Design, synthesis and structural evaluation of peptidomimetics towards foldamers, PNAs and non covalent inhibitors of the 20S proteasome

Dissertation

zur Erlangung des Doktorgrades der Naturwissenschaften

Dr. rer. nat.

an der Fakultät für Chemie und Pharmazie

der Universität Regensburg und der Universität Paris XI (Frankreich)

vorgelegt von

Andrea Bordessa

aus

Germasino (Italy)

Regensburg 2008

This work was supervised by Prof. Dr. Oliver Reiser in Regensburg and
Dr. Sandrine Ongeri and Prof. Dr. Sames Sicsic in Paris

Thesis submission on November 17th, 2008

Thesis defence on December 3rd, 2008

Examination committee: Prof. Dr. Oliver Reiser
Dr. Sandrine Ongeri
Prof. Dr. Burkhard König
Prof. Dr. Sigurd Elz

The following research work was performed from November 2005 to October 2007 in the Institute of Organic Chemistry of the University of Regensburg under the supervision of Prof. Dr. Oliver Reiser and from November 2007 to October 2008 at the University of Paris XI, in the Laboratoire de Molécules Fluorées et Chimie Médicinale, BioCIS, UMR-CNRS 8076 under the supervision of Dr. Sandrine Ongeri and Prof. Dr. Sames Sicsic.

I would like to thank Prof. O. Reiser, Dr. Sandrine Ongeri and Prof. Sames Sicsic for having given me the opportunity to join their research groups and for their help in these three years.
I also thank the Marie Curie commission for financial support during this PhD programme.

Abbreviations

Ac = Acyl

AcOEt = Ethyl acetate

Ar = Aryl

Bn = Benzyl

Boc = *tert*-Butoxycarbonyl

Bu = Butyl

CAN = Cerium Ammonium Nitrate

Cbz = Benzyloxycarbonyl

CD = Circular Dichroism

COSY =Correlation spectroscopy

DIBAL-H =Diisobutylaluminium Hydride

DIPEA = Diisopropylethyl Amine

DMF = Dimethylformamide

DMSO = Dimethylsulfoxide

DNA = Deoxyribonucleic acid

EDC = Ethyl-N,N-dimethyl-3-aminopropylcarbodiimide

ee = Enantiomeric Excess

EI = Electronic impact

Eq. = equivalent

Fmoc = 9-Fluorenylmethoxycarbonyl

h = hours

HBTU = O-Benzotriazole-N,N,N′,N′-tetramethyluronium hexafluorophosphate

HOBt = Hydroxybenzotriazol

HOAt = 1-hydroxy-7-azabenzotriazole

IR = Infrared spectroscopy

Me = Methyl

MeOH = Methanol

min = Minutes

m.p. = Melting Point

MS = Mass Spectroscopy

NMR = Nuclear Magnetic Resonance

NOE = Nuclear Overhauser Effect

PNA = Peptide Nucleic Acid

PG = Protecting Group

Py = Pyridine

PMB = *para*-Methoxybenzyl

RMSD = Root Mean Square Deviation

ROESY = Rotating Frame NOE Spectroscopy

RT = Room Temperature

TFE = Trifluoroethanol

CHAPTER 1 INTRODUCTION

1.1 Peptide generalities

Peptides (from the Greek *πεπτίδια*, "small digestibles") are short polymers formed from the linking, in a defined order, of α-amino acids. The link between one amino acid residue and the next is known as an amide bond or a peptide bond. Proteins are polypeptide molecules (or consist of multiple polypeptide subunits). The convention is that peptides are shorter than 50 amino acids residues and polypeptides/proteins are longer. Natural peptides and proteins are mainly composed of 20 α-amino acids to which we can add a few other ones which are relatively rare in nature. Amino acids are organic molecules which possess an amine and a carboxylic acid. α-amino acids can present different lateral chains leading to molecules with completely different physical properties. The simplest α-amino acid is the glycine, which is the only achiral amino acid. Natural α-amino acids have been classified in five categories: acidic, neutral, basic, hydrophobic and hydrophilic. When the amino acid is not A glycine, the C_α is a chiral center and natural amino acids are all present in the L-configuration in the nomenclature of Fischer. A few ones extracted from exotic molluscs or in cell walls of some bacterias can be in a D-configuration but their occurrence in nature is anecdotic in comparison to the supremacy of L-amino acids. (Figure 1)

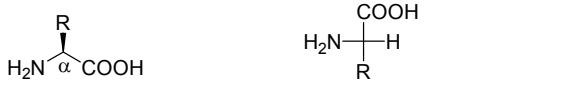

α-amino acid L-amino acid in Fischer representation

Figure 1

Peptides and proteins present four types of primary structure which will be shortly present above.

1.2 Primary structure

In general, polypeptides are unbranched polymers, so their primary structure can often be specified by the sequence of amino acids along their backbone. However, proteins can become cross-linked, most commonly by disulfide bonds, and the primary structure also requires specifying the cross-linking atoms, e.g., specifying the cysteines involved in the protein's disulfide bonds.

1.3 Secondary structure

The remarkable and highly diverse biological activities exhibited by proteins rely on the unique capacity of these intrinsically flexible chains to fold into well-organized and compact structures. Linus Pauli, more than half century ago, first understood that detailed information about these molecular and supramolecular structures are a prerequisite for the comprehension of the biological events in the living cell. The formation of tertiary and quaternary structures relies only on a small set of distinct secondary structural elements: sheets, helices and turns (figure 2). Every conformation has is own nomenclature to describe its hydrogen bonding. A non structured conformation is called random coil.

1.3.1 α-helix

Helices present a periodic folding having a curly shape. Most of the time, the helix turns clockwise and is called right-handed helix. In the other case, it is a left-handed helix. In the family of helices can be differentiated a few subcategories depending on the periodicity of the helix. The most common is the α-helix, and it is characterised by the presence of an hydrogen bond between the carbonyl of an i residue with the nitrogen of the residue i+4, forming a 13-

membered ring. Every loop has a length of 0.54 nm and contains 3.6 residues. The dihedral angles ψ and φ are between 45 and 60 degrees. The structure is very compact and the lateral chains of the amino acids point out of the helix (figure 1).

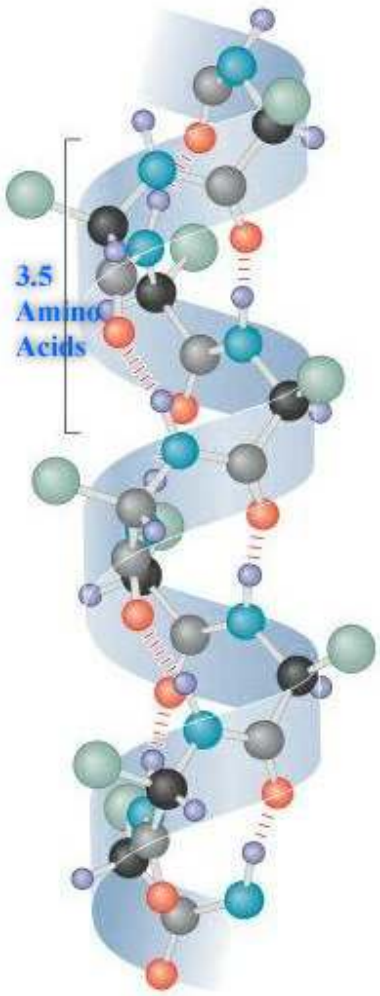

Figure 2 α-helix

1.3.2 β-sheet

β-sheet are another typical conformation adopted by proteins. This is a planar conformation adopted by two fragments far one to each other. The structure is stabilized by the presence of

intermolecular hydrogen bonding between the two fragments. The lateral chains of the amino acids point outside the plane, alternatively under and over. It exists 2 different types of β-sheet, the parallel (both fragments are orientated in the same direction) and the anti-parallel, when the fragments are oriented in opposite directions (Figure 3).

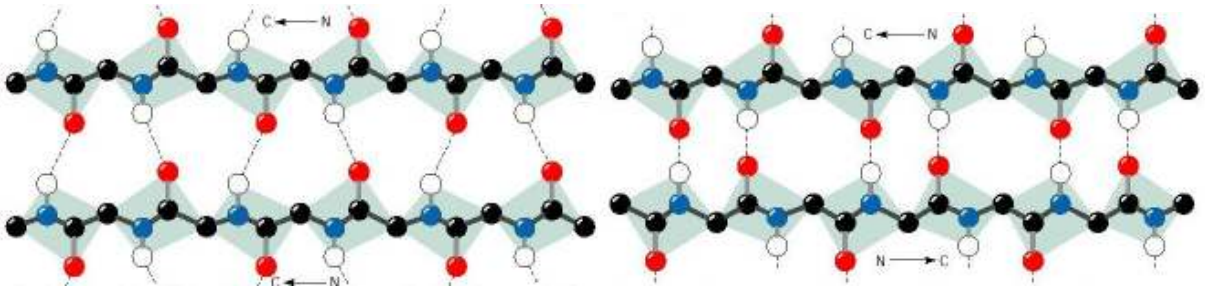

parallel β-sheet **antiparallel β-sheet**

Figure 3

1.3.3 turns

Turns are small secondary structures that form an elbow in the peptide sequence and can induce antiparallel β-sheet by placing two fragments in front one to each other. There are classified depending on the ring size of the hydrogen bond forming the turn. β-turns are the most common turns and involve hydrogen bonding between the *i* residue and the *i+3* residue with a ten-membered ring. There are three types of β-turn depending on the dihedral angles: I, II and III (the type III corresponds to a single turn of 3_{10} helix). The mirror images of these turns are called I', II' and III' (Figure 4).

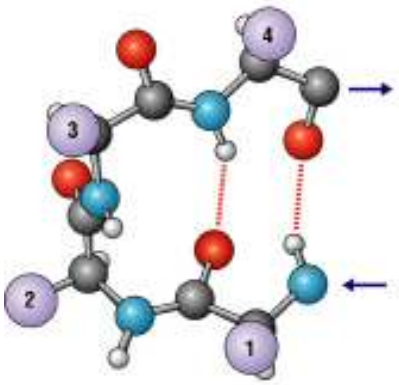

Figure 4

1.4 Tertiary structure

The tertiary structure of a protein or any other macromolecule is its three-dimensional structure, as defined by the atomic coordinates. So, we can say it is essentially the way as the different secondary structures present in a protein organize them one to each other. For example, some residues which are far in the peptidic chains can be close in the three-dimensional structure.

1.5 Quaternary structure

Many proteins are actually assemblies of more than one polypeptide chain, which in the context of the larger assemblage are known as protein subunits. In addition to the tertiary structure of the subunits, multiple-subunit proteins possess a quaternary structure, which is the arrangement into which the subunits assemble. Enzymes composed of subunits with diverse functions are sometimes called holoenzymes, in which some parts may be known as regulatory subunits and the functional core is known as the catalytic subunit.

1.6 Conformational studies of the secondary structure

It is possible to perform more different analysis for the characterization of the secondary structure. The most important are the NMR, IR, circular dichroism and X-ray.

1.6.1 NMR studies

Since the hydrogen bonds are the principal responsible for the formation of the secondary structure, signals of amide protons are fundamental for the understanding of the peptide organization.

1.6.2 Choice of the solvent

The choice of the solvent is of fundamental importance in the NMR studies. In effect, the solvent can largely affect the ability of a peptide to form a secondary structure, and it is also quite commune that a peptide shows different conformations in different solvents.

1.6.3 2D NMR

2D NMR analysis is one of the most powerful tools for the study of the secondary structure of proteins. With unlabelled protein the usual procedure is to record a set of two dimensional homonuclear nuclear magnetic resonance experiments through correlation spectroscopy (COSY), of which several types include conventional correlation spectroscopy and nuclear Overhauser effect spectroscopy (NOESY).[1] A two-dimensional nuclear magnetic resonance experiment produces a two-dimensional spectrum. The units of both axes are chemical shifts. The COSY transfers magnetization through the chemical bonds between adjacent protons. The conventional correlation spectroscopy experiment is only able to transfer magnetization between protons on adjacent atoms, so it is transferred among all the protons that are connected by adjacent atoms. Thus in a conventional correlation spectroscopy, an alpha proton transfers magnetization to the beta protons, the beta protons transfers to the alpha and gamma protons, if any are present, then the gamma proton transfers to the beta and the delta protons, and the process continues. Thus this

experiment is used to build so called spin systems, that is build a list of resonances of the chemical shift of the peptide proton, the alpha protons and all the protons from each residue's side chain. Which chemical shifts corresponds to which nuclei in the spin system is determined by the conventional correlation spectroscopy connectivities and the fact that different types of protons have characteristic chemical shifts. To connect the different spin systems in a sequential order, the nuclear Overhauser effect spectroscopy experiment has to be used. Because this experiment transfers magnetization through space, it will show crosspeaks for all protons that are close in space regardless of whether they are in the same spin system or not. The neighbouring residues are inherently close in space, so the assignments can be made by the peaks in the NOESY with other spin systems.

1.6.4 Hydrogen deuterium exchange and variation of temperature

This two different studies allows to identify which protons of a molecule are involved in an intramolecular hydrogen bond. In the case of the hydrogen deuterium exchange, to a peptide solved in a solvent which does not present exchangeable deuterium will be added CD_3OD. The amide protons in the protein exchange readily with the deuterium of the solvent, so the hydrogen deuterium exchange by NMR spectroscopy follows the disappearance of the amide signals. How rapidly a given amide exchanges reflects its solvent accessibility. Thus amide exchange rates can give information on which parts of the protein are buried, hydrogen bonded etc.
The same principle is at the base of the variation of temperature studies. Generally it is accepted that an amide proton involved in a strong intramolecular hydrogen bond has a low temperature dependence coefficient ($\Delta\delta<3$ ppb/K), while for a weak intramolecular hydrogen bond is significantly higher ($\Delta\delta>8$ ppb/K).

1.6.5 Circular dichroism

Circular dichroism (CD) is a form of spectroscopy based on the differential absorption of left- and right-handed circularly polarized light. It can be used to help to determine the structure of macromolecules (including the secondary structure of proteins and the handedness of DNA). CD was discovered by the French physicist Aimé Cotton in 1896. This analysis is performed in

solution in high dilution (typically <1 mM, to avoid peptide aggregation) in the absorption band of amide bonds (180-250 nm). Circular dichroism measures the ellipticity of a peptide in this band with UV polarised light. In this band can be observed the absorption $\pi \rightarrow \pi^*$ of amides and the absorption will vary according to the hydrogen bonded or non hydrogen bonded state of the amides, therefore it will give information on the presence of a secondary structure. Indeed, a peptide being a chiral molecule, it will present an optical rotation on polarised light but this optical rotation can vary with the wavelength. The analysis is often performed in quartz cells of 1 mm length or less as the solvent absorption can create some parasite noise. All solvents can not be used in CD spectroscopy as the circular dichroism must be measured in a band where the solvent does not absorb, methanol (limit at 195 nm for a cell 1 mm long), trifluoroethanol (TFE) or mixtures methanol/water can be used. Other common organic solvents as THF, acetonitrile, chloroform or dichloromethane can not be used in this case as they absorb in the same region as amides.

The ellipticity θ follows the Beer-Lambert law and can be calculated namely:

$\theta = CD_{measured}/(Cxlxn)$

with θ: ellipticity in $deg.cm^2.dmol^{-1}$

C. concentration in $mol.L^{-1}$

l: length of the cell in dm

n: number of NH in the molecule

This technique has the advantage to be fast and one can see almost immediately if the peptide adopts a secondary structure or not. The limitation is that one can not deduce exactly which amides are involved in hydrogen bonding. It is nevertheless very useful since CD curves of α-peptides are typical of a certain secondary structure and so new peptide curves can be confronted with references. There has been also a lot of work in the field of β-peptides and some references are available but when a peptide containing unnatural amino acids is analysed, this comparison can not be always done with certainty as the curves may differ a lot for a same secondary structure.

1.6.6 IR in solution

Another powerful tools to detect the presence of intramolecular hydrogen is the IR in solution. The technique consist in the measurement of an IR spectrum at high dilution (usually in dichloromethane or chloroform) to avoid the peptide aggregation. It is so observed the region of amide bond, which present, in the case of intramolecular hydrogen bond, two different bands, one at less than 3400 cm^{-1} bonded amides and another at more than 3400 cm^{-1} for non bonded amide. Limits of this technique are the impossibility to use solvent which can form hydrogen bond with the peptide or which adsorb in the interesting region (DMSO, methanol, etc.).

1.6.7 X-ray crystallography

This is the most potent tools to directly study the secondary conformation of a peptide. Unfortunately, it is not simple to obtain a crystal of a peptide, especially for the high flexible linear ones. Actually, the crystal structure of more and more peptides of biological interest are available on the Protein Data Bank database.

1.7 Peptidic coupling

Generally speaking, a peptide is formed by the linking of more amino acids by formation of amide bonds. The simple mixture of two or more amino acids in solution at room temperature just brings to the formation of a salt, and the condition to transform this salt into an amide bond it is too harsh for the formation of peptides. Thus, it is necessary therefore to activate the carboxylic group of one of the amino acids so that nucleophilic attack by the amino group of the second can take place, forming the desired amide under mild conditions. In peptide chemistry, this process is called coupling.

1.7.1 Coupling reagents

The most common general coupling method is the use of coupling reagents. This reacts with the free carbonyl group, generating a reactive species, which is not isolated and which is sufficiently

reactive to allow the amide bond formation at room temperature and in mild condition. The most commonly used coupling reagents are the carbodiimides[2] (Figure 5).

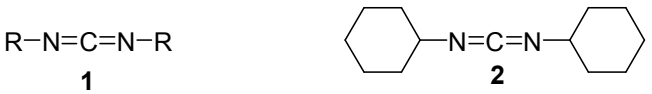

Figure 5

Addition of the carboxyl group of the N-protected amino acid to one of the C=N bonds of the carbodiimmide gives the O-acylisourea intermediate 5, the first active species in the coupling reaction. This highly reactive compound can then undergo aminolysis by the amino component, leading to the formation of the amide **6** and the dialkilurea by-product **7**.

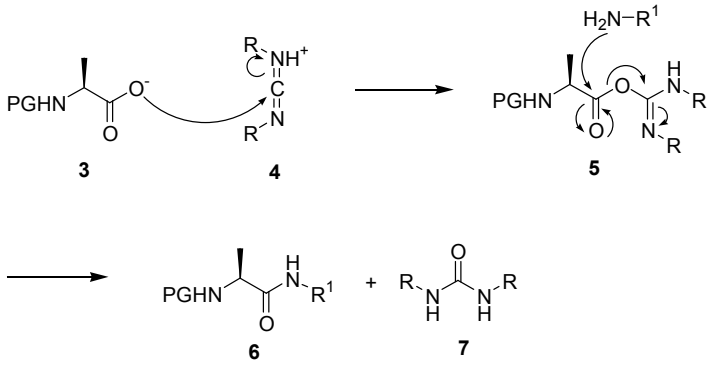

Figure 6

One of the most important side reaction in the coupling promoted by the carbodiimmides is the formation on an oxazolone intermediate which as to be avoid because it can lead to the racemisation of the substrate (Figure 7).

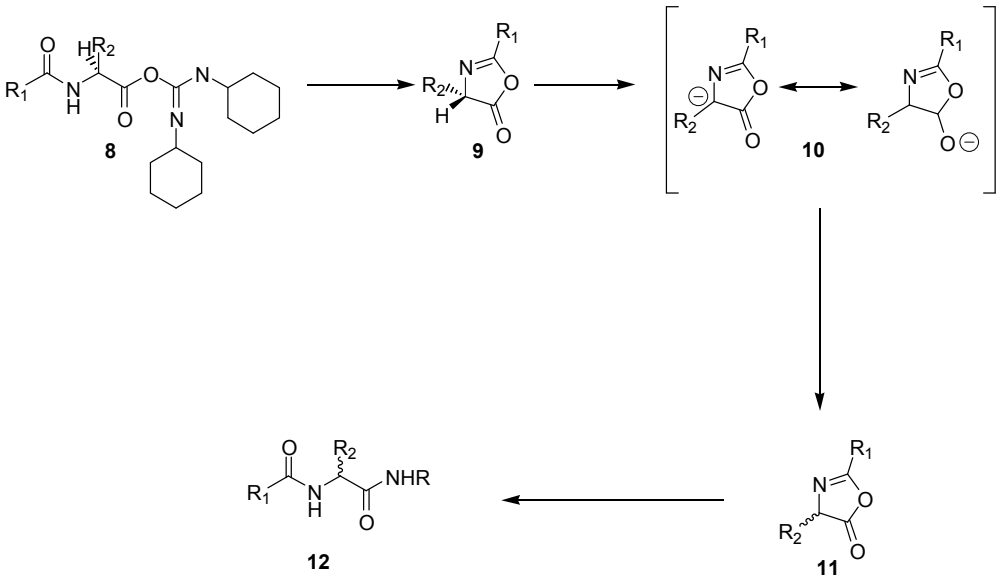

Figure 7

Many of the side reactions that occur when activation is carried out with the carbodiimide alone can be avoid by using some additive. These compounds intercept the O-acylisourea intermediate forming forming a less reactive acylating reagent, which is still potent enough to allow rapid amide bond formation. The most widely used are HOBt (**13**) and the most reactive, but also expensive HOAt (**14**).

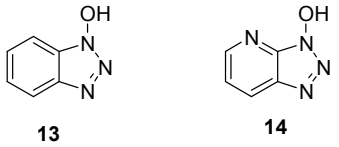

Figure 8

Other reagent coupling widely used are the uronium salt, in particular HBTU and HATU are currently used. X-ray crystallography demonstrate that both HBTU (**15**) and HATU (**16**) crystallized as guanidinium N-oxide (Figure 9).

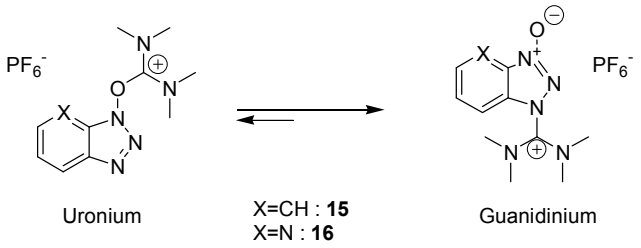

Figure 9

It is possible to perform a peptidic coupling using two different methods, the solution phase and the solid phase synthesis.

1.7.2 Solution phase peptide synthesis

Despite the larger and larger applications of solid phase methods, the synthesis of peptides in solution remains one of the major chemical approaches to these molecules.[3] The principal advantage of this technique is the possibility to isolate and characterize all the intermediates at every step, having a knowledge about the molecular species obtained at every stage. Thus, problems that arise can be immediately identify , when in solid phase synthesis it is possible to do that only after the cleavage to the resin. However, classical peptide synthesis is slower than the solid phase synthesis and it is not suitable for the synthesis of peptide with a large number of residues. In the other hand, it is the most used strategy in some areas, such the high scale synthesis of peptides, the synthesis of peptides composed of unusual or uncommon amino acids (e.g. peptidomimetics) and the synthesis of cyclic peptides.

It exists two different basic strategies: linear or convergent. In the linear strategy the amino acids are coupled singularly to the chain and it is the most suitable method for short peptides. The convergent is based on the condensation of peptidic fragments, and it is adapted for the synthesis

of longer peptides. The advantage of this second method is the possibility to prepare in parallel the different scaffold d, but the coupling of the different fragment can be slow and difficult for the steric reasons due to the use of two big fragments in which the reactive group is not so simply accessible.

1.7.3 Solid phase peptide synthesis (SPPS)

Merrifield's methods for the synthesis of peptides on insoluble polymeric supports has been so succefull that the great majority of peptides are now made using this technique.[4-6] The advantages of this technique over classical synthesis in solution phase are those of simplicity and speed of execution. SPPS can be mechanized and has led to the commercialization of automated peptide synthesizers which can be programmed to carry out repetitive steps in the synthesis of a peptide. In favourable cases, quite complex peptides can be made in a matter of hours by machine-assisted synthesis.

The solid support consists in a polymer chemically inert to all the reagents used in the coupling, insoluble in the reaction's solvent and simple to handle and to filtrate from liquids. It must be also possible to modify the resin to attach the first amino acid of the synthesis by formation of a covalent bond and remove them at the end of the synthesis. The most common resins are the Merrifield resin, which can be cleaved with HBr or HF and it is compatible with the Boc protecting group, and the Wang resin, which can be cleaved in less drastic conditions (TFA) and it is compatible with the Fmoc protecting group.

1.7.4 Protecting group

In both solution and solid phase synthesis, the choice of the protecting groups plays an important role. It is necessary to choice them to have an orthogonal system, which is a system where it is possible to deprotect easily a group without affecting the others. For the synthesis of peptides the N-protecting group is almost always a urethane derivative. The reason of this choice is the simplicity of the protection and deprotection steps and the possibility, choosing an appropriate urethane (figure 10) to deprotect them under acidic (in the case of Boc group, **17**) or basic (in the case of Fmoc group, **18**) conditions or under catalytic hydrogenation (in the case of Cbz group,

19). Usually the N^{α} is protected by using Boc or Fmoc group (the first is most employed is solution phase synthesis and the second in solid phase), when the more stable Cbz is usually used for the protection of the amino group presents in the lateral chains.

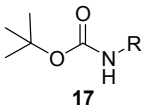

17

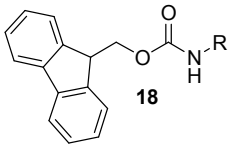

18

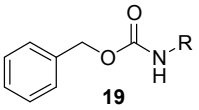

19

Figure 10

The carboxylic group is usually protected by esterification (Figure 11) forming a methyl or ethyl ester (**20**, **21** which can be cleaved in basic conditions by aqueous NaOH or LiOH) or an allyl ester (**22**, cleaved by palladium Tetrakis).

20

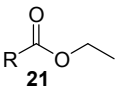

21

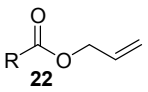

22

Figure 11

1.8 Peptidomimetics

In recent years, the understanding of the folded and self-assembly processes at work in proteins, which are essentially governed by non-covalent forces, have led to major advances in the *de novo* design of individual protein secondary structure elements and protein folds from α-polypeptides.[7-11] Parallel to this field, chemists have been creating new synthetic oligomers that can self organize spontaneously to form defined secondary structures. These molecules aim at mimicking peptide structure through substances having controlled spatial disposition of functional groups, and for this reason are called peptidomimetics. Peptidomimetics have general features analogous to their parent structure, polypeptides, such as amphiphilicity. They have been developed, to a large extent, for the purpose of replacing peptide substrates of enzymes or peptide ligands of protein receptors.[12-15] Peptidomimetic strategies include the modification of amino acid side chains, the introduction of constraints to fix the location of different parts of the molecule,[16] the development of templates that induce or stabilize secondary structures of short chains,[17, 18] the creation of scaffolds that direct side-chain elements to specific locations, and the modification of the peptide backbone. Of these strategies, systematic backbone modifications and structural alterations of the repeat units are most relevant to the field of foldamers. Backbone modifications may involve isosteric or isoelectronic exchange of units or the introduction of additional fragments. For some of these backbones, monomers and sequences giving rise to helical, extended (i.e., "strand"), and turn conformations have been identified. In this field, pseudo-amino acids (β, χ, and δ), due to their ability of these compounds to adopt in solution well-organised secondary structure, can be used as scaffold to place and orient pharmacophores in a predictable manner for the design of molecules with an interesting biological activity. In addition, in contrast with the natural α-peptides, pseudo-peptides display a remarkably *in vitro* stability to degradation by peptidases from bacterial, fungal and eukaryotic origins (e.g. leucyl aminopeptidase, trypsin, amidase, elastase, 20S proteasome, etc.) which makes them even more attractive for biomedical applications.[19] Altogether, such unnatural oligomers designed to reproduce or mimic essential protein structural elements could be of considerable value in the drug discovery.[20] In this field, geminal works by the groups of Gellman[21] and Seebach[19] showed that properties such as folding and structural diversity are not limited to the α-polypetides, but that are also shared with other

peptides containing different amino acids, such as β and χ. Later, it was also demonstrated that the more restricted δ-amino acids can lead to folded oligomers, argument which is exhaustively treated in the next chapter.

CHAPTER 2 δ-AMINO ACIDS TOWARDS FOLDAMERS AND PNAs

2.1 Synthesis of cyclic δ-amino acids

In the biomedical research, the synthesis of compound with similar structures to the bioactive peptides (peptidomimetics) is very important to obtain molecules with an improved potency or stability than the natural compound. In this field, cyclic or polycyclic unnatural amino acids, due to the rigidity of the scaffold and to the highly preorganisation of the substituents, are able to offer a conformational bias to obtain a desired structural behaviour as part of oligopeptide or foldamers. Due to the proper spacing between the amino and the carboxylic function δ-cyclic amino acids can be designed as conformationally restricted dipeptide. A first simple classification of cycle δ-amino acids can be done on the base of the number of the atom in the ring. A large part of cyclic amino acids are carbohydrate derivatives bearing both an amine and a carboxylic acid functionality also referred to as sugar amino acid (SAA). In particular furanoid and pyranoid amino acids found a large application due to the cheap sugar starting materials, the simplicity of the synthesis and the possibility of an high functionalisation by reaction of the hydroxyl functions present in the molecule.

2.1.1 Three membered ring δ-amino acids

In 1990 Kaltenbronn et al.[22] synthesised a dipeptide isostere replacing the amide bond with an epoxide ring. The key step of the synthesis was the epoxidation of an alkene by mCPBA, obtaining the desired product as a mixture of diastereomers (Figure 12).

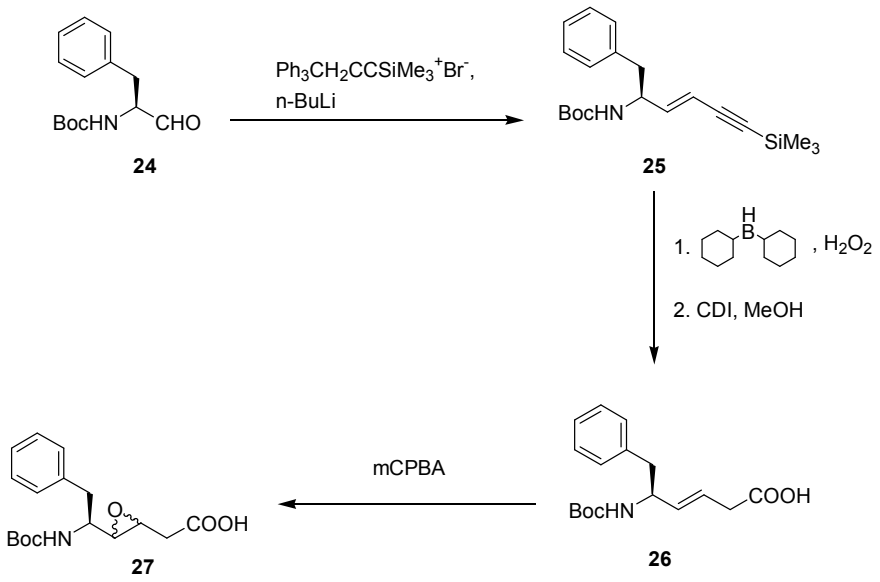

Figure 12: synthesis of epoxy amino acids by Kaltenbronn et al.

After this first example, the same strategy was followed by others groups[23-25] obtaining δ-amino acids with different substituents and diastereomeric ratio of the epoxide ring. In 1996 Mann et al.[26] (Figure 13) published another synthesis of this promising type of δ-amino acids using a Mukaiyama aldol type reaction between the nonstereogenic sylilketene acetal **31** and the chiral aldehyde **30**. The reaction performed in the presence of boron trifluoride etherate gave product **32** in a single diastereomers which was then treated with mCPBA obtaining the epoxide δ-amino ester **33**.

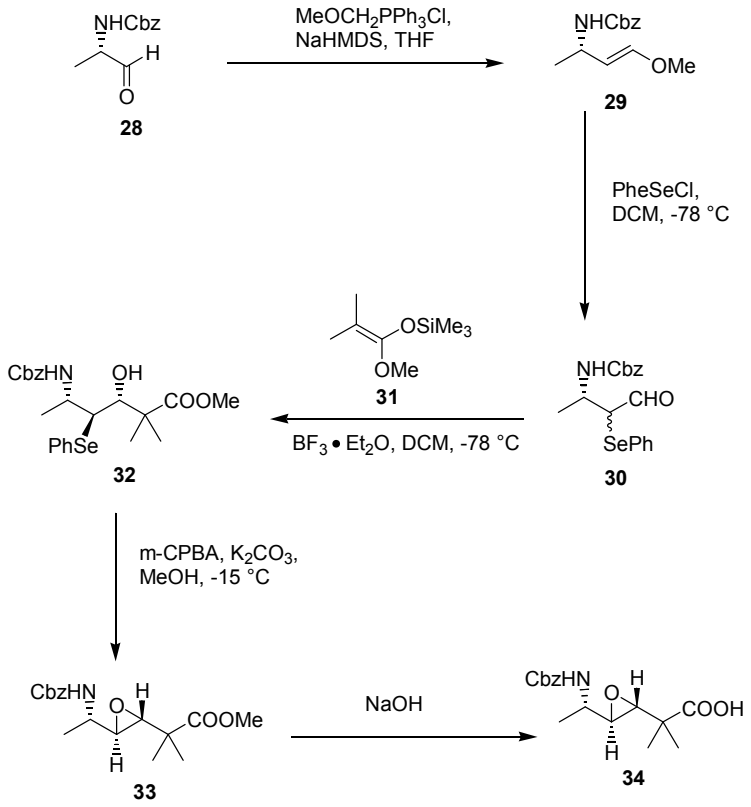

Figure 13: route for epoxy amino acid by Mann et al.

A different approach to 3 membered ring δ-amino acid has been performed by Wipf in 2005[27] which synthesised substituted cyclopropane dipeptide isostere (Figure 14). Methyl alkyne **36** was hydrozirconated with Cp_2ZrHCl, transmetalated to Me_2Zn and added to (diphenylposphinylimino)phenylarene to provide the corresponding allylic amide, which was converted to the desired cyclopropane **37** after treatment with CH_2I_2. Simultaneous N and O deprotection followed by selective N-Cbz protection afforded the alcohol **38a** and **38b** as a separable mixture of diastereomers. The desired δ-amino acid **39** was then obtained by a two step oxidation of the hydroxyl function to carboxylic acid.

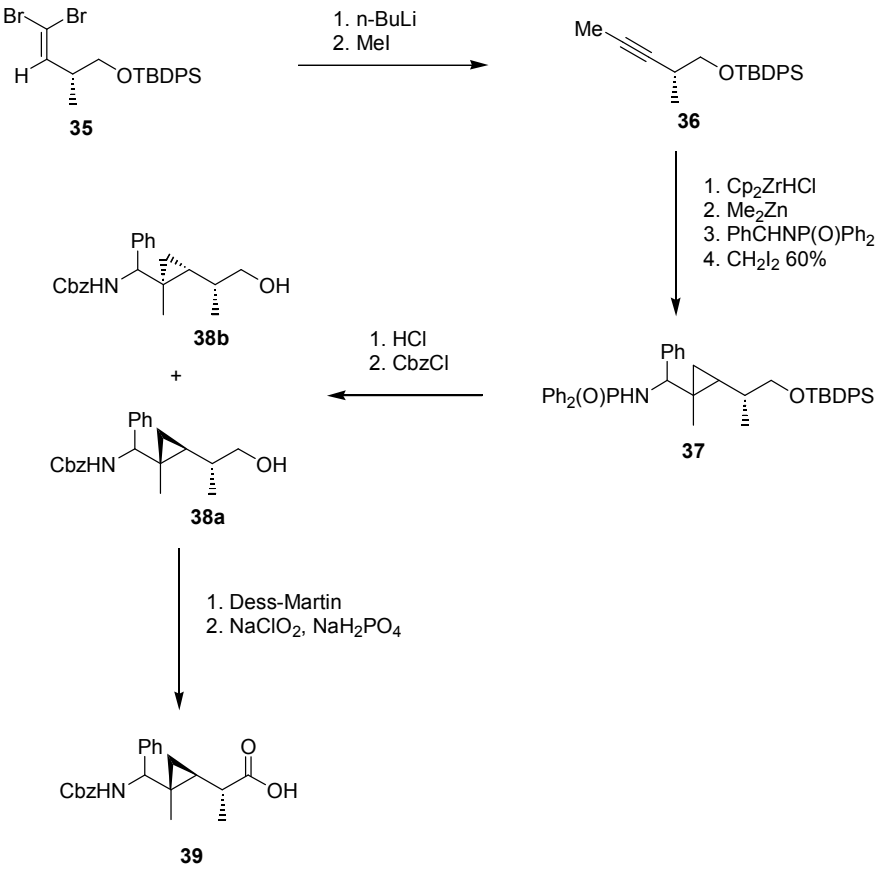

Figure 14: synthesis of cyclopropane dipeptide isostere by Wipf et al.

2.1.2 Four membered ring δ-amino acids

Only few works have been published about the synthesis of δ-amino acid with 4 ring atoms. Very active in this field, Fleet's group published different works reporting the synthesis and/or the secondary structural investigation of δ-2,4 oxetane amino acids.

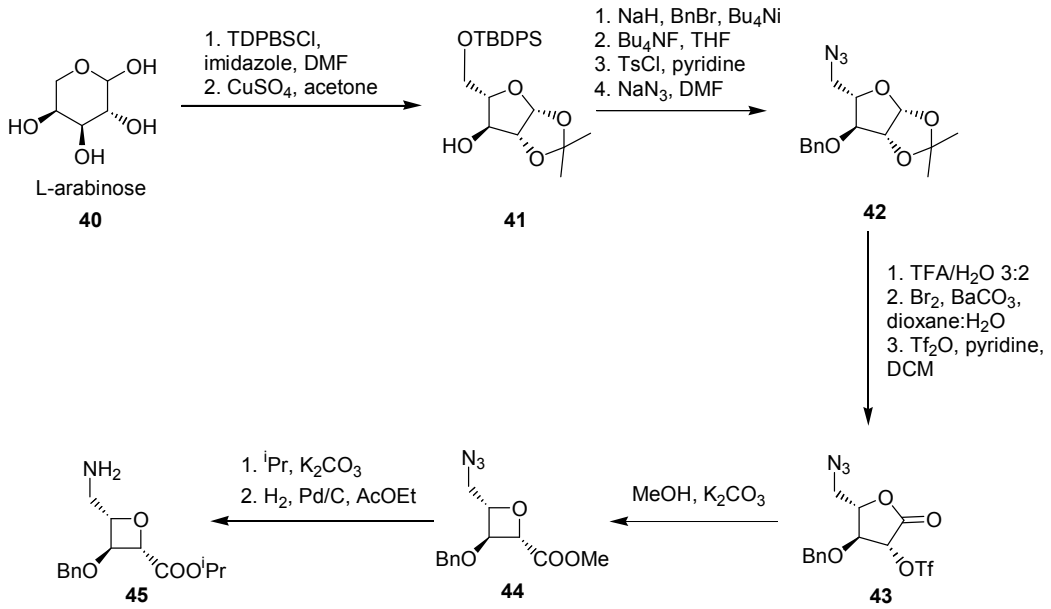

Figure 15: route for oxetane amino acid by Fleet et al.

For example in 2008[28, 29] (Figure 15) 2,4-cis oxetane monomers have been synthesised starting from inexpensive L-arabinose. Key step of the synthetic route is the ring closure of an α-triflate of a γ-lactone in basic methanol, which provide the desired oxetane **44**.

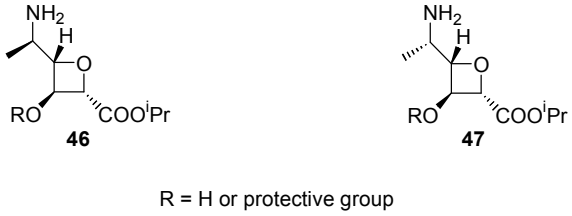

Figure 16: other oxetane amino acids by Fleet. et al.

With the same methodology, but starting from different sugar like L-rhamnose or D-xylose, was possible obtain oxetane with different substituent[30, 31] (figure 16).

2.1.3 Five membered ring δ-amino acids

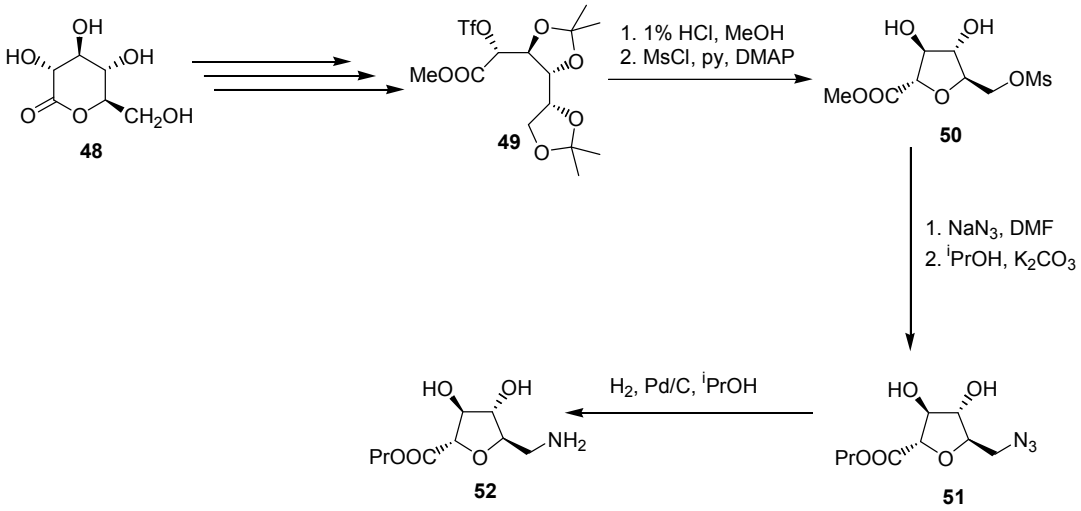

Figure 17: furanoid amino acid by Smith et al.

In 1999 Smith et al.[32] proposed a synthesis of a tetrapeptide based on the trans-5-aminomethyl-tetrahydrofuran-2-carboxylate (figure 17). Treatment of the open chain triflate **49** with methanolic hydrogen chloride give the furan ring via an S_N2-like closure of the C-5 hydroxyl onto C-2 with inversion of configuration. Treatment of primary mesylate **50** with sodium azide afforded the azido ester which was reduced by catalytic hydrogenation to give the free amino group.

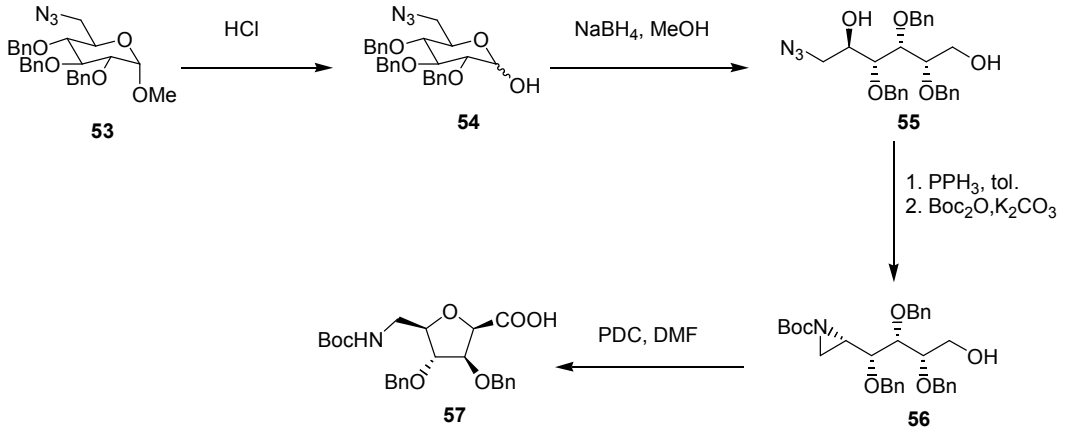

Figure 18: route for furanoid amino acids by chakraborty et al.

In 2000 Chakraborty et al.[33] proposed a synthesis of the furanoid δ-amino acid **57** from the hexose substrate **53,** involving an unusual 5-exo opening of the terminal aziridine ring of **56** by the γ-benzyloxy during the oxidation of the primary hydroxyl group by pyridinium dichromate, with a complete stereocontrol of the ring opening under these conditions (Figure 18).

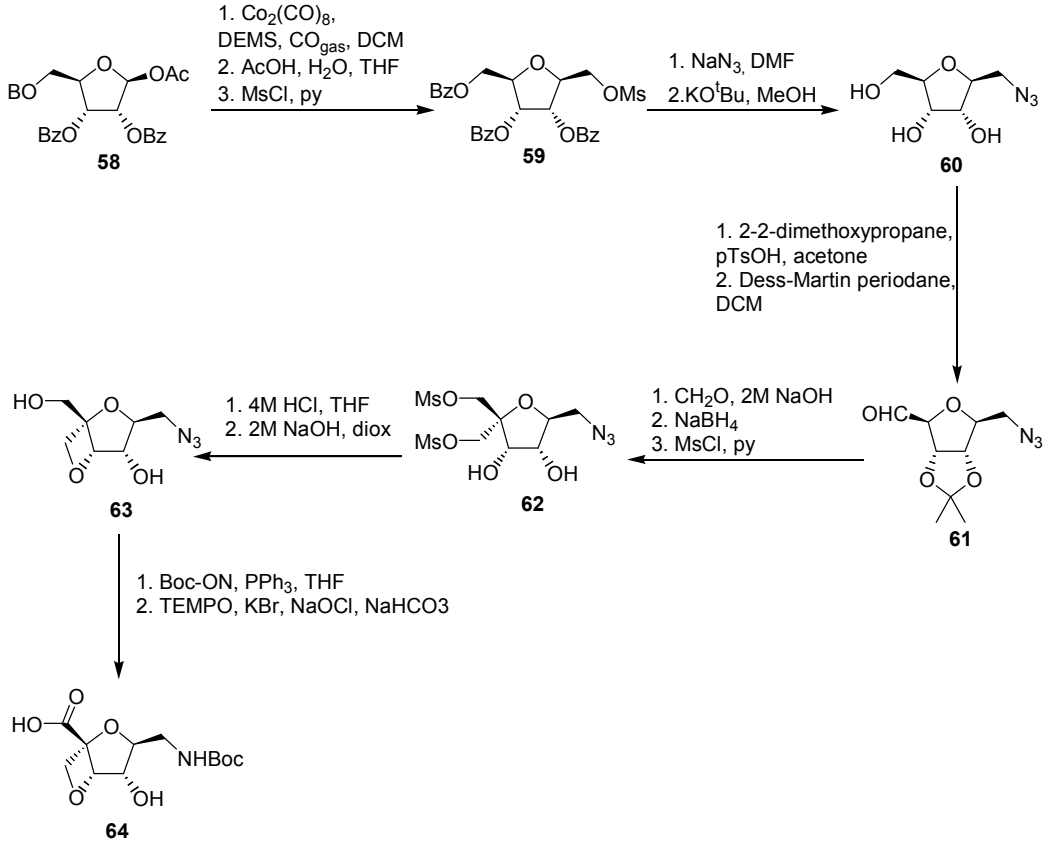

Figure 19: route for constrained amino furanoid amino acid by Van Well et al.

An original structure was synthesised by Van Well et al.[34] in 2003, which synthesised a locked furanoid amino acid (figure 19): the key step of the synthesis is the regioselective ring closure of the dimesylate **62** to exclusively afford the four-membered ring.

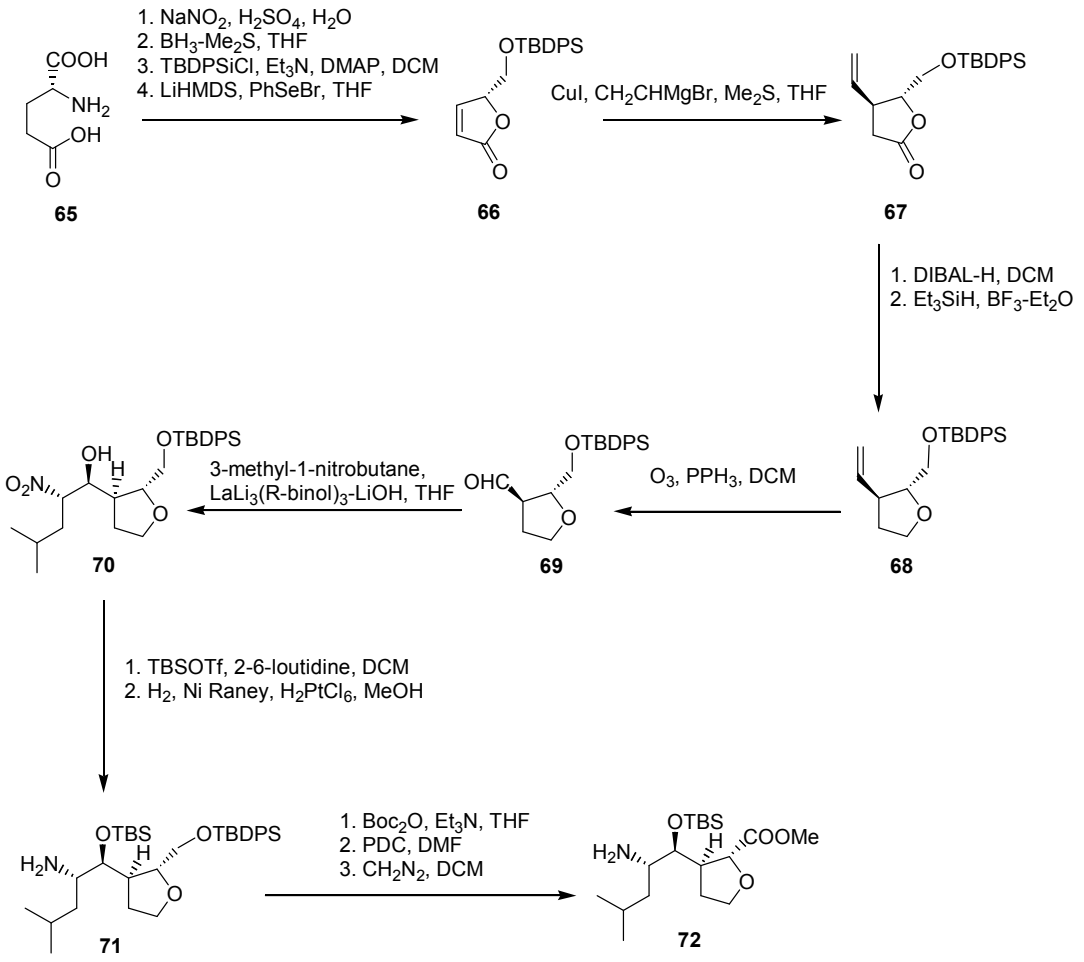

Figure 20: route for furanoid amino acid by Hanessian et al.

In 2004 Hanessian and Brassard[35] (figure 20) synthesised a constrained oxacyclic hydroxyethilene isostere of aspartyl protease inhibitors. Introduction of the nitrogen moiety was performed by a nitroaldol reaction utilising the Shibasaki binol catalyst to obtain **70** as a major isomer in moderate yield.

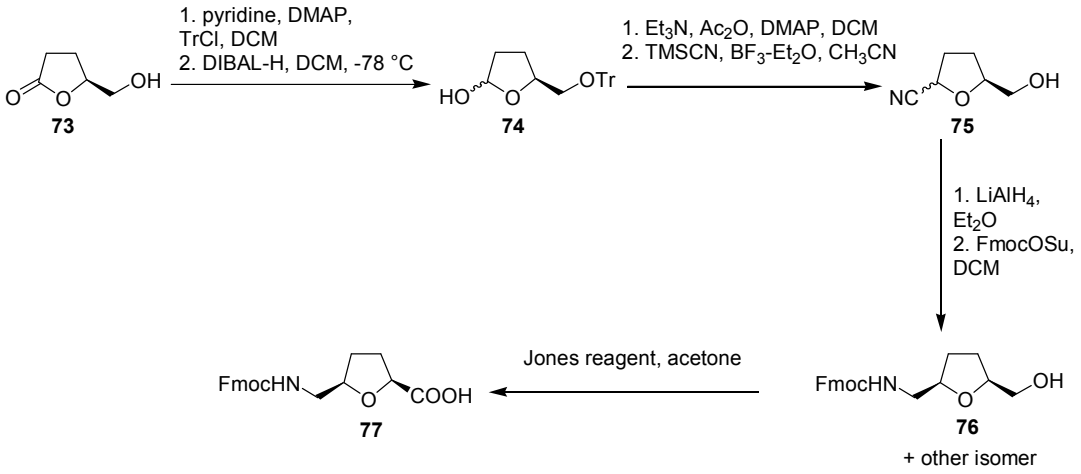

Figure 21: furanoid amino acid by Chakraborty et al.

Another synthesis of a Fmoc protected furanoid δ-amino acid (figure 21) was proposed by Chakraborty in 2004.[36] After protection of the primary hydroxyl group the starting material was reduced with DIBAL-H to the lactol **74**. Acylation of the hydroxyl group was followed by treatment with trimethylsilyl cyanide in the presence of BF_3 etherated to give **75** as a mixture of diastereomers. Reduction of the cyanide group followed by in situ N-Fmoc protection give the intermediate **76**, which can be easily converted into the desired δ-amino acid by oxidation of the hydroxyl group with the Jones' reagent.

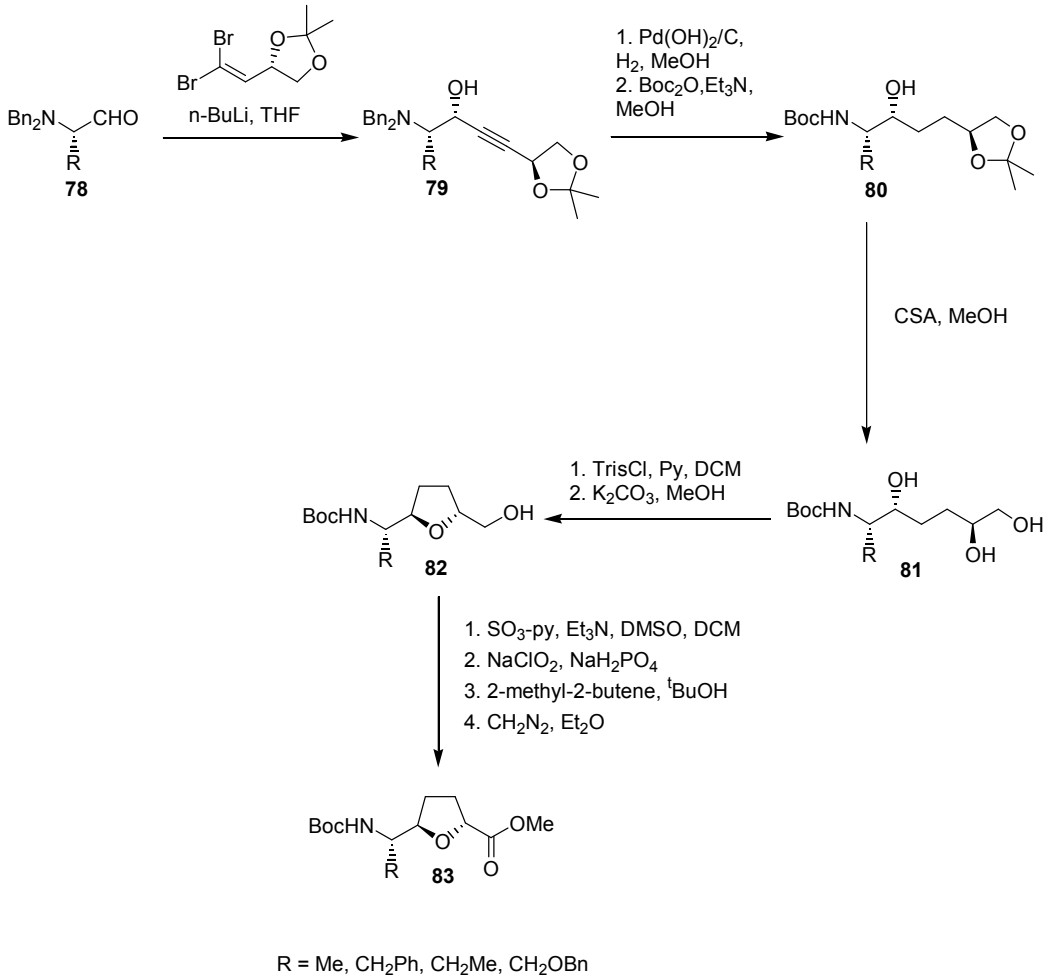

Figure 22: route for C6-substituted furanoid amino acid by Chakraborty et al.

The same group in 2005[37] synthesised a large variety of C6-substituted furanoid amino acid with a completely different strategy (figure 22). Key step of the synthetic route is the selective sulfonylation of the primary hydroxyl group of **81** using 2,4,6-triisopropylbenzenesulfonyl chloride (TrisCl) which gave a sulfonate intermediate that was treated with anhydrous potassium carbonate to carry out an intramolecular ring closure reaction via an epoxide intermediate to give the tetrahydrofuran framework **82**. The subsequent three steps oxidation of the primary hydroxyl group gives the desired δ-amino acid **83**.

2.1.4 Six membered ring δ-amino acids

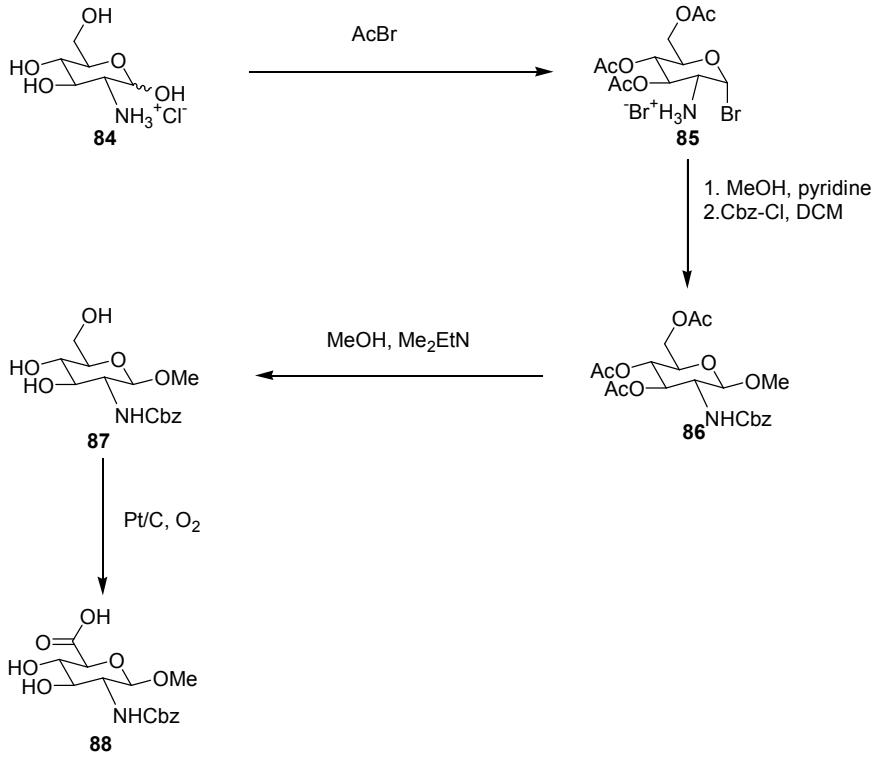

Figure 23: route for pyranoid amino acid by Graf Von Roedern et Al.

In 1996 Graf von Roedern et al.[38] synthesised a pyranoid δ-amino acid starting from glucosamine (figure 23). The anomeric hydroxyl was transformed to glycosyl bromide with acetyl bromide, which was treated with methanol and pyridine to give the β-methyl glycoside. Benzyloxycarbonyl protection of the free amino group was followed by the methanolysis of acetyl group and selective oxidation of the primary hydroxyl group obtaining the desired δ-amino acid **88**.

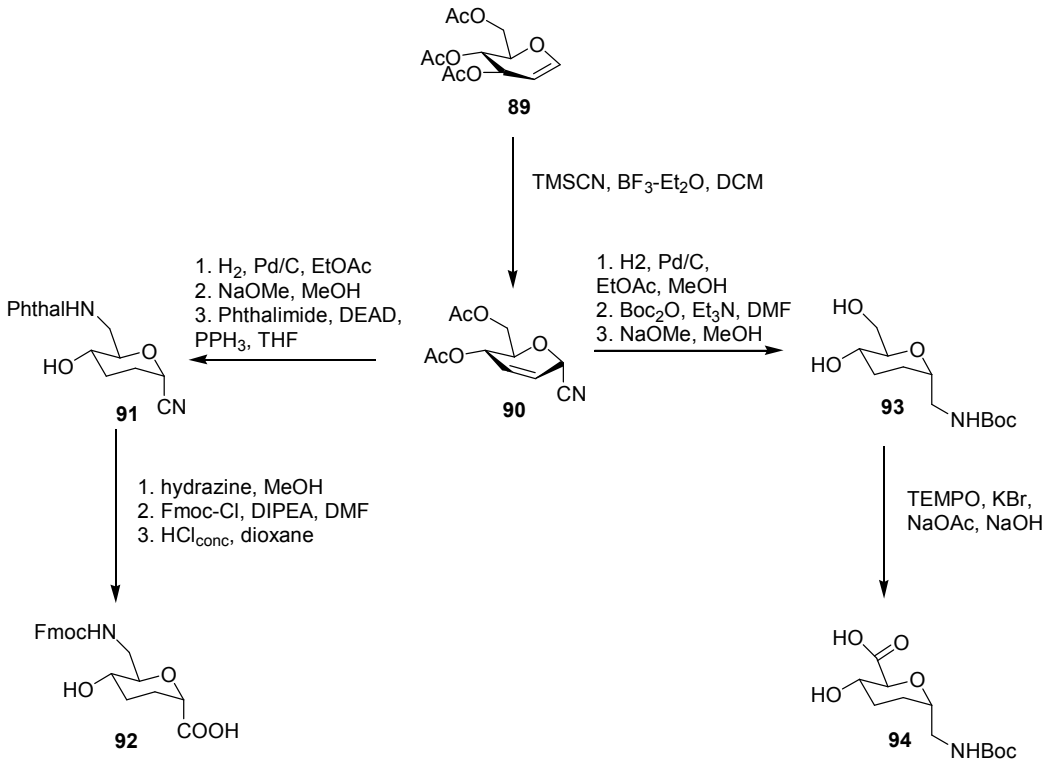

Figure 24: synthesis of pyranoid amino acids by Overkleeft et al.

In 1999, Overkleeft et al.[39] synthesised a farnesyltransferase inhibitor based on sugar amino acids (figure 24). First step of the synthesis is a Ferrier rearrangement of 3,4,6-tri-O-acetyl-D-glucal **89** with trimethylsilyl cyanide and a catalityc amount of BF_3 etherate to give a mixture of separable cyanides. Starting from the major isomer **90** after few steps was possible to obtain the 2 enantiomeric pure δ-amino acids **91** and **92**.

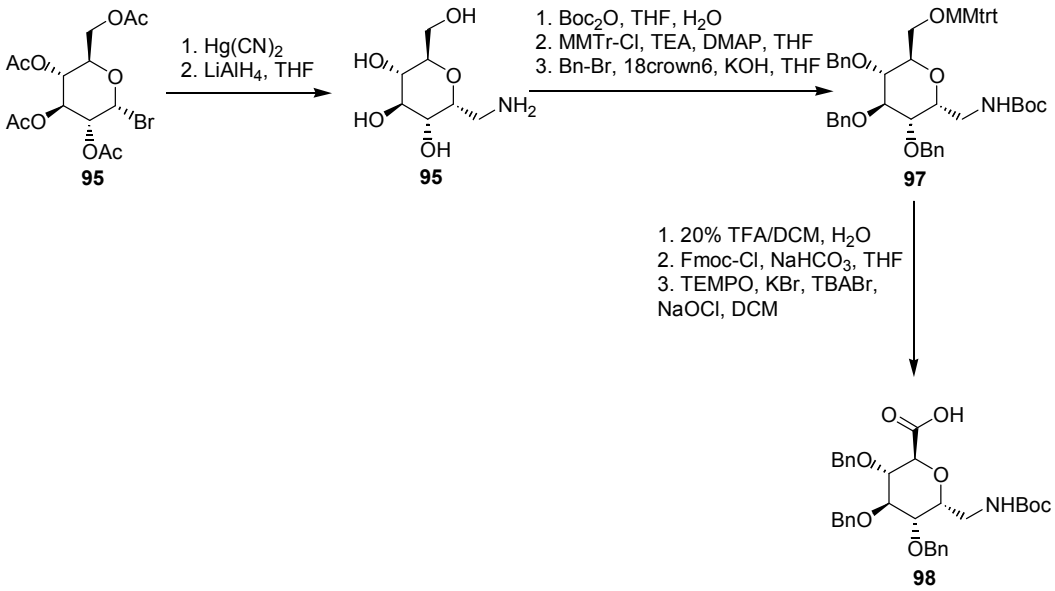

Figure 25: Stockle's pyranoid amino acid

A different synthetic route was proposed by Stockle et al.[40]. O-acetyl-α-glucopyranosyl bromide was reacted with $Hg(CN)_2$ in melt to give the cyanide which was reduced to amine and then protected as tert-butoxy-carbonyl in situ with Boc anhydride. Carboxylic group was then introduced by a TEMPO oxidation of the primary hydroxyl group (figure 25).

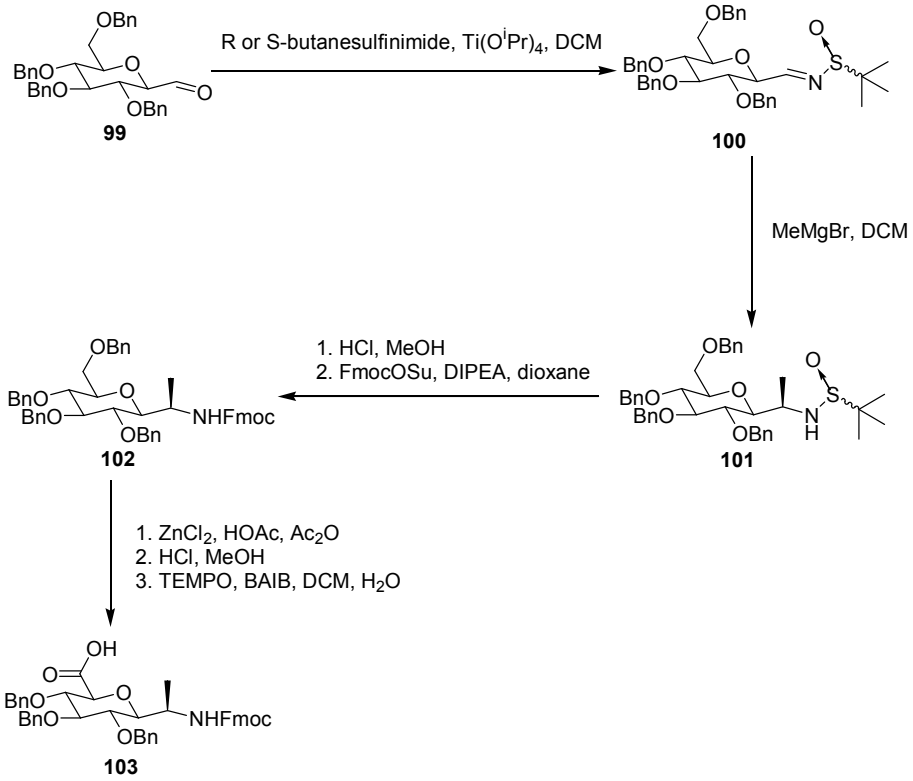

Figure 26: sugar amino acid by Risseuw et al.

In 2007 Risseuw et al.[41] proposed a synthesis of an alkylated sugar δ-amino acid by condensation of formil glucopyrasonide **99** with both R o S-butanesulfinimide in presence of Ti(O^{i}Pr)$_4$, followed by the alkylation of the resulting imide with MeMgBr, giving the adduct **101** with an excellent diastereomeric excess (figure 26). Hydrolysis with methanolic HCl afforded the free amino group which was the protected by treatment with Fmoc succinimide. Selective debenzylation of the primary hydroxyl group followed by a TEMPO oxidation allowed to introduce the carboxylic function in the desired position.

2.1.5 Bicyclic δ-amino acids

Between the bicyclic δ-amino acids, azabicyclo[X.Y.0]alkane amino acids or heteroatom analogues are particularly attractive dipeptide mimetics because their ability to adopt a

conformation which can surrogate a β-turn. Additionally, it is possible easily change some characteristics of the scaffold as rigidity or solubility by inclusion of substituents in different positions, insertion of heteroatoms or other modifications affecting the ring size. A quite general synthesis was proposed by Belvisi et al.[42] in 2004, based on a radical approach (figure 27). Starting from proline derivatives **104**, after deprotection and alkylation of the amino group, was possible to obtain a small library of amides **105**. Conversion of the alcohols to the corresponding brominated products **107** was performed by treatment with mesyl chloride followed by displacement with lithium bromide, whereas the selenides were prepared directly from the alcohols by treatment with N-phenylphtalimide and tributylphosphine.

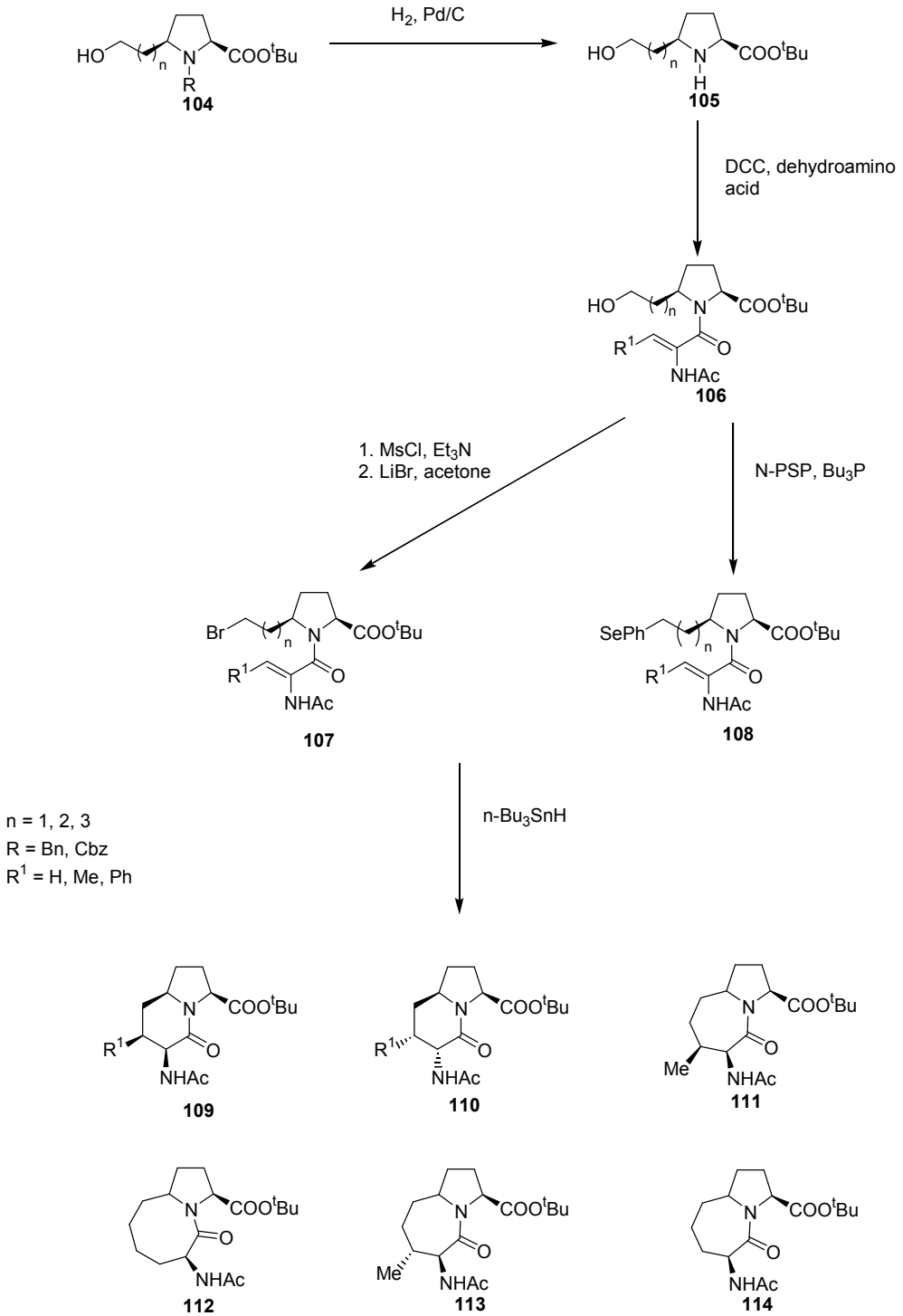

Figure 27: radical approach for azabicycloalkane by Belvisi et al.

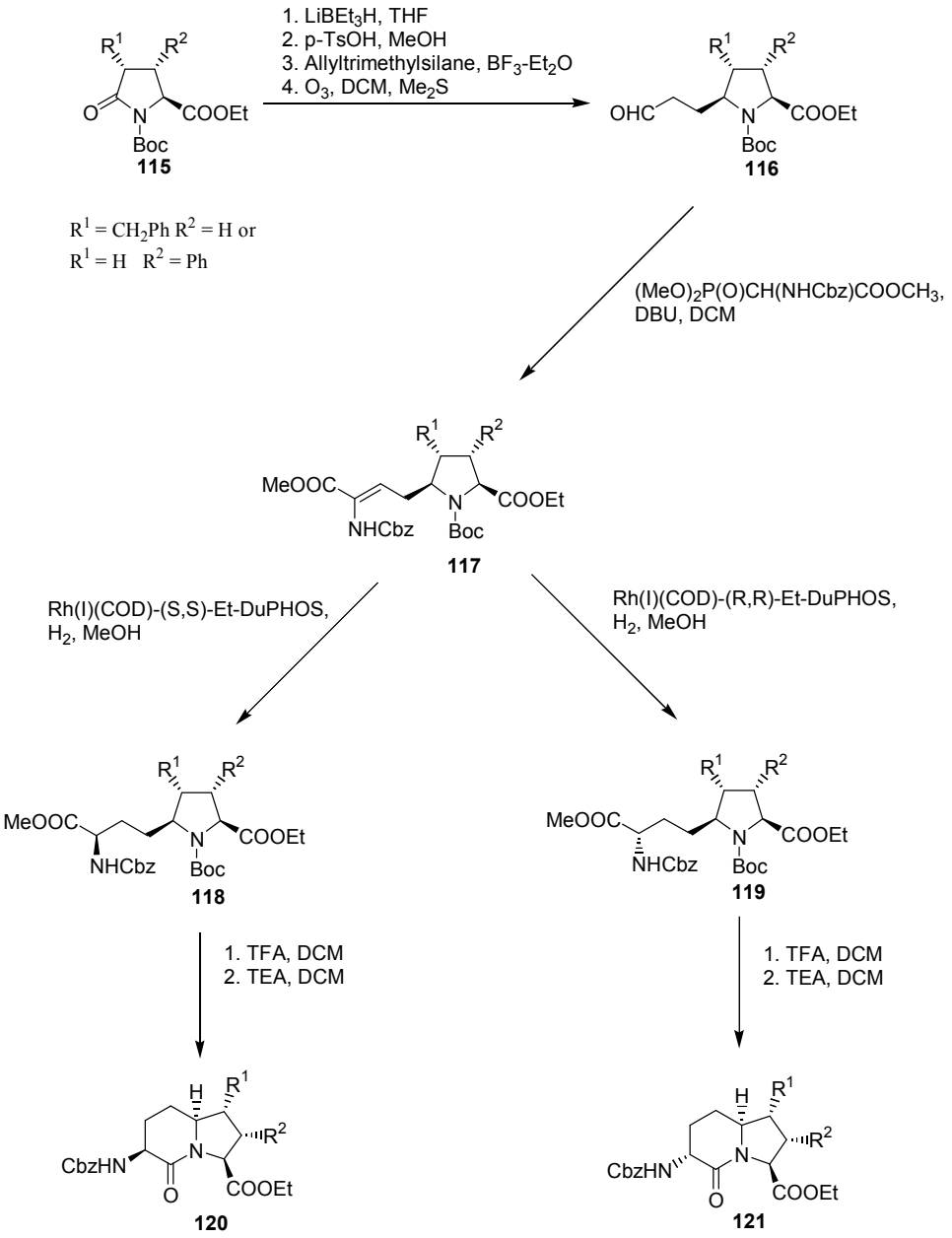

Figure 28: route for azabicycloalkane by Wang et al.

A non radical approach was proposed by Wang et al.[43] in 2002 (figure 28) and Belvisi at al.[42] The aldehyde **116** was obtained in few steps starting from the derivative of pyroglutammic acid **115** and then converted in the dehydroamino acid **117** via the Horner-Emmons olefination . Stereoselective reduction of this compound with the Burk's catalyst followed by intramolecular amido bond formation give the 2 desired δ-amino acids **120** and **121**.

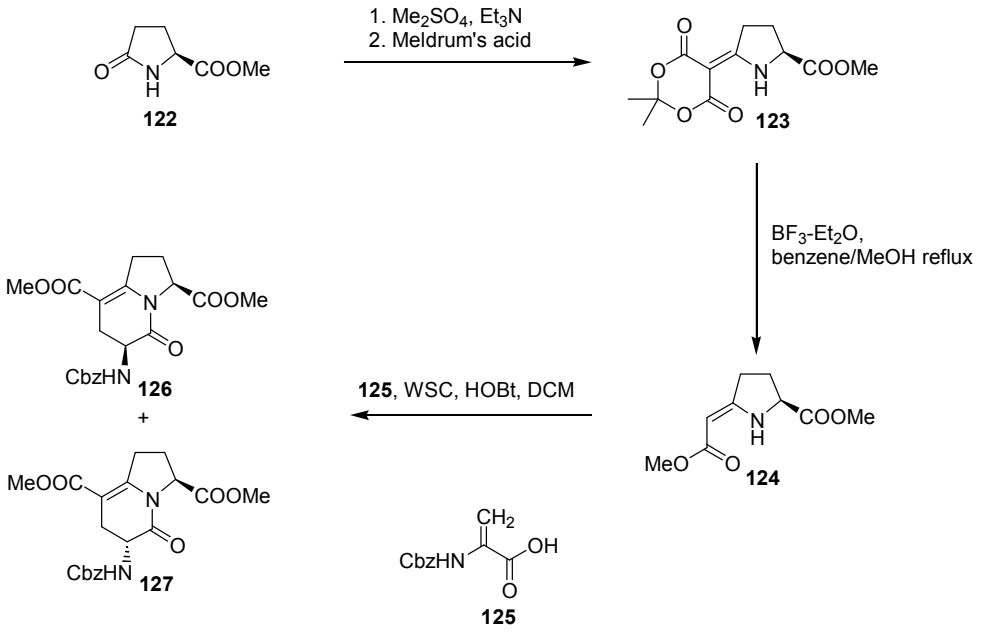

Figure 29: unsaturated bicyclic amino acid by Millet et al.

A synthesis of a more rigid bicyclic scaffold due to the presence of an unsaturation in the 6 member ring cycle was proposed by Millet et al.[44] (figure 29). The enantiomeric pure δ-amino esters **126** and **127** coming from a Michael addition on Cbz-protected dihydroalanine **125** followed by an in situ cyclisation promoted by 1-ethyl-3(3'-dimethylaminopropyl)-carbodiimmide(WSC).

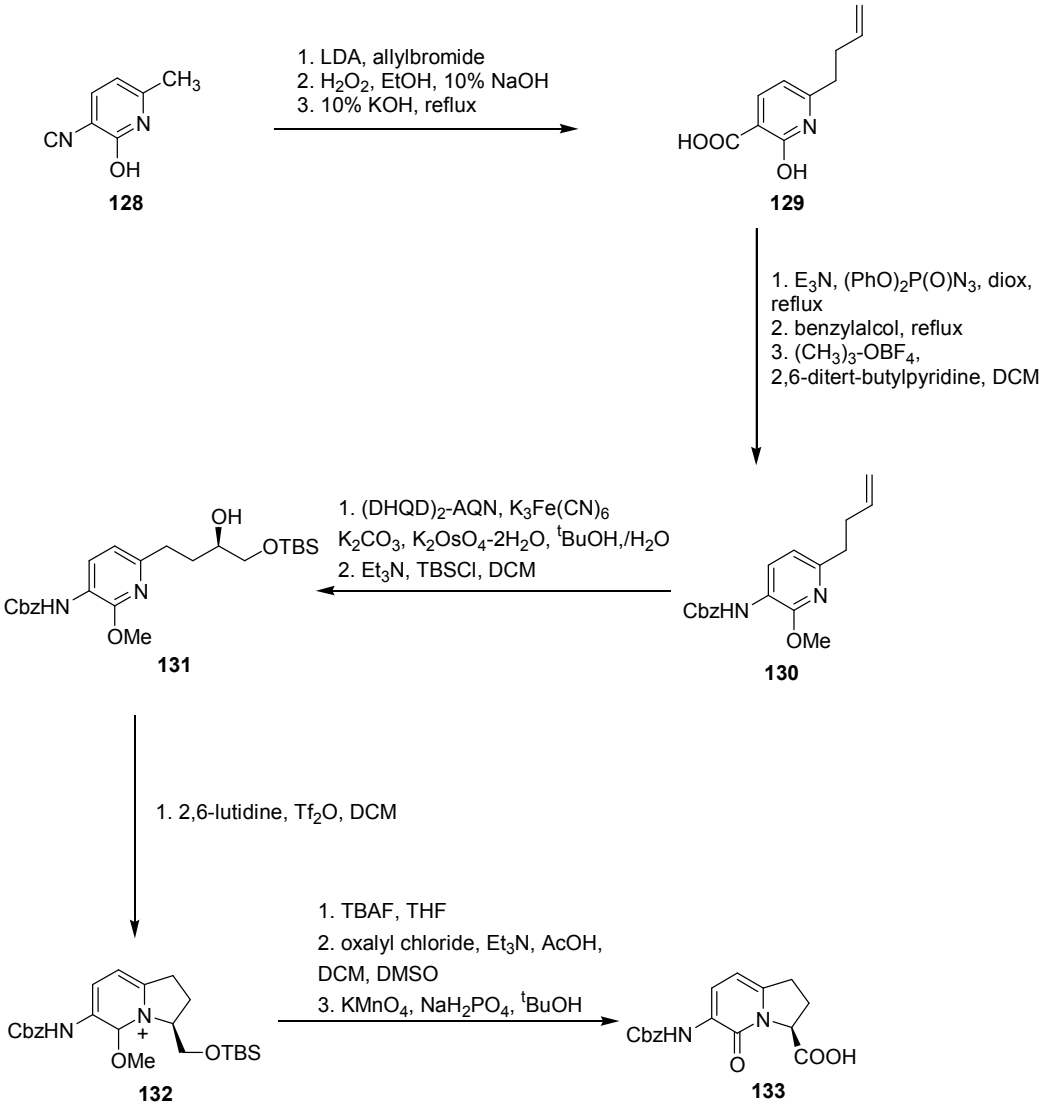

Figure 30: polyunsaturated scaffold by Dragovich et al.

A polyunsaturated scaffold was synthesized by Dragovich et al.[45] in 2002. Cyclisation of pyridine derivative **131** by treatment with an excess of trifluoromethanesulfonic triflate anhydride in the presence of 2,6-lutidine give the pyridium salt **132**. Simultaneous O-demethylation and desilylation by exposure to tetrabutylammonium fluoride followed by a double step oxidation of the hydroxyl function give the desired δ-amino acid **133** (figure 30).

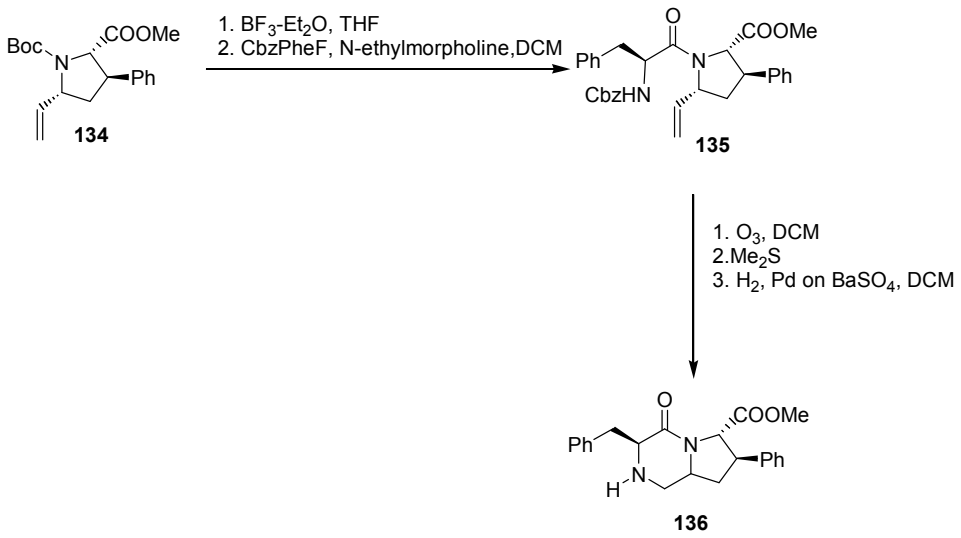

Figure 31: route for diazabicycloalkane by Tong et al.

Often, the free amino function was directly incorporated on the ring.[46] The proline derivative **134** (figure 31) was coupled , after deprotection of the Boc group, with the fluoride acid derivative of the Cbz-protected phenylalanine. The vinyl group of **135** was oxidized using an ozonolysis reaction, which bring, after the reductive workup with dimethyl sulfide, to a spontaneous cyclisation to form a six-membered ring hemiaminal. Reduction with hydrogen in the presence of a catalityc amount of Palladium on Barium sulfate give the desired peptidomimetic **136**.

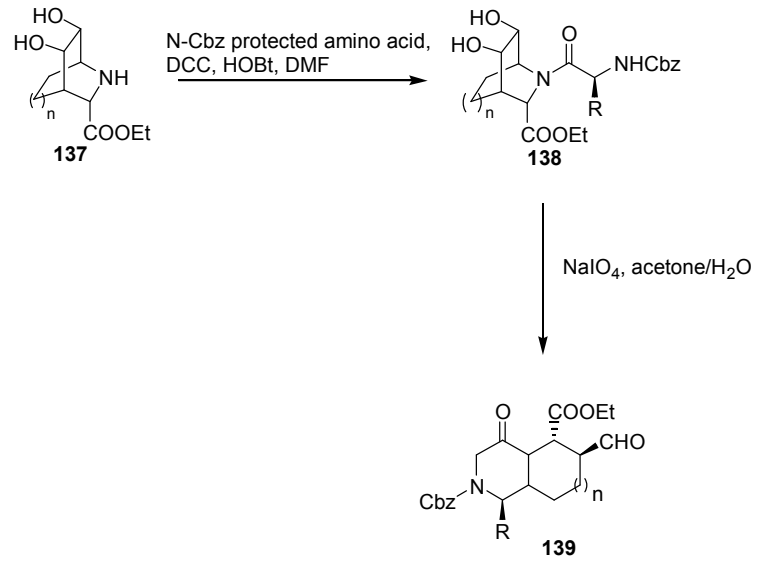

Figure 32: route for diazabicycloalkane by Maison et al.

In 2004 Maison et al.[47] proposed a short synthesis of a number of diazabicycloalkane as useful mimetics of dipeptide. Compound **137** (figure 32) was obtained by an aza-Diels-Alder condensation and then coupled with different natural amino acids to give a small library of molecules **138**. Oxidative cleavage of this compound followed by a spontaneous cyclisation give the desired compound **139** which can further functionalized in few steps.

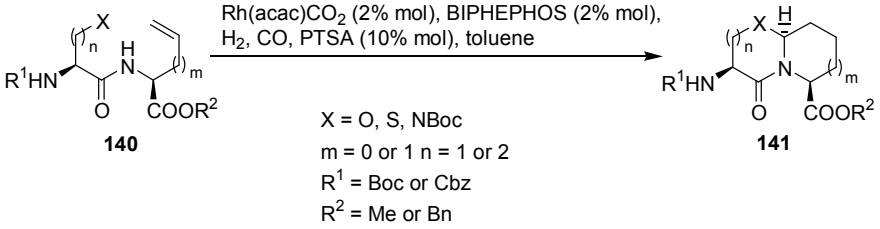

Figure 33: one step synthesis of bicyclic amino acids by Chiou et al.

Chiou et al.[48] proposed a versatile one step synthesis of diaza- or oxoazabicycloalkane trough a Rhodium catalyzed cyclohydrocarbonylation that induces a cascade double cyclisation with an extremely high regio- and stereoselectivity (figure 33).

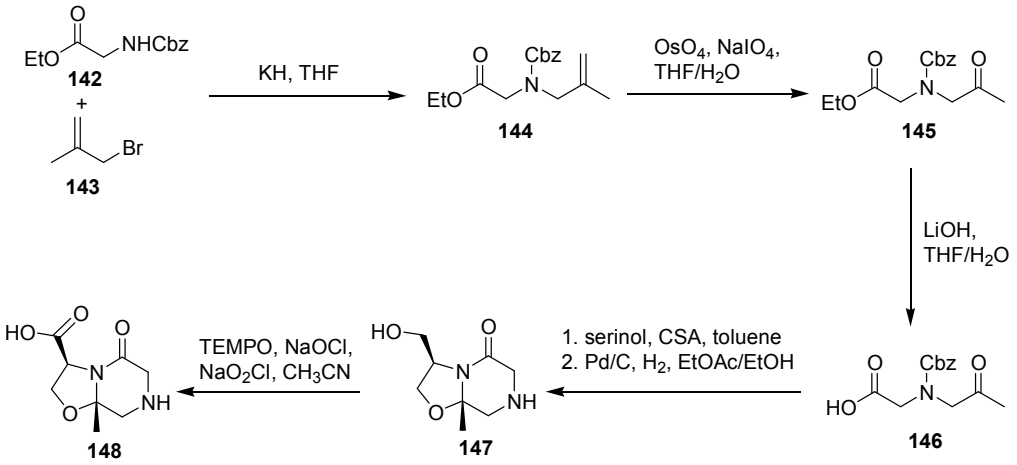

Figure 34: synthesis of oxoazabicycloalkane by Bencsik et al.

Another way to oxoazabicycloalkane δ-amino acid was adopted by Bencsik et al.[49] through the condensation of 3-aza-1,5-ketoacids **146** with the racemic serinol (figure 34) followed by a TEMPO oxidation of the hydroxyl function.

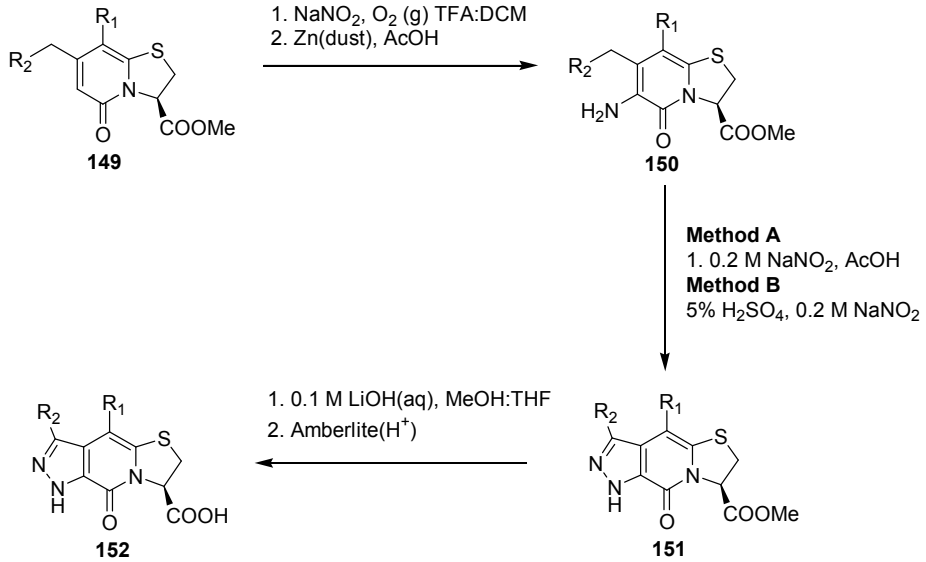

Figure 35

Recently,[50] Sellstedt et al. synthesized the new δ-bicyclic amino ester **150** by a regioselective nitration of the thioazabicycloalkane **149** followed by reduction of the nitro group. diazotation of aminofunctionalized 2-pyridones followed by the hydrolisation of the methyl ester brings to the very rigid ring-fused pyrazole-pyridone scaffold **152** (figure 35).

2.2 δ-amino acids in foldamers

Because δ-amino acids are isosteric to the α-dipeptide, one of their major applications is the introduction of them in active α-peptides to replace part of them, making the oligopeptide more stable versus the enzymatic hydrolysis. Applications as enkephalin analogues[34, 51-54], human -secretase inhibitors[55-59] have been reported. The great interest in this field is also demonstrated by the synthesis of the very potent non peptidic renin inhibitor Aliskiren®[60] from Novartis which has received the approval of the U.S. Food and Drug Administration for the treatment of hypertension. In most of the cases, δ-amino acids are not placed in a part of the peptide highly involved in the formation of the secondary structure, but their role is limited to avoid the enzymatic cleavage.

Nevertheless, δ-amino acids have a great potential for secondary structures induction for the same reasons as they have been used in inhibitors: their backbone mimics α-dipeptides and they may offer folding properties similar to the α-peptides. Hofmann et al. calculated the possible secondary structures that could be adopted by δ-amino acids.[61] The calculations revealed that homopeptides of δ-amino acids could adopt a large variety of helical structures presenting 8-, 10-, 14-, 16-, 20- and 22-membered rings closed by hydrogen bonding. In addition, δ-amino acids can induce β-turns, especially cyclic ones which confirmed the importance of a rigid conformation to stabilise secondary structures.

It exists many examples of δ-amino acids used to induce a secondary structure. A first example was proposed by Gellman et al. which prepared the dipeptide isostere **153** and investigated his ability to induce a secondary structure preparing the protected monomer **154** and the tripeptide

155[62] (Figure 36). NMR and IR in solution studies showed the presence for both of a β-hairpin conformation due to the presence of a ten-membered ring formed by the strong intramolecular hydrogen bond in the molecule **154**. Same behaviour was obtained[63] studying other tetrasubstituted alkenes isosteres. It was explained that the hairpin structures are stabilised by the avoidance of allylic strain compared to the non substituted one which exhibited less stable structures.

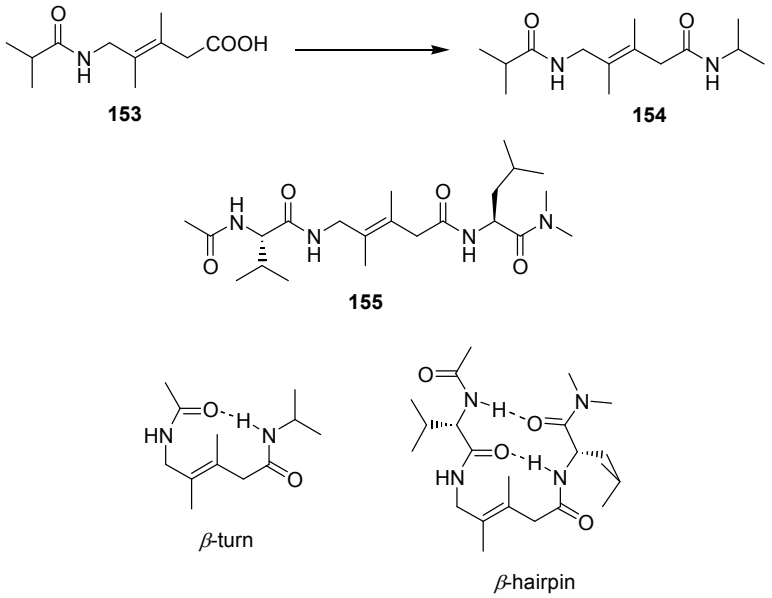

Figure 36

A folded δ-peptide based on ornithine was proposed by Zhao et al.[64] and based his folding properties on donor-acceptor interactions (Figure 37). The peptide could adopt a zipper-featured foldamers since the secondary structure was stabilised by π-stacking between the electron-rich 1,5-dioxynaphtalene (DAN) and the electron deficient pyromellitic diimide (PDI). The peptide **156** was named zipper-featured foldamer as the appendages DAN and PDI linked to the a-NH of ornithine were arranged alternatively one between each other as in a zipper.

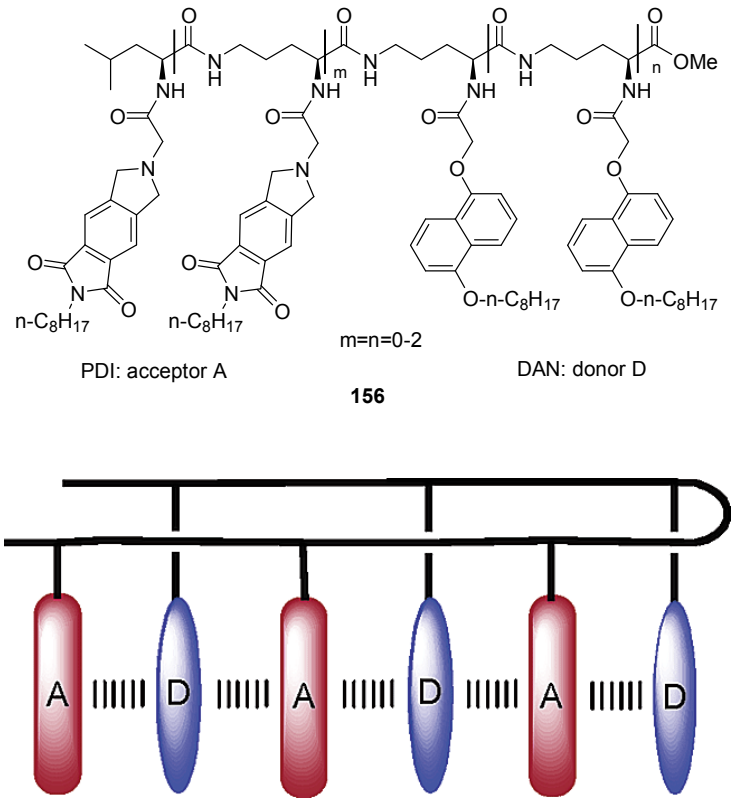

Figure 37 Figure with cordial authorisation by Prof. ZhanTing

Cyclic amino acids, in particular sugar amino acids, found a large application in the field of foldamers due to their rigid structure and the relative simple possibility to introduce different substituents due to presence of the hydroxyl groups. One of the most active groups in this field is the group of Fleet, which synthesised and study a large number of δ-amino acids with different ring size (figure 38).

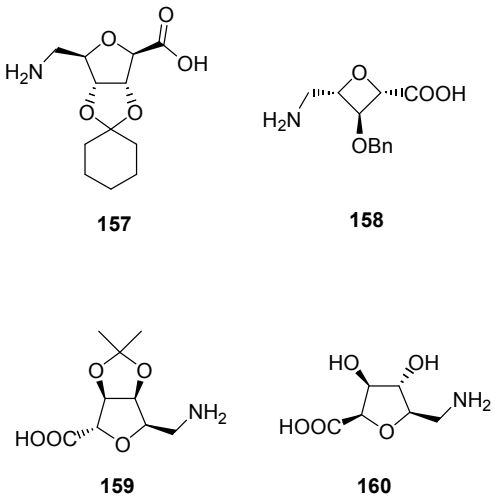

Figure 38

It has been proved that the secondary structure of these three analogous furanoid δ-amino acid is largely affected by the different substituents present on the ring. In particular, a tetramer and an octamer of the molecule **157** showed a β-turn conformation,[65] when the octamer of **159** adopts an helix with repeated 16-membered rings[66] and the tetramer of **160** a β-bend ribbon like structure,[67] as well as the hexamer of the oxetane amino acid **158**.[29]

Folded structures have been found also in the case of hetero-peptides containing series of α-δ-amino acids. One of the major examples was presented by Chakraborty et al.[68] which synthesised the short α-δ-oligopeptide **161** where was possible to observe a series of β-turns plus a nine-membered ring at the C-terminal of the peptide between an OH of the furanoid δ-amino acid and the terminal leucine (Figure 39).

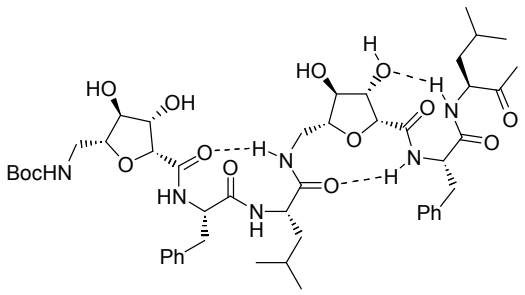

161

Figure 39

A large part of bicyclic amino acids are designed to mimic peptidic motifs of natural compounds which adopt a U-shape conformation (β and γ turns). These conformations are characterized by specific torsional and angular parameters, so the correctly positioning of the amino and the carboxylic group in the peptidomimetic is of fundamental importance. For these reasons, δ-amino acids, which are dipeptide isosteres, found a large application, in particular to replace the *i* + 1 and

i + 2 residues in β-turns systems (Figure 40). In particular, azabicyclo[X.Y.0]alkane amino acids or heteroatom analogues are particularly attractive dipeptide mimetics because their ability to adopt a conformation which can surrogate a β-turn. Additionally, it is possible easily change some characteristics of the scaffold as rigidity or solubility by inclusion of substituents in different positions, insertion of heteroatoms or other modifications affecting the ring size.

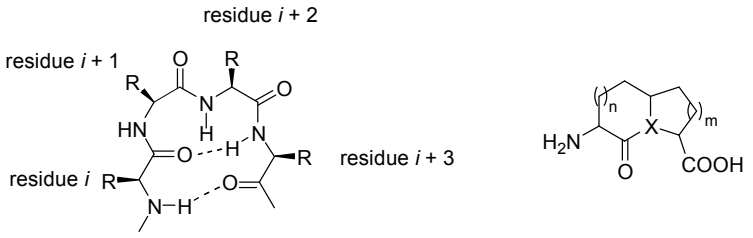

Figure 40: comparison between a β-sheet (on left) and a generic δ-bicyclic amino acid (on right)

For example, in 2003 Davies et al.[69] synthesised the azabycicloalkane **162** as rigid scaffold to induce an external β-turn GLDV motif which can be recognized by integrins.

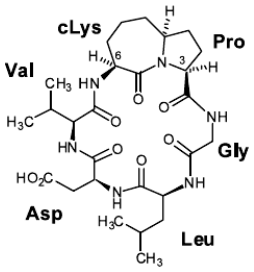

162

Figure 41

2.3 δ-amino acid in peptide nucleic acid (PNA)

Peptide nucleic acids are molecules that are hybrids or chimeras between peptides and nucleic acids. In the broadest definition PNAs are composed of a peptide bearing as lateral chain nucleobase groups. Due to the identical number of bonds (6) along the backbone of DNA, δ-amino acids found a large application in this field of research. The first PNA, based on an aminoethylglicine (Aeg) oligomer, was synthesized by Nielsen et al.[70, 71] in 1991 (Figure 42).

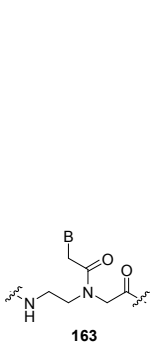

163

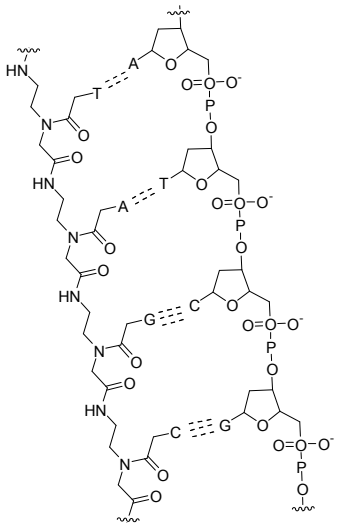

164

Figure 42 Chemical structure of the aminoethylglycine monomer **(163)** and structure of the Aeg-PNA compared to DNA **(164)**

This very simple structure and his interesting applications in the DNA recognition inspired many research's groups to synthesised analogues and derivatives in order to understand and/or improve the properties of this new class of DNA mimics. In particular, many efforts have been done to introduce elements of chirality or to rigidify the structure with cyclic amino acids. Because is not in the aim of this work to be a review about PNA, this part treats in particular the synthesis and the structure of the δ-amino acid scaffolds used in this field without investigate the interactions of PNA with DNA or RNA. To investigate these and other parts which are not exhaustively treated in this paper, many reviews about PNA can be consulted.[72-74]

2.3.1 PNA based on aminoethylglicine

Many synthetic ways have been reported for the synthesis of this PNA.
The preparation of the monomer can be divide in the synthesis of a suitable N-protected aminoethylglicine backbone, which will then acylated with a nucleobase acetic acid derivative. Three different synthetic routes have been employed to aminoethylglicine. First is the alkylation of diaminoethane by an α-halogenated carboxylic acid (figure 43).

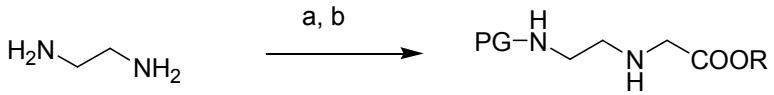

165 **166**

PG	R	A	B	Ref.
Boc	Me	1 $ClCH_2COOH$ 2 MeOH, HCl	Boc_2O, diox/H_2O	Heimer et al. 1984[75]
Fmoc	t-But	$ClCH_2COOtBut$, Et3N, DCM	FmocOSu, DIEA	Thomson et al. 1995[76]
Mmt	Et	1 $ClCH_2COOH$ 2 EtOH, HCl	Mmt-Cl, Et_3N, DCM	Stetsenko et al. 1996[77]

Boc	t-But	Boc_2O, Et_3N, DCM	$ClCH_2COOtBut$, Et_3N, DCM	Breipohl et al. 1997[78]
Boc	Me	Boc_2O, DCM	1 $ClCH_2COOMe$	Kofoed et al. 2001[79]
Dde	Me	1 $ClCH_2COOH$ 2 MeOH, $SOCl_2$	Dde-OH, DIPEA, DCM/EtOH	Bialy et al. 2005[80]
Fmoc	Allyl	1 $ClCH_2COOH$ 2 Allyl-OH	FmocOSu, DIEA	Hudson et al. 2005[81]
NVOC	t-But	1 $BrCH_2COOt$-But	NVOC-Cl, DIEA	Liu et al. 2005[82]
Bts	Et	1 $ClCH_2COOH$ 2 EtOH, HCl	Bts-Cl, Et_3N, DCM	Lee et al. 2007[83]
Boc	Et	Boc_2O, THF	$BrCH_2COOEt$, Et_3N	Vysabhattar et al. 2008 [84]
Fmoc	Benzyl	1 $ClCH_2COOH$ 2 BenzylOH, TsOH, Tolune	FmocOSu, DIPEA	Wojciechowski et al. 2008[85]
Fmoc	Allyl	1 $ClCH_2COOH$ 2 AllylOH, TsOH, Benzene	FmocOSu, DIPEA	Wojciechowski et al. 2008[85]
Fmoc	p-nitrobenzyl	1 $ClCH_2COOH$ 2 p-nitrobenzylOH, TsOH, Toluene	FmocOSu, DIPEA	Wojciechowski et al. 2008[85]

Figure 43 Aminoethylglicine backbone by alkylation of diaminoethane

Second route is the reductive amination of a N-protected aminoacetaldehyde with glicine esters (figure 44).

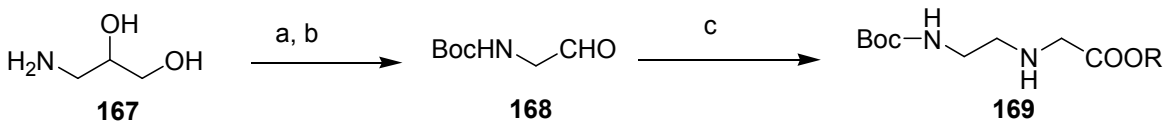

167 **168** **169**

R	a	b	C	Ref.
Me	Boc_2O, NaOH, H_2O	KIO_4, H_20	$H_2NCH_2COOMe.HCl$, NaOAc, H_2, Pd/C	Dueholm et al. 1993[86]
Et	Boc_2O, NaOH, H_2O	KIO_4, H_20	$H_2NCH_2COOMe.HCl$, NaOAc, H_2, Pd/C	Dueholm et al. 1993[86]
Et	Boc_2O, NaOH, H_2O	$NaIO_4$, H_20	$H_2NCH_2COOMe.HCl$, $NaBCNH_3$, MeOH	Finn et al. 1996[87]

Figure 44 synthesis of Boc Aeg derivative by reductive amination of aminoacetaldehyde with glicine esters

Third route is a reductive amination using 1,2-diaminoethane and glyoxylic acid (figure 45)

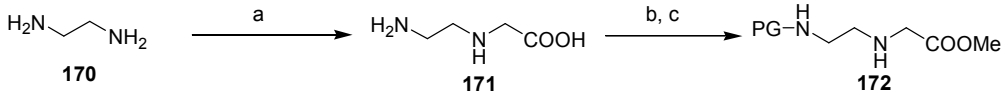

170 171 172

PG	a	b	C	Ref.
Mmt	glyoxylic acid, H_2, Pd/C, MeOH	MeOH, HCl	Mmt-cl, DMF, Et_3N	Will et al. 1995[88]
Fmoc	glyoxylic acid, H_2, Pd/C, MeOH	MeOH, HCl	FmocOSu, dioxane, H_2O	Breipohl et al. 1996[89]

Figure 45 Synthesis of Aeg derivatives by reductive amination of 1,2-diaminoethane and glyoxylic acid

The second step of the synthesis is then the coupling of the secondary not protected amide with a nucleobase acetic acid derivative. In figure 46 is showed as example the synthesis of the thymine acetic acid derivative and his coupling with the aminoethyl glycine backbone. The same strategy can be adopted to couple the other nucleobases, but in this case an additional protection/deprotection step of the free amino function is necessary.

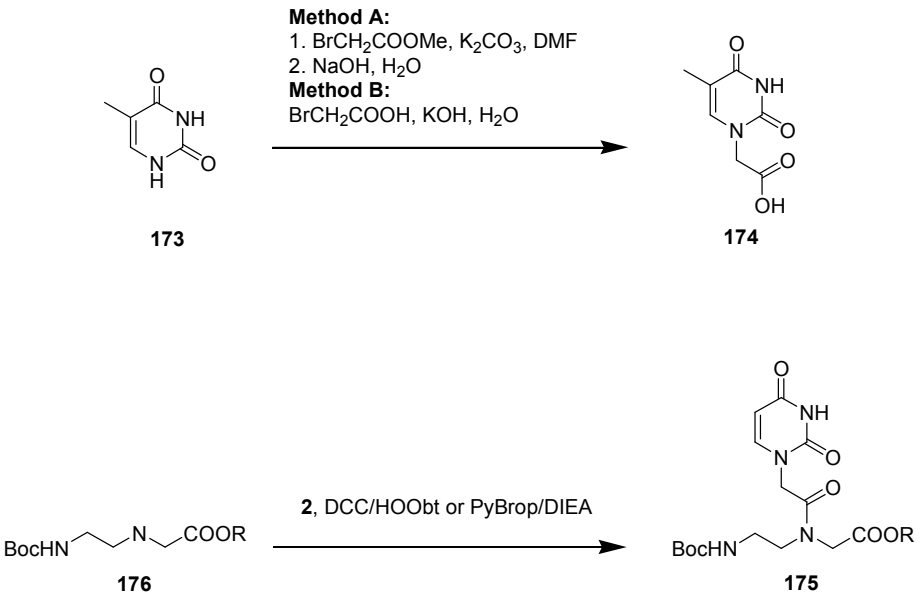

Figure 46 Synthesis of acetic acid thymine derivative and his coupling with the Aeg backbone

2.3.2 Linear analogues of Aeg-PNA

A large variety of linear analogues of Aeg-PNA have been synthesised. First attempts were done by the same group to investigate the change of the affinity with the DNA just replacing the lateral chain bearing the nucleobase, for example adding one bond[90] or by alkylation of the free amino group with an halogeno alkane[91] (**167** and **168**, figure 47). Additionally, because the central nitrogen is not involved in an hydrogen bond, a PNA with a different position of the nitrogen (retro-inverso PNA, **169**) was synthesised.[92-94]

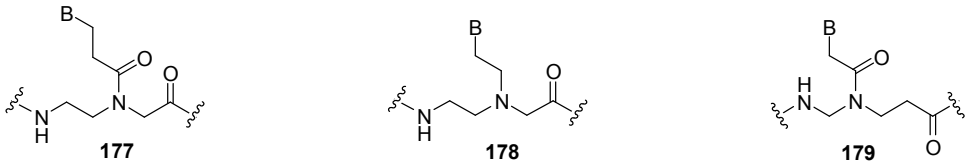

Figure 47 Other PNA by Nilsen's group

Elements of chirality can be simply introduced in the scaffold by replacing the glycine with other amino acids (figure 48), for example using the L or D lysine (**180**).[95] Recently, Balaji et al.[96] proposed a versatile solid phase synthesis to give PNA containing different lateral chains (**181**). Additionally, Ganesh et al.[97] described a dimethyl substitution in the same position (**182**) to introduce a conformational rigidity into backbone and to pre-organized the PNA backbone to attempt selective hybridisation properties.

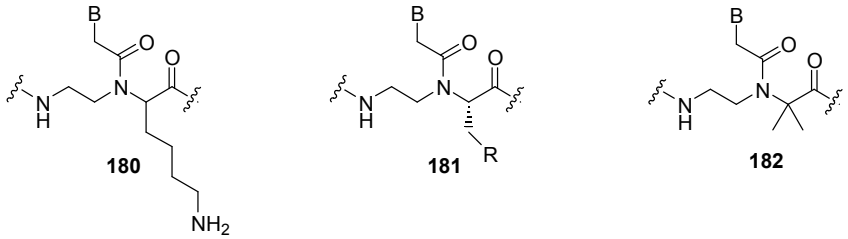

Figure 48 Chiral PNA where the glicine was substituted with other amino acids

The possibility of a functionalisation of the ε position (figure 49) was also explored. Introduction of a methyl (**183**)[98] or of an amino function (**184**)[99, 100] has been done by a variant of the synthesis of AegPNA described previously in this chapter (figure 44) starting respectively from N-protected L-alanine aldehyde and L-lysine aldehyde instead of the glicine aldehyde. Of particular interest is the presence of the free amino group in the molecule **184**, which not only allows to solve the problem of the poor aqueous solubility of PNA, without affecting the affinity to the DNA, but is also a group suitable of further modifications.

Figure 49 ε-functionalised PNA

In 1997 by Altmann et al.[101] proposed a new PNA scaffold which was readily available in few steps starting from L-serine or L-homoserine (figure 50, **185** and **186**). Most important difference with the Aeg-PNA is the presence of an oxygen at the place of the central nitrogen and the subsequent change of the position of the lateral chain bearing the nucleobase.

Figure 50 Serinol PNAs synthesised by Altmann et al.

In order to investigate the effect of the pre-organisation of the monomeric PNA unit in either the trans and the cis form of the amide bond, analogues E-OPA (**193**) and Z-OPA (**194**), in which the central amide bond was replace by a configurationally defined double bond, have been synthesised.[102, 103] Unfortunately, the too rigid structure has a result a decrease of the affinity to DNA in both the case (figure 51).

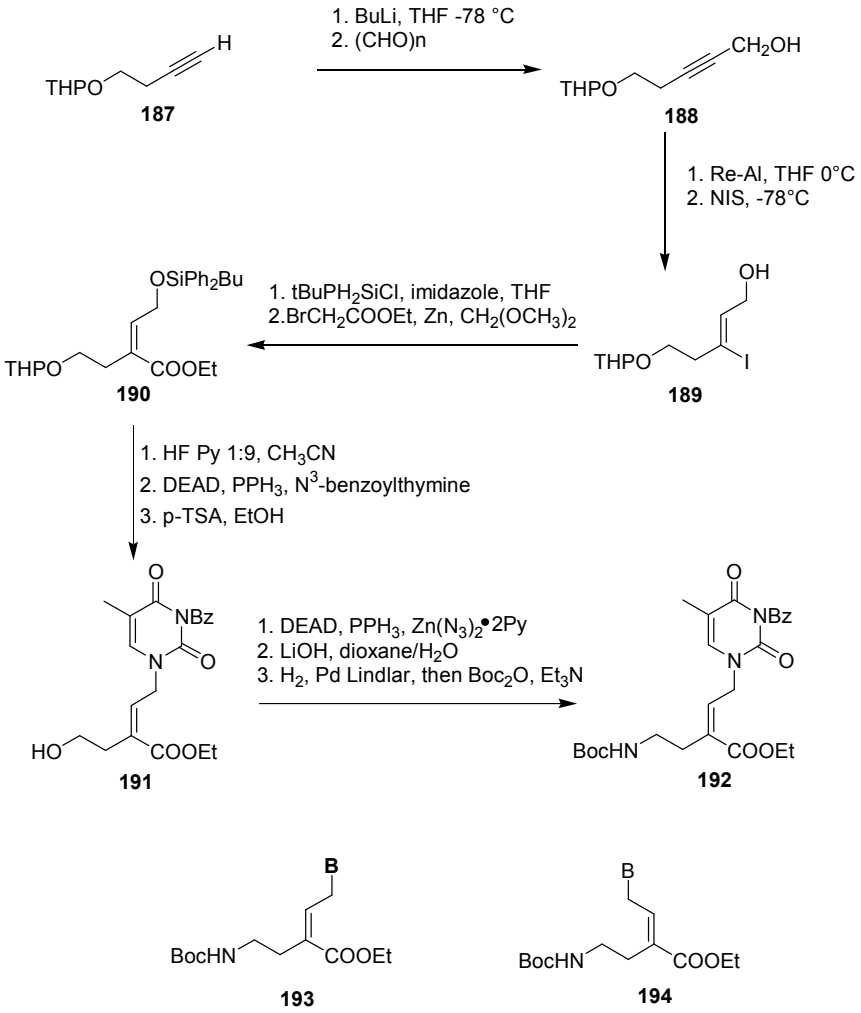

Figure 51 synthesis of the Z-OPA bearing the thymine as nucleobase and general structure of E and Z-OPA

In 1997, Bergmeier et Fundy developed a synthesis of a very flexible PNA based on an aminopentanethyl linker,[104] which was obtained starting from δ-valerolactam in few steps (figure 52).

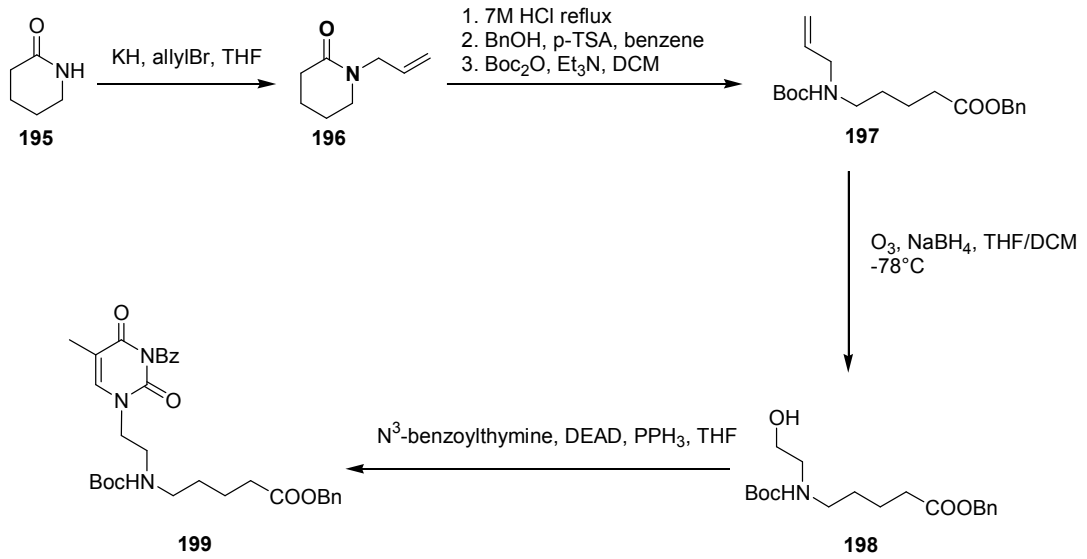

Figure 52 Synthesis of aminopentanethyl-PNA

2.3.3 Cyclic PNAs

The main difference about linear PNAs and DNA is the major flexibility of the firsts comparing with the phosphodiester ribose backbone. For this reason, in the aim to improve the stability of PNA-DNA or PNA-RNA complex, an adequate restriction of the flexibility can be an interesting strategy. This has led to the synthesis of a large series of conformationally constrained cyclic PNA. Particular success had the synthesis of the aminoethylprolil PNA (Aep-PNA), which is one of the few structure able to significantly stabilize the DNA-PNA interaction.[105, 106] Aep-PNA was synthesised in few steps starting from natural (2S,4S)-4-hydroxyproline (figure 53).

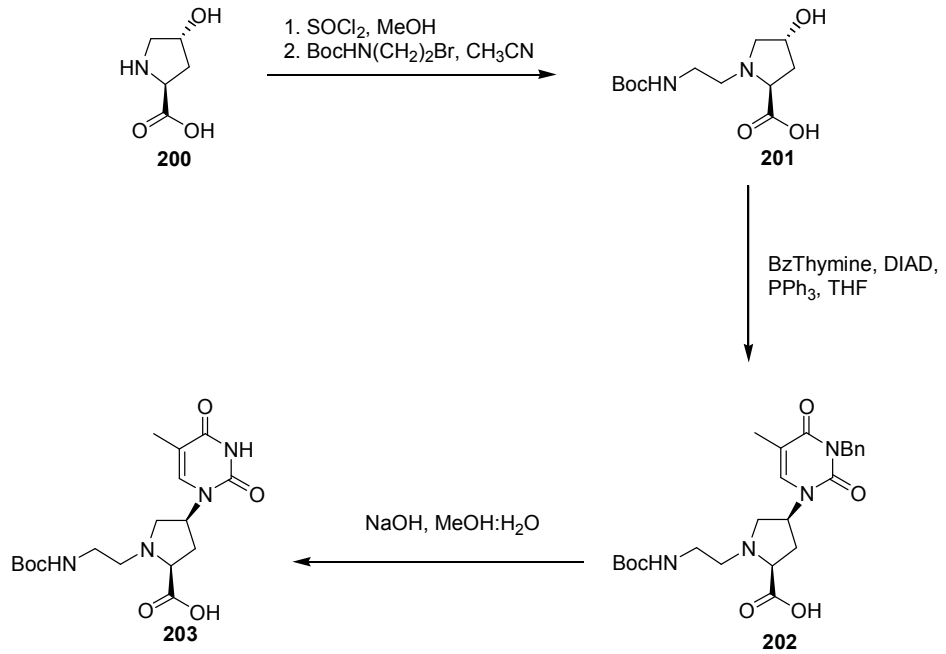

Figure 53 Synthesis of Aep-PNA

From the same starting material, a pyrrolidine-PNA[107] was also synthesised (figure 54).

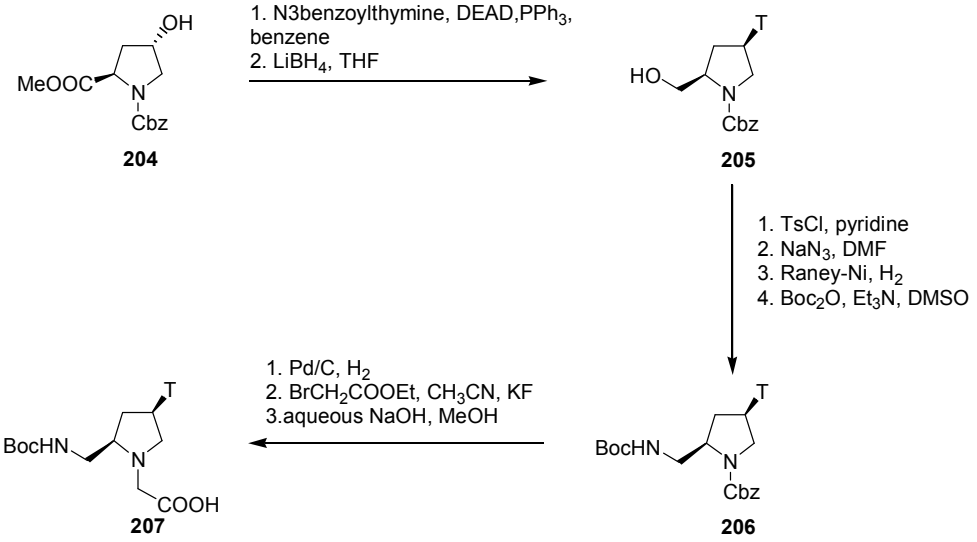

Figure 54 Synthetic route for pyrrolidone-PNA by Kumar et al.

In order to further rigidify the structure of the Aep-PNA a selective oxidation of the C5 carbon has been performed.[108] This modification brings to the aminoethylpyrrolidinone-PNA (Aepone-PNA, figure 55). The tetrahedral nature of pyrrolidine nitrogen in Aep-PNA is switched to the planar amide in Aepone-PNA, as in unmodified PNA, with a consequent influence on the backbone conformation. Unfortunately, the affinity to DNA is lower than Aep-PNA, but more than Nielsen's Aeg-PNA.

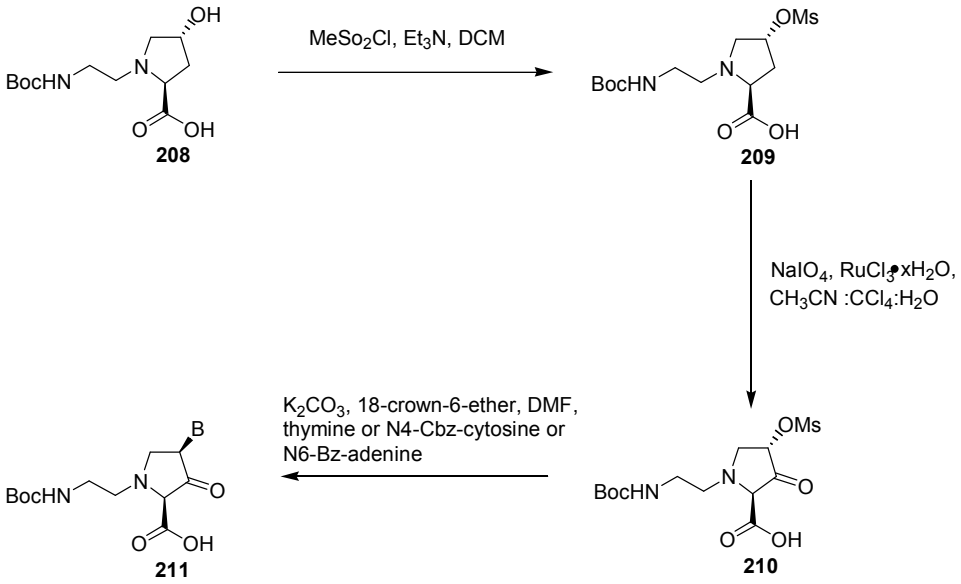

Figure 55 Synthesis of Aepone-PNA by Sharma et al.

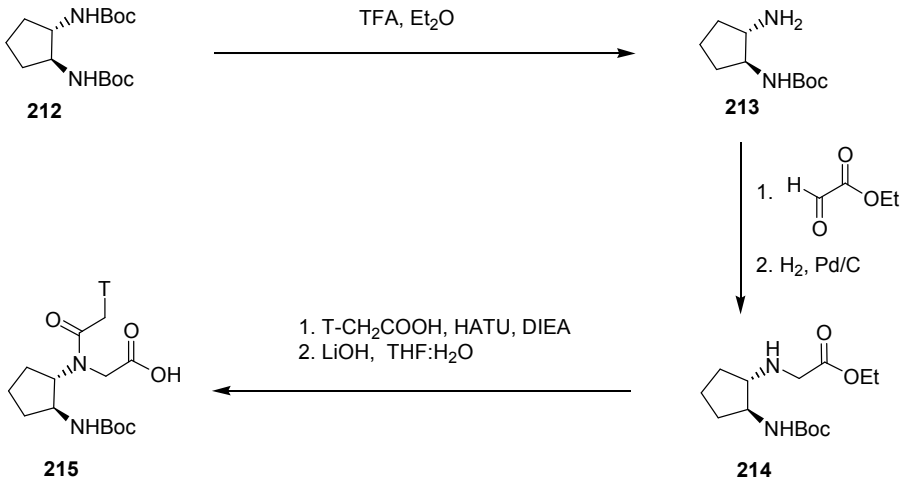

Figure 56 Synthetic route of cyclopentane-PNA by Myers et al.

A cyclopentane conformational restraint PNA was also synthesized.[109] The single deprotection of the di-amine **212** (figure 56) was performed in moderate yield by treatment with just 1 equivalent of tri-fluoroacetic acid. Reductive amination of the free amino group with ethylglyoxalate give the δ-amino ester **214**, which was then alkylated by the acetic acid thymine derivative, to give, after hydrolisation of the ethyl ester, the desired PNA **215**.

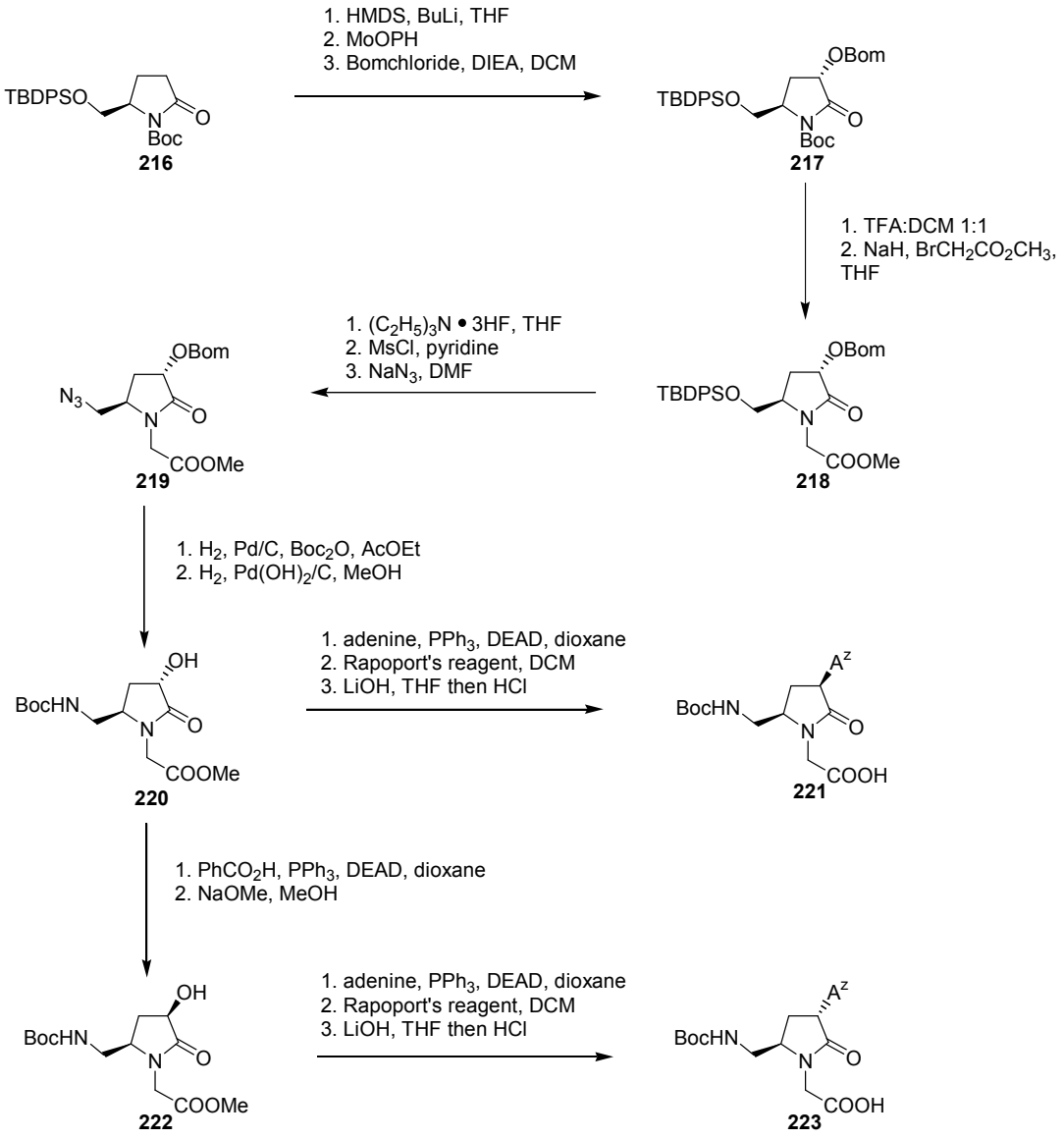

Figure 57 Synthesis of Aepone-PNA by Püschl et al.

Another way to Aepone-PNA was presented also by Püschl et al.[110] in 2001 which synthesised the 2 different diastereomers (3R,5R) and (3S,5R) containing adenine as nucleobase (scheme 17). Moreover, starting from the enantiomer of compound **216** the (3R, 5S) and (3S, 5S) monomers have been obtained (figure 57). With the same strathegy,[110] but starting from the 6-membered ring (6*R*)-6-(*tert*-butyldiphenylsilyloxymethyl)piperidin-2-one, the same research's group obtained the piperidinone-PNA **225** and **226** (figure 58).

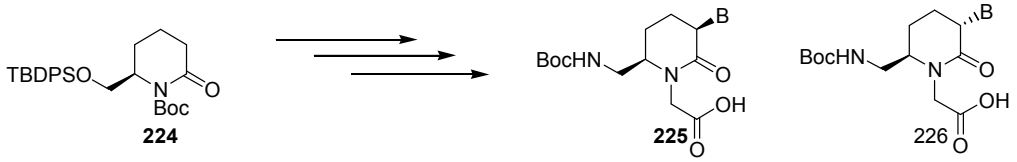

Figure 58 Piperidinone-PNA by Püschl et al.

6-membered ring δ-amino acids found less applications in the PNA's field. The principal reason is the rigidity of the chair/boat conformation compared to the more flexible 5-membered ring, which is often detrimental for the affinity to DNA or RNA. For example, aminoethylpipecolic-PNA (Aepip-PNA)[111] is one the most promising target., and was obtained in few steps starting from the cis-5(S)-hydroxy-2(S)-N1-benzyloxycarbonyl pipecolic acid methyl ester **227** (figure 59).

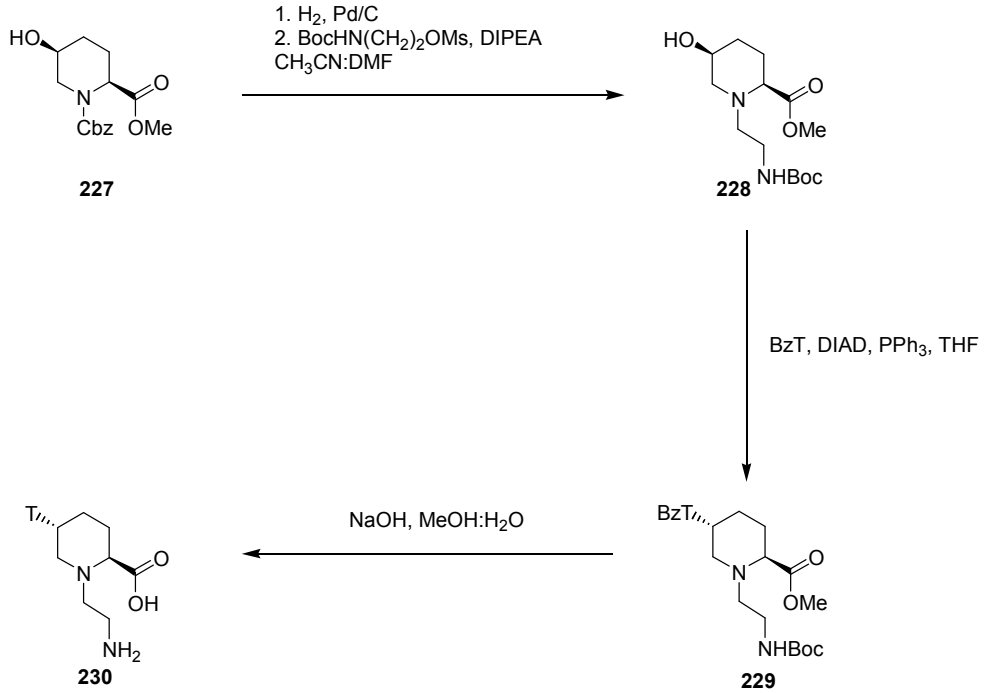

Figure 59 Synthetic route for Aepip-PNA by Shirude et al.

Less applications found the sugar-PNAs. In figure 60 is reported the synthesis of a sugar-PNA by Goodnow et al.[112, 113] Key step of the synthesis is the selective glycosylation of the nucleobase which gave as result the α-isomer with just few impurities of the β-one.

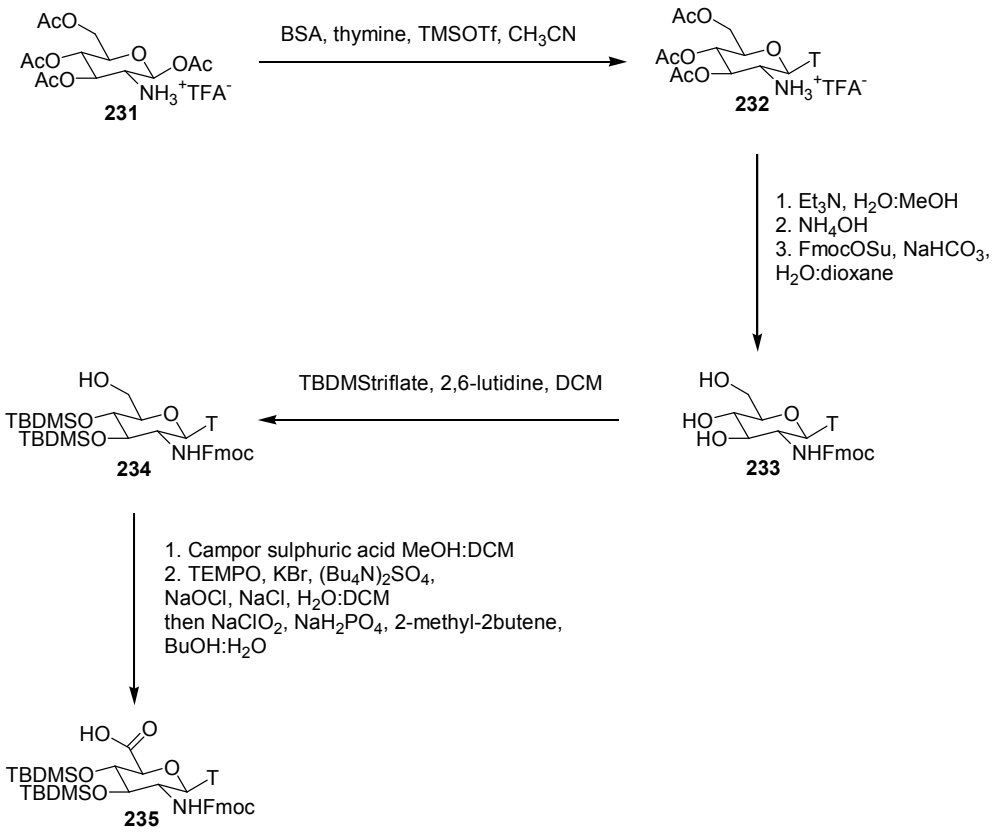

Figure 60 Synthesis of a sugar-PNA by Goodnow et al.

2.4 Synthesis of δ-amino acids

2.4.1 Aim of this work

Previously in our group, the synthesis of a novel γ-butyrolactone aldehyde δ-amino acid and a homo-tetramer based on this scaffold was performed. The CD analysis of this tetrapeptide suggested the presence of an helical conformation, but not other proof have been produced. The purpose of my work is the synthesis of the enantiomer of that δ-amino acid (**256)** and his incorporation in short α-δ-oligopeptides to study his ability to induce a secondary structure. The retrosynthetic scheme is shown in the figure 61. The δ-amino acid can be obtained starting from the asymmetric cyclopropanation developed in our group. The cyclopropanated compound **237** is then submitted to ozonolysis and Sakurai allylation affording a chiral allylated cyclopropane alcohol. This compound can be lactonised very easily to form the corresponding χ-butyrolactonaldehyde **249** on which is added a nitrogen moiety by reductive amination. After Boc protection, PMB cleavage and oxidation can be obtained the δ-amino acid **256** ready for peptide coupling.

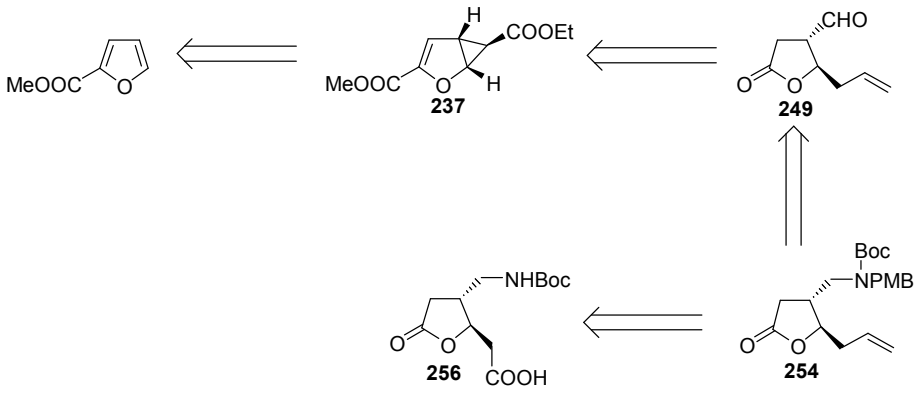

Figure 61

2.4.2 Cyclopropanation

Due to the structural rigidity of the ring and their present in a large series of natural compound, substituted cyclopropanes have been widely employed in the organic synthesis.[22-27] In our lab, it was developed a regio and enantioselective cyclopropanation[114] of the 2-furanoic acid methyl ester **236** (figure 62) with the ethyl diazoacetate in the presence of a catalytic amount of cupper triflate, the R,R bis-oxazoline ligand **241** (its synthesis is showed in figure 63)[115] and the phenylhydrazine. The bis-oxazoline, complexed to the copper carbene, allows the approach of the substrate only by the less hindered double bond. Then, the positioning of the substrate is controlled by the steric hindrance of the isopropyl groups of the bis-oxazoline ligand and the cyclopropanation of the double bond is then directed almost only on one face of the substrate. The enanctioselectivity of the reaction, measured by chiral phase HPLC, is of 94% and it can improved to up of 99% by a single crystallisation in dichloromethane-pentane at low temperature (-27°C).

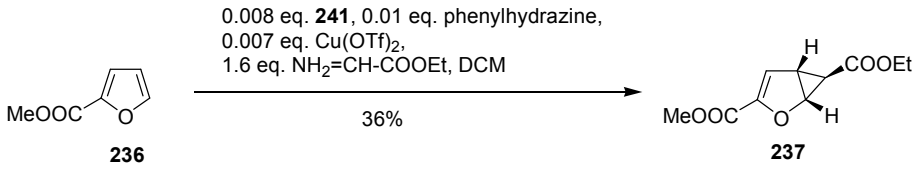

Figure 62

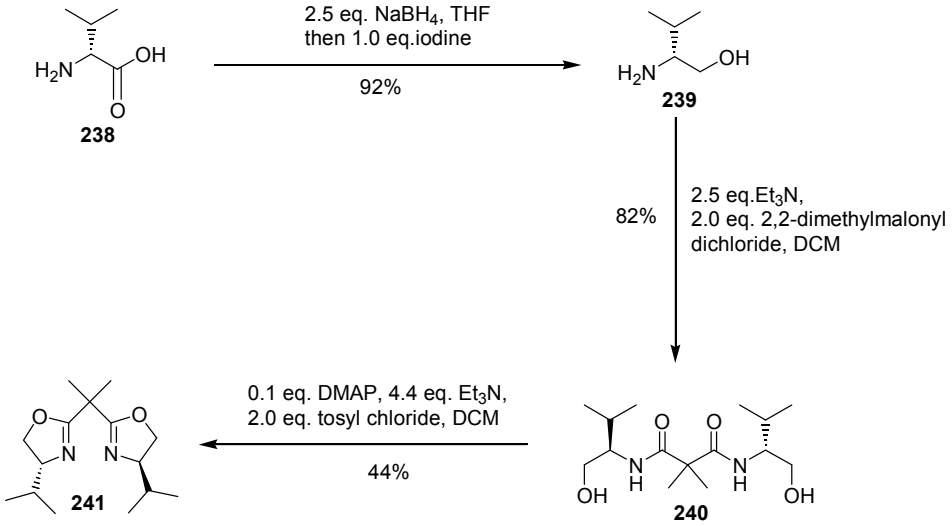

Figure 63

2.4.3 Ozonolysis

Second step of the synthesis is the ozonolysis of the compound **237** to give the cyclopropane aldehyde **242**. The ozone was gurgled in a dichloromethane solution of **237** until the colour of the solution turned to blue, indicating a presence of an excess of ozone. The solution was then purged by oxygen for 5 minutes and successively reacted overnight in presence of an excess of dimethyl sulphide to avoid the oxidation of the aldehyde to carboxylic acid. A simple extraction afforded the desired product in an excellent yield.

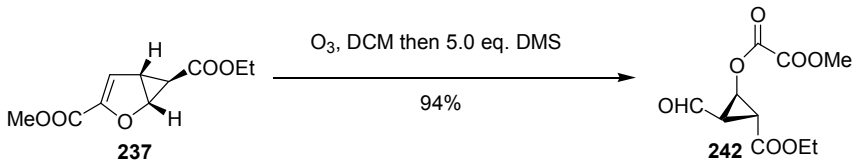

Figure 64

2.4.4 Sakurai allylation

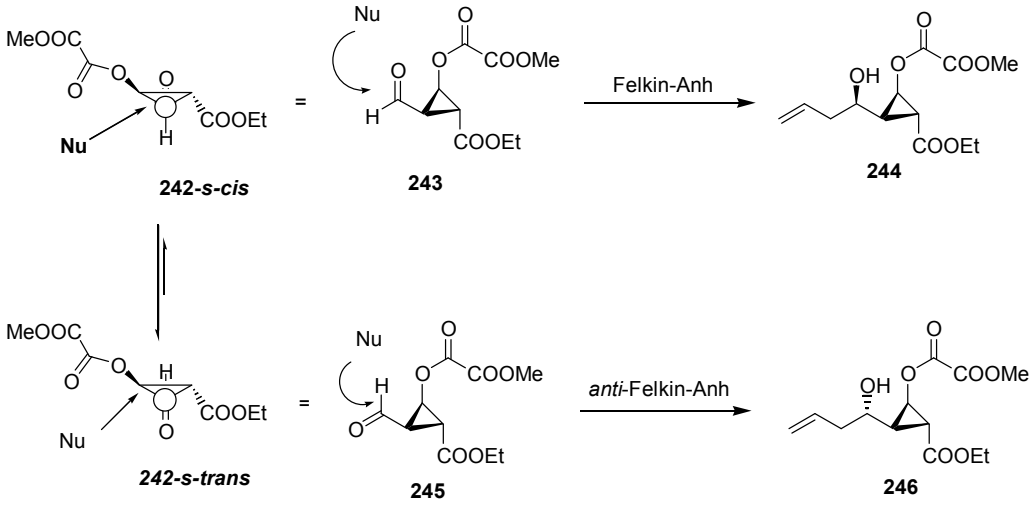

Figure 65

The stereoselectivity of addition of nucleophiles to α-chiral carbonyl compound was first postulated by Cram[116] and its mechanism was improved by Felkin and Anh.[117, 118] For

stereoelectronic reasons, cyclopropyl-substituted carbonyl compounds are more stable in bisected conformations. In our case, two bisected conformations are possible: *s-cis* and *s-trans*. The *s-trans* conformation should be favoured because of steric interactions and the anti-Felkin-Anh product **246** should be obtained. But in fact it was obtained the Felkin-Anh product **244** and some interactions specific should explain the higher stability of the *s-cis* compound in our case. The reaction of **242** with $BF_3 \bullet Et_2O$ and allytrimethylsilane afforded quantitatively the allylated cyclopropane alcohol **244** in a 95/5 ratio (Scheme 47).

2.4.5 Retroaldol lactonisation

The cyclopropane compound **244** presents many interesting features for further synthetic transformations. The free OH group is located in γ-position relatively to the ethyl ester and the cyclopropyl-methyl oxalic diester should saponify easily under basic conditions. The retro-aldol lactonisation (figure 66, pathway a) can be realised with barium hydroxide in methanol affording the γ-butyrolactonaldehyde **249** in good yields (60%) with the same excellent diastereoisomeric ratio as the starting material. The problem relied to this protocol are the difficult purification, in particular the very tedious removal of the barium hydroxide, and the dramatic drop of the yield when the reaction was performed in high scale (up to 1 gram). To avoid these problems, other different base have been employed. First attempt was done with a strong basic Dowex resin in methanol, which allows to improved the yield to 70% (also in gram scales reaction) and to simplify the work-up. The resin could be then simply filtrated and reused for a further reaction after reactivation by treatment with aqueous sodium hydroxide. The problem of this procedure was a progressive decrease of the resin activity after several utilisations, which makes this protocol inapplicable for economical reasons. During the tests of this protocol, it was possible to observe by TLC the formation of an unknown product which was not present in the reactions carry out with the most reactive barium hydroxide. Of particular interest, the fact that collecting this product and reacting them in the same conditions with other strong basic Dowex resin, it was possible to obtain a further amount of the lactone **249**. This observation clearly indicates as the unknown product should be an intermediate of the lactonisation reaction. The unknown compound could be purified and fully characterised by 2D-NMR. It resulted from the

rearrangement of the starting material to an acetal in a diasteromeric ratio of 80/20 of the anomeric carbon (**251**). This suggested a new mechanism of the reaction (pathway b, figure 42). A last protocol was done employing organic amines, in particular triethyl amine, in methanol. It resulted in a very simple protocol (after the reaction it was enough evaporated the solvent and do directly the column), and it was possible to have a good yield (up to 70%) also in a 30 grams scale reaction. Also in this case, it was recovered the intermediate **251**, which could reacted in the same conditions to give a further amount of the lactone **249**. It is interesting to mark that it was not possible to obtain a full conversion of the compound **251** to the lactone **249**, which probably indicates the presence of an equilibrium between the two products.

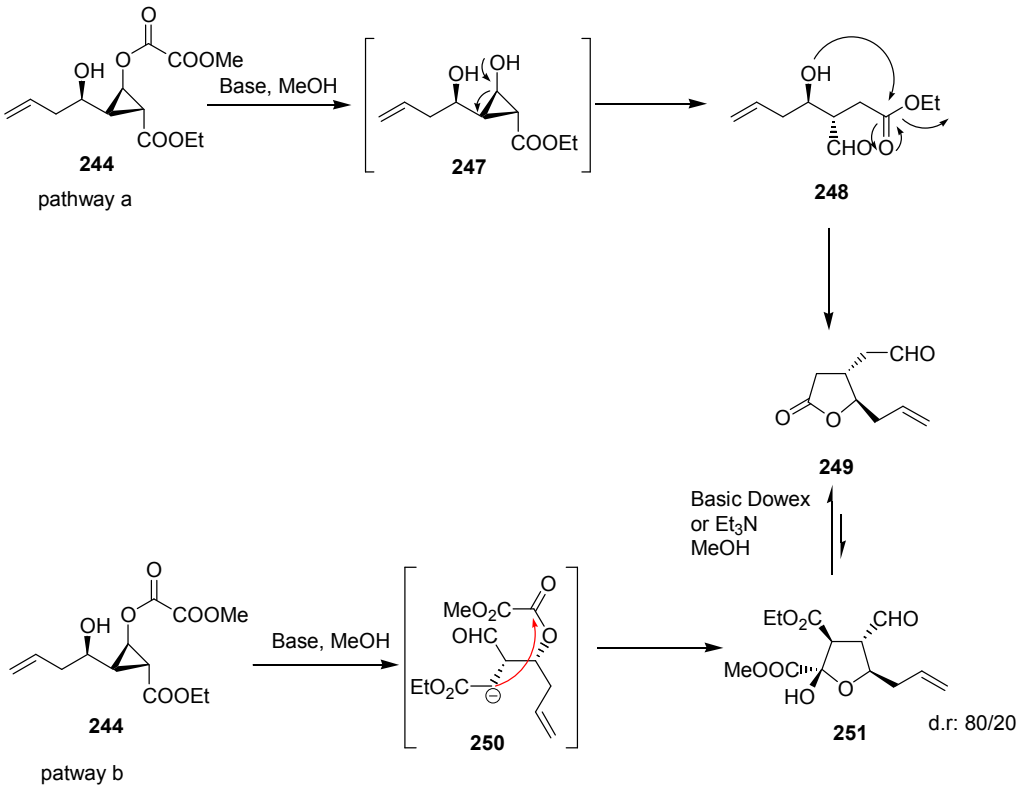

Figure 66

2.4.6 Introduction of the nitrogen moiety

The nitrogen moiety was introduce by a reductive amination of the aldehyde. The mechanism of the reaction consist in a first time in the formation of an imine intermediate which can be then

reducted to amine with different reductive agents as sodium borohydride,[119] $NaBCNH_3$[120], by catalytic hydrogenation[121] etc... This reaction is usually performed in methanol because a source of proton is necessary to complete the reduction. Moreover, the imination step release a molecule of water, for this reason the presence of a drying agent, such as molecular sieves or sodium sulphate, can push the equilibrium to the product. The reductive amination was initially performed with the benzylamine, but the successive cleavage by catalytic hydrogenation of the benzyl group resulted in a very low yield. For this reason, it was decide to use the para-methoxy benzyl amine, which can be cleaved by an oxidative treatment with cerium ammonium nitrate[122] or TEMPO. It was quite hard to find good experimental condition for this reaction, in particular due to two different problems. The first problem was the presence of a parasite lactamisation reaction (figure 54), which was solved by a short reduction time (5-10 minutes at 0°C) and performing the reaction in a dichloromethane-methanol mixture instead of in pure methanol. Second problem was relied to the low stability of the unprotected amine **252** in contact with the silica gel. This problem was overcome by an acidic extraction of the amine **252** by 1M hydrochloric acid, followed by basification of the aqueous phase with solid sodium bicarbonate and re-extraction with dichloromethane. This protocol allowed to obtain the compound **252** in a good yield with an acceptable amount of impurities (less than 5% by proton NMR).

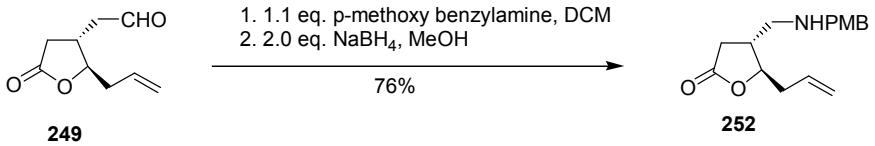

Figure 67

2.4.7 Lactamisation

Heterocycles are among the most important structural classes of chemical substances and are particularly well-represented among natural products and pharmaceuticals. It is estimated that far more then 50% of the published chemical literature concerns heterocyclic structures. One striking structural feature inherent to heterocycles, which continues to be exploited to great advantage by the drug industry, lies in their ability to manifest substituents around a core scaffold in a defined three-dimensional representation, thereby allowing for far less degrees of conformational

freedom than the corresponding conceivable acyclic structures. In addition, as a result of the presence of heteroatoms such as O, N, and S, heterocycles often exhibit altered absorption, distribution, metabolism, and excretion properties. For all these reasons pyrrolidinones are very studied compounds.[123-126] and it can be then interesting develop a synthesis for the enantiomerically pure pirrolidinone **253** which was obtain as parasite product in the reductive amination of the aldehyde **249**. The imination step was then performed in methanol at room temperature for half hour, the $NaBH_4$ was then added portionwise at 0°C and, after a further half hour, the solution was heated to reflux and reacted overnight. In these conditions it was possible to obtain directly in one pot the lactame **253** in a moderate yield. The moderate yield largely depended by the presence, at the end of the reaction, of a considerable amount of the amine **252** (nearly 40%) which can be recovered and converted in a further amount of lactame.

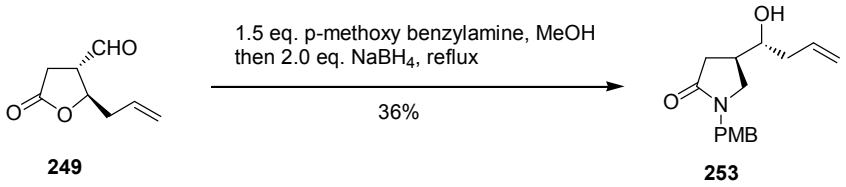

249 **253**

Figure 68

2.4.8 Boc-protection

Boc-protection of the free amino group was performed by a standard protocol by using Boc anhydride in a mixture of dioxane-1M aqueous solution of potassium carbonate with a good yield.

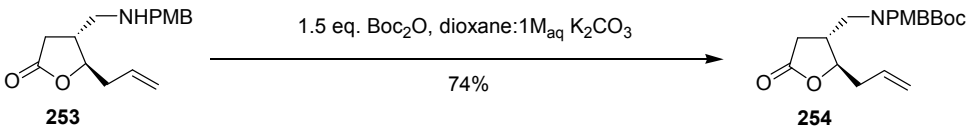

253 **254**

Figure 69

2.4.9 PMB removal by cerium ammonium nitrate

The PMB group was removed in mild condition by oxidation with cerium ammonium nitrate (CAN). As described by Yoshimura et al.[122], the yield of the reaction is very dependent by the concentration of at ammonium cerium nitrate. In particular, with a concentration of the CAN of 0.25M it was possible to obtain the desired product with a yield of 79%, when with a lower concentration as 0.05M the yield dropped to 30%.

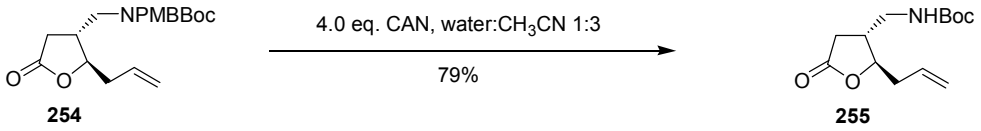

Figure 70

2.4.10 Double bond oxidation

In literature, just few example of one step oxidation of a double bond to carboxylic acid are reported. In particular, the most used protocol consists in a sodium periodate oxidation in the presence of a catalytic amount of hydrate ruthenium trichloride in a mixture of water, acetonitrile and carbon tetrachloride at 0°C.[127] The purification was achieved by a simple extraction with diethyl ether, followed by the filtration of the catalyst, to give the desired acid **256** in a good yield.

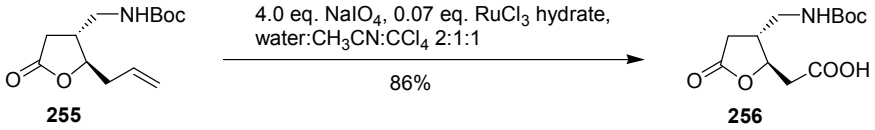

Figure 71

2.5 Synthesis of α-δ-pentapeptide

The lactone δ-amino acid **256** is a suitable building block for the synthesis of oligopeptides. Of particular interest is the synthesis of mixed α-δ-oligopeptides to check the ability of our scaffold to induce a secondary structure. The selected α-amino acid was the natural L-phenylalanine,

which does not present overlap in the proton NMR signals with our lactone, simplifying the NMR studies. In our case, the choice of the Boc protection of the N-terminal amine is suitable for the solution phase synthesis, by using a classical Boc strategy. The first coupling was performed between the δ-amino acid **256** and the trifluoacetic salt of the phenylalanine benzylester **257** in dichloromethane in the presence of HOBt, EDC and DIPEA to give dipeptide **258** in a good yield. Deprotection of the urethane with trifluoroacetic acid followed by coupling of the resulting salt with the Boc-protected phenylalanine in the presence of HOAt, EDC and DIPEA afforded the desired tripeptide **259** in 84% yield. For this and the successively coupling it was employed as coupling reagent the most reactive HOAt instead of the HOBt to achieve better yield. The same protocol was the employed in the next coupling between the tripeptide **259** and the lactone **256** to afford the tetrapeptide **260**. Finally, deprotection of the tetrapeptide **260** and its coupling with the lactone **256** afforded the desired pentapeptide **261**, which was purified by column chromatography and then analysed with different techniques to study its secondary structure. The techniques employed for the conformational analysis were the IR in solution, circular dichroism spectroscopy, NMR analysis and molecular modelling studies. Attempts to obtain stable crystal to carry out X-ray analysis unfortunately had a negative outcome.

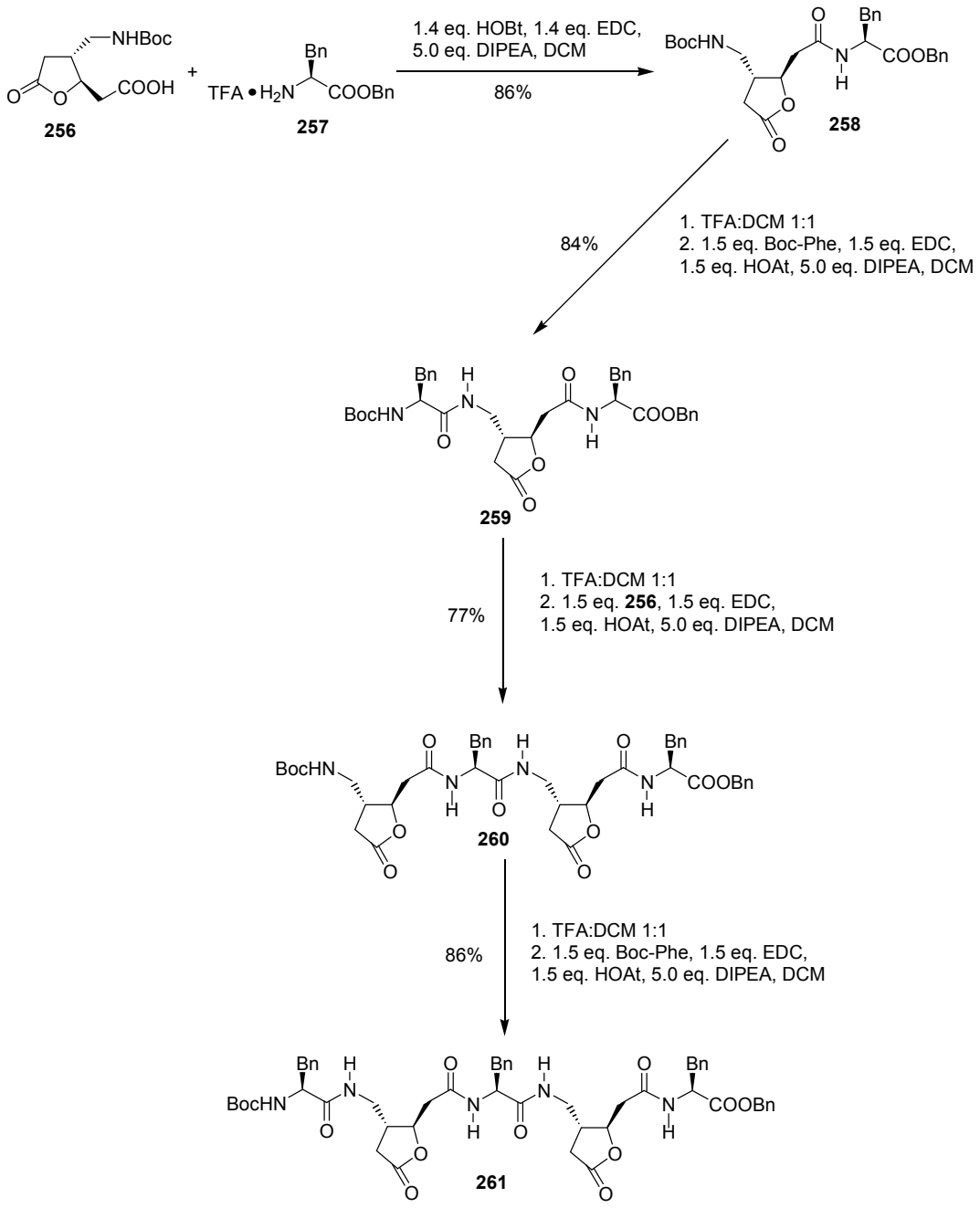
NHBoc
COOH
256
TFA • H2N
Bn
COOBn
257
1.4 eq. HOBt, 1.4 eq. EDC,
5.0 eq. DIPEA, DCM
86%
BocHN
258
84%
1. TFA:DCM 1:1
2. 1.5 eq. Boc-Phe, 1.5 eq. EDC,
1.5 eq. HOAt, 5.0 eq. DIPEA, DCM
259
77%
1. TFA:DCM 1:1
2. 1.5 eq. 256, 1.5 eq. EDC,
1.5 eq. HOAt, 5.0 eq. DIPEA, DCM
260
86%
1. TFA:DCM 1:1
2. 1.5 eq. Boc-Phe, 1.5 eq. EDC,
1.5 eq. HOAt, 5.0 eq. DIPEA, DCM
261

Figure 72

2.6 Conformational analysis of the pentapeptide 261

2.6.1 IR in solution

The IR in solution was performed in dichloromethane at the concentration of 1 mM to avoid the aggregation of the oligopeptide. The result showed in the region of the amide stretching two different peaks (figure 58), one at 3421 cm^{-1}, typical for a not hydrogen bonded amide and a second at 3317 cm^{-1}, which indicates the presence of an amide implicate in an intramolecular hydrogen bond.

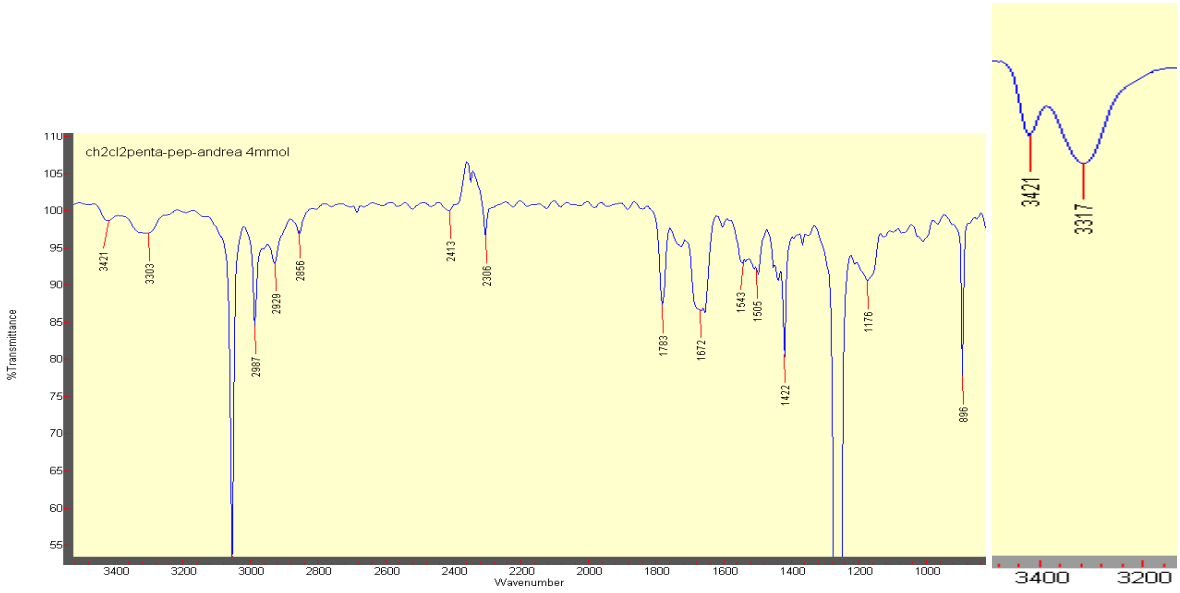

Figure 73 IR spectrum of the pentapeptide **261** and, on right, particular of the amide region signals

2.6.2 CD spectroscopy

CD measurement was performed in trifluoroethanol at the concentration of 0.3 mM. The spectrum (figure 74) showed the presence of two positive peaks at 203 nm and 218 nm, which indicates the presence of a secondary structure. Unfortunately, due to the absence of data about the CD spectra of α-δ-peptides, it is not possible to correlate the spectrum to a particular

conformation. In every case, in literature a similar spectrum was obtained by Claridge et al.[66] for an homo-octamer of the δ-amino acid **159**, which adopted an helix structure in methanol.

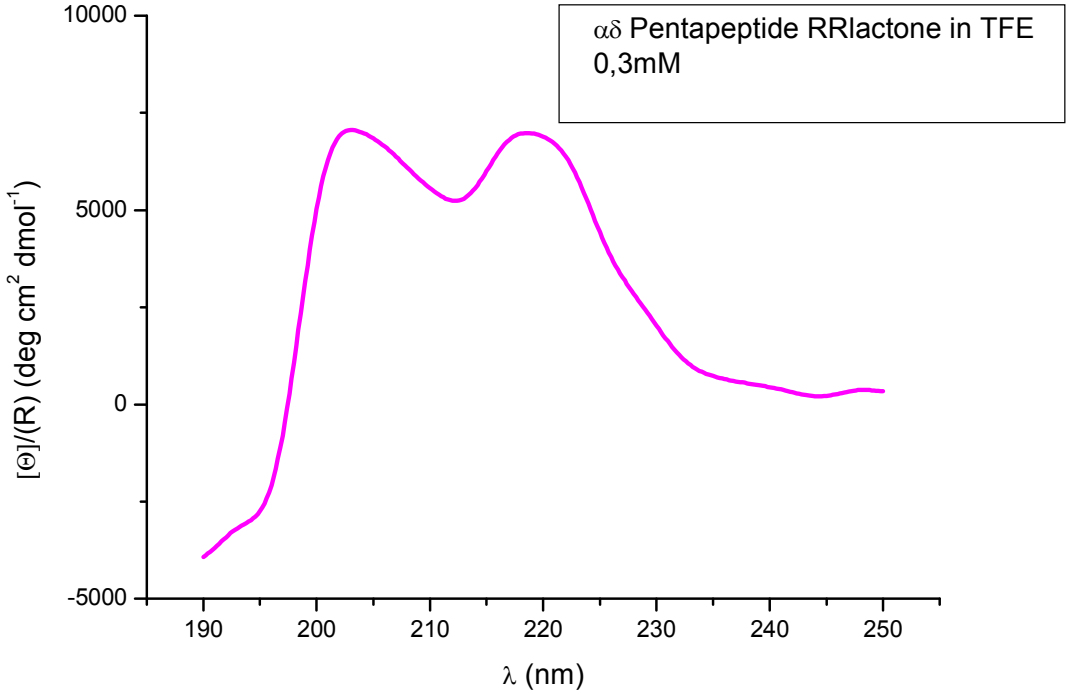

Figure 74

2.6.3 NMR analysis

The NMR analysis were performed at the concentration of 2 mM in $CDCl_3$. To have the maximum possible of information, a set of different analysis has been done. In figure 75 is showed the numeration adopted for the NH of the pentapeptide **261**.

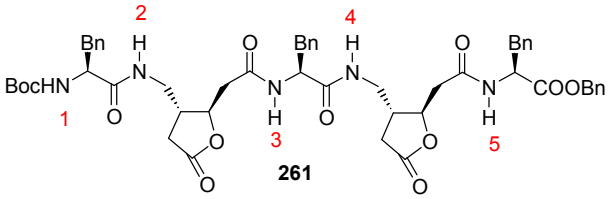

Figure 75

2.6.4 Temperature scan and measurement of the coupling constants

A temperature scan (figure 76) has been performed with two different objectives. The first objective was to find the best temperature to perform the 2D NMR studies, it means the temperature with a better dispersion of the amide signals, in our case 288 K. The second objective was to measure the measure the displacement of the chemical shift at the change of the temperature.

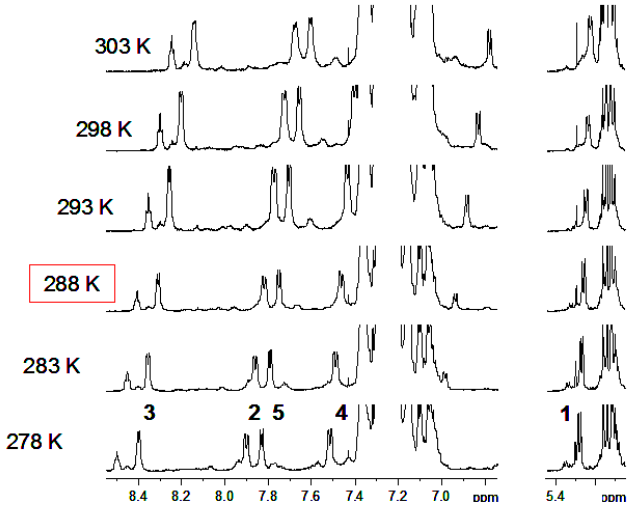

	1	2	3	4	5
Δδ/ΔT	2.0	8.8	10.4	6.0	8.8
^{3}J HN-Hα	8.2		6.2		7.6

Figure 76

Generally it is accepted that an amide proton involved in a strong intramolecular hydrogen bond has a low temperature dependence coefficient (Δδ<3 ppb/K), while for a free hydrogen is significantly higher (Δδ>8 ppb/K). In our case only the NH1 of the urethane showed a low temperature coefficient (2.0 ppb/K) which indicates that it is involved in a strong hydrogen bond. Moreover, the central NH4, with a temperature coefficient of 6.0 ppb/K, is probably also involved in a weak additional hydrogen bond, when the other amides, with coefficients larger than 8 ppb/K are not involved in hydrogen bonds. For the NH1,NH3 and NH5 protons it was also possible to calculate the vicinal coupling constant, which is directly related to the dihedral angle

(and, as consequence, to the conformation) between two protons by the Karplus relationship. In particular, it is usually accepted that a $^{3}J<6$ indicates an helix conformation, while a $^{3}J>8$ indicates a sheet. In the case of vicinal coupling constant between these two values, as in our case, it is possible the presence of an equilibrium between the two conformations.

2.6.5 2D NMR and molecular modelling studies

Despite of the partial overlap between the signals due to the repetition of the same subunit in our oligopeptide, in NOESY and ROESY spectra it was possible to clearly identify some long range contacts. Of particular interest, the strong contacts formed by the NH1, which indicate a presence of well-defined structure in this part of the molecule. Moreover, other interesting contacts can be detected between the NH3 and the NH5 and between the NH4 and the lactone in position 2. Based on these contacts, two different constraints were individuated (the black lines in the scheme 77) and used to perform the molecular modelling studies.

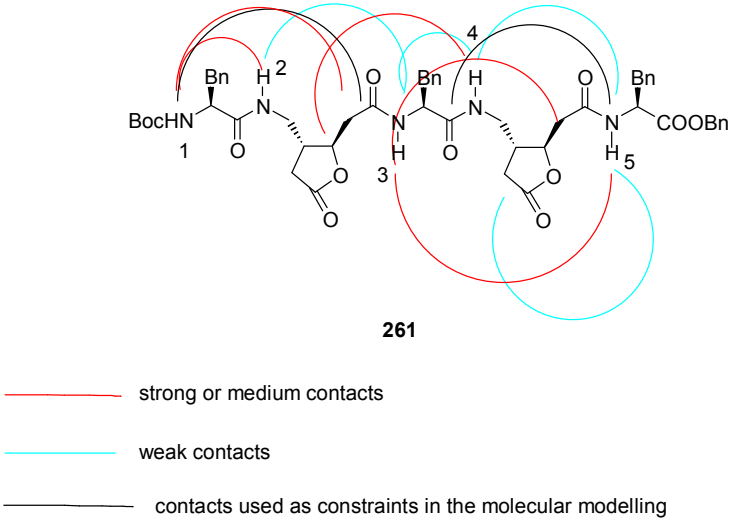

Figure 77

In figure 78 is shown the result of the molecular modelling performed imposing to the model the constraints illustrated above (the molecular modelling studies were done by Lucia Formicola and Karine Guitot), with the presence of an extended helical conformation. In particular, it looks that the part of the molecule between the NH1 and NH3 has a more organised structure, which is partially loose in the rest of the molecule.

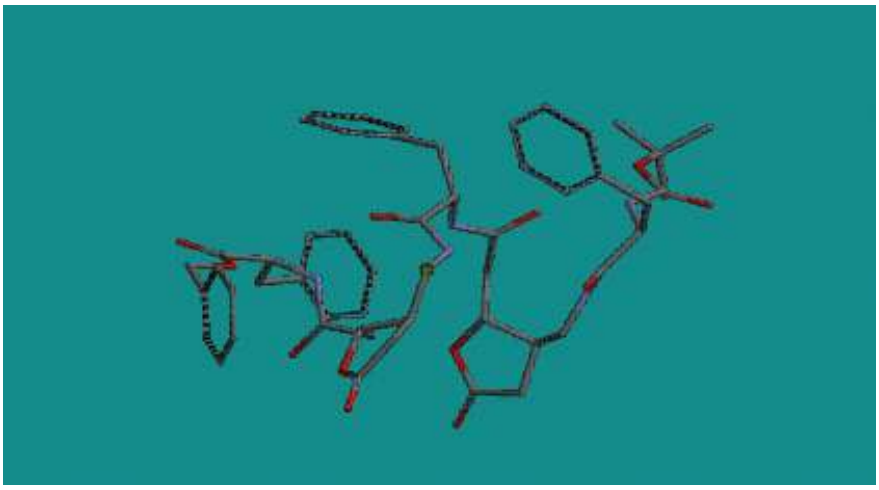

Figure 78

In conclusion, the experiments performed (IR, CD spectroscopy, NMR and molecular modelling studies) indicate the presence of an organised structure for the pentapeptide **261**. In the other hand, the data in our possession are not able to elucidate with certainty the exact conformation of the molecule **261**, but it is probable the presence of an extend helical conformation.

2.7 Synthesis of α-δ heptapeptide

Because the structural analysis about the pentapeptide suggested the presence of a non completely define secondary structure, it was decide to elongate the peptidic chain to investigate if, with a longer peptide, it was possible to obtain a more ordered structure. Thus, starting from the pentapeptide **261** and using the same protocol showed before, two additional solution phase coupling were performed. First step was the TFA deprotection of the pentapeptide **261** followed by the coupling with the δ-amino acid **256** in the presence of DIPEA, EDC and HOAt to give the hexapeptide **262** in good yield. Treatment of this compound with trifluoacetic acid to give the corresponding TFA salt was followed by the coupling in standard conditions with the Boc-phenylalanine to afford the heptapetide **263**. We repeated on compound **263** the same structural investigation performed on the pentapeptide **261**.

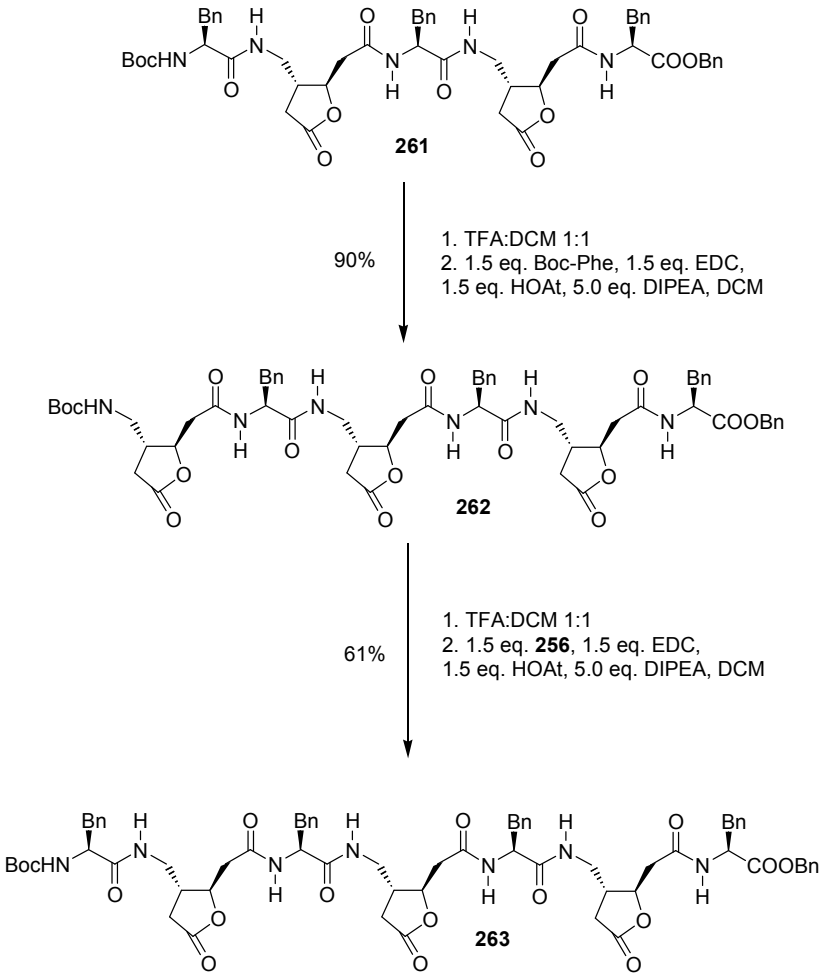

Figure 79

2.7.1 IR in solution

The IR in solution was performed in dichloromethane at the concentration of 1 mM to avoid the peptide aggregation. The result showed in the region of the amide stretching two different peaks (figure 58), one at 3421 cm^{-1}, typical for a not hydrogen bonded amide and a second at 3301 cm^{-1}, which indicates the presence of an amide implicate in an intramolecular hydrogen bond.

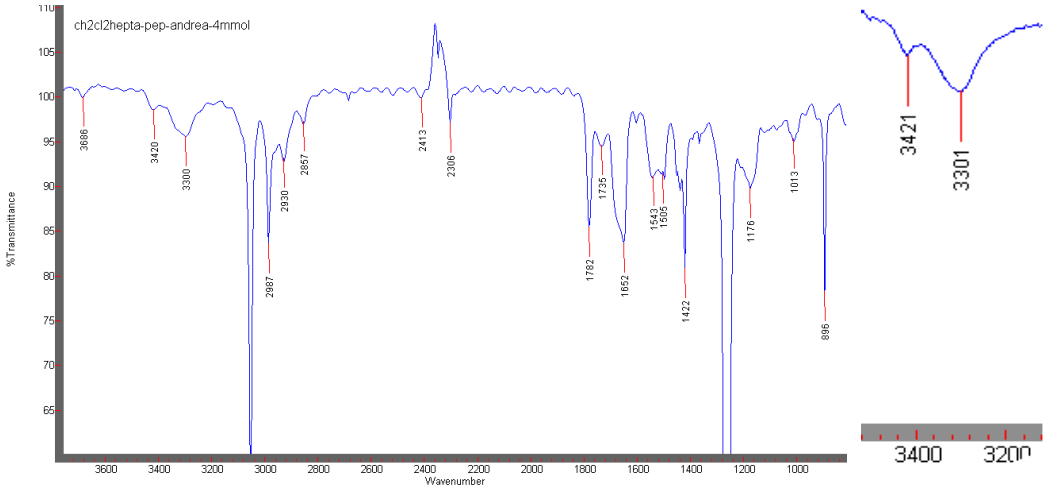

Figure 80 IR spectrum of the heptapeptide **263** and, on right, particular of the amide region signals

2.7.2 CD spectroscopy

CD measurement was performed in trifluoroethanol at the concentration of 0.3 mM. The spectrum (figure 74) showed a positive peak at 218 nm, which indicates the presence of a secondary structure. Unfortunately, due to the absence of data about the CD spectra of α-δ-peptides, it is not possible to correlate the spectrum to a particular conformation.

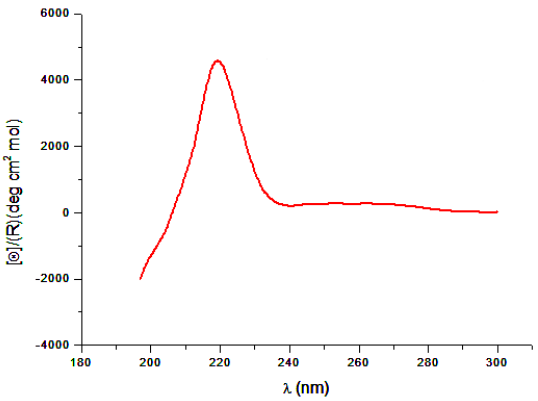

Figure 81

2.7.3 Temperature scan and measurement of the coupling constants

The NMR analysis were performed at the concentration of 2 mM in $CDCl_3$. To have the maximum possible of information, a set of different analysis has been done. In figure 82 is showed the numeration adopted for the NH of the heptapeptide **263**.

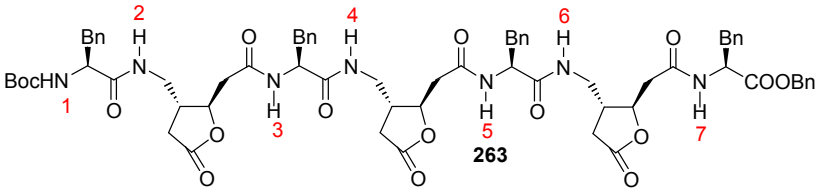

Figure 82

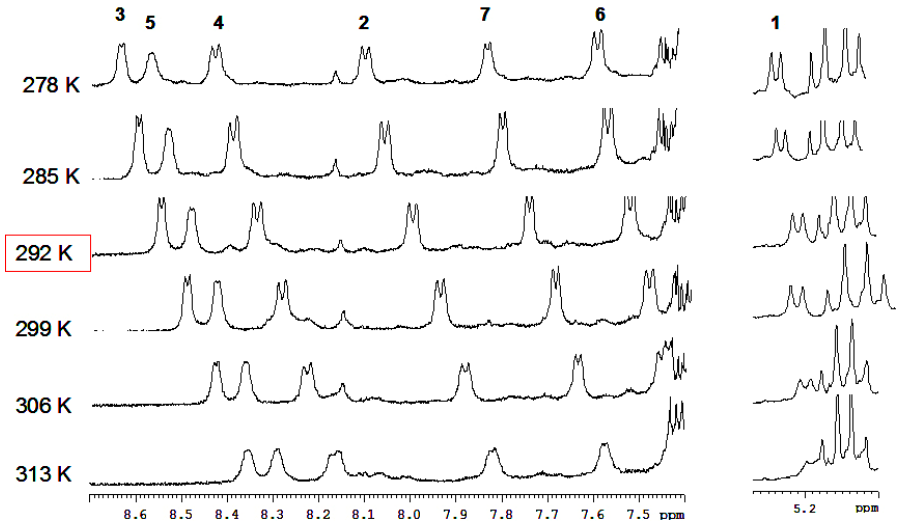

NH	1	2	3	4	5	6	7
Δδ/ΔT	0.7	7.8	7.7	7.3	7.8	3.9	7.2
3J HN-Hα	8.5		5.8		8.5		6.8

Figure 83

As for the pentapeptide **261**, the temperature scan showed a low temperature dependence coefficient (less than 3 ppb/K) only for the NH of the Boc function, which indicates that this proton is involved in a strong intramolecular hydrogen bond. Moreover, the NH6, with a

temperature dependence coefficient of 3.9 ppb/K, is probably involved in a weak intramolecular hydrogen bond. The better dispersion of the NH signals was found at the temperature of 292 K, for this reason the successive 2D NMR experiments were performed at this temperature.

2.7.4 2D NMR and molecular modelling studies

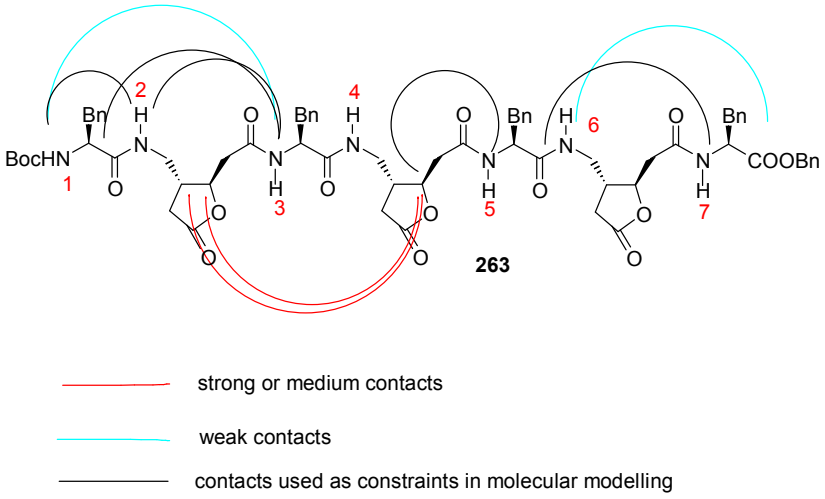

Figure 84

The problem of the partial overlap of the signals due to the repetition of the same subunit, which was found in the pentapeptide **261** is also present in our heptapeptide **263**. In every case, in NOESY and in particularly in ROESY spectra it was possible to clearly identify some long range contacts. Of particular interest, the long range contact between the NH1 and the NH3. Moreover, in the same region of the molecule, additional contacts were found, suggesting a presence of a well defined structure in this part of the molecule. Other interesting contacts can be detected between the lactone in position 2 and the lactone in position 4, indicating a proximity between these two amino acids. Less long range contacts could be identify in the right part of molecule, in particular between the NH6 and NH7 and between the NH6 and the terminal benzylester. These considerations should indicate as, like for the pentapeptide **261**, the heptapeptide **263** is well folded in the region near to the NBoc terminus and less ordered in the region near to the benzylester terminus. The molecular modelling with the constrained indicate in the 84 were performed by Lucia Formicola and Karine Guitot and the result shows in the figure 85 confirmed these hypotheses. In particular, also in this case, the analyses indicates that the most probable conformation adopted is an extended helical structure.

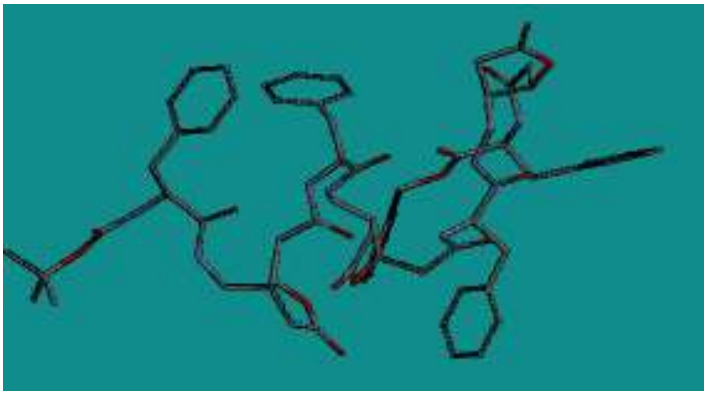

Figure 85

In conclusion, we have demonstrated that the introduction of our δ-amino acid **256** in α-δ-oligopeptides is able to induce a defined secondary structure also in relatively short chains such as the pentapeptide **261**. In particular, in both the penta- and heptapeptide 2D NMR analysis showed the presence of an extended helical structure. In the other hand it is not possible, only on the base of our NMR data, to elucidate the helical secondary structure with certainly.

2.8 Synthesis of PNAs

Since their discovery in 1991,[70] PNAs found a large interest for their ability in DNA and RNA recognition. Aim of this part of my work, is the synthesis of novel PNA based on the δ-amino acid scaffold showed in the previous paragraphs. In figure 86 is showed the retrosynthetic scheme for the synthesis of the PNAs. Starting from the compound **252**, the free amino group was protected as Fmoc, which is a suitable protective group for the solid phase synthesis of

oligopeptides. Next step is the reduction of the lactone followed by acetylation of the alcohol to give the compound **265**. Key step of the synthesis is the coupling of this compound with an activated DNA base in the presence of a Lewis acid (in figure 86 is showed as example the thymine). This reaction bring to the formation of two diastereomers which have to be separate in the following steps. The synthetic route continues with the PMB removal by CAN followed by the oxidation of the double bond with sodium periodate in the presence of a catalytic amount of ruthenium trichloride to afford the desired compound **269**.

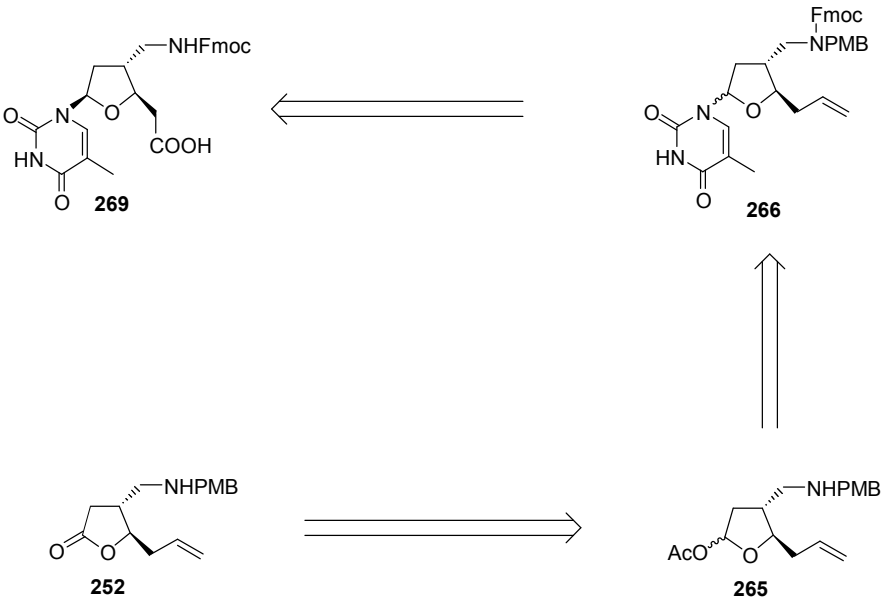

Figure 86

2.8.1 Fmoc protection

The Fmoc protection of the free amino group was performed by treatment with Fmoc succinimide in basic conditions to afford **264** in a good yield. The protection was also performed in the same condition by using the Fmoc chloride, obtaining the desired product in a non satisfactory yield (65%).

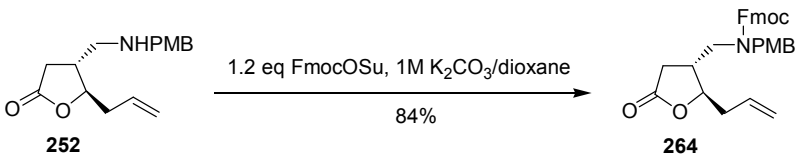

Figure 87

2.8.2 Reduction of the lactone

Reduction of the lactone moiety with DIBAL-H in dry dichloromethane at low temperature[128] was directly followed by the acetylation of the alcohol the afford the acetylated product **265** in a overall yield of 86% with a diastereomeric ratio of 3:1 measured by ^{1}H-NMR.

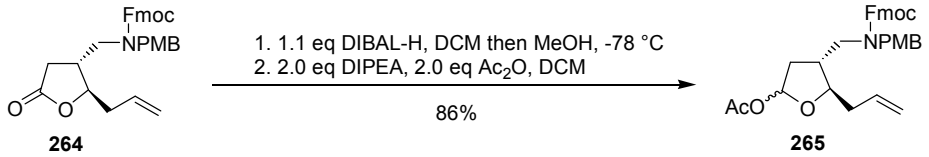

Figure 88

The reaction coupling was performed first using as nucleobase the persilylated thymine in the presence of a Lewis acid.[113] Thymine was chosen for the absence of a free amino group which required an additional protection step. The persilylated thymine was freshly prepared by standard methodology[129] by refluxing overnight the thymine in hexamethyldisilazane in the presence of a catalytic amount of ammonium sulphate and used after coevaporation of the solvent with toluene without further purification. The reaction was performed in the presence of different Lewis acids (TMSOTf, $EtAlCl_2$), but the best result was obtained reacting the acetylated compound **265** with 1.5 eq. of persilylated thymine in the presence of 1.0 eq. of $SnCl_4$ in dichloromethane, obtaining the desired product **266** in 75% yield with a diastereomeric ratio of 1.7:1 measured by ^{1}H-NMR. Also the effect of the solvent has been studied. In effect, the reaction in acetonitrile is faster and with a slightly better yield than in dichloromethane, but, as reported in literature,[130] in this solvent the reaction completely loose the diastereoselctivity.

2.8.3 Coupling with thymine

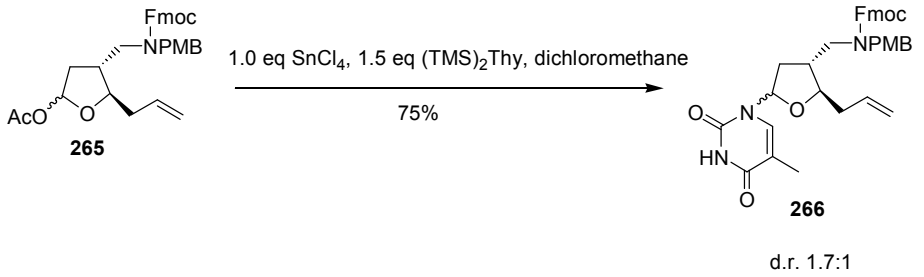

Figure 89

Next step is the PMB removal by CAN, which was performed in the same conditions used in the case of the compound **254**. At this stage it is also possible to separate the two diastereomers by column chromatography.

2.8.4 PMB removal by CAN

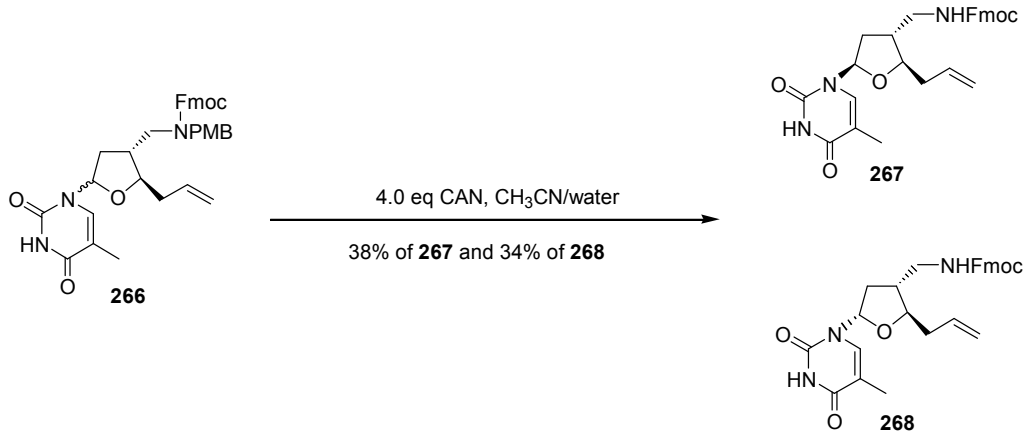

Figure 90

The analysis of the 2D-NMR (NOESY and ROESY spectra) indicated the configuration of the anomeric carbon for the two diastereomers. In particular (figure 91), it was possible to identify for the compound **267** a set of ROESY contacts between the methyl of the thymine and the allylic protons, indicating a special proximity between the thymine and the allyl group. In the other hand, compound **268** presented some ROESY contacts between the same methyl and some protons of the Fmoc group, indicating a special proximity between the thymine and the Fmoc group.

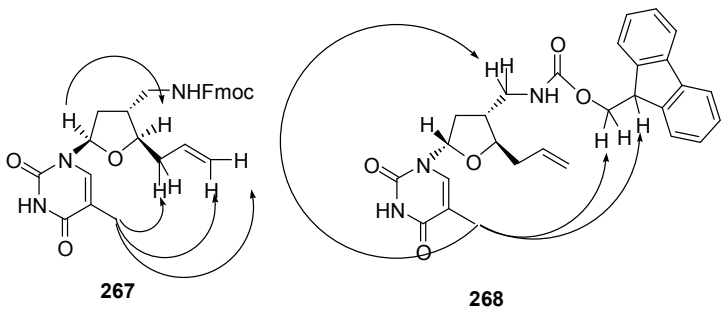

Figure 91 ROESY contacts of the two diastereomers

The oxidation of the double bond to give the desired PNA **269** was tried with the same methodology applied in the synthesis of the δ-amino acid **256** by treatment of the compound **267** with $NaIO_4$ in presence of a catalytic amount of hydrate $RuCl_3$ (figure 92). Unfortunately, in this case, it was not possible to isolate the desired δ-amino acid **269**. The problem was probably relied to the presence of an additional double bond in the thymine. In fact, the less hindered allylic double bond did not be enough more reactive of the thymine double bond , and, for this reason, the result of the reaction was a complex mixture of products which was not possible to separate and to completly characterise. In every case, it was possible to identify (by means of NMR and mass spectra) in the mixture also the presence of the desires product **269**. As reported in literature,[131] one of the undesired products present in the mixture was due to the oxidation of the internal double bond to give a diol. Furhter attempts with a more strictly control of the reaction conditions (in particular the time, the temperature and the concentration of the reaction) can maybe allow to give the desired compound **269** avoiding the undesired side reactions.

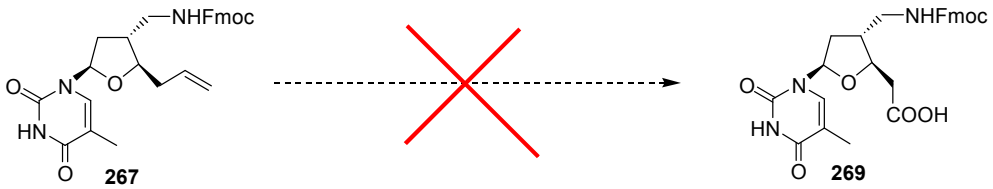

Figure 92

2.8.5 Coupling with adenine

The coupling was performed in the same conditions also with the persilylated adenine. In this case, it was chosen to do the reaction in acetonitrile, because the reaction in dichloromethane was too slow and was not completed also after several days.

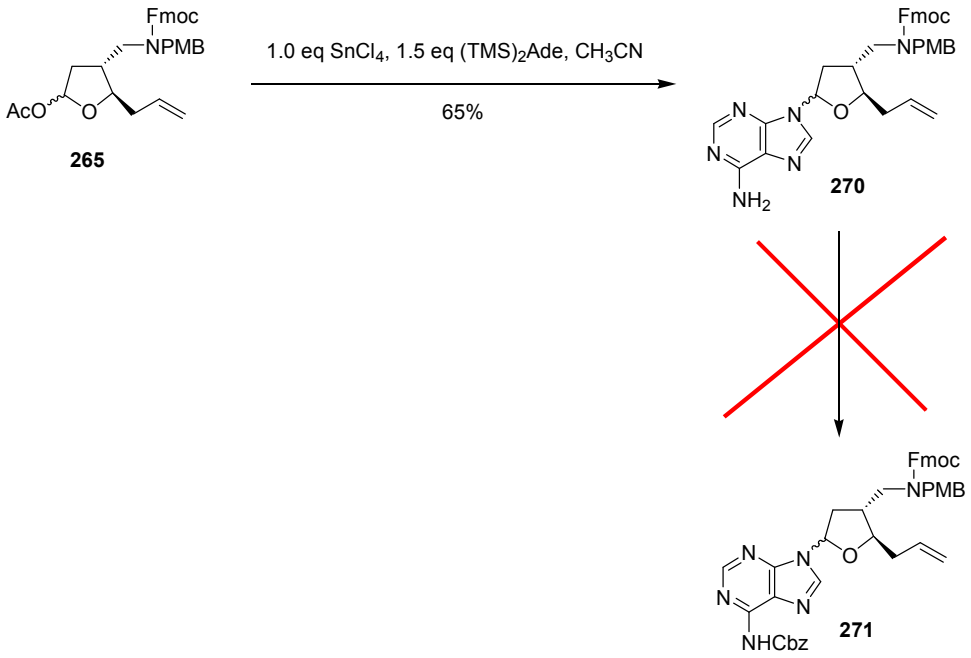

Figure 93

The Cbz protection of the adenine was first tried in standard condition by reaction with Fmoc succinimide, but in these conditions it was possible to collect only the starting material. The reaction was then performed by means of the Rapoport's reagent,[132] which is commonly used for the Cbz protection of the adenine. Unfortunately, following the standard protocol, we just observed the degradation of the starting material, without recovering the desired compound **271**. To overcome this problem it was then decide to perform the coupling directly with the Cbz protected adenine **273**.[133] In this case, the adenine cannot activated by persilylation, and for this reason it resulted not enough reactive to perform the substitution in the same conditions used with the persilylated thymine. It was so decided (figure 94) to activate the compound **265** by bromination with trimethylsilyl bromide. The resulting intermediate **272** was not isolated and was directly reacted with **273** to afford the desired compound **271** in a good yield.

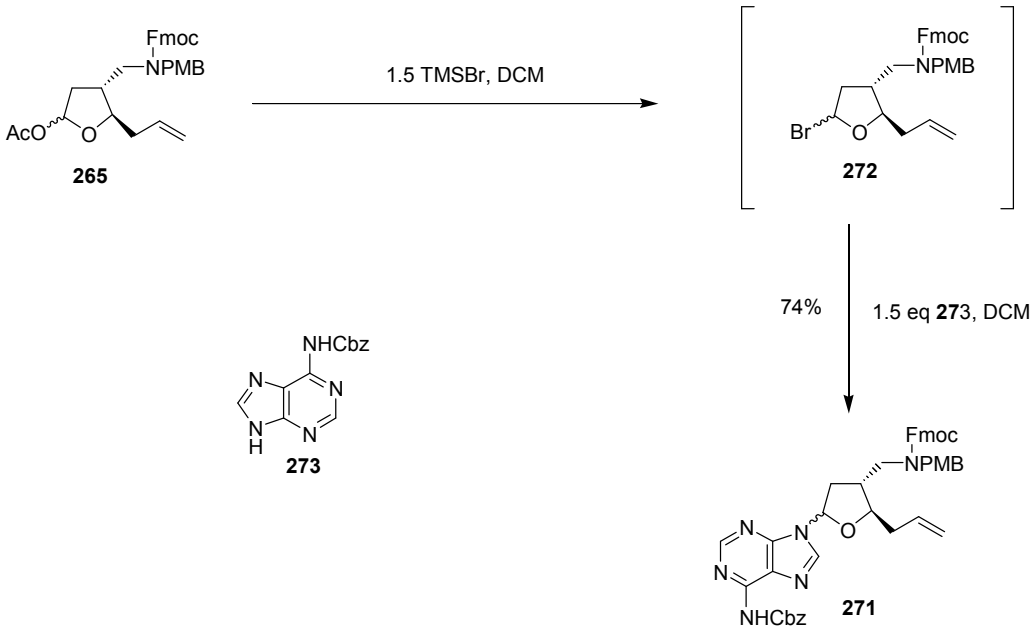

Figure 94

In conclusion, we showed a synthetic way to introduce a nucleobase (thymine or Cbz-protected adenine) in our furanoid scaffold previous reduction and acetylation of the lactone functionality. The obtained compounds **267** and **271** are suitable intermediates for the synthesis of new PNAs based on our δ-amino acid scaffold.

CHAPTER 3 PROTEASOME AND INHIBITORS

3.1 Role of 20S proteasome

Intracellular proteolysis is a fundamental cellular process. In eukaryotes the non-lysosomial protein degradation is performed by the ubiquitin-proteasome pathway. Since the proteasome is responsible of the degradation of a large number of proteins regulating cell cycle, transcription factors and antigenic proteins, it is a promising target for the development of drugs potentially useful for the treatment of a range of pathologies such as cancer,[134, 135] inflammation[136, 137] or immune diseases.[138] Another important function of the proteasome is the degradation of mutated, damaged or unfolded proteins. A large part of the newly synthesized proteins (maybe until one third) cannot fold properly and for this reason are degraded by the proteasome.[139] This function is really important because these abnormal proteins are responsible of many genetic diseases such cystic fibrosis[140, 141] and hereditary α_1-antitrypsin deficiency, which can be a cause of emphysema.[142]

3.2 Mechanism of the ubiquitin-proteasome pathway

The mechanism of the protein's degradation is strictly successive (Figure 95). First, the substrate is marked by covalent attachment of multiple molecules of ubiquitin, a small 8 kDa protein.[134] The covalent bond is usually an isopeptide bond with a free amino group on the lateral chain of the substrate, usually a lysine. A chain of ubiquitin is then formed by reaction of an ubiquitin molecule with the Lys48 of the preceding ubiquitin. This is an ATP depending process which is accomplished by three enzymes, E1, E2 and E3. The resulting ubiquitinylated complex is then recognized and degraded to amino acids or small peptides by the 20S proteasome, a 2.4 MDa multicatalytic enzyme.

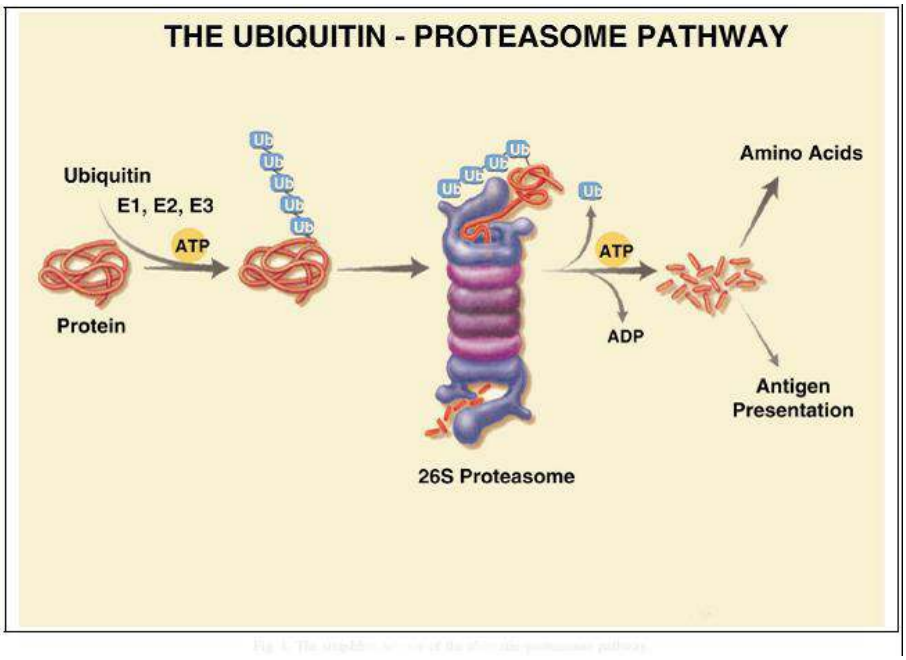

Figure 95 Figure with cordial authorisation by Prof. Kisselev

The 26S proteasome is a multifunctional proteolytic complex which differs in many aspects from typical proteolytic enzymes. In particular, between the unique properties of the proteasome we can mention the enormous size, the substrate recognition by polyubiquitin chain with an ATP dependent mechanism, the presence of 6 active sites with 3 different specificities, the N-terminal threonine-based proteolytic mechanism and the possibility to degrade the globular proteins. The 26S proteasome consist in a proteolytic core particle (CP), the 20S proteasome (720 kDa), sandwiched between two 19S[143] (890 kDa) regulatory cap (Figure 96).

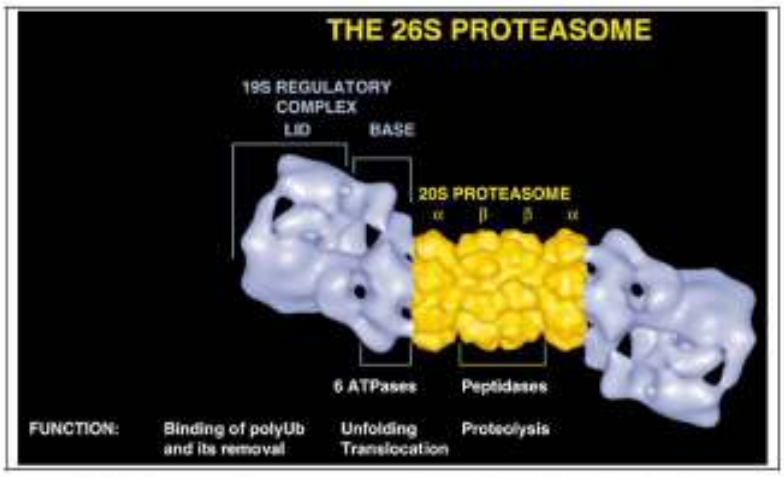

Figure 96 Figure with cordial authorisation by Prof. Kisselev

X-ray analysis of the proteasome crystals from the archaeon *Thermoplasma acidophilum*[144] first showed the proteasome architecture at atomic resolution. The data showed that the CP is composed of four stacked rings, with each ring consisting on seven α- and β-type subunits, following a $\alpha_{1\text{-}7}\beta_{1\text{-}7}\beta_{1\text{-}7}\alpha_{1\text{-}7}$ stoichiometry. Each β-ring contains 3 active sites, β1, β2 and β5, which were identify by X-ray analysis of the proteasome co-crystallized with calpain inhibitor I (Figure 97).[145]

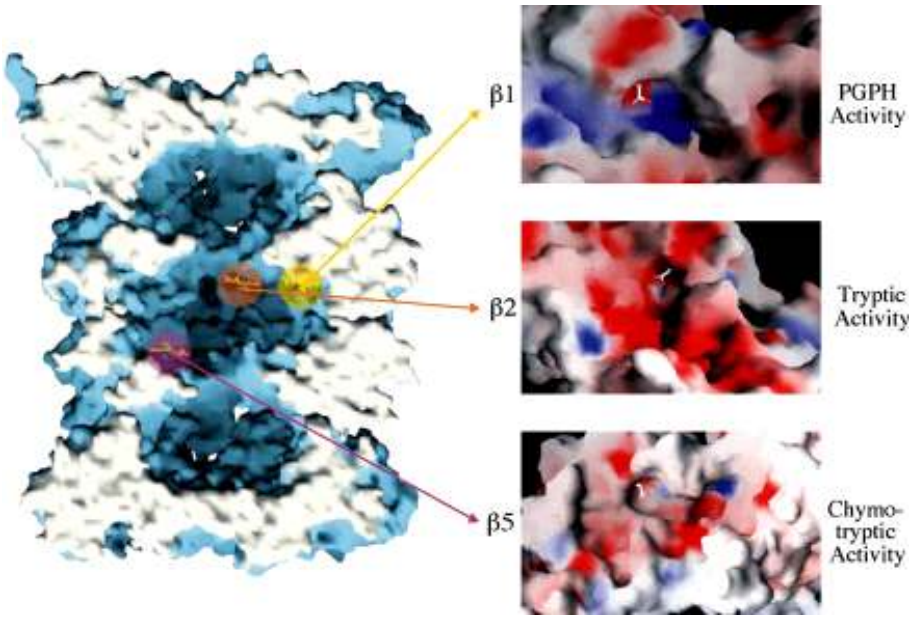

Figure 97 Figure with cordial authorisation by Prof. Groll

The x-ray structure allows also to identify the N-terminal Thr1O$^{\gamma}$ as responsible of proteolytic effect, because from the data it was clear that the functional aldehyde of the inhibitor formed a covalent hemiacetal bond with this residue.[146] Mutagenesis studies confirmed than Thr1, with Glu17 and Lys33, is the major responsible of the activity of this enzyme. This structure showed that 20S proteasome belongs to the new class of proteolytically active enzymes named threonine proteases. The versatility of the proteasome in the protein degradation is demonstrated by its ability to cleave the peptidic chain *in vivo* almost after each amino acid.[147, 148] However, *in vitro* assays with chromogenic substrates showed that proteasome activity is limited to five different cleavage preferences: chymotrypsin-like (CL), trypsin-like (TL), peptyl-glutamyl-peptide-hydrolysing (PGPH), branched chain amino acid-preferring (BrAAP) and small neutral amino acid-preferring (SNAAP). The three different active sites show a specific activity which could be identify by structural an mutational studies.[146, 149, 150] The X-ray structure showed that every active site contains two different hydrophobic pockets (called S1 and S3), which are responsible of the peculiar activities of the active site. Generally, the major responsible for the formation of the S1-specificity pocket is locate in the position 45. Additionally, adjacent subunits in the β-rings to the S1 pockets contribute to their selectivity. β1 subunit presents in position 45 a charged arginine, for this reason electrostatic interactions have a fundamental role in the activity of this subunit. It was demonstrate than this site is the major responsible for the PGPH activity, and for this reason it was traditionally called "peptidyl glutamyl peptide hydrolase",[151] however it has been found that it cleaves after aspartic acid residues faster than after glutamates[152, 153], and for this reason this site is commonly called "post-acidic" (PA) or "caspase-like".[154] (Caspase is an intracellular cysteine protease involved in cytokine processing and apoptose, which cleaves peptides only after aspartates[155]). In the subunit β2, glycine is situated in position 45. For this reason, S1 pocket in this subunit is very spacious and suitable for very large residues. Additionally, the presence of a glutamic acid in position 53 explains the high preference of this subunit for the cleavage after basic amino acid residues. For this reason the active sites present in this subunits are usually referred as "trypsin-like". β5 subunit present in the key position 45 a methionine, which minimize the space of the S1 pocket. The active sites present in these subunits cut preferably after hydrophobic residues and are usually called "chymotrypsin-like".

However, mutational analysis showed also that β2 and β5 subunits have the tendency to cleave after small neutral and branched side chains assigning to these subunits also the BrAAP and the

SNAAP activities[152, 156]. These names of the active sites are useful just to indicate the similarity to the substrate specificities of "classical" proteases, but they do not imply a similarity in the hydrolysis mechanism.

Proteasome activity is in effect completely different and involve for all the proteolytic sites the N-terminal threonine as the active site nucleophile. Much of our understanding about this mechanism is due to mutagenesis studies or by using inhibitors.[152, 157]

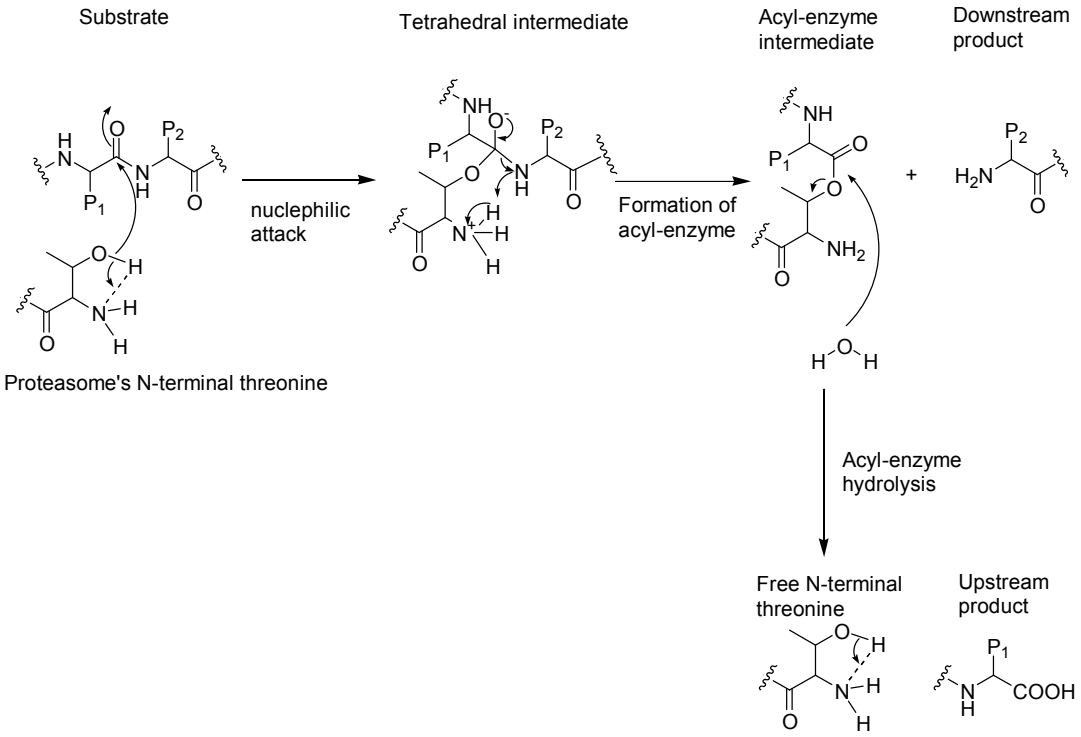

Figure 98

The mechanism is similar to that of serine proteases. First, the hydroxyl group attacks a scissile bond (figure 98). This attacks results in the formation of a tetrahedral intermediate which collapsed in an acyl-enzyme with the release of the downstream product. Deacylation promoted by a molecule of water leads the upstream product and the free N-terminal threonine, which is in this way able to promote the cleavage of a new substrate. This hypothesis was confirmed by X-ray analysis, which showed the acyl-intermediate formed by proteasome and a β-lactame inhibitor.[146]

3.3 Proteasome inhibitors

3.3.1 Covalent inhibitors

Covalent proteasome inhibitors are usually short peptides bearing a reactive group, generally linked to the C-terminus. The pharmacophore interacts with the catalytic residue forming a reversible or irreversible bond, while the peptide portion is design to mimic the natural proteasome substrate. Although the proteasome has many active sites, inhibition of every active site is not necessary to significantly reduce the protein degradation. In fact, it has been proved that the inhibition of chymotrypsin-like site permit to reduce significantly the protein degradation rate.[150, 158] In contrast, the inhibition of trypsin-like or caspase-like site, does not affect the most of the activity of the proteasome. In addition, the hydrophobic residues necessary for the inhibition of the chymotrypsin-like site are more cell-permeable than the inhibitors of the trypsin-like or caspase-like activity which usually contain charged residues. As consequence, most of the synthetic inhibitors are designed for the chymotrypsin-like site, but they usually have also some inhibition activity versus the other catalytic sites. We can classify the covalent proteasome inhibitors in different classes according to their chemical structure. They can be classified more generally in reversible covalent inhibitors and irreversible covalent inhibitors. In the first class we have for example peptide aldehydes and peptide boronates and in the second peptide vinyl sulfones or the peptide epoxyketones. In the class of reversible inhibitors we have also lactacystin and its derivatives, which differs from the other inhibitors because they are not peptidic but based on a β-lactame ring.

3.3.2 Peptide aldehydes

Peptide aldehydes (figure 99) were the first proteasome inhibitors which have been developed and are actually widely used to study proteasome activities and properties.[158] They are also well-known as general inhibitors of cysteine and serine proteases, and thus they are not selective for proteasome. For example, ALLN (Ac-Leu-Leu-Nle-al) was first study as inhibitors of calpains and cathepsins, and for this reason it is usually called as Calpain inhibitor I, **274**). Despite its lack of specificity it has been widely used to study the effect of the proteasome inhibition *in vivo*.[159] Calpain inhibitor I react with the Thr1O^{γ} forming an hemiacetal bond in all the active sites, as confirmed by X-ray structure of the complex. The tripeptide aldehyde adopts a β-conformation and fills the gap between β-strands, forming covalent bonds with the residues 20, 21 and 47 with consequent generation of an anti-parallel β-sheet. The terminal norleucine P1 is inserted in the S1 proteasome pocket, when the leucine P3 interacts with residues in the S3 pocket. It was so clear that a good filling of both S1 and S3 pockets of the proteasome are important for the affinity between inhibitors and proteasome.[146] These inhibitors have fast dissociation rates and are rapidly oxidized into inactive compounds by cells. Consequently, in experiment involving the proteasome, the inhibition effect can be rapidly reversed by removal of the inhibitor. Other peptide aldehydes have been then synthesized, but only few of them are actually widely used. For example MG132 (Z-Leu-Leu-Leu-al, **275**) is not more potent of calpain inhibitor I, but is really more selective and in fact it does not show an appreciable inhibition of calpains or cathepsins at the concentration required for the proteasome inhibition.[160, 161] Other good inhibitors of this class are also PSI (Z-Leu-Glu(OtBu)-Ala-Leu-al, **276**)[162] and CEP1612 (**277**).[163]

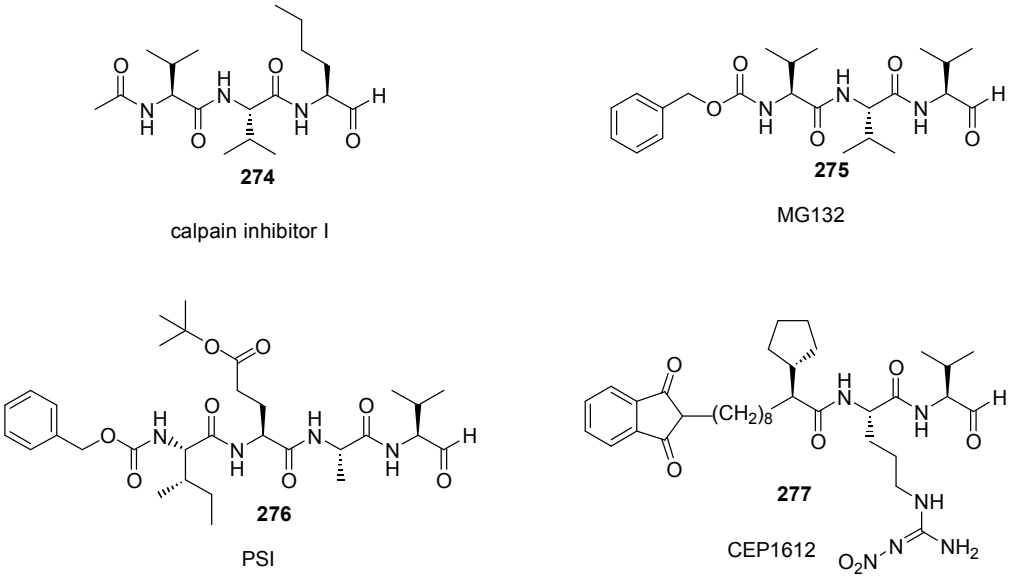

Figure 99

3.3.3 Peptide boronates

Peptide boronates are one of the most important classes of covalent inhibitor of the proteasome (figure 100). They are much more potent than peptide aldehydes, for example the boronate analogue of MG 132, MG262 (Z-Leu-Leu-Leu-boronates, **278**) is 100-fold more potent than the corresponding aldheyde.[164] with a K_i of 18 pM. The boronate-proteasome adducts have a very slow dissociation rate, for this reason, also if they belong to the category of reversible inhibitors, the inhibition is practically irreversible over hours. Another very interesting characteristic of this class of compound is the very high selectivity for the proteasome, for example they are very weak inhibitors of thiol proteases due to the weak interaction between sulphur and boron. Many peptide boronates are also weak inhibitors of serine proteases, such as PS341 (pyrazilcarbonyl-Phe-Leu-boronate, or Bortezomid, **279**), which is 1000-fold a weaker inhibitor of serine proteases than proteasome. For all these reasons, peptide boronates are really interesting compound, and in particular Bortezomid **6** is at the moment the first and the only proteasome inhibitor which reached the market with the commercial name of Velcade®.

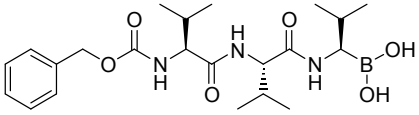

278
MG262

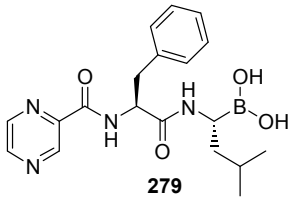

279
Bortezomid

Figure 100

3.3.4 Lactacystin and its derivatives

Lactacystin (**280**, figure 101) is a *Streptomyces* metabolite which has the ability to induce the differential in cultural neuronal cell. It was first discovered by Omura et al.[165, 166] and later synthesized by Corey at al.[167] Lactacystin is able to bind and inactivate the chymotrypsin-like site of the proteasome in a irreversible manner, and to block in a reversible manner also the other two active sites with a really slow dissociation rate.[168] In effect, it was demonstrate that lactacystin is not active, but it spontaneously undergoes at neutral pH to the active *clasto*-lactacystin-lactone (omuraline) **281**.[169] One of the most potent inhibitors of this class is the Salinosporamide A (**282**), a natural compound extracted from the marine bacterium *Salinispora Tropica* and which is currently in development for the treatment of multiple myeloma and other cancers.[170, 171] Recently, a fluorinated analogues of this compound, the fluorosalinosporamide (**283**) has been also synthesised.[172]

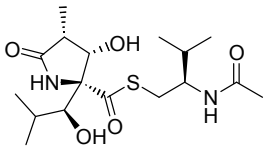

280
Lactacystin

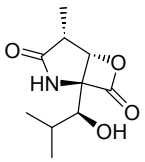

281
Omuralin

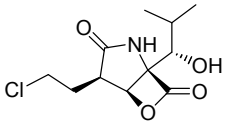

282
Salinosporamide A

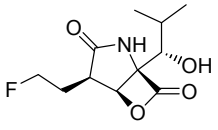

283
Fluorosalinosporamide

Figure 101

3.3.5 Peptide vinyl sulfones

Peptide vinyl sulfones are irreversible inhibitors which were first synthesised and described by Bogyo et al.[173] The mechanism of the reaction is currently studied, but it is currently accepted that the hydroxyl group of the Thr1 of the proteasome reacts by a Michael addition with the double bond of the inhibitor with consequent inactivation of the active site. Vinyl sulfones do not inhibit serine proteases, but have an inhibition effect on cystein proteases, and the selectivity depends essentially to the peptidic part of the inhibitor. For example, the vinyl sulfone analogue of MG 132, ZLVS (**284**), it is also a strong inhibitor of the cathepsins S and B, but when the Z group is substituted with a NIP (3-nitro-4-hydroxy-5-iodophenylacetate) group (NLVS, **285**), this effect decrease considerably (Figure 102).

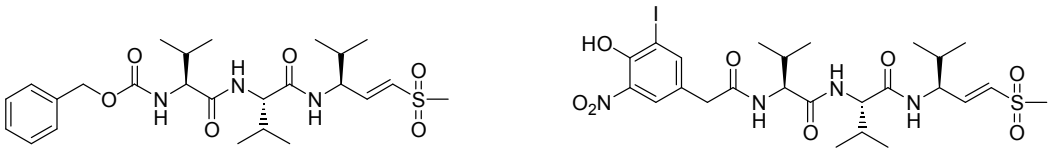

284
ZLVS

285
NLVS

Figure 102

3.3.6 Epoxyketones

Epoxyketones are the most selective proteasome inhibitors known. Epoxomicin (**286**) and dihydroeponemycim (**287**) belong to this class (Figure 103).[136, 174] The reason of their high selectivity is the unique mechanism of binding with the Thr1, which involved both the hydroxyl and the amino functionality, by formation of a cyclic morpholino ring (**288**) , which is not possible in the absence of a free N-terminus as in the case of serine or cysteine proteases. The presence of the morpholino ring was also confirmed by the X-ray structure of the adduct.[145] Moreover, the crystallographic analysis showed a good filling of the S1 and S3 pockets by respectively the lateral chain of the leucine and of the isoleucine, and the presence of an array of hydrogen bonds between the main chain of the epoxomicin and the residues 21, 47 and 49 of the proteasome. This result is very similar to that obtained for the Calpain inhibitor I, which was illustrate previously and confirm the necessity of these features to have a good proteasome inhibition.

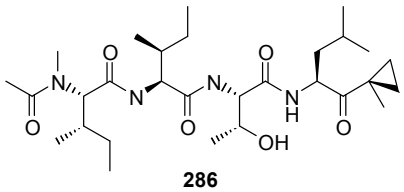

286
epoxomicin

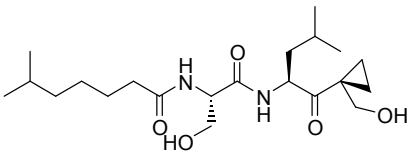

287
dihydroeponemycim

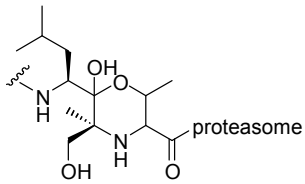

288
morpholine ring

Figure 103

3.3.7 Non covalent proteasome inhibitors

In this class of inhibitors, contrary to the previous classes, there is not a reactive group able to bind covalently the Thr1 in the active site. The binding is due to the formation of an array of hydrogen bond and to the hydrophobic and electrostatic interactions between the inhibitor and the active site. For this reason, the inhibitory effect is reversible and time-limited. Because a irreversible inhibition of the proteasome usually induce apoptosis and cause cell death[175], it can be expected that the cytotoxic effects may be reduced using this class of inhibitory. In addition, because the interaction is possible only in the presence of a particular conformation of the active site, it is also reasonable to think that this class of compounds can show a really good selectivity for the proteasome, without affecting the activity of the other proteases. Actually, just few compounds show this mechanism of inhibition. One of the most study is a natural compound isolated from *Apiospora Montagnei*, called TMC-95A (**289** figure 104), which blocks the proteolytic activity of all the active sites of the proteasome in a nanomolar range concentration.[176, 177] This compounds is not related to the other known inhibitors and consists in a macrocyclic ring-system made of modified amino acids. In fact, a large contribution to the elucidation of the inhibition mechanism of this compound has been done by Groll and coworkers,[178] which co-crystallized the TMC-95A with the proteasome obtaining the X-ray structure of the complex for all the active sites. It was clear that TMC-95A binds the β subunits without modify their N-terminal threonine. A tight network of hydrogen bonds connects TMC-95A with the proteasome, and stabilizes its position. All these interactions are performed between the main chain atoms of TMC95-A and strictly conserved residues of the protein. The arrangement of the TMC-95A is similar to the already described aldehyde and epoxyketone inhibitors[145] and it is the same in all the active sites. The n-propylene group protrudes into S1 pocket, whereas the lateral chain of the asparagines is deeply inserted into the S3 pocket. The NMR-structure of unbounded TMC95-A in solution[177] superimposed with the crystal structure of the complex showed that the binding with the active site does not comport a conformational rearrangement of the inhibitor, so the optimal binding is probably due to the strained conformation of the TMC95-A, caused by the cross-link between the tyrosine and the oxoindol side chain. Additionally, also the crystal structure of the

unbounded proteasome shows a perfect superimposition with the crystal structure of the complex with the inhibitor,[178] which means that also the structure of the protein is not affected by the presence of the inhibitor. Due to the complexity of the structure of this compound, which does not permit an application of this very interesting compound as drug, some simpler macrocycles mimicking the structure of the TMC-95A have been synthesized (**290**), but unfortunately the new compounds showed a significant decrease in the inhibitory activity.[179]

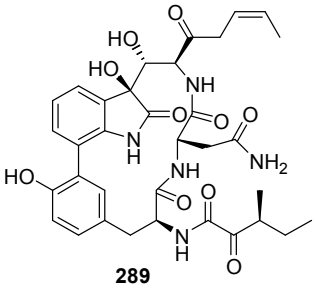

289

TMC95-A

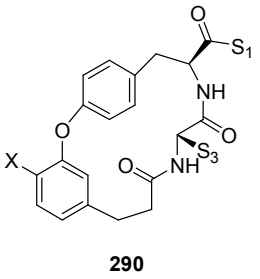

290

S_1 = n-propyl S_3= Asn X=NO_2 or
S_1 = Nle-NH_2 S_3 = Asn X = NH_2 or
S_1 = Arg-NH_2 S_3 = Arg X=NO_2 or
S_1 = Arg-NH_2 S_3 = Arg X = NH_2

Biaryl analogues of the TMC95-A

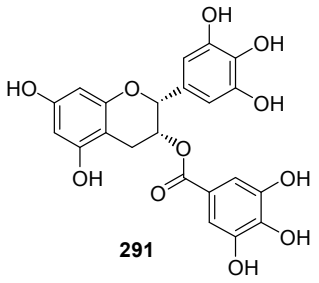

291

(-)-epigallocatechin-3-gallate (ECGC)

Figure 104

Other natural compounds show also an inhibitory activity of the proteasome. For example, green tea contains many polyphenols with this characteristic. The most active between them is the (-)-epigallocatechin-3-gallate (ECGC) (**291**, figure 104).[180] The inhibitory mechanism of this compound is not yet completely explained, but different studies of structure-activity relationship, atomic orbital energy analysis and analysis of the products of interaction between ECGC and proteasome strongly suggest that the ester bond in this molecule is attacked by proteasome leading to the Acylation of the threonine in the active site. Analysis also suggested that this bond is slowly hydrolyzed by water, leading to the reactivation of the proteasome.

In 2007, Basse et al.[181] reported the synthesis and the biological evaluation of a library of 45 linear oligopeptides designed as linear analogues of the TMC95A (the most active in figure 105). Despite the absence of the entropically favourable constrained conformation, some of these compounds presented submicromolar inhibition constants.

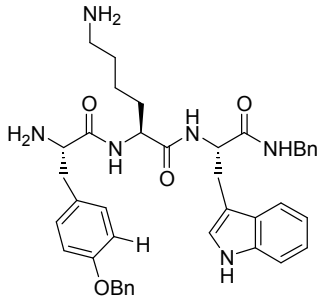

292

Figure 105

Recently, some novel non covalent inhibitors have been synthesized with an activity of nanomolar range. For example, a research's group of Novartis synthesized a new non covalent inhibitor based on an aminostatine skeleton (**293**, figure 106).[182] Despite the nanomolar range activity of this inhibitor *in vitro*, the cellular tests do not expressed its high enzymatic inhibitory activity at the cellular level. Assuming that the reason was the poor cell penetration, the same

group designed new similar scaffolds to decrease the size and the peptidic character of the molecule. These efforts lead to the novel compound **294**, a selective inhibitor of the chymotrypsin-like site of the proteasome, with an IC_{50} of 7 nM. Cellular tests of this new compound are not yet published, for this reason it is not possible to know if this smaller and less peptidic molecule gave better results than the lead molecule **293.** In the binding model proposed by the authors and based on molecular modelling and structure-activity relationship the N-benzyl group of **294** fills the S1 pocket is mimicked when the 3,4,5-trimethoxyphenylalanine interacts with the S3 pocket. Finally, the terminal biphenyl is able to interact with the accessory AS1 and AS2 hydrophobic pocket.

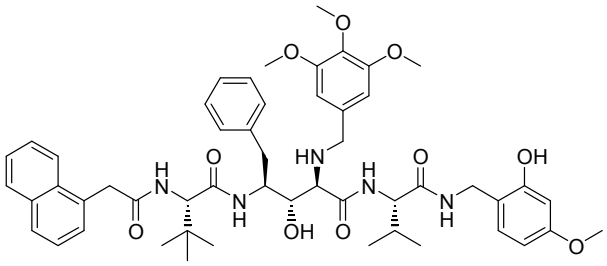

293

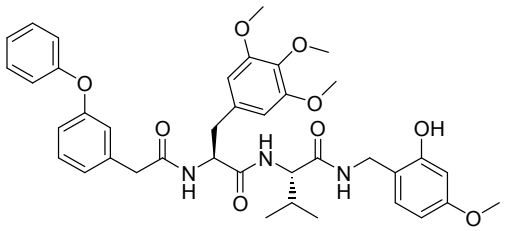

294

Figure 106

3.4 Biological effects of proteasome inhibitors

Since the discovery of specific and efficient inhibitors, a large number of data documenting the critical role of the ubiquitin-proteasome pathway has been produced. These results clearly showed that proteasome performs precise regulated degradations of key proteins to switch off specific pathways. The effects of treatment of cells with proteasome inhibitors can give completely different results which are depending not only by the cell status, but also by the type and the amount of the inhibitor.[183] Additionally, it is not often simple to identify *in vivo* the effect of the inhibition of the proteasome, because most of the inhibitors affect also the activity of other proteases, and a part of the biological effects observed can be explain by this secondary effect.

Because the degradation of many proteins regulating the cell cycle (G1 and mitotic cyclins, CDK, inhibitors, p53) is regulated by the proteasome, cell proliferation is significantly affected by the proteasome inhibition. In effect, it was demonstrated that proteasome inhibition can arrest the cell cycle at various stages.[184] Of particular interest is the ability of proteasome inhibitors to induce the apoptosis in proliferating cells and to inhibit the angiogenesis[185], which makes these compounds attractive candidates as drugs for the cancer treatment. In particular, several studies demonstrated that proliferating cells are usually more sensitive that non proliferating ones,[185-187] and they may undergoes to apoptosis in 4-48 hrs.[186, 188]

In addition, proteasome inhibitors affect also other biological process as inflammatory and immune responses. The critical biochemical event in the initiation of the inflammatory response is the rapid destruction of the inhibitory protein IkB which occurs in response to various toxic stimuli. IkB was the first substrate of the ubiquitin-proteasome pathway identified by using the proteasome inhibitors.[160] IkB is an inhibitor of transcription factor NF-kB, which actives the expression of many genes encoding inflammatory mediators (e.g. tumor necrosis factor), enzymes (cyclooxygenase, nitric oxide synthetase) and leukocyte adhesion molecules.[189] Consequently, in cultured cells and *in vivo*, proteasome inhibitors, by stabilizing IkB, maintain NF-kB in the inhibited state and prevent production of these proteins, decreasing significantly the inflammatory state.

3.5 Molecular modeling

The use of theoretical models which allow to understand or predict structures, properties or molecular interactions is known as molecular modeling. It allows to give some informational data that can't be easily empirically obtained, such, for example, the structure of a transition state. One of the most interesting application is the virtual screening (VS), i.e. the possibility to screen *in silico* the interactions between large libraries of small-molecular-weight ligands and therapeutically relevant macromolecules to identify leads or able to complex the selected targets. Among the most commonly VS tools are docking methods, which have been able to predict the binding modes of many potent enzyme inhibitors as well as receptor antagonist. As result, many drugs designed computer-aided methods are in late-stage clinical trial or reached the market.[190]

3.5.1 Docking

Docking's programs allow the systematic exploration of the configurations of a ligand interacting with a receptor. To date, over of 60 docking programs are avaible[191], but just few of them are widely used (Autodock, Dock, Flex, FREED, Glide, GOLD, ICM, QXP/Flo+, Surflex). Each docking program has 2 different components:

- A methodology to explore the conformational space of the ligand and of the protein target
- A scoring function which allows to evaluate the result

The first aspect is the most important to have an accurate prediction of the binding mode. The second allows to distinguish between the highly active compounds, which should have a better score, and non-binders or poor-binders. For this reason, the score function is critical in virtual screening, where it is necessary to extract information about the possible hits from a large library. Between the different algorithms used in academic and pharmaceutical context, we choose to use Autodock.[192-194] This program allows to predict the conformation of a ligand interacting with a rigid or semi-rigid receptor. The knowledge of the structure of the receptor is an essential pre-

requirement to use this technique, but fortunately the structure of a large number of proteins or enzymes obtained by X-ray or NMR studies is available on "Protein data bank PDB" database.
The first algorithm used by Autodock was of Monte Carlo type, which in the actual version is replaced by a genetic algorithm of Lamarckian type.[195] In effect it was demonstrated that this type of algorithm has a better fitting with X-ray structures of ligand-receptor complexes.[194] The energy of interaction is calculated with a methodology which is based on the use of grid of potential interactions.
Autodock is the most cited docking program in the scientific literature.[196] The first version of 1989 was the first docking program able to consider the conformational flexibility of the ligand and the last version (Autodock 4) introduces also the possibility of calculate the flexibility of the lateral chains of the receptor, for example a protein.

3.5.2 Genetic algorithm

The genetic algorithm of Lamarckian type in commonly used for the conformational analysis of the ligands, in particular dihedral angles. The name Lamarckian comes from Jean-Baptiste Lamarck and his theory about the genetic inheritance, now rejected.
This algorithm describes the states of freedom of the ligand as a suite of binary number which is considered as a gene. The state of the ligand corresponds to the genotype and its coordinates to the phenotype. An initial population of different genes is generated by chance and every gene is evaluated by the energy function of the program (score function). The genes are selected on the base of there score to form the next population. The genes can also combine to have a better solution starting from 2 conformations with a good score. Is it also possible for some genes to have a mutation which generate a hazardous modification.
Because a gene is represented by a suite of binary numbers, also the combination or mutation of the genes are represented by binary operations. For these reasons, these operators can generate a large number of non interesting solutions, which can slowdown the calculation. A number of methods has been adopted to avoid this problem, but as often as not these solutions are really expensive for the time of the calculation.[197] The methodology adopted by Autodock 3 is to associate a local research of the minimum to the genetic algorithm.

The difference between a genetic algorithm based on the Darwin and Mendel theory and another based on Lamarckian genetic algorithm is shown in the figure 107. In particular, in the case of Lamarckian theory **(part B)** accepted idea is that an organism can pass on characteristics that it acquired during its lifetime to its offspring (also known as based on heritability of acquired characteristics or "soft inheritance"), which is not allowed in the Mendel theory **(part A)**.
In this figure, the function f(x) is the score function. It represents the force, or health, of a subject with a determined genotype and phenotype: a structure with a low energy is a subject with a good health. In the part B, which depicts the Lamarckian genetic algorithm, it is possible to explore the phenotype space to find a local minimum of the score function. In Autodock case, the algorithm[194] try to minimize the score function in the genotype space (configuration of the ligand: torsion angles) instead of the phenotype space (coordinates). For every generation, a part of the population (parameter which can be change by the user, in our case 0,06) follow this route of local research.

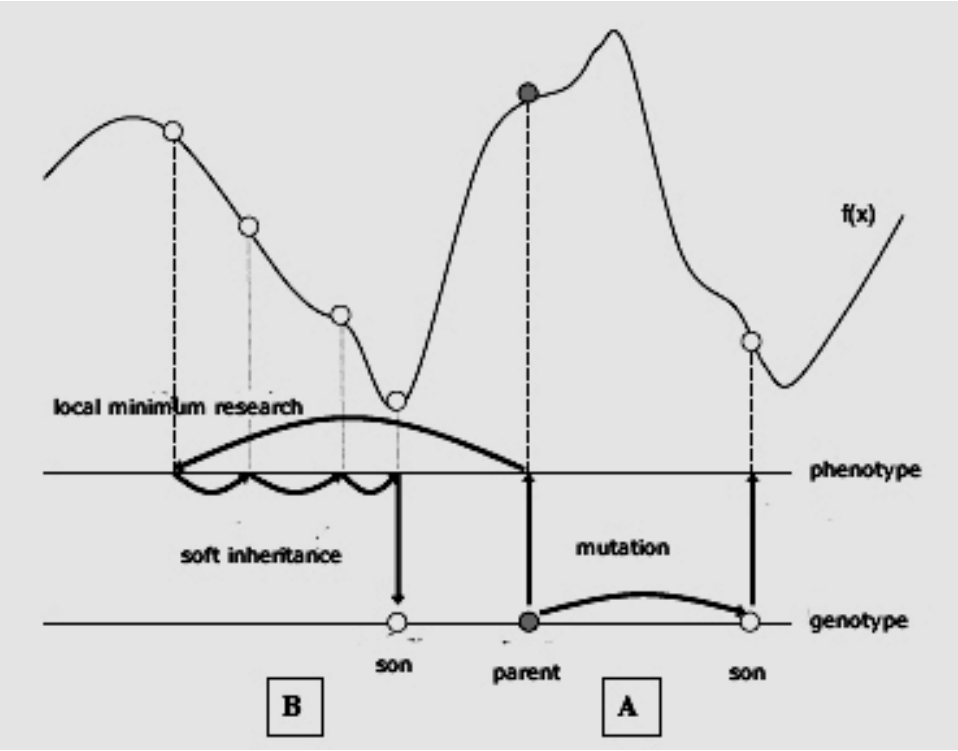

Figure 107 The principle of the genetic algorithm

3.5.3 Free energy function

The free energy function used by Autodock was optimized using as references 188 complexes protein-inhibitor with structure and inhibition constant known. The thermodynamic cycle of the receptor (R) - inhibitor (I) complexation in both the gas and liquid phase take care of the mechanism of de-solvatation at the base of the hydrophobic interactions.

$$\Delta G_{complex/solvent} = \Delta G_{Solvatation\ (R + I)} + \Delta G_{complex/vacuum} + \Delta G_{solvatation\ (RI)}$$

where $\Delta G_{complex/solvent}$ and $\Delta G_{complex/vacuum}$ are the free energies of the complex in the solvent and in the vacuum and $\Delta G_{Solvatation\ (R + I)}$ and $\Delta G_{solvatation\ (RI)}$ are the free energies of solvatation of the separated entities and of the complex.

Autodock allows to calculate the free energy of complexation in the vacuum and can estimate the change of the free energy of the separated species and of the complex after solvatation. It is possible to calculate the free energy of complexation in solution and consequently the inhibition constant.

3.5.4 3D grids

Autodock use 3D grids which are calculated before the docking. It generates a grid for every element present in the molecule (at exclusion of the carbon, which is just differentiate between aliphatic and aromatic). This improve the calculation's speed because the grids are generated just once and then can be re-used to calculate the docking between others ligands (but containing the same atoms) and the same inhibitor. Autodock's grids are constituted by a three-dimensional set of points (it is possible to parameter the distance and the number of points) which forms a region containing the active site of the receptor. In every point of this grid, the potential energy of an atom-probe or of a functional group in interaction with the atoms of the receptor is calculated and stored.

A supplementary 3D grid of the electrostatic potential calculated by the interactions between the receptor and a probe of charge |e| is also necessary. To simulate the presence of the solvent, a dielectric function ε depending of the distance is used.

3.5.5 Hydrogen bonds

Hydrogen bonds are essential in a complexation process. For this reason, they are explicit in the Autodock calculations. Only the hydrogen able to form an hydrogen bond (hydrogen bonded to an heteroatom as nitrogen, oxygen or sulphur) are defined in the 3D grid of the atoms. A potential of the type Lennard-jones is used, and a function depending of the angle θ (figure 108) is also imposed.

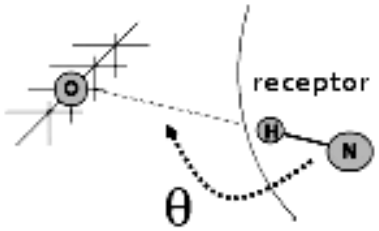

Figure 108

An hydrogen bond has the maximum of strength for an angle θ of 180° between the donor, the polar hydrogen and the acceptor. If the angle decreases, it decreases also the energy of the hydrogen bond. In the case of an angle between 0 and 90° the hydrogen bond is not possible.

3.5.6 The torsional term

A measurement of the loss of entropy due to the loss of degree of freedom after the complexation is also required. This term is proportional to the number of torsional angle (N_{tor}) of the ligand.
In particular:

$$\Delta G_{tor} = W_{tor} * N_{tor}$$

where W_{tor} is an empirical parameter.

3.6 Previous works in this lab and aim of this work

In the last two years, the challenge of the design and the synthesis of novel non covalent inhibitors of the 20S proteasome has been tackled by Lucia Formicola. Her efforts brought to the synthesis of a fluorinated pseudo amino acid (**295**) which, opportunely substituted, allows to inhibit the different active sites of the proteasome. Fluorine has become a fundamental tool in drugs development.[198, 199] In particular trifluoromethyl group is often used in medicinal chemistry to improve metabolic stability and/or biological activity.[200] It is hydrophobic, electron-rich, bulky and it can mimic functional groups as methyl, isopropyl and phenyl. Consequently, incorporating trifluoromethyl group in peptides or peptidomimetics can greatly alter their structural properties and thus their ability to interact with receptors and enzymes. The incorporation of a trifluoromethyl group into peptidomimetics to produce potent inhibitors of various enzymes has been extensively studied. In particular, the scaffold **295** was chosen because the presence of the trifluomethyl group can greatly improve the acidity of the neighbouring hydrazine functional group and thus improve its hydrogen bond donor ability.[199] In particular, the biological tests of a short library of molecules based on this peptidomimetics showed the ability of four of them to inhibit the 20S proteasome in a micromolar range (figure 109). Molecular modelling was the tool used for the conception of these molecules. The superimposition of two inhibitors (TMC-95A **289**, figure 104 and epoxomicin **286**, figure 103) crystallized in the chymotrypsin-like site of the proteasome showed a perfect superimposition of the main chain of these two inhibitors, with the presence of the hydrogen bonds with the same residues of the proteasome (T21, G47 and A 49). Moreover, also the lateral groups of the two inhibitors showed the same filling of the S1 and S3 pockets of the proteasome. In addition, Novartis research's group also demonstrated by molecular modelling and structure-activity relationship that the same hydrogen bonds were also formed by the aminobenzylstatine **294** (figure 106)**.** The design of these molecule was inspired by the

structure of the aminobenzylstatine inhibitor **294** synthesised by Novartis. Based on this model, the N-benzyl group of **294** which fills the S1 pocket is mimicked by a phenylalanine methyl ester, when the 3,4,5-trimethoxyphenylalanine interacting with the S3 pocket is substituted by a dimethoxypheylalanine or by the lysine, which is particularly able to bind the S3 pocket of the trypsin-like site and improve the solubility of the compound.[181] These two parts are then connected by the fluorinated peptidomimetic **295**. Finally, the terminal biphenyl was directly taken by the Novartis inhibitors for his ability to interact with the accessory AS1 and AS2 hydrophobic pocket. Superimposition of the resulted molecules with **294** was followed by a minimisation in vacuum using the MMFF94 Force Field[201] to prove that the inhibitors candidates were able to mimic the conformation of the known inhibitors.

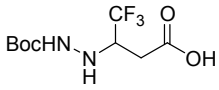

295

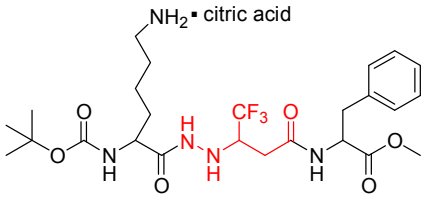

296

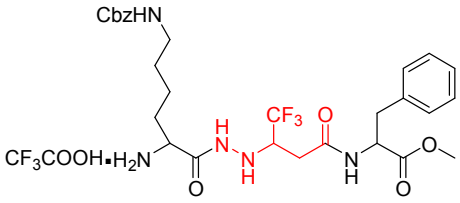

297

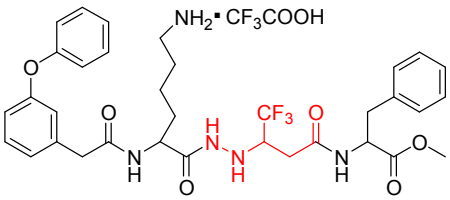

298

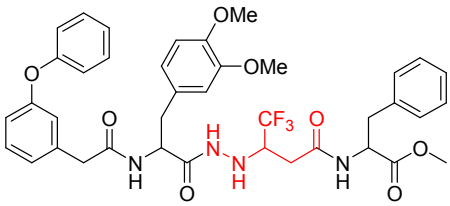

299

	CT-L	PA-L	T-L
296	32±2	6±0.5	30%
297	5.9±0.5	NI	4.4±1.2
298	1.6±0.1	2.7±0.1	8,4±1.3
299	85±15	72±0.7	x4

Figure 109 Chemical structures and IC_{50} or % of inhibition at 100 µmolar of the active molecules previously synthesised in our lab of rabbit 20S proteasome at pH 7.5 and 37°.
x: activation factor

On the other hand, other similar molecules (figure 110) containing the same peptidomimetic didn't show any inhibitory effect. In particular, molecules **300** and **301** are precursor of the active **296** and **298** with the amino group of the lateral chain of the lysine protected as Cbz, when in the molecule **302** the biphenyl is directly attached to the peptidomimetic scaffold without the presence of an additional amino acid.

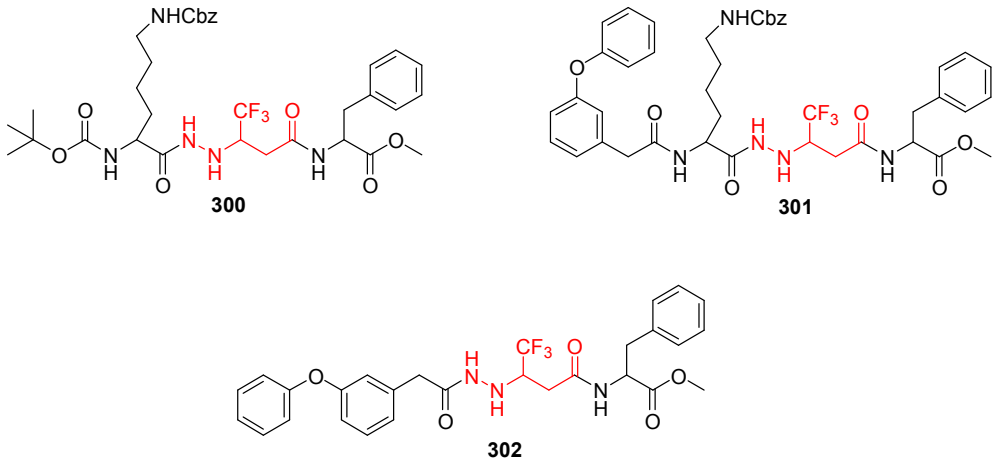

Figure 110

The understanding of the mechanism of interaction between these molecules and the different active sites of the proteasome is of great importance for the rational design of new inhibitors. In the aim to develop a useful tool able to supply some important indications for the synthesis of new inhibitors, a docking approach, which allows to evaluate the interactions between a ligand and a receptor, has been choose.
My one year research project was divided in the following steps:

1. Identification by means of literature and crystallography studies of the mechanism of interaction between the known inhibitors and the proteasome. This allows to identify the essential features (occupation of hydrophobic pockets, hydrogen bonds etc.) necessary for the inhibition of the proteasome.

2. Docking of known inhibitors to compare our results with the crystallised structures or with the reported molecular modelling studies. This allows to define the docking parameters and to validate the model.

3. Docking of the lead molecule (**296**) to formulate a first hypothesis of interaction.

4. Systematic modification of the lead molecule and subsequently docking of the suggested molecules to address the synthetic work.

5. Use of the biological evaluation results of the synthesised molecules to refine the docking parameters and for a well understanding of the binding interaction between molecules and proteasome.

3.6.1 Literature and crystallographic studies

Protein data bank is as useful tool which allows to obtain the X-ray structure of a large number of proteins crystallised both alone and in the presence of an inhibitor. The structures are available in a .pdb file format, which can be read by the most common molecular modelling and docking program (such, in our case, Sybyl, Accelrys DS Visualizer, Autodock4 and Pymol). In particular, it is possible to find different X-ray structures of the 20S proteasome crystallised alone[146, 202] or in complex with non covalent[178, 179] or covalent[145, 203, 204] inhibitors. As reported in literature, the structure of the active site does not differ substantially in the case of yeast, rabbit or mammalian proteasome. The differences are just limited to the presence of different amino acids in not-key position, without affecting the structure of the active site. In addition, it is also demonstrate that the X-ray structure of the proteasome in presence of an inhibitor is perfectly super-imposable to the crystal structure of the proteasome alone,[205] which simplify the docking studies because it is possible to consider the proteasome as a rigid structure without affecting the accuracy of the results.

The bibliographic research allowed to identify some "ligand-receptor" (in docking studies receptor is a general macromolecule which interacts with the ligand) interactions which are common to all the non covalent inhibitors of the proteasome and which are also often present in the covalent inhibitors. The first and most important characteristic is the ability of these low-yield molecules to have a good filling of both the S1 and S3 pockets (in figure 111 it is showed as example the binding mode of the TMC-95A in the CT-like site). The region between the two pockets is also very important for the stability of the complex. In effect this region is sandwiched between two β-sheets, for this reason the inhibitor has to present functional groups which are able to stabilise the complex by means of the formation of hydrogen bonds. In particular, it was demonstrated that the hydrogen bonds with some residues, i.e. T21, G47, A49, are necessary for the formation of a stable receptor-ligand complex. In addition, other hydrogen bonds can be suitable, such as with G23, D114 (which is present only in the chymotrypsin-like and the trypsin-like site, but not in the caspase) and D120 (which is present at the bottom of the S3 pocket only in the trypsin-like site). A last common feature is the distance between the part ligand which protrudes in the S1 pocket and the T1, which is usually between 3 and 4 Å.

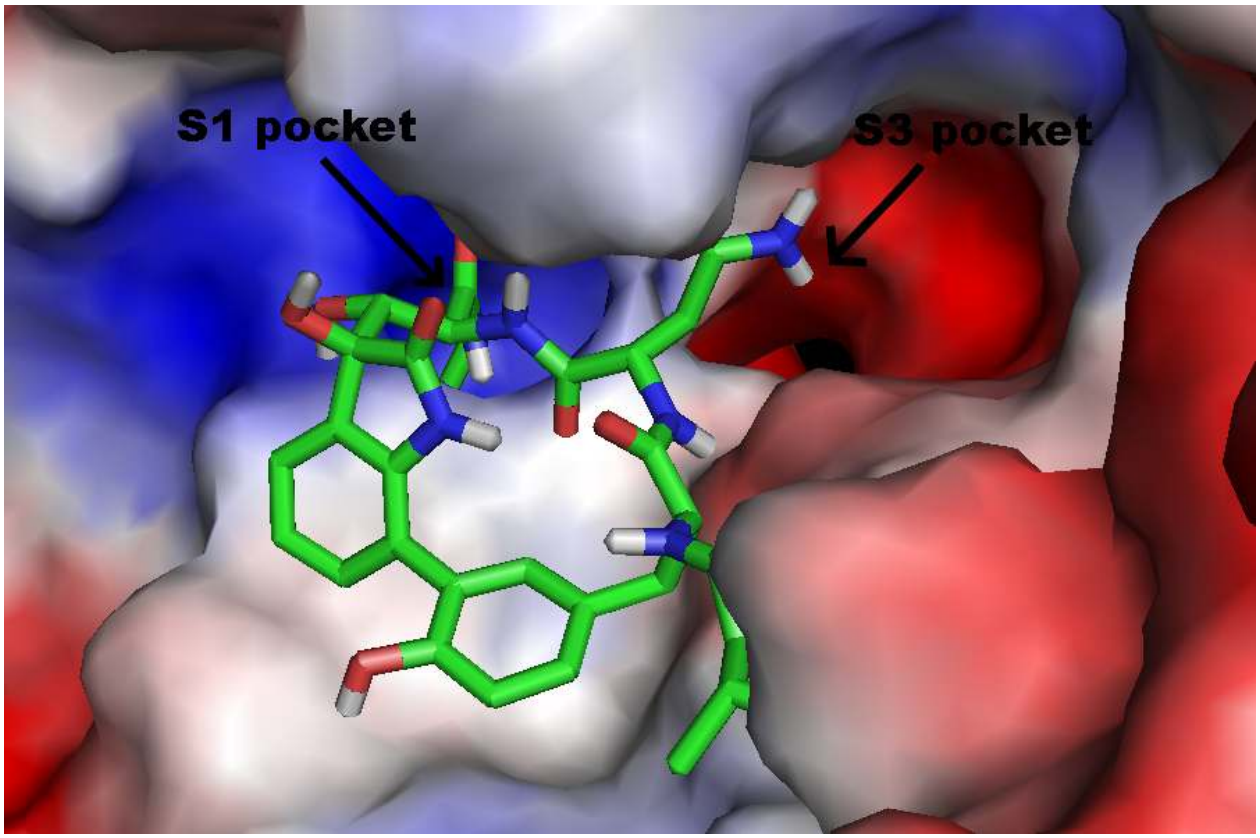

Figure 111: Binding mode of the TMC95-A in the 20S proteasome

3.6.2 Choice of docking parameters and docking of the known inhibitors

A docking experiment with Autodock consists in different steps. The first step is the preparation of both the receptor and the ligand. The file containing the three-dimensional structure of the proteasome co-crystallised with the TMC95-A was obtained directly by the professor Groll in the .pdb format and converted by autodock4 in a .pdbqt file, which is the format required by this docking program. In effect, just the two β-subunits forming the different active sites have been

used, reducing the calculation time. The ligands were prepared by using the program Sybyl as .mol2 format and then automatically converted by Autodock4 in .pdbqt files.

The second step is the preparation of a potential grid containing the active site where the ligand has to be free to explore the conformational space. This grid was centred on the position of the TMC95-A and was big enough to allows a good mobility to the ligand (the box was of 60-60-50 points with a spacing of 0.375Å for all the three active sites).

The third step is the choice of the docking parameters and this is the trickiest step. Approaching our problem, it was immediately clear that it was necessary not only to have a technique able to give us good docking results, but also, due to the large number of molecules to test, able to give a result in a relatively short time (less than 24 hrs.). These two exigencies go in opposite directions because a most accurate calculation needs obviously more time, which is in contrast with the exigency to screen a large number of molecules.

In particular, Autodock4 program allows to modify different parameters which are directly related with the quality of the results and the running time machine. The two most important are the number of conformations generated by the program and the number of evaluations done by the program for every conformation generated. The different conformations generated by the program are organised in clusters, it means groups of molecules which adopt similar conformation. Autodock generate automatically the clusters using the RMSD parameter and assign for every cluster a binding energy obtained by its score function. More molecules are present in the same cluster, better is the docking result. Typically a larger number of evaluations for every conformation leads to have clusters of bigger dimensions, and theoretically an infinitive number of evaluations leads to just one cluster containing always the same conformation. In figure 112 is represented a typical example of the variation of the clusters at the variation of the number of evaluations (ga_num_eval in the scheme). In the first case, with 250K evaluations for every conformation, we can see as the best cluster is not the cluster with the lower binding energy (indicate here as Best Dock), but with 2.5M evaluations the best dock and the best cluster are coincident and contains up to 70% of the conformation generated. In this case the situation joined the convergence and a larger number of evaluations does not change significantly the result. In the scheme it is also indicated the running time machine, which is proportional to the number of evaluation.

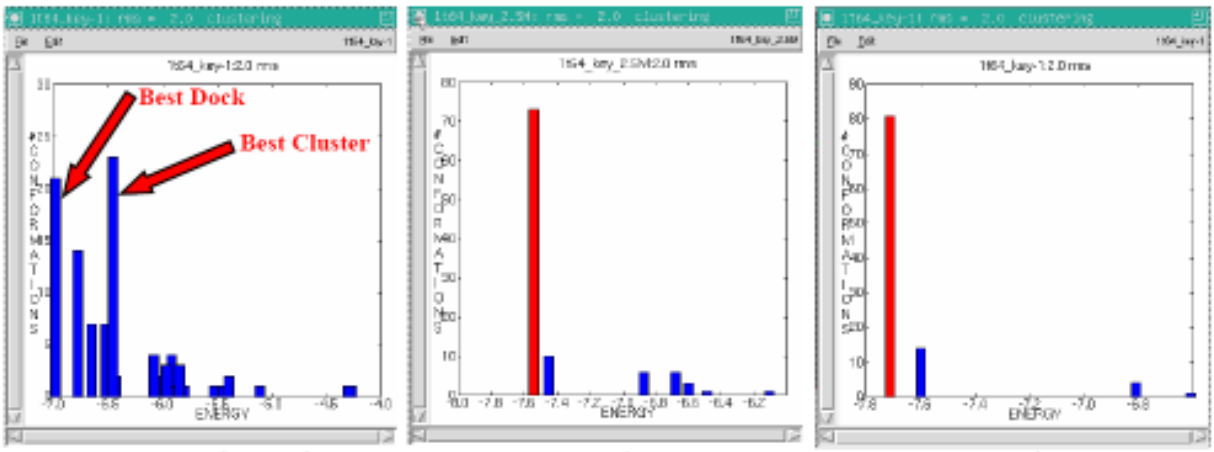

ga_num_eval = 250k
11m 49s

ga_num_eval = 2.5M
1h 43m

ga_num_eval = 25M
17h 3m

Figure 112

Our first docking experiments was done on the TMC95-A and its biaryl analogues (figure 89), because they are the only non covalent inhibitors co-crystallised with the 20S proteasome. In this case it was simple to join the convergence after 2.5M evaluations and the docking results fitted the experimental structure in an excellent way, with an RMSD less than 2.0 Å (figure 113).

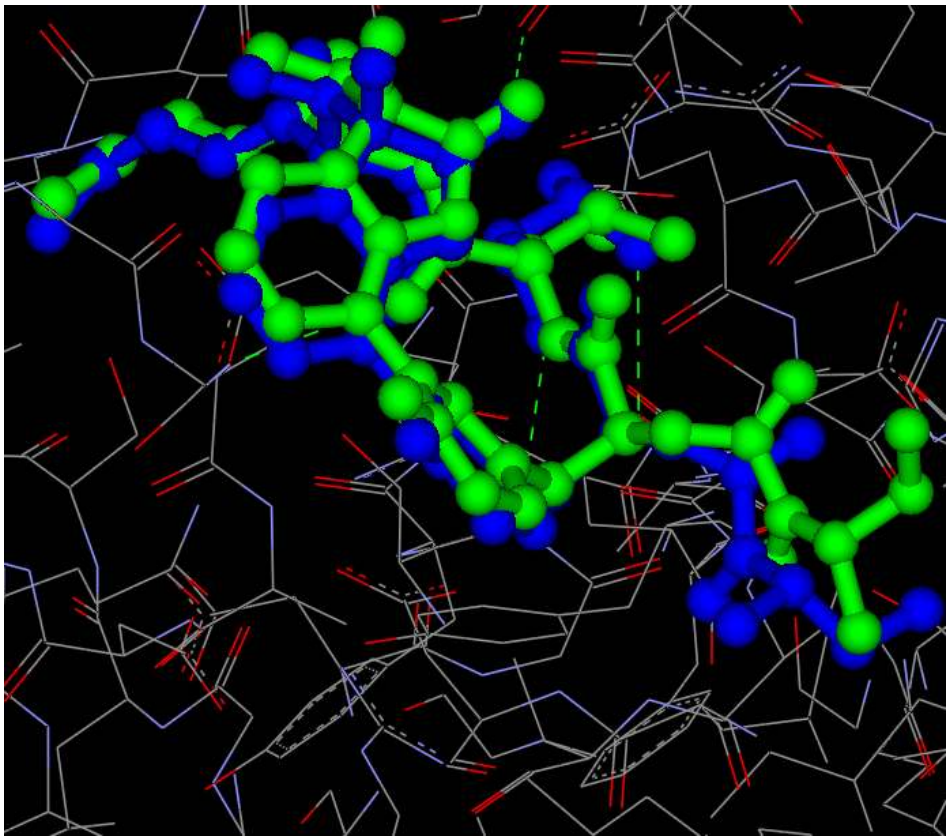

Figure 113 In green the crystallised structure of the TMC95-A in chymotrypsin-like site, in blue the calculated one.

Due to its rigidity, this macrocycle is unfortunately simpler than the linear and flexible molecules in our job. For this reason, we started to analyze other non covalent inhibitors with a well-known binding interaction (obtained by molecular modelling and structure-activity relationship), but without a crystallographic proof. The major contributions have been obtained from some animostatine based inhibitors (**293** and **294**, figure 106) synthesised by a research group of Novartis.[182] In particular, the docking result for the molecule **294** (figure 114) in CT-L site fitted quite good the molecular modelling studies reported. In effect, in our calculation it was possible to find the filling of the S1 and S3 pockets by the same groups described by the authors, and also the presence of the same principal hydrogen bonds, between the main chain of **294** and the residues 21, 47 and 49 of the proteasome and between the methoxy groups of the central 3,4,5-trimethoxyphenylalanine and some serines (in particular the residues 118) present at the bottom of the S3 pocket. The main problem was that in the case of a so flexible inhibitor, similar to our molecules for the number of torsions, the system could not join the convergence after several days (only 4 conformations on 50 generated in the main cluster after 3 days), which was not compatible with the purpose of our project.

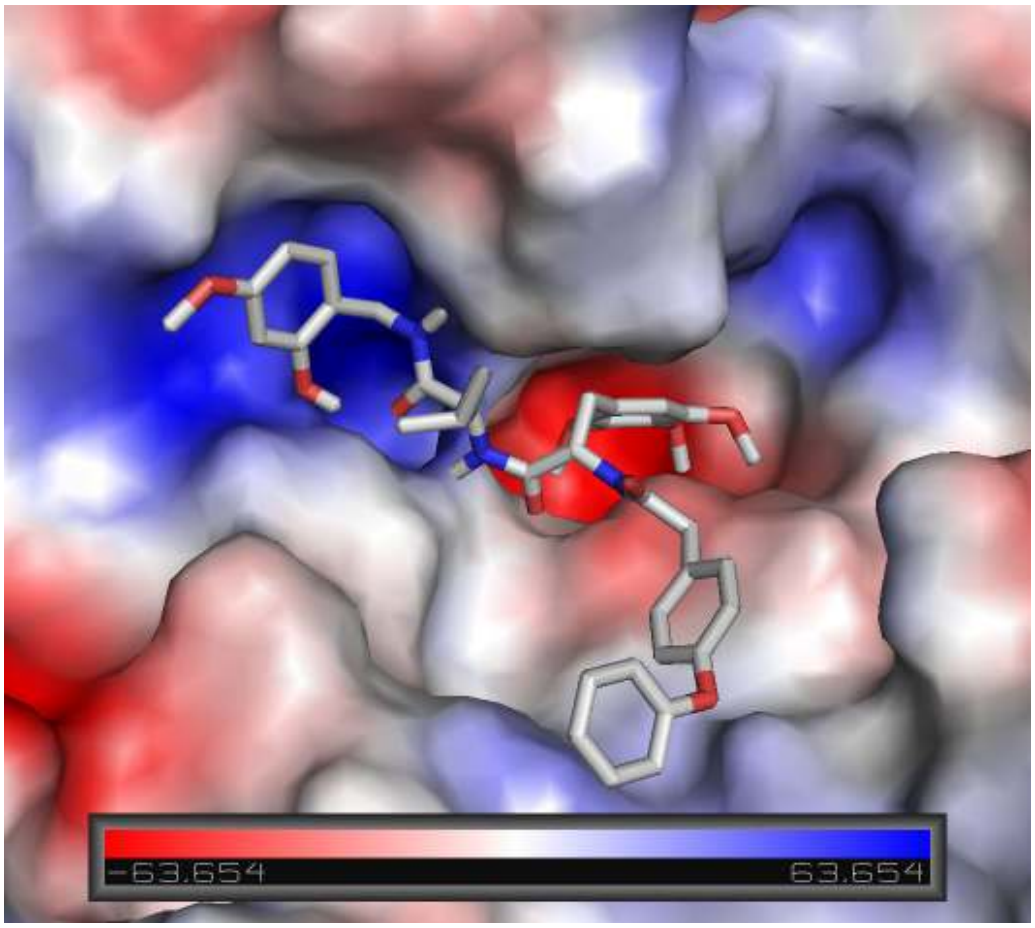

Figure 114

To overcome this problem another strategy has to be adopted. An interesting idea was obtained by Smith et al.,[206] which reported a docking study about some polyphenols of the green tea showing an inhibitory effect of the 20S proteasome (for example the (-)-epigallocatechin-3-gallate (ECGC) **291**, figure 89). In this paper the authors overcome the problem of the lack of a good clustering by analysing the clusters obtained with a better free energy of binding and choosing the most probable conformation following as criteria the distance between the ester carbonyl carbon of the ligand and the hydroxyl group of the Thr1 and the occupation of the S1 pocket by the A-C ring of the polyphenol. With this procedure they could obtain a linear correlation between the ΔG of binding calculated by Autodock and the experimental K_i. Another input has been obtained by a publication of Cozzini et al. in 2004[207] who explored the possibility to use docking methodology in case of few (or lack of) crystallographic data to produce new lead candidates. Based on the crystal structures of just three ligand-ERα receptor complexes they

identify common features, in particular hydrogen bonds with some residues of the receptor, present in all the complexes. They then docked a small set of known ligands assigning them a rate on the base of the Autodock binding energy, the distance between the ligand and the key residues of the receptor and the HINT score function (which essentially measure the hydrophobic interactions). For the same admission of the authors, with this approach it is difficult to obtain a quantitative range or scoring scales (specially because the error associated with the scoring Autodock function is of nearly 2 Kcal/mol), but these results are able to drive further QSAR analysis and even the synthesis.

Adapting these main guides to our case, we decided to set the parameters to 50 conformations generated and 10 millions evaluations. We were aware of with these conditions it was not possible to join the convergence, but we were able to limit the time to 16-18 hours for every calculation, depending of the number of torsions present in the ligand. Because it was not possible to clearly identify the best conformation due to the absence of a good clustering, we decide then to analyse the most favourable conformations (at least 5) searching for the criteria discussed in the last paragraph. In particular, for every candidate, the simultaneous occupation of both S1 and S3 pockets was the first discriminating. In other words, it has been supposed that to have an inhibitory effect, a molecule have to fill both this two hydrophobic pockets, and the absence of this feature lead to discard the molecule. Related to this characteristic, it was also measured the distance between the ligand and the T1, which should be between 3 and 4 Å and help to indicate a good filling of the S1 pocket. Secondary, it was analysed the presence of intermolecular hydrogen bonds between the ligand and the active site, in particular with T21, G47 and A49, which indicate a good filling of the region between the 2 β-sheet indispensable for a stabilisation of the complex. Moreover, the presence of additional hydrogen bonds, such as with G23, D114 and D120 (these last two not always present), and a good binding energy calculated by Autodock, were considered important features.

3.6.3 Docking of the lead molecule and virtual screening of new candidates

At the begin of my work, from the molecules with an inhibitory effect presented above, only the molecule **296** was tested and for this reason all the efforts to propose a first mechanism of binding were done only on the base of the molecule **296**. Moreover, the biological test was done

only on the chymotrypsin-like site, and for this reason the first studies were done in the CT-L site. In this case, different dockings changing the Autodock parameters were performed to find the best conditions and to obtain a more reliable result, the docking was done with a larger number of evaluations (25 millions). Additionally, because the pseudo amino acid **295** is obtained as racemic, it was necessary to perform two different calculations, respectively with the S and R configuration of the chiral centre bearing the CF_3. The result suggested that the Boc group was inserted in the S1 pocket and the phenylalanine in the S3, whereas the free amino group of the lateral chain of the lysine was involved in an hydrogen bond with the residue T21 (in figure 115 is represented the result for the S configuration, in green dashed the intermolecular hydrogen bonds). Deeply analysing this result, it was possible to see as the Boc group is inserted in the S1 pocket, with a distance between the tert-butyl group and the T1 of 3.1 Å, which indicates a good filling of this pocket. The phenylalanine is inserted in the S3 pocket and the methoxy group could form an additional hydrogen bond with the serine 118, which is at the bottom of the S3 pocket. This hydrogen bond, also if is not on of fundamental for the interaction with the proteasome, is also reported by Novartis[208] as useful to stabilise the complex. In the region between the two hydrophobic pockets, the ligand formed hydrogen bonds with the residues G47 and A49 respectively with the oxygen and the nitrogen of the urethane moiety, and with T21 with the free amino group on the lateral chain of the lysine and with the hydrazine moiety. It was also present a strong interaction between the trifluoromethyl group and the residue D114. Moreover, the binding energy calculated by Autodock was excellent, with a value of -9.20 Kcal/mol. In addition, the other clusters generated by the program, presented an higher binding energy (more than -6.0 Kcal/mol) suggesting as this is the most probable conformation. Thus, we can conclude than in this active molecule it was possible to find all the features common to the other proteasome inhibitors. Less clear was the result obtained for the molecule with the R configuration of the carbonyl bearing the CF_3. In every case, when the cluster at minor binding energy did not present a good conformation, the second better cluster presented a result quite similar to that obtained for the S diastereomer, with the Boc group in the S1 pocket and the phenylalanine in the S3. The Boc group was less inserted in the S1 pocket (the distance with the T1 was of 4.8 Å), when the phenylalanine had a good filling of the S3 pocket (also in this case it was observed the hydrogen bond with the S118). Less intermolecular hydrogen bonds could be found (only with T21 and D114) and this fact was reflected in an higher binding energy (-6.30 Kcal/mol).

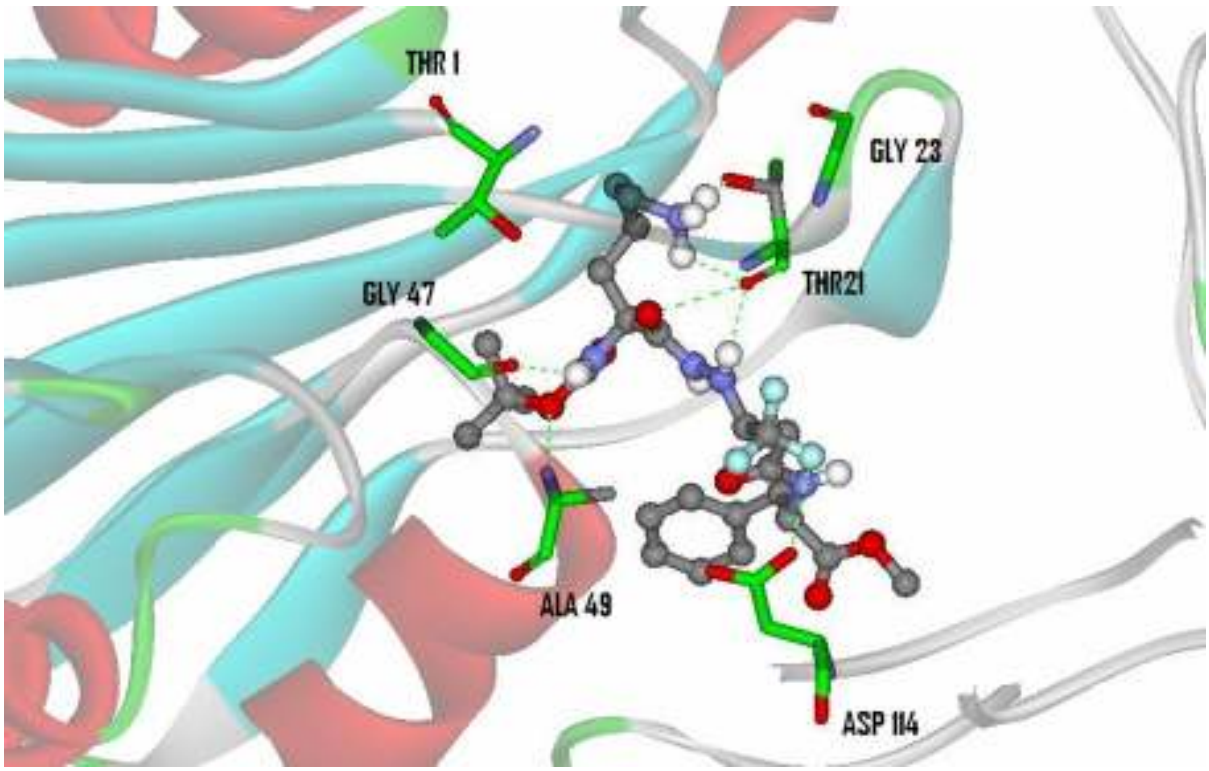

Figure 115

Based on this first model, we decided to perform pharmacomodulation on the lead molecule **296** to evaluate the influence of each part of the molecule to try to establish structure-activity relationship and to try to obtain better proteasome inhibitors. We decided to substituted the Boc group with other adapt to fill better the S1 pocket, the phenylalanine with group able to fill the S3, the lysine with other amino acids and we also tried to see the influence of the substitution the central core of the molecules (in figure 116 the groups tested and, with a red bar, the rejected).

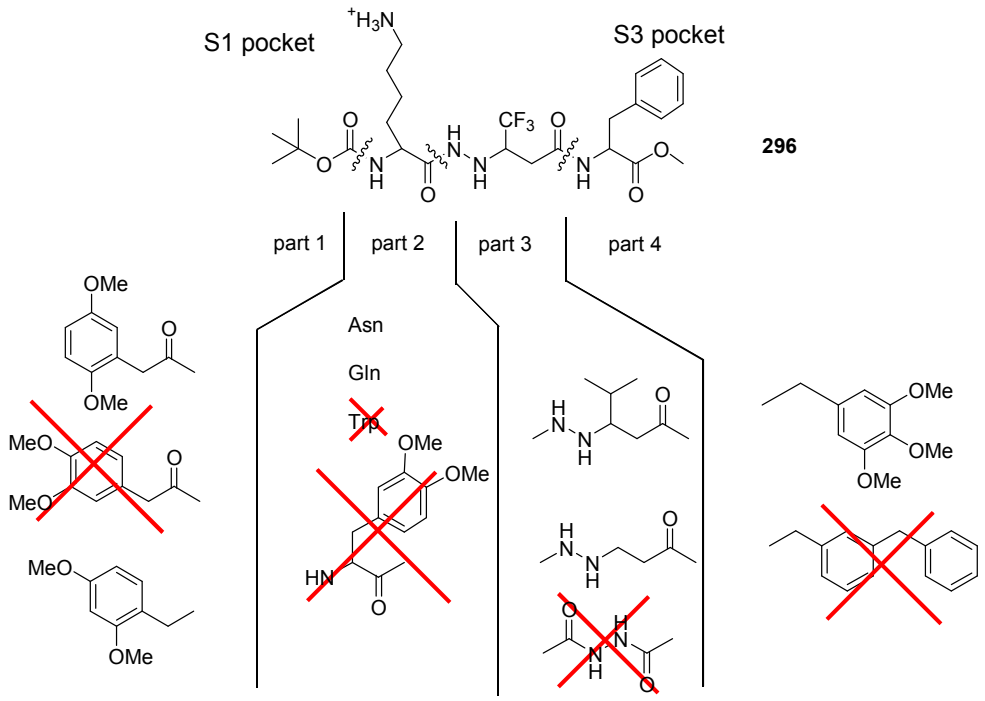

Figure 116

It was decided to substitute the Boc group with a dimethoxy-phenylacetic acid group and the docking result showed that a trimethoxyl group in position two of the ring was the most favourable to have a good interaction with the T1. The lysine was substituted by different amino acids and the docking results showed that the most favourable amino acids were asparagine and glutamine, whereas tryptophan and the unnatural 3,4-di-(trimethoxy)-phenylalanine have the tendency to fill the S3 pocket without leaving enough space for a good filling of the S1 pocket by the part 1. For the part 3 other peptidomimetics used as β-sheet mimetics and non fluorinated analogues of the same peptidomimetic have been evaluated. In particular, this is interesting to prove the role of the fluorine to reinforce the hydrogen bond of the adjacent groups. In the part 4 it was decide to substitute the phenylalanine with a trimethoxy-benzylamine, which is particularly able to form hydrogen bonds with the serines present at the bottom of the S3 pocket of the CT-L site, as proved by Novartis.[182, 208]

Herein, we present the synthesis of a small library of peptidomimetics, their biological evaluation and a first attempt of a rational explication of the binding mode based on our model.

3.6.4 Synthesis of the fluorinated peptidomimetic 295

First step of the synthesis is the preparation of the fluorinated ethyl acrylate **305** by reduction of the 4,4,4-Trifluoro-3-oxo-butyric acid ethyl ester **303** with sodium boro hydride and successive hydrolysis in presence of hydrochloric acid gave the alcohol **304** which was then dehydrate by heating in the presence of P_2O_5 (figure 117), to give the desired compound **305** in 52% overall yield.

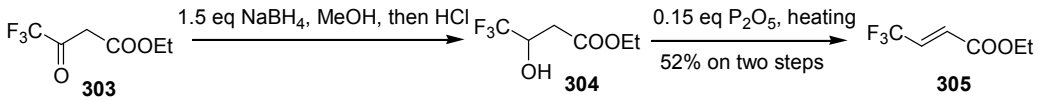

Figure 117

Michael addition with Boc-hydrazine was performed in methanol to give the β-hydrazino ester **306** in excellent yield. Due to the low boiling point of the acrylate **305** (comparable with that of the methanol) the reaction was performed in a seal tube with an oil bath temperature of 80°C. The reaction is completely non stereoselectivity and the product **306** was obtained as a racemic mixture. Unfortunately, also in the next steps, it was not possible the two compounds, for this reason the molecules were tested as a mixture of diastereomers.

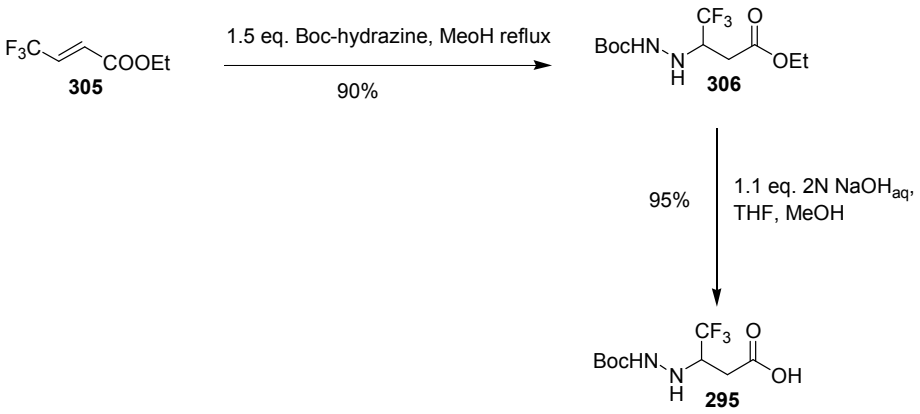

Figure 118

2.6.5 Solution phase synthesis of the inhibitors

Starting from the pseudo amino acid **295** a set of different molecules has been synthesised. The first diversity was introduced at the level of the first coupling with the free carboxylic group of **295**. This coupling has been performed both with L-phenylalanine methyl ester hydrochloride and 3,4,5-trimethoxy benzylamine in good yield (Figure 119).

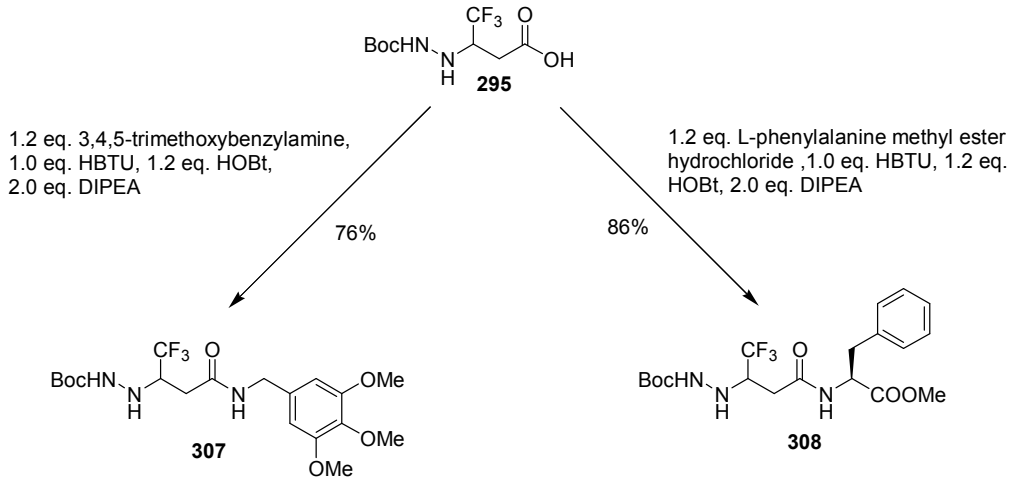

Figure 119

At this point, it was possible to introduce a second element of diversity coupling the fragments **307** and **308** with different amino acids. In particular L-lysine and L-asparagine have been choiced (Figure 120).

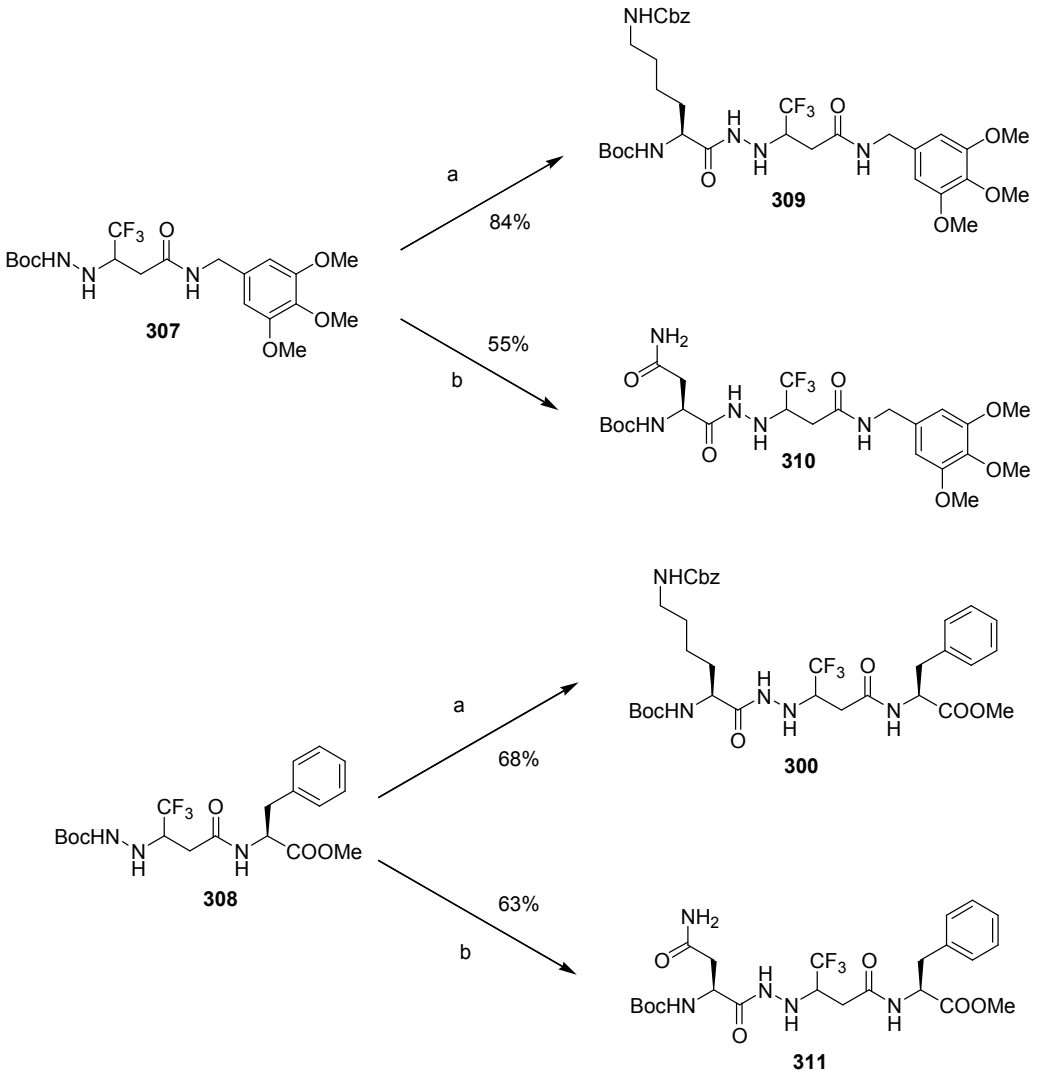

Figure 120 a. 1)TFA:DCM 1:1 2) 1.2 eq. NαBocNεLysine, 1.2 eq. HBTU, 1.2 eq. HOBt, 5 eq. DIPEA b. 1)TFA:DCM 1:1 2) 1.2 eq. NBocAsn, 1.2 eq. HBTU, 1.2 eq. HOBt, 5 eq. DIPEA

Starting from the molecule **309** the following molecules were prepared (Figure 121). Molecule **312** was obtained by a standard Boc deprotection of **309** as trifluoroacetic acid salt in quantitative yield and it was then coupled in standard conditions with the 2,5-dimethoxyphenylacetic acid to give the product **313**. Unfortunately, hydrogenolysis of the Cbz group in the presence of 10% Pd/C did not give the desired product, but only starting material has been recovered. Addition of a further amount of catalyst or of acetic acid did not give the desired compound **314**, but, also after more days, only the starting material and some unidentified subproducts were recovered.

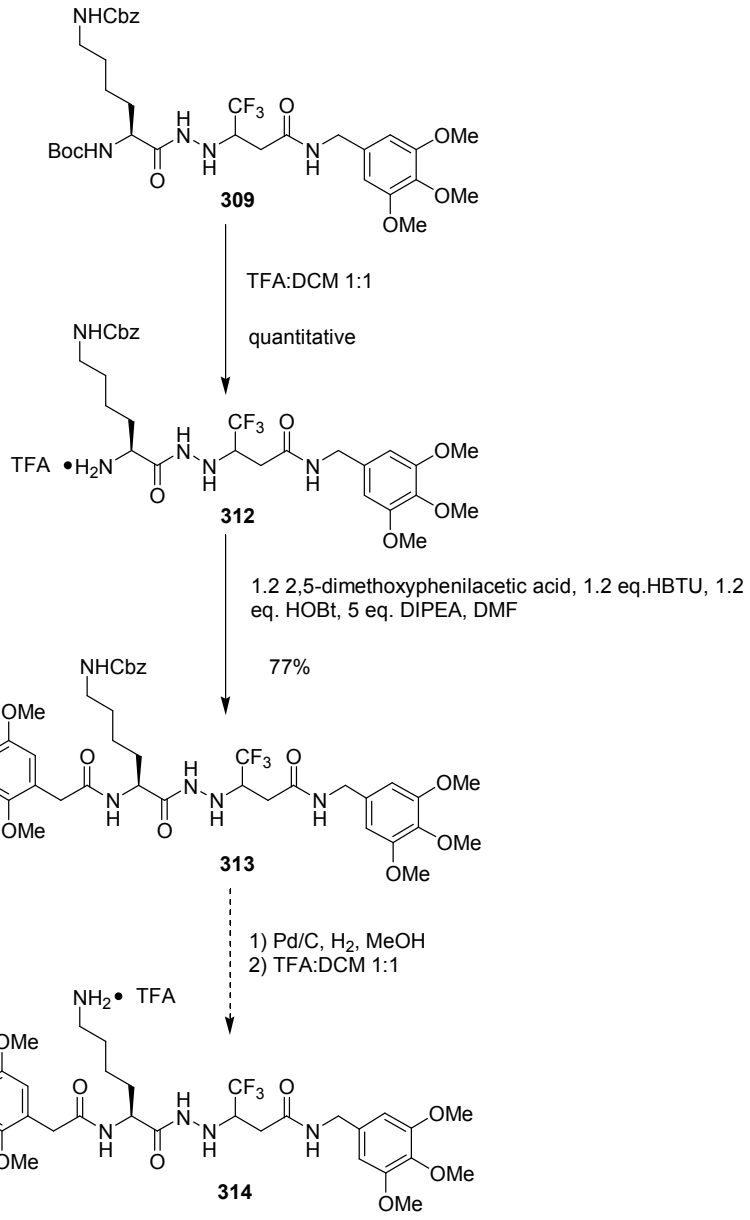
NHCbz
BocHN
CF3
OMe
OMe
OMe
309
TFA:DCM 1:1
quantitative
TFA •H2N
312
1.2 2,5-dimethoxyphenilacetic acid, 1.2 eq.HBTU, 1.2 eq. HOBt, 5 eq. DIPEA, DMF
77%
313
1) Pd/C, H2, MeOH
2) TFA:DCM 1:1
NH2• TFA
314

Figure 121

The same protocol were followed to obtain compounds **297**, **315**, and **316** from **300 (**figure 122) i.e.,

i. Cleavage of the Boc group ton give the **297** in a quantitative yield

ii. Coupling with 2,5-dimethoxyphenylacetic acid to give the intermediate **315** in 84% yield

iii. Cleavage of the Cbz group to afford **316** in 82% yield

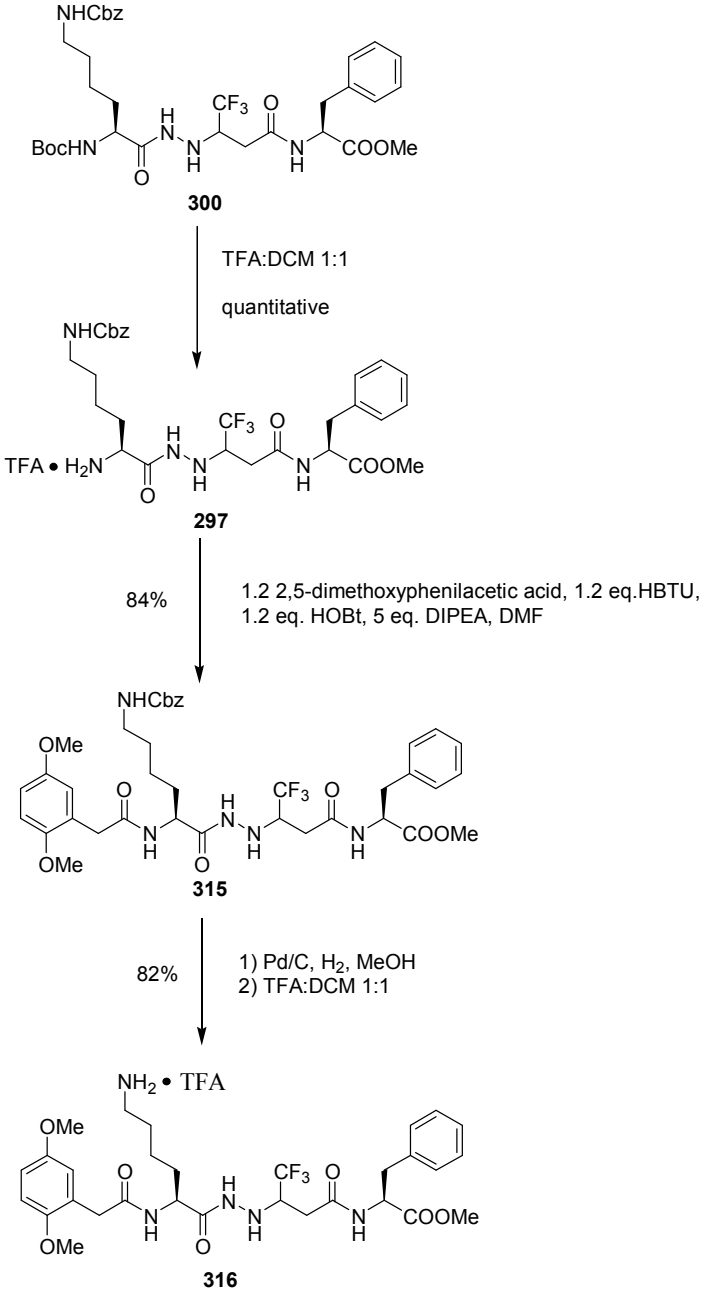

Figure 122

The cleavage of the Boc group of **311** followed by a coupling with 2,5-dimethoxyphenylacetic acid afforded the desired compound **317** in 65% yield after two steps (Figure 123).

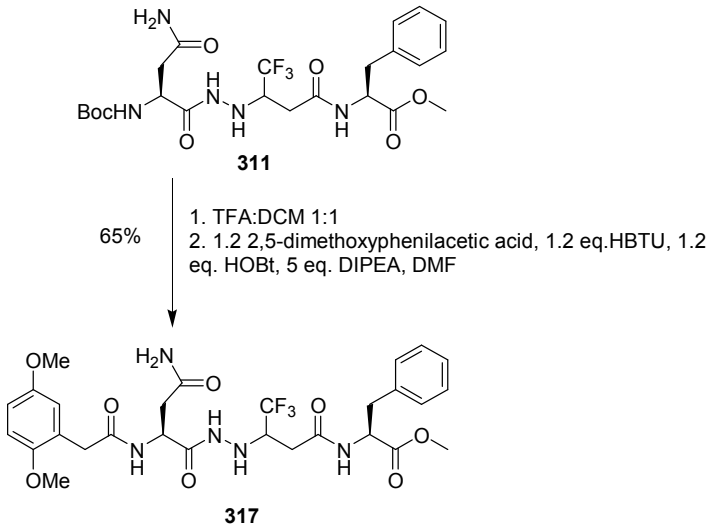

Figure 123

Because our pseudo amino acid **295** could be a spacer enough long to maybe bear directly the groups filling the S1 and S3 pockets, the molecule **318** has been also designed and synthesized (Figure 124).

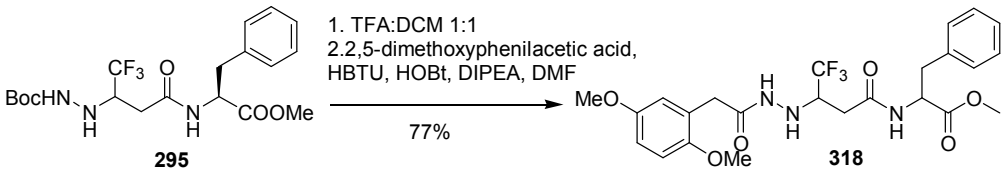

Figure 124

In addition, to verify the influence of the fluorine in the binding with the proteasome, some non fluorinated analogues of these molecules have been also designed and synthesized. It was so decided to synthesize the pseudo amino acid **324** (Figure 125). The first attempt was a Michael addition of Boc-hydrazine **320** and the methyl acrylate **319** in the conditions used for the fluorinated scaffold. Unfortunately the methyl acrylate resulted a too reactive substrate and for this reason instead of the desired product **321**, which was recovered just in traces, was obtained

the product **322**. The same result was obtained performing the reaction at low temperature and for a short time reaction. Thus, it was decided to synthesized the pseudo amino acid reacting the ethyl bromoacetate **323** with Boc-hydrazine **320.**[209, 210] The desired product **323** was obtained in a moderate yield. Basic hydrolysis of this compound gave the desired Boc-protected amino acid **324**.

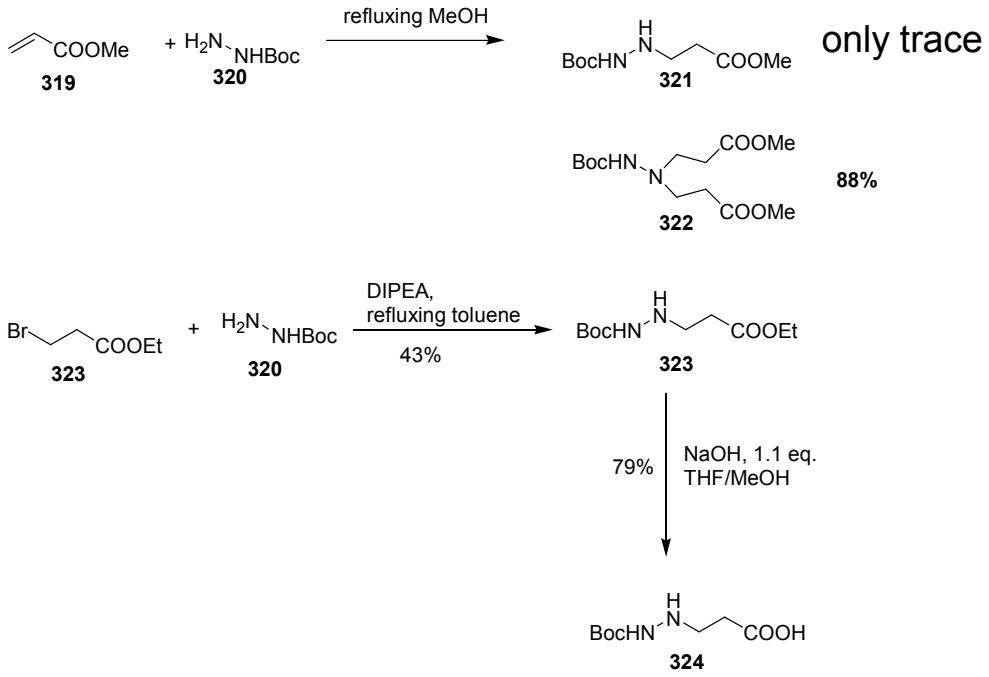

Figure 125

Following the same synthetic ways of the fluorinated scaffold, the peptidomimetic **324** was then coupled with at the free carboxylic group with the phenylalanine ethyl ester hydrochloride to give the product **325** in a good yield. Compound **325** was then deprotected at the N-terminus by reaction with trifluoroacetic acid and coupled with the NαBocNεCbz-L-Lysine to obtain the molecule **326** in a good yield. A further deprotection of the urethane brings to the molecule **327** as TFA salt. Coupling reaction with the 3-phenoxy-phenyl acetic acid gives the product **328**. Unfortunately, the deprotection of the Cbz group by hydrogenolysis was difficult and only starting material and some unidentified subproducts were recovered (figure 126). Hydrogenolysis of the compound **328** under different conditions (more pressure, a different amount of catalyst or in the presence of acetic acid) was not carried out.

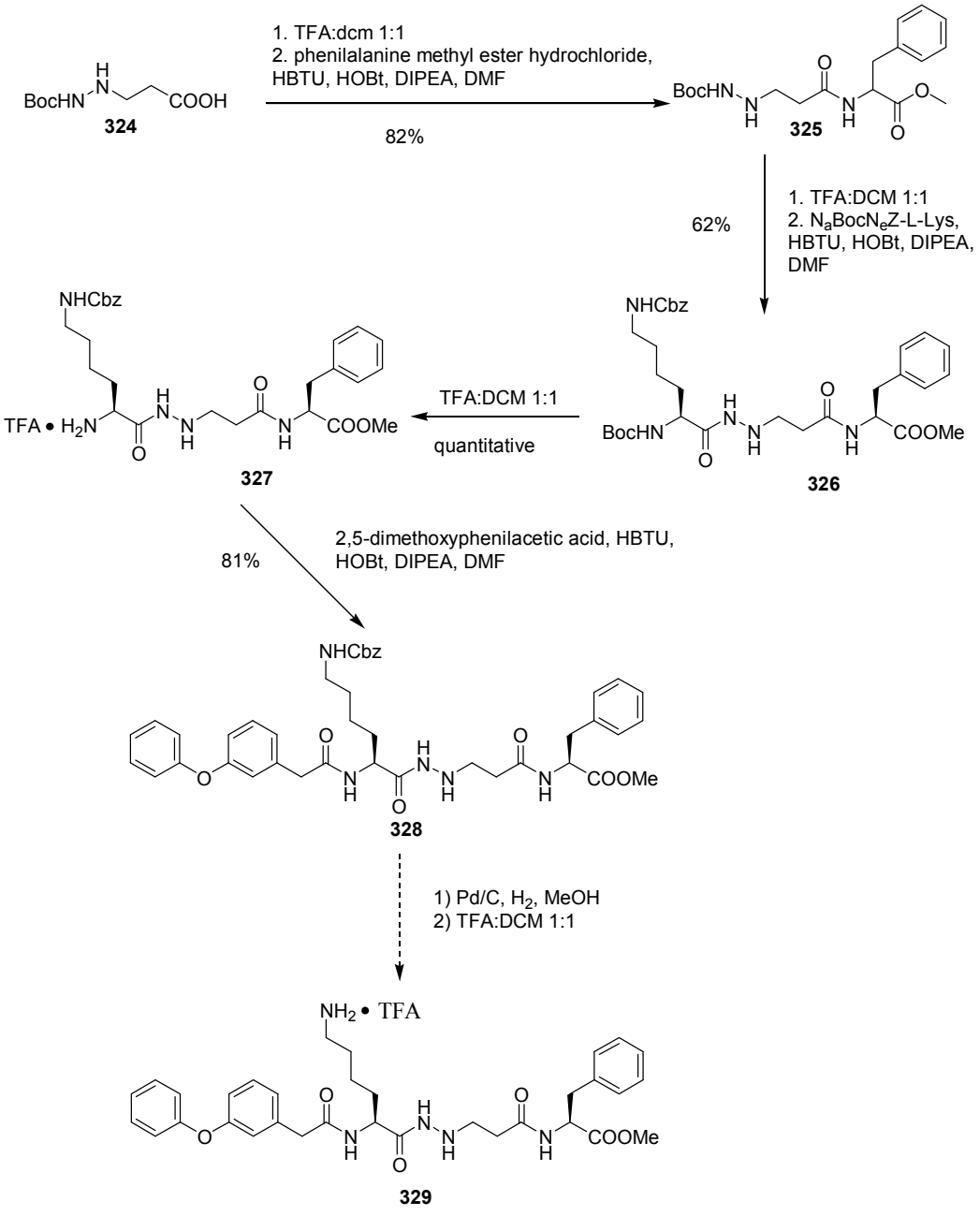
1. TFA:dcm 1:1
2. phenilalanine methyl ester hydrochloride, HBTU, HOBt, DIPEA, DMF
82%
1. TFA:DCM 1:1
2. NaBocNeZ-L-Lys, HBTU, HOBt, DIPEA, DMF
62%
TFA:DCM 1:1
quantitative
2,5-dimethoxyphenilacetic acid, HBTU, HOBt, DIPEA, DMF
81%
1) Pd/C, H2, MeOH
2) TFA:DCM 1:1

Figure 126

3.7 Results and discussion

In figure 127 are represented the final molecules and the intermediates which were purified and prepared for the biological tests. Due to the relatively low number of experimental data and to the quite different structures of the tested molecules it is not possible to have a structure-activity relationship, but it is possible to do some general considerations about the binding mode of the selected molecules. Moreover, it is possible to explain the different behaviour of quite similar molecules in the binding with the active sites of the proteasome. To integrate the results also the seven molecules previously synthesized by Lucia Formicola (molecules **296-302**) have been studied. Moreover, all the fluorinated molecules, were tested as a mixture of diastereomers. The diastereomeric ratio for each molecule have been determine by ^{19}F-NMR and it is reported in the experimental part of this thesis. The biological tests have been carried out in the laboratory of Enzymologie Moléculaire et Functionelle, FRE2852, CNRS-UPMC (Université Paris VI) by Nicolas Basse and Xavier Maréchal under the supervision of Professor Michèle Reboud-Ravaux. CT-L, PA and T-L activities were determined by monitoring the hydrolysis of Suc-LLVY-AMC, Z-LLE-bNA and Boc-LRR-AMC and, respectively, for 45 min at 37 °C in the absence (control) or presence of test compounds (0.1-200 μM). The buffers (pH 7.5) were 20 mM Tris, 1 mM DTT, 10 % glycerol, 0.02 % (w/v) SDS for CT-L and PA activities, and 20 mM Tris, 1 mM DTT, 10 % glycerol for T-L activity. The IC_{50} values (inhibitor concentrations giving 50 % inhibition) were obtained by plotting the percent inhibition against inhibitor concentration to equation % inhibition = $100[I]/(IC_{50}{}^{nH} + [I]^{nH})$ or equation % inhibition = $100[I]^{nH}/(IC_{50}{}^{nH} + [I]^{nH})$ where n_H is the Hill number. The K_m values of the fluorogenic substrates in our experimental conditions were: XX (Suc-LLVY-AMC), YY (Z-LLE-bNA) and ZZ (Boc-LRR-AMC).

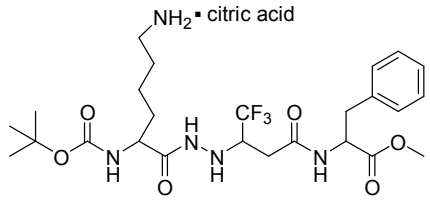

296

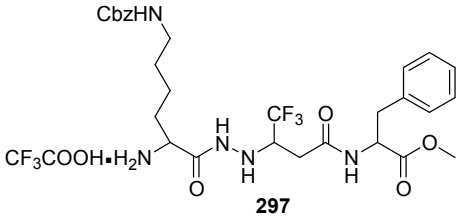

297

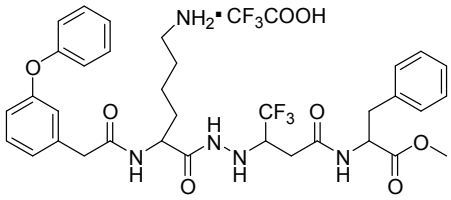

298

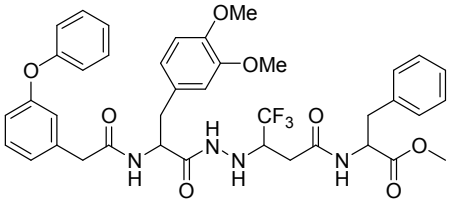

299

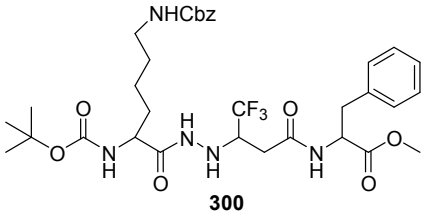

300

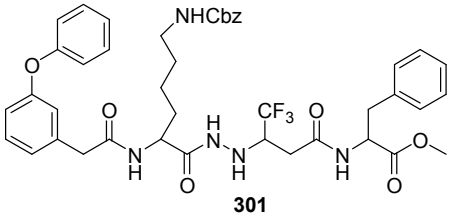

301

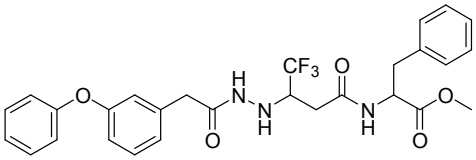

302

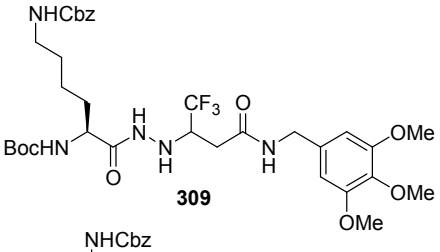

309

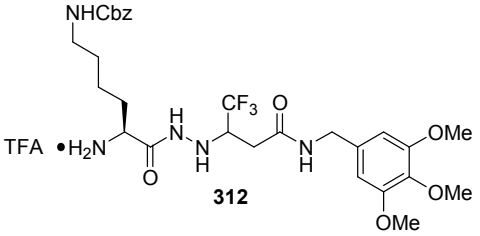

312

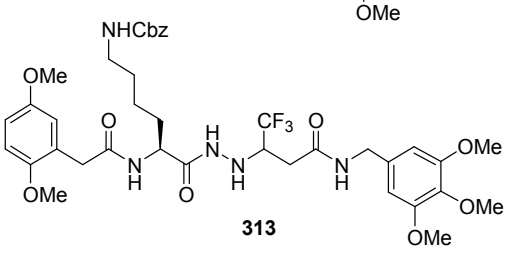

313

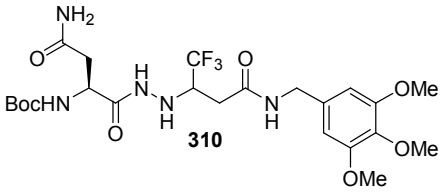

310

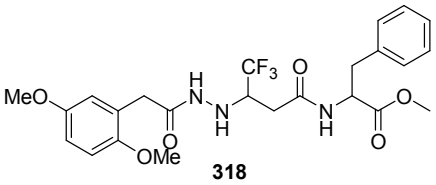

318

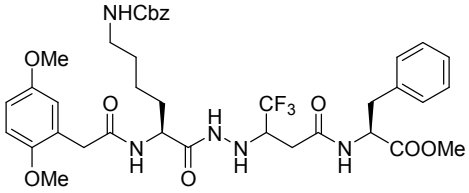

315

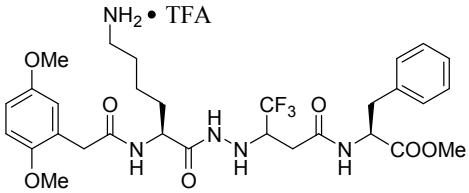

316

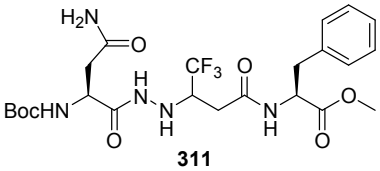

311

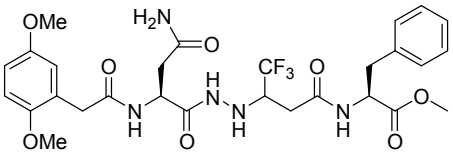

317

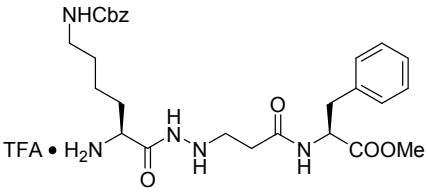

327

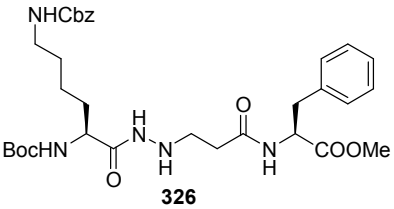

326

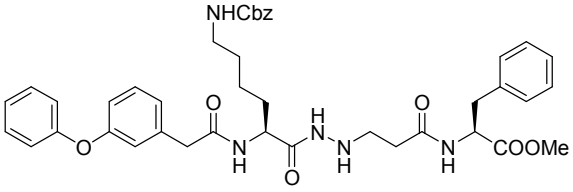

328

Molecule	CT-L	PA	T-L
296	32±2	6±0.5	30%
297	5.9±0.5	NI	4.4±1.2
298	1.6±0.1	2.7±0.1	8,4±1.3
299	85±15	72±0.7	X4
300	N.I.	N.I.	N.I.
301	N.I.	N.I.	N.I.
302	N.I.	N.I.	N.I.
309	N.T.	N.T.	N.T.
310	30%	77	x2.7
311	N.T.	N.T.	N.T.
312	10.1±0.4	I	I
313	N.I.	N.I.	x1.8
315	30%	54	x1.6
316	8.6±0.3	I.	I.
317	N.I.	N.I.	N.I.
318	N.I.	N.I.	N.I.
326	48.5±2.4	I.	I.
327	18.2±0.4	I.	I.
328	N.T.	N.T.	N.T.

Figure 127 Chemical structures and IC_{50} or % of inhibition at 100 μmolar of the active molecules previously synthesised in our lab of rabbit 20S proteasome at pH 7.5 and 37°.

x: activation factor I. = inhibition at 200 μM, 100 μM and 50μM N.I. = not inhibition N.T. = not tested

NB : Due to complex variations of inhibition percentages according to the inhibitor concentrations, IC_{50} could not be determined for molecules **312**, **316**, **326**, **327** for PA and T-L activities.

Due to the large variety and the flexibility of the molecules, it is not possible with these few data to establish some reliable structure-activity relationship, but in every case it is possible to explain the different activities of series of similar molecules which probably interact in the same way with the active sites of the proteasome. The first step of the analysis was to find, between the clusters at lower energy generated by Autodock, the conformations corresponding to the criteria expose above (see paragraph **3.6.2**). In particular, the first thing was to recognize the conformations able to fill both the S1 and the S3 pockets of the proteasome. Whereas this research was quite simple for the active molecules, in the case of the inactive compounds it was often not possible to find conformations with these characteristics. The second step was the research of the intermolecular hydrogen bonds between the ligand and the receptor, in particular with the residues T21, G23, G47, A49 and D114 (this last residue not present in the caspase), and with D120 (in T-L), which are, as illustrated above, the most important for the interaction with the active site of the proteasome. When possible, additionally hydrogen bonds were identified. Last element analyzed was the distance between the ligand and the T1, which can give us additional information about the filling f the S1 pocket. All these analysis have been repeated twice for all the molecules, one for the S configuration of the carbon bearing the trifluoromethyl, and one for the R configuration. For these analysis, two different programs have been used, Pymol Visualizer, which allows to fast generate an electrostatic surface of the receptor (the following images have been prepare with this program) and Accelerys DS Visualizer, which is useful to find the intermolecular hydrogen bonds and to measure distance or angle between different atoms. The results of these studies have been then reported in a table, which present also other features derived by the Autodock program, such as the number of cluster in which the conformation was found (the clusters are classed by the program in the base of the binding energy, so the first cluster is that at lowest energy), the number of conformations present in the cluster and the binding energy (see Annex 1). Analyzing the data, it was possible to do some general considerations. In the case of the molecule with the C-terminus in the S1 (or S3) pocket and the N-terminus in the S3 (or S1) pocket, the number of bonds between the two groups was larger than that of the known inhibitors, and for this reason the rest of the molecule adopt a conformation quite folded which does not allow to form a large number of hydrogen bonds in the crucial region of the proteasome between the two β-sheets. In effect, the pseudo amino acid **295** contains two more bonds than the valine present in both the TMC-95A and in the Novartis

inhibitor, and this can probably explain why the peptidomimetics is sometimes docked outside of the region of the proteasome between the two β-sheets. Another consideration is that the result obtained for the S and R diastereomers often differ, which can suggest a different activity between the two diastereomers. For this reason, an interesting future work can be the separation of the mixture of diastereomers to carry out the biological tests on the diastereomerically pure products. Moreover, the presence of a free amino group is often decisive for the activity. In fact, all the compounds presenting a free amino group (**296, 297, 298, 312, 316** and **327**) are active, when the protected precursors are or inactive (**300, 301, 309, 313**) or in every case less active (**315, 326**).

Analyzing the biological results, it was possible to see that very similar molecules could present a completely different activity. It was so interesting to limit the analysis of the docking results to small set of similar molecules to try to understand their behaviour. A first set can be obtained by the molecule with the free amine in the lateral chain of the lysine. For all this molecules, the docking in the trypsin-like site showed as driving force of the interaction a strong hydrogen bond between this free amino group and the aspartic acid 120 situated at the bottom of the S3 pocket. This is also confirmed by precedent studies which indicate the formation of a ionic bond with this residue, making the lysine a good amino acid to target the trypsin-like site.[181] In particular molecule **296**, **298**, and **316** differ just in the group present at the N terminal, which is respectively a *tert*-butoxy carbonyl, a 3-phenoxyphenyl acetic acid and a 2,5-di-methoxyphenyl acetic acid (figure 128a, b and c respectively, if not indicates all the images in the next pages are referred to the S configuration of the carbon bearing the trifluoromethyl).

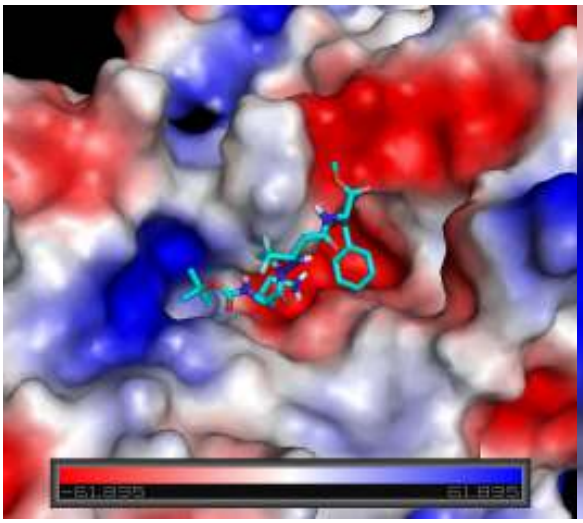

Figure 128a molecule **296** in trypsin-like site

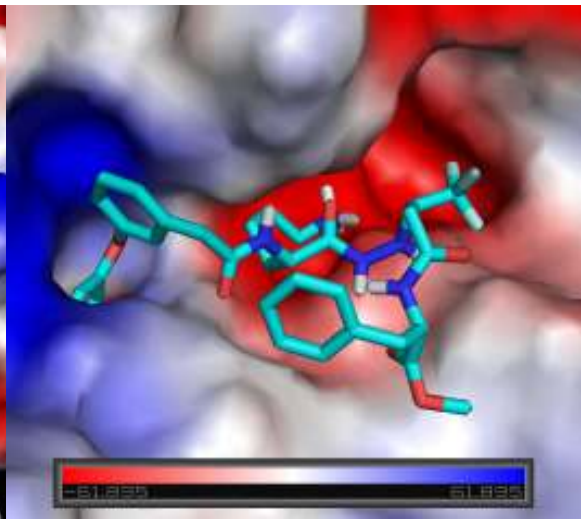

Figure 128b **298** in trypsin-like site

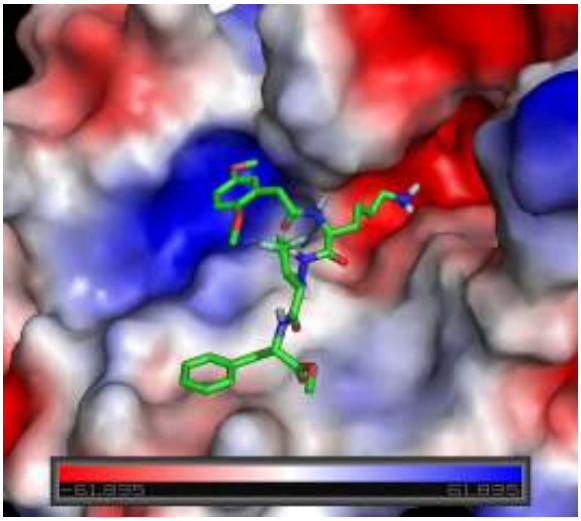

Figure 128c molecule **316** in trypsin-like site

Comparing the images, it is possible to see as the biphenyl of the molecule **298** is deeply inserted in the S1 pocket when the Boc group of **296** is just at the entry of the S1 pocket. This is reflected by the different activity of the two molecules, with an IC_{50} of 8.4 for **298** and an inhibition of 30% at 100 μM for **296**. In the case of **316**, the phenyl ring is less inserted in the S1 pocket, but, on the other hand the molecule in this region is more flexible and the methoxy group in the position 2 of the ring is close to the T1 with the formation of an hydrogen bond.

Another set is that formed by the molecules **300**, **301** and **315**. In this case, the only active molecule is the **315** with an IC_{50} of 54 in the caspase site (figure129a, b and c respectively).

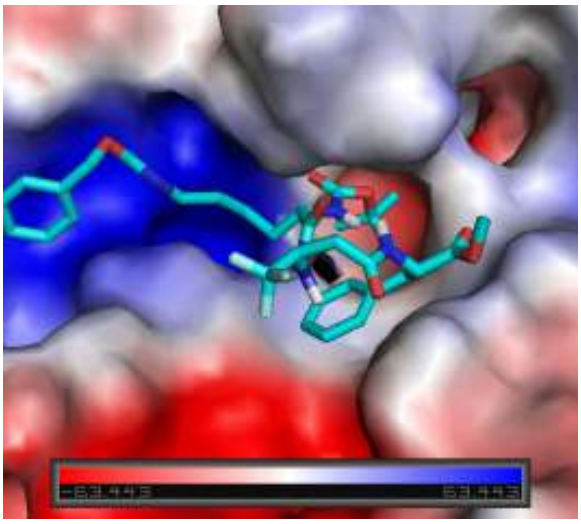

Figure 129a molecule **300** in caspase

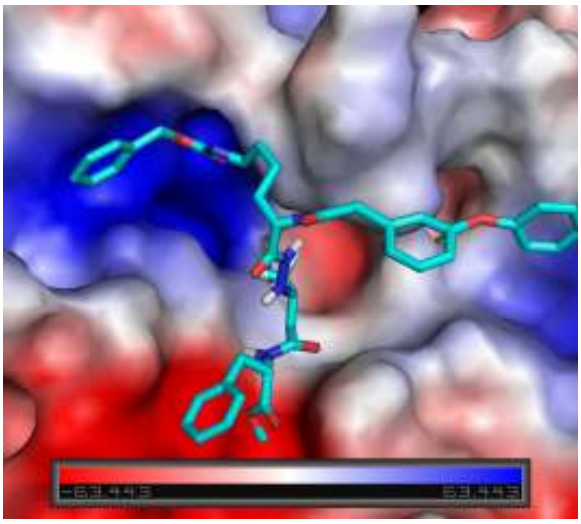

Figure 129b molecule **301** in caspase

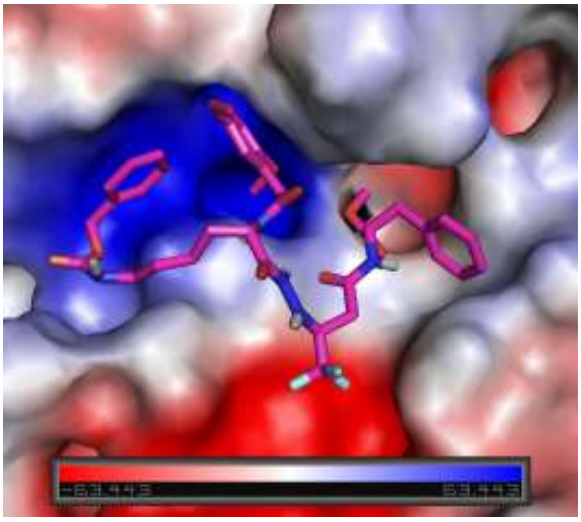

figure 129c molecule **315** in caspase

In this case, we can see as for the molecules **300** and **301** no groups interact with the S1 pocket, whereas for the molecule **315** the phenyl ring is slightly inserted in this pocket, explaining the weak activity of this compound.

Molecule **297** present a quite good activity in chymotrypsin-like and trypsin-like site, but it is not active at all in caspase (figure 130a, b and c).

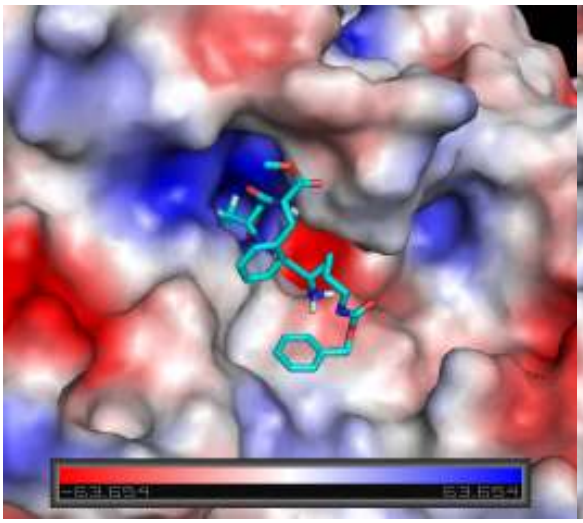

Figure 130a molecule **297** in chymotrypsin-like

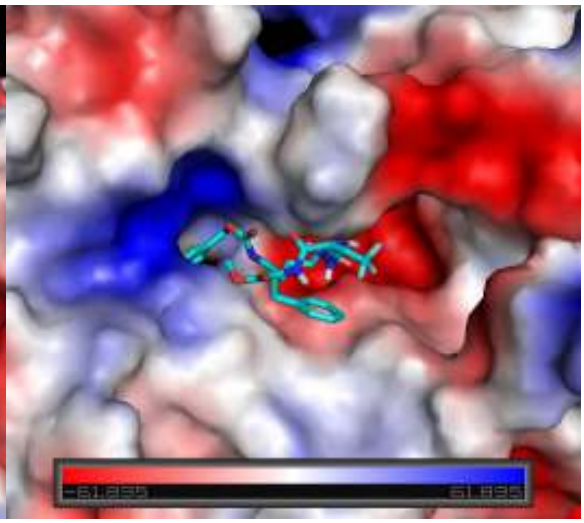

Figure 130b molecule **297** in trypsin-like

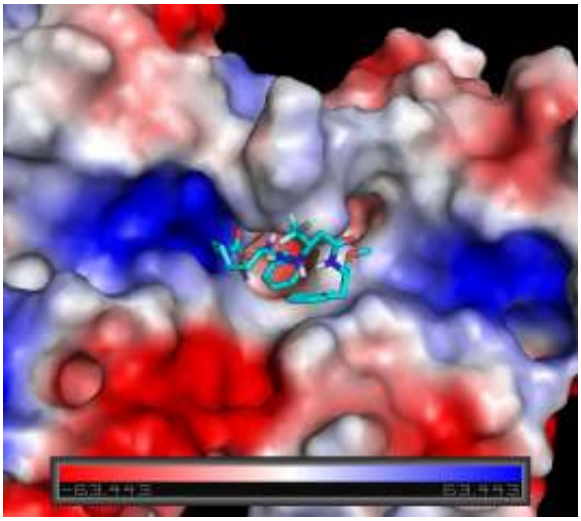

Figure 130c molecule **297** in caspase

As shown, the most favourable conformation of the molecule **297** interacts with both the S1 and S3 pockets in the chymotrypsin-like and trypsin-like active sites, but in the case of caspase it was not possible to find a good conformation analysing the ten clusters with a lower binding energy (in figure 130c the conformation with a lowest binding energy generated by Autodock4). Similar to the molecule **297** is the molecule **312** which differs from the first only for the presence of a trimethoxybenzyl amine at the place of the phenylalanine (in Figure 131 as example the docking in the trypsin-like site). As expected, also this molecule shows an inhibitory activity of the

proteasome, inhibiting all the three active sites. In particular, in the chymotrypsin-like site the order of magnitude of the IC_{50} is the same of the molecule **297**, suggesting that this substitution has not a large effect in the inhibitory activity of this active site. It is also interesting to see as molecule **312** resulted active in the caspase, when the molecule **297** was not active.

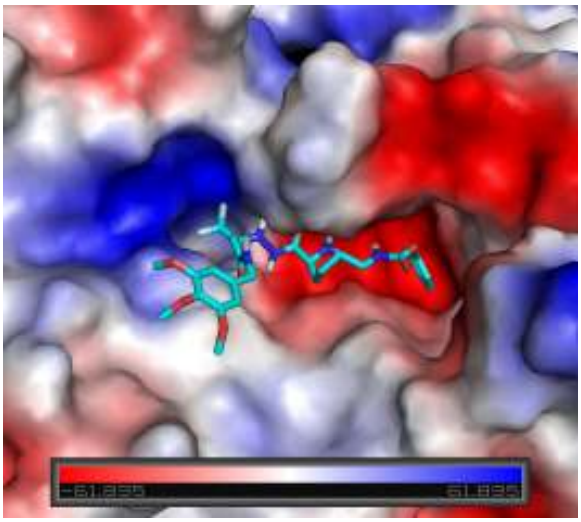

Figure 131 molecule **312** in trypsin

In the aim to synthesise molecules with a lower molecular weight, which is an important parameter for the absorption of a drug in the cell, molecule **318** was prepared. The molecule **302**, which differs from the **318** just by the presence of a 2-phenoxy phenyl instead of a dimethoxy-phenyl was tested with negative response. The comparison between the 2 molecules (figure 132a and b) showed that the phenylalanine is inserted in S1 pocket for both the molecules, but whereas the phenoxyphenyl group of **302** was too big to fill the S3 pocket, the dimethoxyphenyl is enough small and flexible to be inserted in this pocket. Unfortunately, despite the good docking result, also the molecule **318** did not show an inhibitory activity of the proteasome. In effect, all the known non covalent (and the most of covalent) proteasome inhibitors present in literature are molecule with a quite high molecular weight, thus probably the presence of additional groups which can help to stabilise the position of the molecule is required.

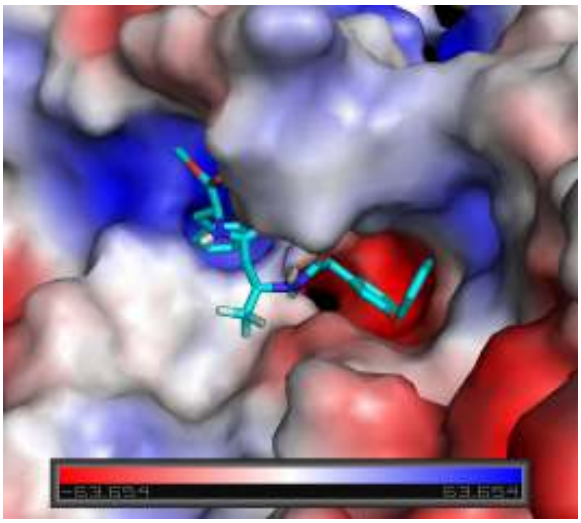

Figure 132a molecule **302** in chymotrypsin-like

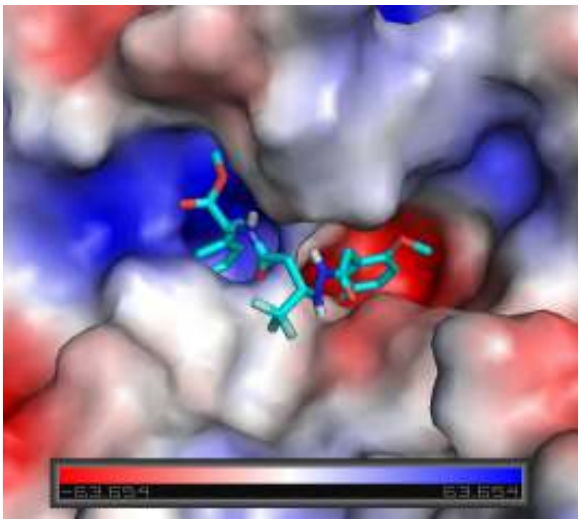

figure 132b molecule **312** in chymotrypsin-like

A last consideration can be done about the presence of the trifluoromethyl group in our scaffold. At the moment, just few non fluorinated analogues have been synthesised and tested, but it is possible to do some consideration. The molecule 327, which is the analogue of the fluorinated **297**, shows an inhibitory effect of all the active sites of the proteasome. The IC_{50} of molecule **327** was calculated only for the chymotrypsin-like active site, but also if this molecule resulted slightly less active of the molecule **297**, it was in the same order of magnitude (18.2 μM for **327** and 5.9 μM for **297**). We can also observe the apparition of a PA inhibition with the non-fluorinated molecule **327**. A greater difference was found between the behaviour of molecule **300**, which is not active, and its non fluorinated analogue **326**, which has an inhibitory activity in all the three active sites. Also if they are just preliminary results and a larger series of non fluorinated compounds is necessary to have a good comparison, it seems that the presence of the trifluoromethyl group does not greatly improve the activity of our inhibitors. In fact, we generally observed for the non fluorinated compounds an improvement of the solubility, which can also play an important role in the difference of reactivity observed between the molecules **300** and **327**. Moreover, as observed previously, the presence of a free amine is often very important for the activity. Thus, in the non fluorinated compounds the behaviour of the nitrogen of the hydrazine group is more similar to that of a free amine, due to the lack of the effect of the vicinal trifluoromethyl group.

In conclusion, we demonstrated here that the docking can be a useful tool for a better understanding of the binding mechanism between small molecules and 20S proteasome. In particular, it is possible to explain the differences in the activity between sets of similar molecules which bind the receptor in a similar manner. The limits in our methodology are particularly relied to the high number of torsions of the inhibitor candidates, which does not allow to obtain a good clustering. Moreover, the structural diversity of the molecules synthesised joined with their high flexibility, makes plausible that it does not exist just one mechanism of binding interaction common to all the molecules, making more complicated the establishment of a structure-activity relationship. Although these problems, our methodology can be an useful tool to support and to drive the synthesis of new candidates for the inhibition of the 20S proteasome.

3.8 Conclusions

From these biological results we can establish some preliminary structure-activity relationship that will have to be confirmed in the future with the synthesis and the docking of a large number of analogues :

- The presence of a free amino group is often decisive for the activity. In fact, all the compounds presenting a free amino group (**296, 297, 298, 312, 316** and **327**) are active, when the protected precursors are or inactive (**300, 301, 309, 313**) or in every case less active (**315, 326**).
- *Concerning the part 1 of the molecules* (*Vide supra*, Paragraph 3.6.3, Fig 116) : the 2,5-dimethoxyphenyl acetic group is comparable (**316** versus **296** and **298**) or slightly superior (**315** versus **300** and **301**) to a Boc group or to the 3-phenoxyphenylacetic acid.
- *Concerning the part 2 of the molecules*, a Lysine residue is favourable, specially a free Lysine residue which is superior to the 3,4-dimethoxyphenylalanine residue (compare **298** and **299**) specially on the T-L activity. Moreover a protected or a free Lysine residue is slightly superior to the asparagine residue (compare **315** to **317**, **316** to **317** and **311** to **296**).
- *Concerning the part 3 of the molecules*, non fluorinated scaffold do not seem to decrease the activity. However, diastereoisomeric fluorinated compound must be separated and biologically evaluated individually as we really observe a big influence of the chiral center stereochemistry on the Docking analysis.

- *Concerning the part 4 of the molecules*, the phenylalanine residue is comparable to the 3,4,5-trimethoxy benzylamine (compare **312** and **297**). Even then an inhibitory activity on the PA site is observed with **312** while no inhibitory activity was shown on this site with **297**. This result would be very interesting if it is confirmed because in this case we suppressed the peptide character of the C-terminal part of our pseudo-peptides.

CHAPTER 4 EXPERIMENTAL PART

4.1 Instruments and general techniques

^{1}H-NMR spectra were recorded on Bruker AC 250 (250 MHz), Bruker Avance 300 (300 MHz), Bruker Avance 400 (400 MHz) and Bruker Avance 600 (600 MHz). The chemical shifts are reporter in δ (ppm) relative to chloroform ($CDCl_3$, 7.26 ppm), dimethylsulfoxide (DMSO-d_6, 2.49 ppm), methanol-d_3 (CD_3OH, 3.34 ppm) with presaturation to eliminate attenuate the OH peak and tetramethylsilane (TMS, 0.00 ppm) as an internal standard. The spectra were analysed by first order, the coupling constant (*J*) are reported in Hertz (Hz). Characterisation of signals: s= singlet, bs= broad singlet, d= doublet, t= triplet, q= quartet, m= multiplet, bm= broad multiplet, dd= double doublet, dt= double triplet, ddd= double double doublet. Integration is determined as the relative number of atoms. Diastereoisomeric ratios were determined by comparing the integrals of corresponding protons in the ^{1}H-NMR spectra.

^{13}C-NMR spectra were recorded on Bruker AC 250 (62.9 MHz), Bruker Avance 300 (75.5 MHz), Bruker Avance 400 (100.6 MHz) and Bruker Avance 600 (150.9 MHz). The chemical shifts are reported in δ (ppm) relative to chloroform ($CDCl_3$, 77 ppm), dimethylsulfoxide (DMSO-d_6, 39.52 ppm), methanol-d_3 (CD_3OH, 49 ppm) and tetramethylsilane (TMS, 0.00 ppm) as an internal standard.

2D-NMR spectra (COSY, NOESY, ROESY, HETCORR) were recorded on Bruker Avance 400 (400 MHz) and Bruker Avance 600 (600 MHz).

IR spectra were recorded with a Bio-Rad Excalibur series FT-IR

MS spectra were recorded in the mass spectroscopy departments of Regensburg

Optical rotations were measured on a Perkin-Elmer-polarimeter 241 with sodium lamp at 589 nm in the specified solvent.

CD spectra were measured on a JASCO model J-710/720 at the Institute of Bioanalytic and Sensoric of the University of Regensburg at 21°C between 250 and 190 nm in the specified solvent, with 10 scans. The length of the rectangular cuvette was 0.1 mm, the resolution was 0.2 nm, the band width 1.0 nm, the sensitivity 10-20 mdeg, the response 2.0 s, the speed 10 nm/min. The background was substracted for each spectrum. The absorption value is measured as molar ellipticity per residue ($deg.cm^2.dmol^{-1}$). The spectra were smoothed by adjacent averaging algorithm or FFT filter with the Origin 6.0 program.

Thin layer chromatography (TLC) was performed on alumina plates coated with silica gel (Merck silica gel 60 F 254, layer thickness 0.2 mm) or glass plates coated with flash chromatography silica gel (Merck silica gel 60 F 254, layer thickness 0.25 mm). Visualisation was accomplished by UV light (wavelength λ = 254 nm), permanganate solution, ninhydrin/acetic acid solution, vanillin/H_2SO_4 solution and paramethoxybenzaldehyde solution.
The solvents were purified according to standard laboratory method. DMF was distilled over CaH_2 before use. After distillation, dry THF was stored in a Schlenk flask under nitrogen over molecular sieves 4 Å. BF_3•Et_2O was distilled under nitrogen and stored in a Schlenk flask under nitrogen in the refrigerator. In Regensburg dichloromethane were purified by a solvent purification system apparatus, when in Paris was distilled over CaH_2

4.2 Synthesis of the compounds

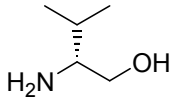

239

(D)-amino-3-methylbutan-1-ol 239

To a solution of NaBH4 (8.1g, 214 mmol,2.5 eq.) in dry THF (135 mL) was added L-valine (10.0 g, 85.3 mmol, 1.0 eq.) under nitrogen atmosphere. The reaction mixture was cooled to 0°C in an ice bath and a solution of iodine (21.6 g,85.3 mmol, 1.0 eq.) in dry THF (50 mL) was slowly added over 1 h, resulting in production of hydrogen. After gas ceased, the reaction mixture was refluxed for 20 h and then cooled to room temperature. Methanol was added cautiously until the stirred solution became clear. The solution was stirred for 30 minutes and concentrated in vacuo to give a white paste, which was dissolved in 20% aqueous KOH (50mL).The solution was further stirred for four hours and extracted with DCM (3 x 140 mL). The combined organic layers were dried over anhydrous MgSO4, filtered and concentrated in vacuo to afford **239** (8.15 g, 92%) as a colourless oil.

Analitycal data are accorded with the literature

^{1}H NMR (250 MHz, CDCl3): δ 3.64 (dd, *J* = 10.6, 8.7Hz, 1H),3.31 (dd, *J* = 10.6, 8.7 Hz, 1H), 2.57 (ddd, *J* = 8.6, 6.4, 3.9 Hz, 1H), 2.20 (bs, 2H), 1.5-1.7 (m, 1H), 0.93 (d, *J* = 6.8 Hz, 3H), 0.91 (d, *J* = 6.8 Hz, 3H).

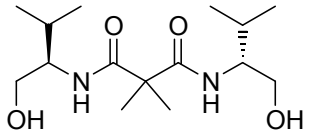

240

(+)-(R, R)-N,N'-bis-(1-hydroxymethyl-2-methyl-propyl)-2,2-dimethyl-malonamide 240

To a cold solution (0°C) of L-valinol **239** (15.4 g, 150.0 mmol, 2.0 eq.) in dry DCM (150 mL) were slowly added triethylamine (52.3 mL, 375mmol, 5 eq.) and a solution of 2,2-dimethylmalonyl dichloride (10 mL, 75 mmol, 1 eq.) in dry DCM (70 mL). Then, the ice bath was removed and the reaction mixture was stirred for 45 minutes to room temperature, resulting in a colourless precipitate which was dissolved again by addition of dry DCM (350 mL). After addition of 1M HCl (100 mL), the aqueous layer was separated and extracted with DCM (3 x 50 mL). The combined organic layers were washed with saturated NaHCO3 (100 mL) and brine (100 mL), dried over MgSO4, filtered and concentrated in vacuo. Crystallisation of the crude product from ethyl acetate (100 mL) and subsequent recrystallisation of the residue of the mother liquor afforded **240** (18.76 g, 83%) as colourless crystals.

R_f = 0.26 (SiO2, EtOAc/MeOH 95:5); m.p. = 98-99°C; $[\alpha]_D^{20}$ = +6.3 (c=0.50, DCM).

^{1}H NMR (250 MHz, $CDCl_3$): δ ppm 6.41 (d, *J* = 8.8 Hz, 2H), 3.84-3.72 (m, 4H), 3.56-3.48 (m, 2H), 3.21 (bs, 2H), 1.80 (hept., *J* = 6.8 Hz, 2H), 1.49 (s, 6H), 0.95 (d, *J* = 6.74, 6H), 0.92 (d, *J* = 6.74 Hz, 6H)

^{13}C NMR (62.9 MHz, $CDCl_3$): δ ppm 174.6, 64.0, 57.2, 50.1, 29.1, 23.6, 19.7, 18.8

IR (KBr): 3326, 2963, 2877, 1642, 1543, 1391, 1368, 1287, 1186, 1071, 1024, 899, 651 cm^{-1}

MS (DCI, NH3): m/z (%) = 304.5 (16), 303.5 (100) [$M+H^+$]

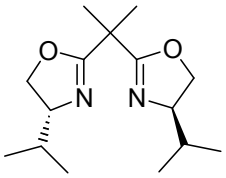

241

(+)-(R,R)-isopropylbisoxazoline 241

To a mixture of (-)-(S, S)-N,N'-bis-(1-hydroxymethyl-2-methylpropyl)-2,2-dimethylmalonamide **240** (18.76 g, 620.0 mmol, 1.0 equiv.) and 4-dimethylamino pyridine (0.75 g, 6.2 mmol, 0. 1 equiv.) in dry CH_2CI_2 (400 mL) was slowly added triethylamine (37.6 mL, 270.0 mmol, 4.4 equiv.) over 15 min. Subsequently a solution of tosyl chloride (23.65 g, 124.0 mmol, 2.0 equiv.) in dry CH_2CI_2 (50 mL) was added dropwise via the addition funnel. The reaction mixture was stirred for additional 48 h at room temperature where the colour changed to yellow and cloudy precipitate occurred. The precipitate was dissolved in CH_2CI_2 (150 mL). The reaction mixture was then washed with saturated NH_4Cl (250 mL) followed by water (150 mL) and saturated $NaHC0_3$ (200 mL). The combined aqueous layers were extracted with CH_2CI_2 (3 x 200 mL) and the combined organic layers were dried over Na_2SO_4. After filtration and concentration in vacuo the residue was purified by hot n-pentane extraction to afford **241** (7.466 g, 44%) as a colourless oil.

R_f = 0.26 (Si02, DCM/MeOH 19: 1); $[\alpha]_D^{20}$ = +108.1 (c = 1.01, CH_2CI_2)

^{1}H NMR (250 MHz, $CDCl_3$): δ ppm 4.27-4.09 (m, 2 H), 4.04-3.92 (m, 4 H), 1.91-1.72 (m, 2 H), 1.52 (s, 6 H), 0.92 (d, J = 6.84 Hz, 6 H), 0.85 (d, J = 6.79 Hz, 6 H);

^{13}C NMR (100.6 MHz, $CDCl_3$): δ ppm 168.8, 71.5, 69.9, 38.6, 32.2, 24.4, 18.5, 17.3

IR (Film): $\bar{\upsilon}$ = 3411, 3225, 2960, 1660, 1468, 1385, 1352, 1301, 1247, 1146, 1109, 980, 925, 795, 737 cm-1

MS (DCI, NH3): m/z (%) = 391.6 (7), 313.5 (7), 268.4 (17), 267.4 (100) [M + NH_4^+]

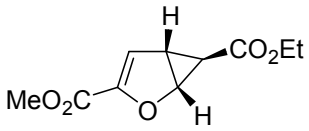

237

(1R,5R,6R)-(+)-2-Oxabicyclo[3.1.0]hex-3-ene-3,6-dicarboxylic 6-ethylester-3-methyl ester 237

In a three-neck flask equipped with a slow addition funnel under nitrogen at 0°C were added successively 53.2 g (421 mmol, 1 eq.) of furanoic acid methylester, 0.88 g (3.32 mmol, 0.008 eq.) of ligand **241** and 1.08 g (2.98 mmol, 0.007 eq.) of $Cu(OTf)_2$. The inner walls of the flask were rinsed with a few millilitres of dry DCM to allow all of the copper to dilute in the solution. After 10 minutes, three drops of phenylhydrazine were added in the solution which turned from a deep blue to a dark red colour testifying of the reduction of the metal complex. The slow addition funnel was then filled with 500 mL of a solution of diazoacetate in DCM ($153.97 g.L^{-1}$, 76,98 g, 675 mmol, 1.6 eq.). After half an hour, the solution was added dropwise at the frequency of one drop every 6 seconds and the reaction was let at 0°C for four days. Once the solution was totally added, the reaction mixture was filtered on a 10 cm pad of basic alumina and washed with 500 mL of DCM. The solution was evaporated under vacuum and column chromatographed on silica gel with a solution hexanes/Ethyl acetate 5:1 as eluent. The fractions were collected and the solvent evaporated under vacuum. The product was obtained as a slightly yellow oil and was crystallised in pentane/DCM affording 29.6 g (139.5 mmol, 33%) of **237** as enantiomerically pure white crystals (ee>99% measured by chiral HPLC).

R_f (PE/EE 5:1)= 0.14; m.p. 42 °C; $[\alpha]_D^{20} = +272$ (c=1.0, CH_2Cl_2)

^{1}H NMR (250 MHz, $CDCl_3$): δ ppm 1.16 (dd, *J*=2.7, 1.1 Hz, 1H), 1.23 (t, *J*=7.1 Hz, 3H), 2.87 (ddd, *J*=5.3, 2.9, 2.7 Hz, 1H), 3.78 (s, 3H), 4.12 (q, *J*=7.1 Hz, 2H), 4.97 (dd, *J*=5.3, 1.1 Hz, 1H), 6.39 (d, *J*=2.9 Hz, 1H)

^{13}C NMR (62.9 MHz, $CDCl_3$): δ ppm 14.2, 21.5, 31.9, 52.1, 61.0, 67.5, 116.0, 149.3, 159.5, 171.7

IR (KBr): 3118, 2956, 1720, 1617, 1428, 1380, 1297, 1166, 1124, 1041, 954, 831, 725 cm^{-1}

MS (70 eV, EI): m/z (%): 212.1 [M^+] (9.8), 153.0 [M^+-CO_2Me] (11.5), 139.0 [M^+-CO_2Et] (100), 124.9 (24.4), 98.9 (28.6), 96.9 (31.7), 78.9 (11.3), 59.0 (13.5), 52.1 (11.5);

Elemental Analysis calcd (%) for $C_{10}H_{12}O_5$ C 56.60, H 5.70; found C 56.51, H 5.73.

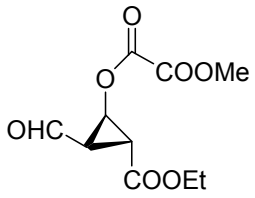

242

(1R,2R,3R)-(+)-Oxalic acid 2-ethoxycarbonyl 3-formyl-cyclopropyl ester methyl ester 242

A solution of **237** (2.50 g, 11.78 mmol) in dry CH_2Cl_2 (125 mL) was cooled to -78°C and treated with ozone until the mixture turned blue. Excess ozone was expelled by passing oxygen through the solution, followed by addition of dimethyl sulfide (4.3 mL, 58.91 mmol, 5.0 equiv). The reaction mixture was allowed to warm to room temperature and stirring was continued for 24 h. Saturated NaHCO3 (10 mL) was added and layers were separated. The organic layer was washed with water (2 x 10 mL), dried, filtered and evaporated. The residue was recrystallized from Et_2O at -27°C to give **242** as a colourless solid (2.70 g, 94%).

M.p. 52°C; $[\alpha]_D^{20}$=+37.7 (c=1.0, CH_2Cl_2)

^{1}H NMR (250 MHz, CDCl3): δ ppm 1.28 (t, *J*=7.1 Hz, 3H), 2.79 (ddd, J_7.3, 6.0, 4.0 Hz, 1H), 2.90 (dd, *J*=6.0, 3.6 Hz, 1H), 3.91 (s, 3H), 4.19 (q, *J*=7.1 Hz, 2H), 4.83 (dd, *J*=7.3, 3.6 Hz, 1H), 9.45 (d, *J*=4.0 Hz, 1H)

^{13}C NMR (62.9 MHz, CDCl3): δ ppm 14.1, 26.4, 34.9, 54.0, 58.9, 62.0, 156.6, 156.9, 168.1, 192.7

IR (KBr): $\bar{\upsilon}$= 3066, 3015, 2963, 2892, 1785, 1751, 1735, 1706, 1445, 1345, 1313, 1210, 1167, 1086, 1011, 963, 867, 790, 715, 613, 495 cm^{-1}

MS (DCI, NH_3): m/z (%): 262.0 [M^++NH_4] (100), 176.0 (20), 160.0 (55), 120.9 (15);

Elemental Analysis calcd (%) for $C_{10}H_{12}O_7$ (244.2): C 49.19, H 4.95; found C 49.22, H 4.99.

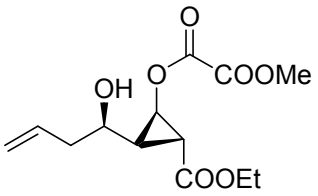

244

(1R, 1'R/R,2R, 3R)-Oxalicacid-hydroxy-but-3'-enyl-3-ethoxycarbonyl-cyclopropylester methylester 244

A solution of **242** (5.00 g, 20.5 mmol) in dry CH_2Cl_2 (200 mL) was treated with BF_3•Et_2O (3.0 mL, 20.5 mmol) at -78°C. After 10 minutes allyltrimethylsilane (5.0 mL, 30.75 mmol, 1.5 equiv) was added and stirring was continued for 24 h. The reaction was quenched with saturated $NaHCO_3$ (6.0 mL) and the mixture was allowed to warm to 0°C. After separation of the organic layer and drying with MgSO4 , the solvent was evaporated under vacuum to yield the corresponding alcohol **244** as a colourless oil (5.82 g, 100% crude yield, dr 95:5).

^{1}H NMR (250 MHz, $CDCl_3$): δ ppm 1.25 (t, *J*=7.0 Hz, 3H), 1.81 ± 1.92 (m, 1H), 2.15 (dd, *J*=6.2, 2.7 Hz, 1H), 2.31 ± 2.51 (m, 4H), 3.70 (ddd, *J*=7.3, 7.3, 5.4 Hz, 1H), 3.88 (s, 3H), 4.13 (q, *J*=7.0 Hz, 2H), 4.72 (dd, *J*=7.5, 2.8 Hz, 1H), 5.14 ± 5.22 (m, 2H), 5.76 ± 5. 93 (m, 1H), characteristic signals of the diastereomer: δ ppm 4.14 (q, *J*=7.0 Hz, 2H), 4.67 (dd, *J*=6.9, 3.0 Hz, 1H).

^{13}C NMR (75.5 MHz, $CDCl_3$): δ ppm 170.6, 133.0, 118.9, 61.3, 58.8, 41.7, 31.2, 24.6, 14.1

MS (DCI, NH_3): 304.2 [$M+NH_4^+$], 287.2 [MH^+], 269.1 [MH^+-H_2O]

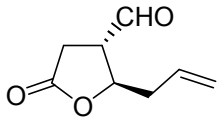

249

(2R/S,3R)-2-Allyl-5-oxotetrahydrofuran-3-carbaldehyde 249

A solution of **244** (6.15 g, 21.48 mmol, 1 eq.) in 100 mL dry MeOH was put in an ice bath. 5.96 mL of triethylamine (4.35 g, 42.99 mmol, 2 eq.) were then slowly added and the reaction was let at 0°C for two hours. The ice bath was then removed and the reaction was warmed to room temperature until no more evolution could be seen on TLC. The reaction mixture was evaporated under vacuum and the residue was chromatographed on silica gel (hexanes/ethyl acetate 1:1) and afforded 2.21g of **249** (yield=67%) as a slightly yellow coloured oil with a diastereomeric ratio of 95/5. During the reaction, the stable intermediate **251** could be isolated and fully characterised in a diastereomeric ratio of 80/20.

R_f (hexanes/EA 1:1) = 0.17; $[\alpha]_D^{20}$=+31.7 (c=1.35 in CH_2Cl_2)

^{1}H NMR (250 MHz, $CDCl_3$): δ ppm 2.35 ± 2.59 (m, 2H), 2.71 (dd, J_18.2, 9.9 Hz, 1H), 2.89 (dd, *J*=18.2, 7.5 Hz, 1H), 3.19 (dddd, *J*=10.0, 7.3, 6.0, 1.2 Hz, 1H), 4.74 (dd, *J*=11.9, 6.2 Hz, 1H), 5.10 ± 5.27 (m, 2H), 5.75 (dddd, *J*=17.3, 10.0, 7.0, 3.5 Hz, 1H), 9.69 (d, *J*=1.2 Hz, 1H), characteristic signals of the diastereomer (2R): δ ppm 3.00 (dd, *J*=17.7, 5.8 Hz, 1H), 9.82 (d, *J*=1.7 Hz, 1H)

^{13}C NMR (75.5 MHz, $CDCl_3$): δ ppm 197.3, 174.0,130.9, 120.5, 78.0, 51.3, 39.2, 28.9, characteristic signals for the minor compound: δ ppm 198.0, 131.3, 120.0, 49.6, 39.4, 28.7

IR (film): $\bar{\upsilon}$ = 3080, 2980, 2939, 2841, 1774, 1727, 1642, 1419, 1359, 1193, 1111, 1000, 924 cm^{-1}

MS (EI, 70 eV): m/z (%): 154.2 (5) [M^+], 113.1 (100) [M^+-C_3H_5], 85.1 (95), 57.1 (95);

Elemental Analysis calcd (%) for $C_8H_{10}O_3$ (154.2): C 62.33, H 6.54; found: C 62.36, H 6.83.

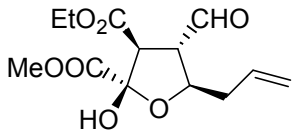

251

(2R/S, 3R, 4R, 5R)-5-Allyl-4-formyl-2-hydroxy-tetrahydro-furan-2,3-dicarboxylic acid 3-ethyl ester 2-methyl ester 251

R_f (hexanes/EA 1:1) = 0.67

^{1}H NMR (300 MHz, $CDCl_3$): δ ppm 9.79 (d, *J* = 1.4 Hz, 0.8H, major), 9.75 (d, *J* = 1.9 Hz, 0.2H, minor), 5.83-5.68 (m, 1H), 5.22-5.13 (m, 2H), 4.50 (s, 0.2H, minor), 4.46 (s, 0.8H, major), 4.37-4.07 (m, 3H), 3.95 (dd, *J* = 11.5H, *J* = 1.2 Hz, 1H), 3.87 (s, 2.4H, major), 3.79 (s, 0.6H, minor), 3.65-3.57 (ddd, *J* = 1.4 Hz, *J* = 9.0 Hz, *J* = 11.5 Hz, 1H), 2.77-2.44 (m, 2H), 1.22-1.17 (t, *J* = 7.13 Hz, 3H)

^{13}C NMR (300 MHz, $CDCl_3$): δ ppm 198.3, 169.5, 167.3, 132.7, 119.0, 100.3, 80.6, 61.6, 55.9, 53.9, 53.6, 40.8, 13.9

MS (LR): m/z (%): 304.2 (100) [$M+NH_4^+$], 286.3 (7.35) [$M+NH_4^+-H_2O$]

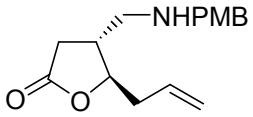

252

(4R,5R)-5-Allyl-4-[(4-methoxy-benzylamino)-methyl]-dihydro-furan-2-one 252

To a solution of **249** (880 mg, 5.24 mmol, 1.0 eq.) in dry DCM (50 ml) were added sequentially sodium sulphate (1.49 g, 10.48 mmol, 2.0 eq.) and 4-methoxybenzylamine (750 µL, 5.77 mmol, 1.1 eq.). The reaction mixture was stirred at room temperature for 3 h. The resulting slightly yellow solution was cooled at 0°C in an ice bath and $NaBH_4$ (397 mg, 10.48 mmol, 2.0 eq.) and dry MeOH (15 ml). The reaction mixture was stirred for further 30 min at 0°C and then filtrated on a celite pad. The solution was cooled at 0°C in an ice bath and a 1M solution of HCl was added until the pH solution was 1. The organic phase was separated and extracted with 1M solution of HCl (2 x 50 ml). The combined aqueous layers were washed with EtOAc (2 x 50 ml) and cooled at 0°C in an ice bath. Solid sodium hydrogen carbonate was added until the pH of the solution was 8.

The aqueous phase was the extracted with diethyl ether (3 x 80 mL), the combined organic layers were dried over Na_2SO_4, filtered and concentrated in vacuo to give **252** as a slightly yellow oil (1.101 g, 4.00 mmol, 76%) which was used for the next step without further purification.

An analytic sample was obtained by column chromatography (ethylacetate).

R_f = 0.40 (SiO_2, ethylacetate); $[\alpha]_D^{20}$ = +19.42 (c=1.04, DCM)

^{1}H-NMR (300 MHz, $CDCl_3$): δ ppm 7.23 (dd, *J* = 11.5, 8.5 Hz, 2H), 6.89-6.81 (m, 2H), 5.79 (m, 1H), 5.20-5.13 (m, 2H), 4.34 (dd, *J* = 11.7, 5.4 Hz, 1H), 3.80 (s, 3H), 3.71 (s, 2H), 2.73-2.61 (m, 2H), 2.53-2.20 (m, 5H)

^{13}C-NMR (75.5 MHz, $CDCl_3$): δ ppm 176.4, 158.8, 132.4, 132.0, 129.2, 119.0, 113.9, 83.1, 55.3, 53.3, 51.4, 39.9, 39.1, 33.2

IR (KBr): $\bar{\upsilon}$ = 3329, 3070, 2924, 2831, 2357, 2057, 1772, 1679, 1611, 1508, 1454, 1288, 1176, 1029, 985, 819

MS (CI, NH_3): m/z (%) = 276.3 (100) [M+ H^+]

HRMS (EI, 70 eV): Calculated for [$C_{16}H_{21}NO_3$]: 275.1521, found 275.1515 [M^+]

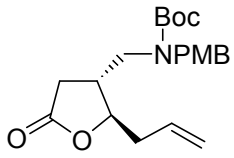

254

(2R,3R)-(2-Allyl-5-oxo-tetrahydro-furan-3-ylmethyl)-(4-methoxy-benzyl)-carbamic acid tert-butyl ester 254

To a solution of **252** (1.28 g, 4.65 mmol, 1.0 eq.) in dioxane / 1M aqueous solution of K_2CO_3 (12 mL / 16 mL) was added di-*tert*-butyldicarbonate (1.52 g, 6.99 mmol, 1.5 eq.). The reaction mixture was stirred at RT overnight and extracted with EtOAc (3 x 50 ml). The combined organic layers were washed with 10% aqueous solution of citric acid (2 x 30 ml) and brine (2 x 30 ml), dried over Na_2SO_4, filtrated and evaporated in vacuo to give a slightly yellow oil which was purified by column chromatography (PE:EtOAc 3:1) to afford **254** (1.294 g, 3.44 mmol, 74%)as a colourless oil.

R_f = 0.35 (SiO_2, PE:EtOAc 3:1) ; $[\alpha]_D^{20}$ = + 10.37 (c = 0.96, DCM)

^{1}H-NMR (300 MHz, $CDCl_3$): δ ppm 7.20-7.11 (m, 2H), 6.92-6.84 (m, 2H), 5.85-5.67 (m, 1H), 5.23-5.10 (m, 2H), 4.40 (s, 2H), 4.24 (bs, 1H), 3.80 (s, 3H), 3.26 (bs, 2H), 2.59-2.22 (m, 5H), 1.50 (s, 9H)

^{13}C-NMR (75.5MHz,$CDCl_3$) δ ppm 175.7, 159.1, 155.8, 132.1, 129.6, 128.8, 119.1, 114.1, 82.5, 80.7, 55.3, 48.4, 39.9, 38.6, 33.0, 28.4

IR (film): $\bar{\upsilon}$ = 3076, 2976,2931, 2837, 2372, 1778, 1690

MS (EI, 70 eV): m/z (%) = 375.3 (100) [M^+]

HRMS (EI, 70 eV): Calculated for [$C_{21}H_{29}NO_5$]: 375.2046, found 375.2046 [M^+]

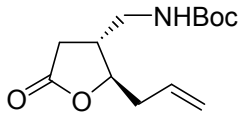

255

(2R,3R)-(2-Allyl-5-oxo-tetrahydro-furan-3-ylmethyl)-carbamic acid tert-butyl ester 255

To a cold (0°C) solution of **254** (633 mg, 1.69 mmol, 1.0 eq.) in water / acetonitrile (7mL / 21mL) cerium ammonium nitrate (3.70 g, 6.75 mmol, 4.0 eq, c = 0.25 M) was added portionwise.
The reaction was stirred at 0°C for 1 h and then at RT for additional 2 h until the total consumption of the starting material. Water (30 ml) was added and the aqueous phase was extracted with EtOAc (3 x 50 mL). The combined organic layers were washed with a saturated aqueous solution of $NaHCO_3$ (30 mL), dried with Na_2SO_4, filtrated and evaporated in vacuo to give an oil which was purified by column chromatography (PE:EtOAc 3:1) to afford **255** (340 mg, 1.33 mmol, 79%) as a colourless solid.

R_f = 0.29 (SiO_2, PE:EtOAc 3:1) ; $[\alpha]_D^{20}$ = + 21.58 (c = 1.01, DCM)

^{1}H-NMR (300 MHz, $CDCl_3$): δ ppm 5.81 (ddd, *J*= 17.8, 16.5, 7.1 Hz, 1H), 5.25-5.15 (m, 2H), 4.72 (bs, 1H), 4.31 (dd *J* =11.8, 5.8 Hz, 1H), 3.33-3.17 (m, 2H), 2.68 (dd *J* =17.2, 8.1 Hz, 1H), 2.59-2.42 (m, 3H), 2.34 (dd *J*=17.3, 7.1 Hz, 1H), 1.41 (s, 9H)

^{13}C-NMR (75.5MHz,$CDCl_3$): δ ppm 175.7, 156.0, 131.0, 119.3, 82.3, 80.0, 40.2, 38.7, 38.5, 28.3

IR (KBr): $\bar{\upsilon}$ = 3474, 2976, 2931, 2837, 2372, 1778, 1690, 1168,910, 855

MS (CI, NH_3): m/z (%) = 273.2 (71.32) [$M+NH_4^+$], 256.1 (1.07) [NH^+]

Elemental analysis calcd (%) for [$C_{13}H_{21}NO_4$]: C 61.16, H 8.29, N 5.49; found C 61.04, H 7.86, N 5.35

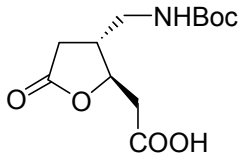

256

(2R,3R)-[3-(tert-Butoxycarbonylamino-methyl)-5-oxo-tetrahydro-furan-2-yl]-acetic acid 256 or (+)-GBA

To a cold (0°C) solution of **255** (340 mg, 1.33 mmol, 1.0 eq.) in water / acetonitrile / carbon tetrachloride (6 mL / 3 mL / 3 mL) were added sodium periodate (1.14 g, 5.32 mmol, 4 eq.) and $RuCl_3 \bullet xH_2O$ (25 mg, 0.09 mmol, 0.07 eq.). The solution was stirred for 1 h at 0°C and for 2 h at RT. Water (10 ml) was added and the solution was then extracted with diethyl ether (3 x 50 mL). The combined organic layers were dried over Na_2SO_4, filtrated through a celite pad and evaporated in vacuo to obtain **256** (317 mg, 1.15 mmol, 86%) as a colourless solid.

R_f= 0.15 (SiO_2, EtOAc) ; $[\alpha]_D^{20}$ = + 7.41 (c = 1.01, DMSO)

^{1}H-NMR (300 MHz, DMSO d_6): δ ppm 12.75-12.20 (bs, 1H), 7.07 (t *J* = 5.9 Hz, 1H), 4.55 (m, 1H), 3.15-2.96 (m,2H), 2.74-2.25 (m, 5H)

^{13}C-NMR (75.5MHz, DMSO d_6): δ ppm 175.8, 171.3, 155.8, 78.9, 77.8, 41.3, 39.8, 39.0, 31.6, 28.0

IR (KBr): $\bar{\upsilon}$ = 3327, 3101, 2989, 2938, 2569, 1783, 1658, 1256

MS [ESI, DCM/MeOH + 10 mmol/L NH_4Ac)NH_3]: m/z (%)= 290.8 (100) [M+NH_4^+], 273.3 (4.7) [NH^+]

Elemental analysis calcd (%) for [$C_{12}H_{19}NO_6$]: C 52.74, H 7.01, N 5.13; found C 52.40, H 6.73, N 5.03

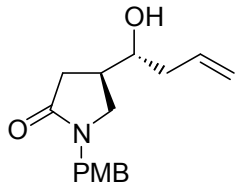

253

(4R, 1'R)-4-(1-Hydroxy-but-3-enyl)-1-(4-methoxy-benzyl)-pyrrolidin-2-one 253

To a solution of **249** (288 mg, 1.87 mmol, 1.0 eq.) in MeOH (15 ml) was added the 4-methoxy benzylamine (360 μL, 3.80 mmol, 1.5 eq.). The solution was reacted at RT for 4 h, then the $NaHB_4$ was added and the solution was stirred for 2 h at RT and refluxed overnight. The mixture was cooled at RT, washed with 1M aqueous solution of HCl (2 x 15 ml) and brine (2 x 15 ml), dried over Na_2SO_4, filtrated and evaporated in vacuo to obtain a sticky solid which was purified by column chromatography (EtOAc) to afford **253** (187 mg, 0.68 mmol, 36%) as a slightly yellow oil.

R_f = 0.2 (SiO_2 EtOAc) $[\alpha]_D^{20}$ = + 16.42 (c=1.04, DCM)

^{1}H NMR (300 MHz, $CDCl_3$): δ ppm 7.18-7.15 (d, J = 8.7 Hz, 2H), 6.87-6.84 (d, J = 8.7 Hz, 2H), 5.81-5.68 (m, 1H), 5.19-5.10 (m, 2H), 4.42-4.32 (d, J = 4.2 Hz, 2H), 3.81 (s, 3H), 3.60-3.53 (m, 1H), 3.29-3.23 (dd, J = 8.4Hz, J = 9.7Hz, 1H), 3.12-3.06 (dd, J = 6.6Hz, J = 9.8Hz, 1H), 2.54-1.98 (m, 6H)

^{13}C NMR (75 MHz, $CDCl_3$): δ ppm 173.9, 159.1, 133.9, 129.5, 128.5, 119.1, 114.1, 71.5, 55.3, 48.6, 45.9, 39.7, 36.5, 32.9

MS (LR): m/z (%): 293.2 (9.6) [$M+NH_4^+$], 276.2 (100) [$M+H^+$]

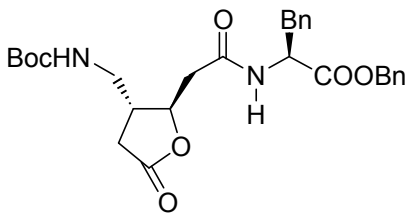

258

Boc-(+)-GBA-L-Phe-COOBn 258

A solution of Boc-(L)-Phe-COOBn (640 mg, 1.78 mmol, 1.5 eq.) in DCM/TFA 50:50 (10 ml) was stirred for 1 h at RT. The solvent was evaporated in vacuo and the resulting TFA salt was precipitated by addition of diethyl ether. The solvent was removed and the resulting colourless solid was dissolved in DCM (10 ml) and DIPEA (1.02 mL, 6.0 mmol, 5.0 eq.) was added. Meanwhile a solution of **256** (317 mg, 1.16 mmol, 1.0 eq.) and EDC•HCl (307 mg, 1.60 mmol, 1.4 eq.) in DCM (5 mL) was stirred for half an hour at RT and added to the phenylalanine solution. After further 5 min HOBt (245 mg, 1.60 mmol, 1.4 eq.) was added and the solution was stirred for 20 h at RT. The solution was diluted with ACOEt (50 mL) and washed with 10% aqueous solution of citric acid (2 x 30 mL) and a saturated aqueous solution of $NaHCO_3$ (2 x 30 mL), dried over Na_2SO_4, filtrated and evaporated in vacuo to give a slightly yellow solid which was purified by column chromatography (EtOAc) to give **258** as a colourless solid (501 mg, 0.99 mmol, 85%).

R_f= 0.3 (SiO_2, EtOAc) $[\alpha]_D^{20}$ = +12.10 (c=1.05, DCM)

^{1}H-NMR (300 MHz, $CDCl_3$) δ ppm 1H-NMR (300 MHz) 7.40-7.20 (m, 8H), 7.09-6.90 (m, 2H), 6.78 (s, 1H), 6.44 (d, 1H, J=7.9Hz), 5.22-5.06 (m, 2H), 4.90 (dd, 1H, J=6.3Hz, J=14.1Hz), 4.65 (q, 1H, J=6.1Hz), 3.26-3.02 (m, 4H), 2.63-2.48 (m, 2H), 2.38-2.26 (m, 2H), 1.42 (m, 9H)

^{13}C-NMR (75.5MHz, $CDCl_3$) δ ppm 175.2, 171.2, 168.5, 156.3, 135.7, 135.0, 129.3, 128.7, 128.5, 128.4, 127.1, 121.3, 79.8, 79.2, 67.4, 53.3, 41.0, 40.7, 37.8, 32.4, 28.4

IR (KBr): $\bar{\upsilon}$ = 3332, 2189, 1789, 1722, 1661, 1529, 1456, 1369, 1251, 1170, 1009, 752, 699 cm^{-1}

MS (LR): m/z (%): 528.3 (100) [$M+NH_4^+$], 511.3 [MH^+]

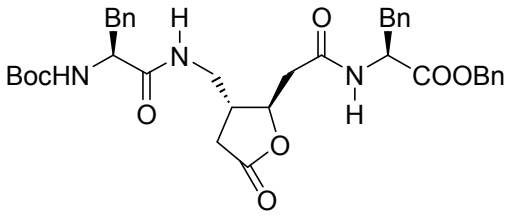

259

Boc-(L)-Phe-(+)-GBA-(L)-Phe-COOBn 259

A solution of **258** (382 mg, 0.75 mmol, 1.0 eq.) in DCM/TFA 50:50 (8 ml) was stirred for 1 h at RT. The solvent was evaporated in vacuo and the resulting TFA salt was precipitated by addition of diethyl ether. The solvent was removed and the resulting colourless solid was dissolved in DCM (8 ml) and DIPEA (650 μL, 3.75 mmol, 5.0 eq.) was added. Meanwhile a solution of Boc-Phe (300 mg, 1.13 mmol, 1.5 eq.) and EDC•HCl (217 mg, 1.13 mmol, 1.5 eq.) in DCM (5 mL) was stirred for half an hour at RT and added to the solution of **6** derivative. After further 5 min HOAt (154 mg, 1.13 mmol, 1.5 eq.) was added and the solution was stirred for 20 h at RT. The solution was diluted with ACOEt (40 mL) and washed with 10% aqueous solution of citric acid (2 x 30 mL) and a saturated aqueous solution of $NaHCO_3$ (2 x 30 mL), dried over Na_2SO_4, filtrated and evaporated in vacuo to give a slightly yellow solid which was purified by column chromatography (PE:EtOAc 1:1) to give **259** as a colourless solid (411 mg, 0.63 mmol, 84%).

R_f= 0.1 (SiO_2, PE:EtOAc 1:1) $[\alpha]_D^{20}$ = +18.03 (c=1.01, DCM)

^{1}H-NMR (300 MHz, $CDCl_3$): δ ppm 740-7.28 (m, 12H), 7.08-6.90 (m, 3H), 6.94-6.88 (m, 1H), 6.85-6.78 (m, 1H), 5.25-5.20 (m, 1H), 5.18-5.10 (m, 2H), 4.91 (dd, 1H, J=7.8Hz, J=13.6Hz), 4.40 (q, 1H, J=5.9Hz), 4.30 (dd, 1H, J=7.2Hz, J=15.5Hz), 3.48 (dt, 1H, J=7.2Hz, J=14.2Hz), 3.13 (d, 1H, J=5.8Hz), 3.05-2.90 (m, 3H), 2.65-2.34 (m, 3H), 2.24-2.18 (m, 2H), 1.40 (s, 9H)

^{13}C-NMR (75.5MHz, $CDCl_3$): 174.1, 171.3, 135.7, 134.8, 133.9, 128.3, 128.2, 127.7, 127.6, 127.4, 126.1, 1259, 79.4, 77.9, 66.5, 59.4, 55.3, 52.5, 39.1, 39.0, 38.4, 37.5, 36.6, 31.2, 27.3, 20.1, 13.2

IR (KBr): $\bar{\upsilon}$ = 3314, 2189, 1650, 1541, 1455, 1175, 1030, 750, 698 cm^{-1}

MS (LR): m/z (%): 658.5 [MH^+]

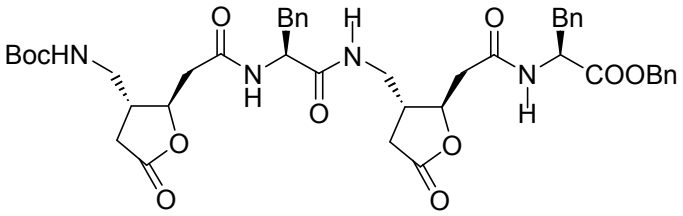

260

Boc-(+)-GBA-(L)-Phe-(+)-GBA-(L)-Phe-COOBn 260

A solution of **259** (312 mg, 0.47 mmol, 1.0 eq.) in DCM/TFA 50:50 (8 ml) was stirred for 1 h at RT. The solvent was evaporated in vacuo and the resulting TFA salt was precipitated by addition of diethyl ether. The solvent was removed and the resulting colourless solid was dissolved in DCM (8 ml) and DIPEA (400 μL, 2.35 mmol, 5.0 eq.) was added. Meanwhile a solution of **249** (194 mg, 0.71 mmol, 1.5 eq.) and EDC•HCl (136 mg, 0.71 mmol, 1.5 eq.) in DCM (5 mL) was stirred for half an hour at RT and added to the solution of **259** derivative. After further 5 min HOAt (109 mg, 0.80 mmol, 1.7 eq.) was added and the solution was stirred for 20 h at RT. The solution was diluted with ACOEt (30 mL) and washed with 10% aqueous solution of citric acid (2 x 20 mL) and a saturated aqueous solution of $NaHCO_3$ (2 x 20 mL), dried over Na_2SO_4, filtrated and evaporated in vacuo to give a slightly yellow solid which was purified by column chromatography (EtOAc) to give **260** as a colourless solid (293 mg, 0.36 mmol, 77%).

R_f= 0.11 (SiO_2, EtOAc) $[\alpha]_D^{20}$ = +15.03 (c=1.00, DCM)

^{1}H-NMR (300 MHz, $CDCl_3$) δ ppm 7.27 (m, 13H), 7.07 (m, 3H), 5.37 (s, 1H) , 5.21-5.07 (m, 2H), 4.80 (td, 2H, J=6.7Hz, J=13.6Hz), 4.75-4.60 (m, 3H), 4.46 (q, 1H, J=6.0Hz), 3.51-3.40 (m, 1H), 3.12-2.93 (m, 8H), 2.60-2.40 (m, 4H), 2.39-2.10 (m, 4H), 1.41 (s, 9H)

^{13}C-NMR (75.5MHz, $CDCl_3$) δ ppm 175.7, 175.6, 172.0, 169.6, 169.1, 136.7, 135.8, 134.9, 129.3, 129.2, 128.6, 128.4, 127.1, 127.0, 79.9, 79.7, 79.4, 67.4, 54.9, 53.7, 40.9, 40.4, 39.5, 37.7, 37.5, 32.3, 28.4

IR (KBr): $\bar{\upsilon}$ = 3416, 2197, 2082, 1646, 1541, 1455, 1175, 1030, 750, 698 cm^{-1}

MS = [ESI (DCM/MeOH + 10 mmol/l NH_4Ac)] : m/z (%) 713.4 [M + H^+ - Boc] (11), 757.4 [M + H^+ - C_4H_8] (25), 813.4 [M + H^+] (80), 830.5 [M + NH_4^+] (100)

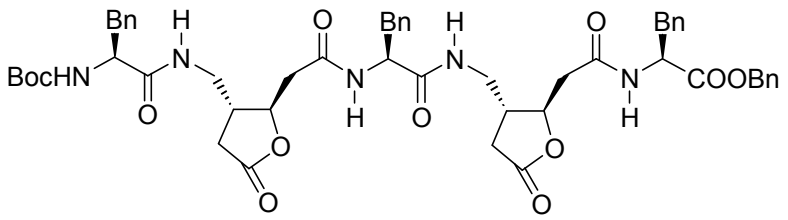

261

Boc-(L)-Phe-(+)-GBA-(L)-Phe-(+)-GBA-(L)-Phe-COOBn 261

A solution of **260** (298 mg, 0.37 mmol, 1.0 eq.) in DCM/TFA 50:50 (6 ml) was stirred for 1 h at RT. The solvent was evaporated in vacuo and the resulting TFA salt was precipitated by addition of diethyl ether. The solvent was removed and the resulting colourless solid was dissolved in DCM (6 ml) and DIPEA (320 µL, 1.85 mmol, 5.0 eq.) was added. Meanwhile a solution of Boc-Phe (146 mg, 0.55 mmol, 1.5 eq.) and EDC•HCl (106 mg, 0.55 mmol, 1.5 eq.) in DCM (4 mL) was stirred for half an hour at RT and added to the solution of **260** derivative. After further 5 min HOAt (75 mg, 0.55 mmol, 1.5 eq.) was added and the solution was stirred for 20 h at RT. The solution was diluted with ACOEt (30 mL) and washed with 10% aqueous solution of citric acid (2 x 20 mL) and a saturated aqueous solution of $NaHCO_3$ (2 x 20 mL), dried over Na_2SO_4, filtrated and evaporated in vacuo to give a slightly yellow solid which was purified by column chromatography (EtOAc) to give **261** as a colourless solid (300 mg, 0.32 mmol, 86%).

R_f= 0.3 (SiO_2, EtOAc); $[\alpha]_D^{20}$ = +19.05 (c=1.03, DCM)

^{1}H-NMR (600 MHz, $CDCl_3$): δ ppm 8.25 (t, 1H, J=5.2Hz), 8.14 (d, 1H, J=5.3Hz), 7.68 (d, 1H, J=7.5Hz), 7.61 (d, 1H, J=6.8Hz), 7.30-6.90 (m, 20H), 5.23 (d, 1H, J=7.8Hz), 5.19-5.06 (m, 2H), 4.85-4.76 (m, 1H) ppm 4.72-4.62 (m, 1H), 4.60-4.50 (m, 1H), 4.48-4.36 (m, 2H), 3.75-3.72 (m, 2H), 3.36 (t, 1H, J=6.2Hz), 3.20-3.10 (m, 2H), 3.10-2.90 (m, 2H), 2.90-2.70 (2H), 2.63-2.50 (m, 6H), 2.45-2.30 (m, 4H), 1.39 (s, 9H)

^{13}C-NMR (125MHz, $CDCl_3$) δ ppm 175.8, 175.7, 175.6, 172.0, 171.3, 169.6, 169.1, 155.8, 136.7, 135.8, 134.9, 129.3, 129.2, 128.6, 128.4, 127.1, 127.0, 79.9, 79.7, 79.4, 79.2, 67.4, 54.9, 53.7, 41.3, 40.9, 40.4, 39.8, 39.5, 39.0, 37.7, 37.5, 32.3, 28.4

IR (KBr): $\bar{\upsilon}$ = 3420, 2190, 2062, 1643, 1521, 1435, 1170, 1035, 760, 698 cm^{-1}

MS = [ESI (DCM/MeOH + 10 mmol/l NH_4Ac)] : m/z (%) 960.5 [M + H^+] (100), 977.5 [M + NH_4^+] (25)

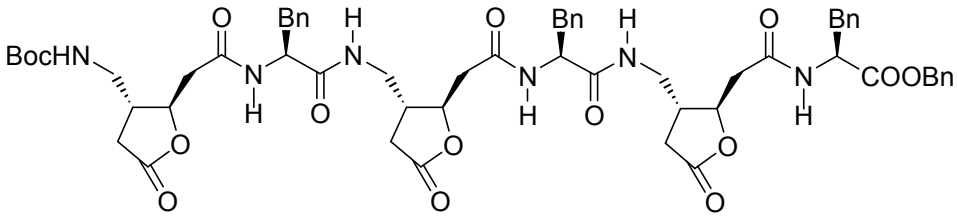

262

Boc-(+)-GBA-(L)-Phe-(+)-GBA-(L)-Phe-(L)-Phe-(+)-GBA -COOBn 262

A solution of **261** (200 mg, 0.21 mmol, 1.0 eq.) in DCM/TFA 50:50 (8 ml) was stirred for 1 h at RT. The solvent was evaporated in vacuo and the resulting TFA salt was precipitated by addition of diethyl ether. The solvent was removed and the resulting colourless solid was dissolved in DCM (5 ml) and DIPEA (180 µL, 1.05 mmol, 5.0 eq.) was added. Meanwhile a solution of **249** (82 mg, 0.32 mmol, 1.5 eq.) and EDC•HCl (61 mg, 1.05 mmol, 1.5 eq.) in DCM (3 mL) was stirred for half an hour at RT and added to the solution of **261** derivative. After further 5 min HOAt (44 mg, 0.32 mmol, 1.5 eq.) was added and the solution was stirred for 20 h at RT. The solution was diluted with ACOEt (20 mL) and washed with 10% aqueous solution of citric acid (2 x 15 mL) and a saturated aqueous solution of $NaHCO_3$ (2 x 15 mL), dried over Na_2SO_4, filtrated and evaporated in vacuo to give a slightly yellow solid which was purified by column chromatography (EtOAc:MeOH 9:1) to give **260** as a colourless solid (211 mg, 0.19 mmol, 90%).

R_f= 0.5 (SiO_2, EtOAc:MeOH 9:1) $[\alpha]_D^{20}$ = +16.12 (c=1.03, DCM)

^{1}H-NMR (300 MHz, $CDCl_3$): 8.55 (d, 1H, J=6.1Hz), 8.48 (d, 1H, J=5.0Hz), 8.34 (d, 1H, J=9.7Hz), 7.75 (d, 1H, J=7.2Hz), 7.53-7.00 (m, 20H), 5.22 (d, 1H, J=8.5Hz), 5.25-5.05 (m, 2H), 4.74-4.67 (m, 1H), 4.65-4.59 (m, 1H), 4.57-4.50 (m, 1H), 4.47-4.42 (m, 1H), 4.24-4.18 (m, 1H), 3.86-3.80 (m, 1H), 3.75-3.72 (m, 1H), 3.10-2.80 (m, 12H), 2.78-2.65 (m, 3H), 2.57-2.47 (m, 3H), 2.42-2.20 (m, 8H), 1.39 (s, 9H)

^{13}C-NMR (75.5MHz, $CDCl_3$): 175.4, 174.8, 172.5, 168.6, 168.0, 167.4, 166.8, 166.5, 166.2, 166.1, 138.9, 138.4, 136.6, 136.3, 135.5, 134.6, 129.1, 128.9, 128.7, 128.6, 128.5, 128.1, 127.2, 127.1, 81.0, 79.9, 79.7, 79.4, 79.2, 67.4, 54.9, 53.7, 41.3, 40.9, 40.4, 39.8, 39.5, 39.0, 37.7, 37.5, 32.3, 28.4

IR (KBr): $\bar{\upsilon}$ = 3425, 2170, 2062, 1633, 1521, 1455, 1140, 1055, 750, 668 cm^{-1}

MS = [ESI (DCM/MeOH + 10 mmol/l NH_4Ac)] : [ESI (DCM/MeOH + 10 mmol/l NH_4Ac)] : m/z (%) 1115.5 [M + H^+] (100), 1132.5 [M + NH_4^+] (40)

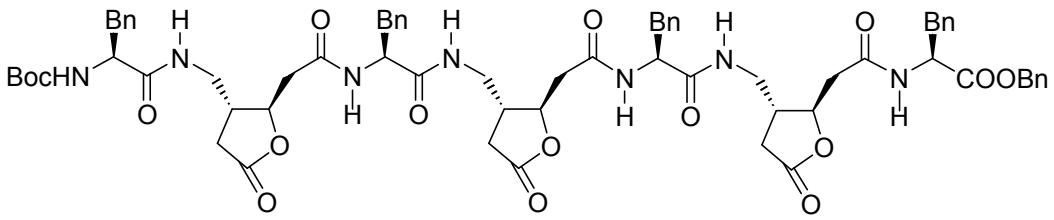

263

Boc-(L)-Phe-(+)-GBA-(L)-Phe-(+)-GBA-(L)-Phe-(+)-GBA-(L)-Phe-(+)-COOBn 263

A solution of **262** (192 mg, 0.17 mmol, 1.0 eq.) in DCM/TFA 50:50 (6 ml) was stirred for 1 h at RT. The solvent was evaporated in vacuo and the resulting TFA salt was precipitated by addition of diethyl ether. The solvent was removed and the resulting colourless solid was dissolved in DCM (6 ml) and DIPEA (150 µL, 0.85 mmol, 5.0 eq.) was added. Meanwhile a solution of Boc-Phe (69 mg, 0.26 mmol, 1.5 eq.) and EDC•HCl (50 mg, 0.26 mmol, 1.5 eq.) in DCM (4 mL) was stirred for half an hour at RT and added to the solution of **260** derivative. After further 5 min HOAt (33 mg, 0.26 mmol, 1.5 eq.) was added and the solution was stirred for 20 h at RT. The solution was diluted with ACOEt (30 mL) and washed with 10% aqueous solution of citric acid (2 x 20 mL) and a saturated aqueous solution of $NaHCO_3$ (2 x 20 mL), dried over Na_2SO_4, filtrated and evaporated in vacuo to give a slightly yellow solid which was purified by column chromatography (EtOAc) to give **261** as a colourless solid (131 mg, 0.10 mmol, 61%).

R_f = 0.3 (SiO_2, EtOAc) $[\alpha]_D^{20}$ = +19.03 (c=1.05, DCM)

^{1}H-NMR (600 MHz, $CDCl_3$): δ ppm 8.55 (d, 1H, J=6.1Hz), 8.48 (d, 1H, J=5.0Hz), 8.34 (d, 1H, J=9.7Hz), 8.00 (d, 1H, J=9.2Hz), 7.75 (d, 1H, J=7.2Hz), 7.53-7.33 (m,19H), 7.31.7-00 (m, 6H), 5.22 (d, 1H, J=8.5Hz), 5.25-5.05 (dd, 2H), 4.81 (dd, 1H, J=7.8Hz, J=14.1Hz), 4.74-4.67 (m, 1H), 4.65-4.59 (m, 1H), 4.57-4.50 (m, 1H), 4.47 (dd, 1H, J=8.7Hz, J=14.5Hz), 4.26-4.18 (m, 1H), 3.90-3.80 (m, 1H), 3.75-3.68 (m, 2H), 3.10-2.80 (m, 14H), 2.78-2.65 (m, 4H), 2.57-2.47 (m, 3H), 2.42-2.20 (m, 8H), 1.39 (s, 9H)

^{13}C-NMR (125MHz, $CDCl_3$): 175.4, 174.8, 172.5, 168.6, 168.5, 168.0, 167.4, 166.8, 166.5, 166.2, 166.1, 138.9, 138.4, 136.6, 136.3, 135.5, 134.65, 134.60, 129.10, 129.05, 128.9, 128.7, 128.6, 128.58, 128.54, 128.51, 128.1, 127.2, 127.1, 81.0, 79.9, 79.7, 79.4, 79.2, 79.1, 67.4, 54.9, 53.7, 41.3, 40.9, 40.4, 39.8, 39.5, 39.0, 37.7, 37.5, 32.3, 28.4

IR (KBr): $\bar{\upsilon}$ = 3445, 2180, 2052, 1646, 1525, 1455, 1150, 1055, 750, 678 cm^{-1}

MS = [ESI (DCM/MeOH + 10 mmol/l NH_4Ac)] : m/z (%) 1261.6 [M + H^+] (100), 1278.6 [M + NH_4^+] (35)

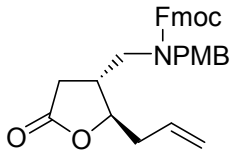

264

(2R,3R)-(2-Allyl-5-oxo-tetrahydro-furan-3-ylmethyl)-(4-methoxy-benzyl)-carbamic acid 9H-fluoren-9-ylmethyl ester 264

To a cold (0°C) solution of **252** (880 mg, 5.44 mmol, 1.0 eq.) in dioxane / 1M aqueous solution of K_2CO_3 (20 ml / 16 ml) was added portionwise FmocSu (1.605 gr, 4.80 mmol, 1.2 eq.). The reaction was allowed to come at RT and stirred overnight. The mixture was poured in water (30 m) and extracted with EtOAc (3 x 50 mL).

The combined organic layers were dried over Na_2SO_4, filtered and evaporated in vacuo to give a sticky solid which was purified by column chromatography (PE:EtOAc 2:1) to obtain **264** (1.679 g, 3.38 mmol, 84%) as a sticky, colourless solid.

R_f = 0.23 (SiO_2, PE:EtOAc 2:1) ; $[\alpha]_D^{20}$ = +10.40 (c = 1.00)

^{1}H-NMR (300 MHz, $CDCl_3$): δ ppm7.75 (d, 2H, J=7.4 Hz), 7.55 (bs, 2H), 7.45-7.22 (m, 4H), 7.07-6.79 (m, 4H), 5.83-5.42 (m, 1H), 5.22-4.93 (m, 2H), 4.83 (s, 1H), 4.63 (s, 1H), 4.27-4.07 (m, 4H), 3.78 (s, 3H), 3.26 (s, 1H), 2.66 (s, 1H), 2.52-2.17 (m, 3H), 2.11-1.84 (m, 2H)

^{13}C-NMR (75.5MHz, $CDCl_3$): δ ppm 159.2, 143.8, 143.7, 141.4, 132.1, 129.1, 129.0, 128.9, 128.8, 127.8, 127.3, 127.2, 124.6, 124.4, 120.0, 118.8, 114.1, 82.2, 77.5, 77.1, 76.7, 67.1, 60.4, 55.3, 50.7, 47.5, 38.7, 38.5, 32.9

IR (KBr): $\bar{\upsilon}$ = 3046, 2966,2921, 2835, 2362, 1768, 1680

MS = [ESI (DCM/MeOH + 10 mmol/l NH_4Ac)] : m/z (%) 498.3 [M + H^+] (21), 515.3 [M + NH_4^+] (100), 1012.6 [2M + NH_4^+] (5)

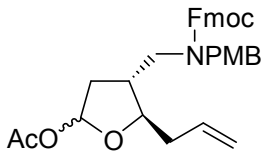

265

(4R,5R)- Acetic acid 5-allyl-4-v-tetrahydro-furan-2-yl ester 265

To a cold (-78°C) solution of **264** (1.47 g, 2.95 mmol, 1.0 eq.) in dry DCM (50 mL) under nitrogen was added portionwise in 30 min a 1M solution in DCM of DIBAL-H (3.0 mL, 3.0 mmol, 1.1 eq.) until the total consumption of the starting material. The reaction was quenched with dry MeOH (4 mL) and warmed to RT. Then DCM (30 mL) and a saturated solution of $NaHCO_3$ (5 mL) were added to the mixture. The organic phase was separated and the aqueous phase was extracted with DCM (3 x 20 mL). The combined organic layers were dried over Na_2SO_4, filtrated through a celite pad, evaporated in vacuo to give a sticky solid which was dissolved in DCM (10 mL) and cooled at 0°C with an ice bath. To the solution were added sequentially acetic anhydride (550 μL, 5.90 mmol, 2.0 eq.) and DIPEA (1.00 mL, 5.90 mmol, 2.0 eq.) and the reaction was then allowed to come at RT and stirred overnight. The solution was diluted with water (20 mL) and extracted with EtOAc (3 x 30 mL). The combined organic layers were dried over Na_2SO_4, evaporated in vacuo to obtain a sticky solid which was purified by column chromatography (PE:EtOAc 2:1) to give **265** (1.374 g, 2.53 mmol, 86%, diastereomic ratio 3:1) as a sticky, colourless solid.

R_f = 0.33 (SiO_2, PE:EtOAc 2:1)

^{1}H-NMR (300 MHz, $CDCl_3$): 7.77 (s, 2H), 7.65-7.49 (m, 2H), 7.45-7.22 (m, 4H), 7.11-6.71 (m, 4H), 6.30-5.95 (m, 1H), 5.85-5.57 (m, 1H), 5.12-4.91 (m, 2H), 4.82-4.49 (m, 2H), 4.46-4.29 (m, 1H), 4.27-4.24 (2H, m), 3.81 (s, 3H), 3.80-3.72 (m, 1H), 3.52-3.18 (m, 2H), 2.41-2.18 (m, 2H), 2.10 (s, 3H), 2.08-2.00 (m, 3H)

^{13}C-NMR (75.5MHz, $CDCl_3$): 170.3, 159.0, 156.4, 143.9, 141.4, 134.0, 133.7, 129.2, 128.7, 127.7, 127.1, 124.7, 120.0, 117.8, 117.5, 114.2, 98.2, 67.2, 60.4, 55.3, 50.1, 47.4, 41.3, 39.0, 21.2, 14.2

IR (KBr): $\bar{\upsilon}$ = 3016, 1750, 1640, 1520, 1318, 1151, 1027

MS = [ESI (DCM/MeOH + 10 mmol/l NH_4Ac)] : m/z (%) 482.3 $[MH^+ - CH_3COOH]^+$ (84), 499.3 $[MNH_4^+ - CH_3COOH]^+$ (6), 559.4 $[MNH_4^+]$ (100)

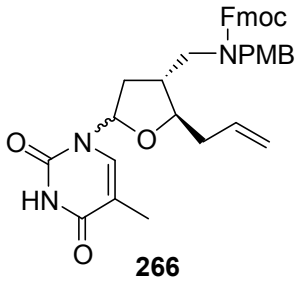

266

(4R,5R)-[2-Allyl-5-(5-methyl-2,4-dioxo-3,4-dihydro-2H-pyrimidin-1-yl)-tetrahydro-furan-3-ylmethyl]- (4-methoxy-benzyl)-carbamic acid 9H-fluoren-9-ylmethyl ester 266

To a cold (-10°C) solution of **17** (542 mg, 1.00 mmol, 1.0 eq.) in dry acetonitrile (20 mL) under nitrogen was added a precomplexed solution of $SnCl_4$ (120 µL, 1.00 mmol, 1.0 eq.) and persilylated thymine (1.5 mmol, 405 mg, 1.5 eq.) in dry acetonitrile (10 ml). The reaction was stirred for 30 min, warmed at RT and stirred for further 20 min until the total consumption of the starting material. The reaction was then quenched with a saturated solution of $NaHCO_3$ (5 mL) and stirred for further 5 min. The organic layer was separated and the aqueous layer was extracted with EtOAc (3 x 15 mL). The combined organic layers were dried over Na_2SO_4, filtrated and evaporated in vacuo to give a sticky solid which was purified by column chromatography (PE:EtOAc 1:1) to give **18** (418 mg, 0.75 mmol, 75%) as a colourless solid.

R_f = 0.2 (SiO_2, PE:EtOAc 1:1)

^{1}H-NMR (300 MHz, $CDCl_3$): 8.81 (bs, 1H), 7.75 (2H, s), 7.64-7.44 (2H, m), 7.45-7.13 (5H, m), 7.07-6.77 (4H, m), 5.99 (d, 1H, J=6.1Hz), 5.88-5.51 (m, 1H), 5.20-4.94 (m, 2H), 4.90-4.71 (m, 2H), 4.67-4.47 (m, 1H), 4.20-4.05 (m, 2H), 3.79 (s, 3H), 3.80-3.75 (m, 1H), 3.25 (bs, 1H), 2.81-2.65 (m, 1H), 2.41-2.28 (m, 1H), 2.10-1.90 (m, 2H), 1.93 (d, 3H, J=6.2Hz), 1.90-1.53 (m, 2H)

^{13}C-NMR (75.5MHz, $CDCl_3$): 163.8, 159.1, 157.8, 156.3, 150.1, 148.6, 143.8, 141.4, 133.5, 133.4, 129.1, 128.8, 127.7, 127.1, 124.6, 120.0, 114.1, 112.8, 110.4, 82.7, 55.3, 47.5, 37.5, 35.8, 31.0, 12.7

IR (KBr): $\bar{\upsilon}$ = 3015, 1718, 1490, 1332, 1170, 1035

MS = ESI (DCM/MeOH + 10 mmol/l NH_4Ac)] : m/z (%) 608.4 [M + H^+] (47), 625.4 [M + NH_4^+] (100)

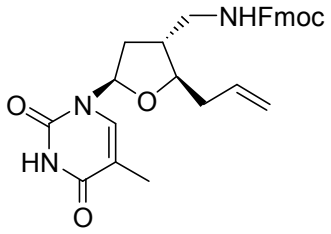

267

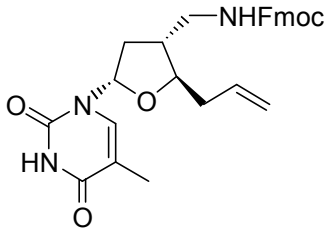

268

(2R, 4R, 5R)-[2-Allyl-5-(5-methyl-2,4-dioxo-3,4-dihydro-2H-pyrimidin-1-yl)-tetrahydro-furan-3-ylmethyl]-carbamic acid 9H-fluoren-9-ylmethyl ester 267

and (2S, 4R, 5R)-[2-Allyl-5-(5-methyl-2,4-dioxo-3,4-dihydro-2H-pyrimidin-1-yl)-tetrahydro-furan-3-ylmethyl]-carbamic acid 9H-fluoren-9-ylmethyl ester 268

To a cold (0°C) solution of **266** (340 mg, 0.56 mmol, 1.0 eq.) in acetonitrile / water (7 mL / 2.4 mL) CAN (1.23 g, 2.24 mmol, 4.0 eq., conc. 0.25 M) was added portionwise. The reaction was stirred at 0°C for 1 h and at RT for 2 additional hours until the total consumption of the starting material. The reaction was then poured in water (30 mL), extracted with EtOAc (3 x 30 mL). The combined organic layers were washed with a saturated solution of $NaHCO_3$ (30 mL), dried over Na_2SO_4, filtered and evaporated in vacuo to obtain a colourless solid which was purified by column chromatography (PE:EtOAc 1:1) to give **267** (104 mg, 0.21 mmol, 38%) and **268** (94 mg, 0.19 mmol, 34%) as colourless solids.

267

R_f = 0.06 (SiO_2, PE:EtOAc 1:1) ; $[\alpha]_D^{20}$ = +8.92 (c = 1.03)

^{1}H-NMR (600 MHz, $CDCl_3$): δ ppm 9.35 (s, 1H) ppm 7.76 (d, 2H, J=7.5Hz) ppm 7.58 (d, 2H, J=7.3Hz) ppm 7.40 (t, 2H, J=7.3Hz) ppm 7.35-7.25 (m, 3H), 6.04-5.95 (m, 1H), 5.92-5.80 (m, 1H), 5.25-5.10 (m, 2H), 4.50-4.42 (m, 1H), 4.24-4.18 (m, 2H), 3.83-3.78 (m, 1H), 3.37-3.27 (m, 1H), 3.25-3.15 (m, 1H), 2.60-2.45 (m, 1H), 2.40-2.15 (m, 2H), 2.08-2.04 (m, 1H), 1.93 (s, 3H), 1.78 (m, 1H)

^{13}C-NMR (150MHz, $CDCl_3$): 163.9, 156.6, 150.4, 143.8, 141.3, 135.3, 133,4, 127.7, 127.0, 124.9, 120.0, 118.5, 110.6, 85.0, 82.7, 82.5, 66.6, 47.3, 42.2, 38.4, 36.6, 12.6

IR (solid): $\bar{\upsilon}$ = 2926, 1685, 1513, 1468, 1244, 1105, 915

MS = [ESI, (DCM/MeOH + 10 mmol/l NH_4Ac)]: m/z (%) 488.4 (8) [M + H^+], 505.4 (100) [M + NH_4^+], 992.8 (16) [2M + NH_4^+]

268

R_f = 0.13 (SiO_2, PE:EtOAc 1:1) ; $[\alpha]_D^{20}$ = +3.10 (c = 1.02)

^{1}H-NMR (600 MHz, $CDCl_3$): δ ppm 9.55 (bs, 1H), 7.75 (d, 2H, J=7.5Hz), 7.60 (m, 2H), 7.39 (t, 2H, J=7.2Hz), 7.31 (m, 3H), 7.13 (s, 1H), 5.88-5.77 (m, 2H), 5.20-5.10 (m, 2H), 4.40-4.28 (m, 1H), 4.22-4.18 (m, 2H), 3.49-3.40 (m, 1H), 3.31-3.26 (m, 1H), 2.52-3.44 (m, 1H), 2.43-3.37 (m, 2H), 2.36-3.27 (m, 1H), 2.26 (m, 1H), 1.94 (s, 3H), 1.91-1.86 (m, 1H)

^{13}C-NMR (7150MHz, $CDCl_3$): 163.8, 156.8, 150.9, 143.9, 141.3, 135.2, 133,4, 127.6, 127.0, 125.1, 120.0, 118.4, 111.1, 88.7, 80.2, 78.8, 66.9, 47.2, 42.0, 39.9, 33.0, 12.7

IR (solid): $\bar{\upsilon}$ = 2985, 1723, 1522, 1473, 1253, 1095, 902

MS = [ESI, (DCM/MeOH + 10 mmol/l NH_4Ac)]: m/z (%) 488.4 (12) [M + H^+], 505.4 (100) [M + NH_4^+], 992.8(18) [2M + NH_4^+

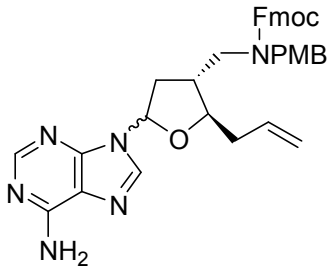

270

(2R/S,3R,5R)-[2-Allyl-5-(6-amino-purin-9-yl)-tetrahydro-furan-3-ylmethyl]-(4-methoxy-benzyl)-carbamic acid 9H-fluoren-9-ylmethyl ester 270

To a cold (-10°C) solution of **265** (450 mg, 0.83 mmol, 1.0 eq.) in dry acetonitrile (20 ml) under nitrogen was added a solution of persylilated adenine (350 mg, 1.25 mmol, 1.5 eq.) and $SnCl_4$ (100 µL, 0.83 mmol, 1.0 eq.) in dry acetonitrile (5 mL). The mixture was stirred at -10°C for 30 min, warmed at RT, stirred for additional 15 min and quenched with a saturated solution of $NaHCO_3$. The organic phase was separated and the aqueous phase was extracted with AcOEt (3 x 15 mL). The combined organic layers were dried over Na_2SO_4, filtrated and evaporated in vacuo to obtain a amorphous solid which was purified by column chromatography (EtOAc) to give **19** (333 mg, 0.54 mmol, 65%) as a colourless solid.

R_f = 0.14 (SiO_2, EtOAc)

^{1}H-NMR (300 MHz, $CDCl_3$): δ ppm 8.37-8.22 (m, 1H), 8.11-7.78 (m, 1H), 7.72 (d, 2H, J=7.3 Hz), 7.63-7.46 (m, 2H), 7.43-7.17 (m, 4H), 7.08-6.71 (m, 4H), 6.64-6.41 (m, 2H), 6.19 (s, 0.6H, first diastereomers), 6.04-5.86 (m, 0.4H, second diastereomers), 5.84-5.50 (m, 1H), 5.16-4.90 (m, 2H), 4.80 (s, 1H), 4.60 (d, 1H, J=4.4 Hz), 4.34-4.14 (m, 2H), 3.89-3.81 (m, 1H), 3.78 (s, 3H), 3.46-3.17 (m, 1H), 2.96-2.69 (m, 1H), 2.57-1.83 (m, 6H)

^{13}C-NMR (75.5MHz, $CDCl_3$): 159.1, 156.4, 155.0, 151.6, 143.0, 143.9, 143.8, 141.5, 139.2, 133.6, 129.1, 128.8, 127.7, 127.2, 124.8, 124.7, 124.6, 124.5, 120.2, 120.0, 118.1, 117.7, 114.0, 82.7, 55.3, 48.1, 47.6, 37.0, 32.0

IR (solid): $\bar{\upsilon}$ = 3320, 3172, 1693, 1639, 1595, 1297, 1367, 1032

MS = [ESI, (DCM/MeOH + 10 mmol/l NH_4Ac)]: m/z (%) = 617.4 (100) [M + H^+]

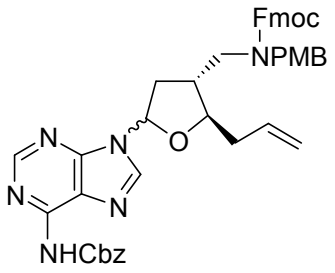

271

[9-(5-Allyl-4-{[(9H-fluoren-9-ylmethoxycarbonyl)-(4-methoxy-benzyl)-amino]-methyl}-tetrahydro-furan-2-yl)-9H-purin-6-yl]-carbamic acid benzyl ester 271

To a cold solution (0°C) of **12** (953 mg, 1.73 mmol, 1 eq.) in dry DCM (20 ml) was added bromotrimethylsilane (340 µl, 2.57 mmol, 1.5 eq.). The reaction was stirred for 4 hours and **20** (930 mg, 3.46 mmol, 2 eq.) was added. The precipitate was then dissolved by addition of DMF (20 ml), the solution was warmed at RT and stirred overnight. The obtained suspension was quenched with a saturated solution of $NaHCO_3$, the aqueous layer was separate and extracted with EtOAc (3 x 20 ml). The combined organic layers were dried with $MgSO_4$, filtrated and evaporated in vacuo to

obtain a sticky solid which was purified by column chromatography to give **21** (962 mg, 1.28 mmol, 74%) as a white solid.

R_f = 0.14 (SiO_2, PE:EtOAc 1:1)

^{1}H-NMR (300 MHz, $CDCl_3$): δ ppm 8.75 (s, 1H), 8.12-7.81 (m, 1H), 7.72 (d, 2H, J=7.0 Hz), 7.61-7.18 (m, 11H), 7.02-6.69 (m, 4H), 6.25-5.87 (m, 1H), 5.83-5.46 (m, 1H), 5.30 (d, 2H, J=3.69), 5.14-4.92 (m, 2H), 4.90-4.74 (m, 1H), 4.66-4.49 (m, 1H), 4.40-4.10 (m, 3H), 3.90-3.81 (bs, 1H), 3.78 (s, 3H), 3.47-3.16 (m, 2H), 2.95-2.62 (m, 1H), 2.60-1.82 (m, 6H)

^{13}C-NMR (75.5MHz, $CDCl_3$): δ ppm 159.1, 156.4, 152.6, 151.0, 149.3, 143.9, 143.8, 141.4, 141.3, 135.4, 133.6, 133.5, 129.1, 129.0, 128.9, 128.8, 128.7, 128.6, 127.7, 127.3, 127.1, 124.8, 124.7, 124.5, 124.4, 123.1, 122.7, 121.4, 120.0, 118.1, 114.0, 67.8, 55.3, 47.4, 42.0, 36.9

IR (KBr): $\bar{\upsilon}$ = 2910, 1754, 1693, 1609, 14460, 1118, 910

MS = [ESI, (DCM/MeOH + 10 mmol/l NH_4Ac)]: m/z (%) 751.3

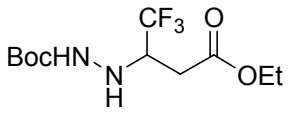

306

3-**(N'-tert-Butoxycarbonyl-hydrazino)-4,4,4-trifluoro-butyric acid ethyl ester 306**

A solution of **1** (1.74 g, 10.35 mmol, 1.0 eq.) and hydrazinecarboxylic acid tert-butyl ester (2.73 g, 20.70 mmol, 2.0 eq.) in MeOH (15 ml) was stirred in a sealed tube at 80°C over 5 days. The solvent was evaporated under vacuum and purified by chromatography (cyclohexane:EtOAc 8:2), obtaining **2** (2.80 g, 9.35 mmol, 90%) as a slightly yellow oil.

^{1}H NMR (200 MHz, $CDCl_3$) δ ppm 6.48 (br s, 1 H), 4.80 (br s, 1 H), 4.46 (q, *J* = 7.2 Hz, 2H), 4.16 (m, 1H), 2.90 (m, 2H), 1.71 (s, 9H), 1.53 (t, *J* = 7.2 Hz, 3H).

^{13}C NMR (75 MHz, $CDCl_3$) δ ppm 169.8, 125.3, 81.3 (CBoc), 61.3, 58.5, 32.1, 28.2 , 14.0

^{19}F (188 MHz, $CDCl_3$) δ ppm -75.3 (d, *J* = 5.6 Hz).

R_f: 0.3 (EtOAc:cyclohexane 1:4)

IR (cm^{-1}): 3193, 1715, 1157, 1121, 774

MS (ESI Positive) m/z: 323 $[M+Na]^+$

Elemental Anal. Calculated for $[C_{11}H_{19}F_3N_2O_4]$ C 44.00, H 6.38, N 9.33 found C 43.72, H 6.16, N 9.69

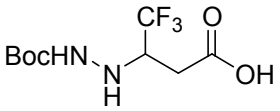

295

3-(N'-tert-Butoxycarbonyl-hydrazino)-4,4,4-trifluoro-butyric acid 295

To a solution of **396** (985 mg, 3.28 mmol, 1.0 eq.) in THF/MeOH (5 ml/5 ml) a 2N solution of NaOH (1.8 ml, 3.6 mmol, 1.1 eq.) was added. The reaction was stirred at RT over 3 hrs. The solvent was removed under vacuum (without distilling the water) and the remaining solution was bring at pH=1 by addition of 1N solution of HCl. The aqueous phase was extracted with EtOAc (3x 20 ml). The combined organic layers were dried with $MgSO_4$, filtered and concentrated under vacuum to obtain the product **295** (844 mg, 3.10 mmol, 95%) as a white solid which was used in the next step without further purification.

^{1}H NMR (300 MHz, DMSO-*d*6) δ ppm 12.54 (br s, 1H) 8.39 (br s, 1H), 3.82 (m, 1H), 2.61 (dd, *J* = 16.6 and 5.4 Hz, 1H), 2.44 (dd, *J* = 16.6 and 6.8Hz, 1H), 1.38 (s, 9H).

^{13}C NMR (75 MHz, DMSO-*d*6) δ ppm 170.8, 156.4, 125.9 (q, *J* = 280.5 Hz), 78.9, 57.4, 32.4, 28.0

^{19}F (188 MHz, DMSO-*d*6) δ ppm -74.1 (d, *J* = 6.8 Hz).

R_f: 0.3 (EtOAc/cyclohexane: 70/30)

mp: 138-140 °C (crude)

IR (cm^{-1}): 3325 (NH), 3100 (OH), 1732 (C=O), 1687 (C=O), 1122 (C-O), 760 (CF_3)

MS (ESI Negative) m/z: 271 $[M-H]^-$

Elemental Anal. Calculated for $[C_9H_{15}F_3N_2O_4]$ C 39.71, H 5.55, N 9.3310.29 found C 39.83, H 5.50, N 10.29

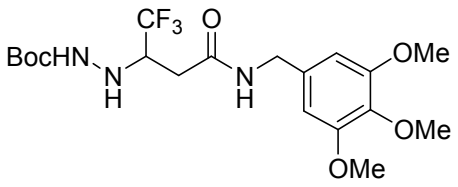

307

N'-{2,2,2-Trifluoro-1-[(3,4,5-trimethoxy-benzylcarbamoyl)-methyl]-ethyl}-hydrazinecarboxylic acid tert-butyl ester 307

To a solution of **295** (1.34 g, 4.92 mmol, 1.0 eq.) and HBTU (2.23 g, 5.90 mmol, 1.2 eq.) in DMF (10 ml) pre-complexed for 30 min. were added in the order HOBt (798 mg, 5.90 mmol, 1.2 eq.), DIPEA (1.65 ml, 9.84 mmol, 2.0 eq.) and phenylalanine hydroxychloride. The reaction was performed under argon atmosphere a RT overnight. The solvent was evaporated over vacuum and the product dissolved in EtOAc (25 ml). The organic layer was washed with 10% aqueous solution of citric acid (2 x 15 ml),water (30 ml), a 10% aqueous solution of K_2CO_3 (2 x 15 ml) and brine (20 ml), dried over Na_2SO_4, filtrated and evaporated in vacuo to give a slightly yellow solid which was purified by column chromatography (EtOAc:cyclohexane 1:1) to give **307** as a colourless solid (1.70 g, 3.76 mmol, 76%).

^{1}H NMR (300 MHz, $CDCl_3$) δ ppm 6.64 (s, 2H), 6.29 (s, 1H), 4.45 (m, 2H), 4.34 (m, 1H), 3.89 (s, 6H), 3.86 (s, 3H), 3.79 (m, 2H), 2.57 (s, 1H), 1.67 (s, 9H)

^{13}C NMR (75 MHz, $CDCl_3$) δ ppm 168.2 ,156.7, 153.2, 137.1, 105.1, 81.5, 60.8, 59.0, 56.1, 44.0, 33.3, 28.2

^{19}F (188 MHz, $CDCl_3$) δ ppm -75.09 (d, 1H, J=7.0Hz)

R_f: 0.5 (SiO_2, cyclohexane:EtOAc 1:1)

mp: 138-140 °C (crude)

IR (cm^{-1}): 3300, 1652, 1506, 1234, 1123

MS (ESI Negative) m/z: 474.2 [M+Na^+]

Elemental Anal. Calculated for [C19H28F3N3O6+1H_2O] C 48,61 H 6.45 N8.95 found C 48.40 H 5.88 N 8.49

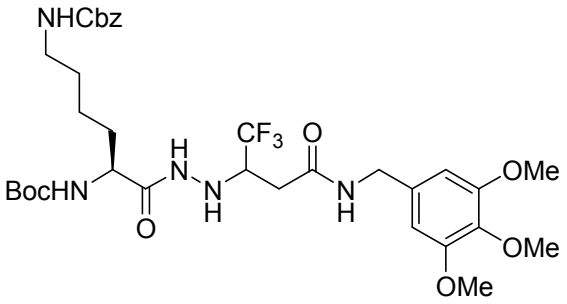

309

[5-tert-Butoxycarbonylamino-5-(N'-{2,2,2-trifluoro-1-[(3,4,5-trimethoxy-benzylcarbamoyl)-methyl]-ethyl}-hydrazinocarbonyl)-pentyl]-carbamic acid benzyl ester 309

A solution of **307** (926 mg, 1.99 mmol, 1.0 eq.) in DCM/TFA 3:1 (12 ml) was stirred for 2 h at RT. The solvent was evaporated in vacuo and the excess of trifluoroacetic acid was coevaporated with methanol. The resulting slightly yellow solid was dissolved in DMF (5 ml), then DIPEA (1.6 ml, 10.0 mmol, 5.0 eq.) and HOBt (323 mg, 2.39 mmol, 1.2 eq.) were added. Meanwhile a solution of NαBocNεZlysine (910 mg, 2.39 mmol, 1.2 eq.) and HBTU (906 mg, 2.39 mmol, 1.2 eq.) in DMF (5 mL) was stirred for half an hour at RT. The two solutions were then combined and the resulting mixture was stirred at RT overnight. The solvent was evaporated under vacuum and the resulting yellow oil was diluted with ACOEt (30 mL) and washed with 10% aqueous solution of citric acid (2 x 20 mL), a 10% aqueous solution of K_2CO3 (2 x 20 mL) and brine (30 ml), dried over Na_2SO_4, filtrated and evaporated in vacuo to give a slightly yellow solid which was purified by column chromatography (cyclohexane:EtOAc 1:1) to give **309** as a colourless solid (1.19 g, 1.67 mmol, 84%).

^{1}H NMR (300 MHz, DMSO-*d*6) δ ppm 1H-NMR (300 MHz) 9.48 (d, 1H, J=5.2Hz), 8.57 (m, 1H), 7.28-7.36 (m, 5H), 7.23 (t, 1H, J=5.3Hz), 6.85 (m, 1H), 6.58 (s, 2H), 5.54 (m, 1H), 5.00 (s, 2H), 4.20-4.27 (m, 3H), 3.85 (m, 1H), 3.74 (s, 6H), 3.62 (s, 3H), 2.97 (m, 2H), 1.52 (m, 2H), 1.42 (m, 9H), 1.22 (m, 4H)

^{13}C NMR (75 MHz, DMSO-*d*6) δ ppm 167.9, 163.2, 163.0, 155.9, 152.6, 137.1, 136.1, 134.6, 128.2, 127.6, 104.3, 104.3, 77.8, 65.0, 59.8, 55.6, 28.9, 28.0, 22.6

^{19}F (188 MHz, DMSO-*d*6) δ ppm -74.62 (d, 1F, J=7.5Hz), -74.89 (d, 1F, J=6.3Hz)

R_f: 0.6 (SiO_2, cyclohexane:EtOAc 1:1)

mp: 112-114 °C

IR (cm^{-1}): 3312, 1637, 1525, 1250, 1126

MS (ESI Negative) m/z: 714.4 [$M+H^+$]

Elemental Anal. Calculated for [$C33H46F3N5O9+1H_2O$] C 54.19 H 6.63 N 9.58 found C 54.17 H 6.19 N 9.43

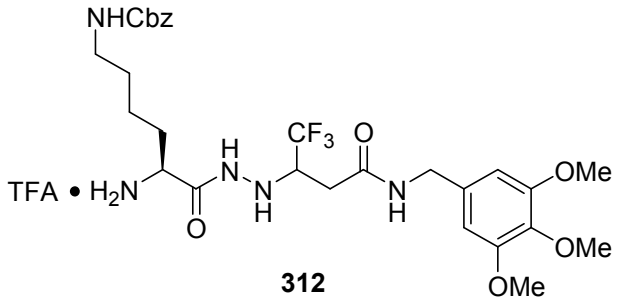

312

[5-Amino-5-(N'-{2,2,2-trifluoro-1-[(3,4,5-trimethoxy-benzylcarbamoyl)-methyl]-ethyl}-hydrazinocarbonyl)-pentyl]-carbamic acid benzyl ester trifluoroacetic acid salt 312

A solution of **309** (741 mg, 1.04 mmol, 1.0 eq) in DCM/TFA 3:1 (15 ml) was stirred for 2 h at RT. The solvent was evaporated in vacuum and the excess of TFA was coevaporated with methanol. The crude was then precipitate with diethyl ether and washed with cyclohexane (3 x 15 ml) to afford **312** (745 mg, 1.04 mmol, quantitative) as a colourless solid.

^{1}H NMR (300 MHz, DMSO-*d*6) δ ppm 9.98 (m, 1H), 8.59 (m, 1H), 8.14 (s, 2H), 7.38-7.26 (m, 5H), 6.57 (s, 2H), 5.00 (s, 2H), 4.20-4.30 (m, 2H), 3.89 (m, 1H), 3.74 (s, 6H), 3.65 (m, 1H), 3.62 (s, 3H), 2.98 (m, 2H), 2.58 (m, 2H), 1.65-1.69 (m, 2H), 1.38-1.42 (m, 2H), 1.25-1.29 (m, 2H)

^{13}C NMR (75 MHz, DMSO-*d*6) δ ppm 171.0, 169.9, 169.8, 159.0, 138.4, 138.2, 135.8, 129.5, 129.0, 128.8, 106.0, 67.4, 61.1, 60.1, 59.7, 56.6, 53.2, 53.1, 44.5, 41.4, 34.7, 34.6, 32.2, 30.5, 23.0

^{19}F (188 MHz, DMSO-*d*6) δ ppm -76.51 (m, 1F), -77.33 (s, 1F)

R_f: 0.3 (SiO_2, EtOAc/MeOH/NH_4OH: 79/20/1)

mp: **136-**138 °C

IR (cm^{-1}): 2924, 1667, 1594, 1123

MS (ESI) m/z: 614 [$M+H^+$]

Elemental Anal. Calculated for [$C30H39F6N5O9+ 1.5 H_2O$] C 47.74 H 5.72 N 9.28 found C 47.52 H 5.04 N 8.80

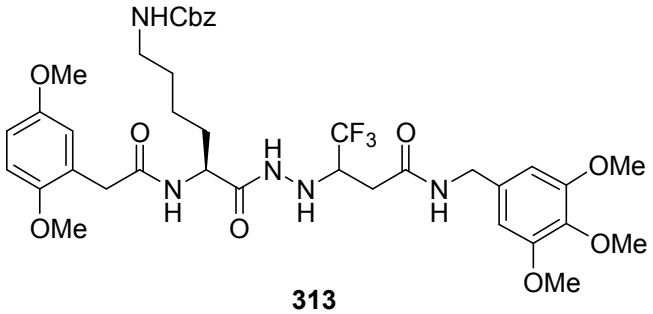

313

[5-[2-(2,5-Dimethoxy-phenyl)-acetylamino]-5-(N'-{2,2,2-trifluoro-1-[(3,4,5-trimethoxy-benzylcarbamoyl)-methyl]-ethyl}-hydrazinocarbonyl)-pentyl]-carbamic acid benzyl ester 313

To a solution of **312** (563 mg, 0.77 mmol, 1.0 eq.) in DMF (4 ml), DIPEA (640 µl, 3.85 mmol, 5.0 eq.) and HOBt (157 mg, 1.16 mmol, 1.5 eq.) were added. Meanwhile a solution of 2,5-dimethoxyphenylacetic acid (227 mg, 1.16 mmol, 1.5 eq.) and HBTU (440 mg, 1.16 mmol, 1.5 eq.) in DMF (4 mL) was stirred for half an hour at RT. The two solutions were combined and the resulting mixture was stirred at RT overnight. The solvent was evaporated under vacuum and the resulting yellow oil was diluted with ACOEt (20 mL) and washed with 10% aqueous solution of citric acid (2 x 15 mL), a 10% aqueous solution of K_2CO3 (2 x 15 mL), brine (20 ml), and distilled water, dried over Na_2SO_4, filtrated and evaporated in vacuo to give a slightly yellow solid which was purified by precipitation in an hot mixture of methanol/EtOAc to give **313** as a colourless solid (434 mg, 0.59 mmol, 77%).

^{1}H NMR (300 MHz, DMSO-*d*6) δ ppm 9.57 (d, 1H, J=5.4Hz), 8.56 (t, 1H, J=5.8Hz), 7.95 (d, 1H, J=8.0Hz), 7.37-7.22 (m, 5H), 7.22 (t, 1H, J=5.4Hz), 6.86-6.76 (m, 2H), 6.70-6.65 (m, 1H), 6.57 (s, 2H), 5.76 (s, 1H), 5.54 (t, 1H, J=4.4Hz), 5.00 (s, 2H), 4.24 (m, 3H), 3.86 (m, 1H), 3.73 (s, 6H), 3.67 (s, 6H), 3.62 (s, 3H), 2.99-2.81 (m, 2H), 2.50-2.40 (m, 2H, under DMSO), 1.57-1.49 (m, 2H), 1.46-132 (m, 2H), 1.30-1.20 (m, 2H)

^{13}C NMR (75 MHz, DMSO-*d*6) δ ppm 171.3, 169.8, 168.0, 156.5, 152.9, 152.7, 151.3, 137.2, 136.3, 134.7, 128.3, 127.9, 127.7, 125.6, 125.5, 116.7, 111.9, 111.6, 104.5, 65.1, 59.9, 55.8, 55.7, 55.2, 51.1, 51.0, 42.4, 36.7, 36.6, 33.2, 31.8, 29.0, 22.4

^{19}F (188 MHz, DMSO-*d*6) δ ppm

R_f: 0.3 (SiO_2, EtOAc)

mp: 138-140 °C (crude)

IR (cm^{-1}): 3298, 1633, 1503, 1228, 1126, 698

MS (ESI) m/z: 793 [M+H$^+$]

Elemental Anal. Calculated for [C38H48F3N5O10+1H_2O] C 56.34 H 6.23 N 8.65 found C 56.55 H 6.38 N 8.41

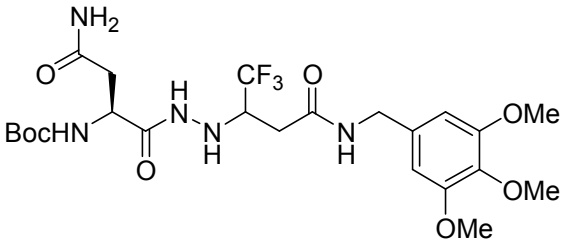

310

[2-Carbamoyl-1-(N'-{2,2,2-trifluoro-1-[(3,4,5-trimethoxy-benzylcarbamoyl)-methyl]-ethyl}-hydrazinocarbonyl)-ethyl]-carbamic acid tert-butyl ester 310

A solution of **307** (547 mg, 1.18 mmol, 1.0 eq.) in DCM/TFA 3:1 (12 ml) was stirred for 2 h at RT. The solvent was evaporated in vacuo and the excess of trifluoroacetic acid was coevaporated with methanol. The resulting slightly yellow solid was dissolved in DMF (3 ml), then DIPEA (1.0 ml, 5.9 mmol, 5.0 eq.) and HOBt (190 mg, 1.41 mmol, 1.2 eq.) were added. Meanwhile a solution of NBocAsn (328 mg, 1.41 mmol, 1.2 eq.) and HBTU (536 mg, 1.41 mmol, 1.2 eq.) in DMF (5 mL) was stirred for half an hour at RT The two solutions were then combined and the resulting mixture was stirred at RT overnight. The solvent was evaporated under vacuum and the resulting colourless solid was washed with Et_2O, EtOAc and petroleum ether to give **16** as a colourless solid (0.65 g, 1.67 mmol, 55%).

^{1}H NMR (400 MHz, DMSO-*d*6) δ ppm 1H-NMR 9.41 (dd, 1H, J=4.9Hz, J=16.2Hz), 8.51 (d, 1H, J=7.8Hz), 7.25 (s, 1H), 6.88 (s, 2H), 6.58 (bs, 1H), 5.53 (m, 1H), 4.24 (m, 3H), 3.83 (m, 1H), 3.74 (s, 6H), 3.62 (s, 3H), 2.60-2.50 (2H under DMSO) 2.39 (m, 2H), 1.36 (s, 1H)

^{13}C NMR (100 MHz, DMSO-*d*6) δ 171.0, 168.0, 154.9, 152.7, 137.2, 137.0, 135.7, 134.8, 128.3, 125.4, 78.9, 59.9, 57.72 (dd, 1H, J=7.8Hz, J=27.1Hz), 53.6, 50.0, 37.6, 33.6, 28.1

^{19}F (188 MHz, DMSO-*d*6) δ ppm -73.5 (m)

R_f: 0.2 (SiO_2, EtOAc:MeOH 9:1)

mp: 174-176 °C

IR (cm^{-1}): 3319, 2361,1637, 1127

MS (ESI Negative) m/z: 566 [M+H$^+$]

Elemental Anal. Calculated for [C23H34F3N5O8+0.5 H_2O] C 48.12 H 6.16 N 12.20 found C 48.27 H 5.88 N 11.86

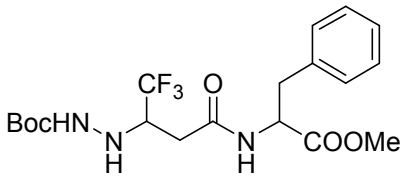

308

2-[3-(N'-tert-Butoxycarbonyl-hydrazino)-4,4,4-trifluoro-butyrylamino]-3-phenyl-propionic acid methyl ester 308

To a solution of **295** (2.55 g, 9.37 mmol, 1.0 eq.) and HBTU (3.56 g, 9.37 mmol, 1.0 eq.) in DMF (20 ml) pre-complexed for 30 min. were added in the order HOBt (1.52 g, 11.24 mmol, 1.2 eq.), DIPEA (3.1 ml, 18.74 mmol, 2.0 eq.) and phenylalanine hydroxychloride. The reaction was performed under argon atmosphere a RT overnight. The solvent was evaporated over vacuum and the product dissolved in EtOAc (30 ml). The organic layer was washed with 10% aqueous solution of citric acid (2 x 25 ml),water (30 ml), a 10% aqueous solution of K_2CO_3 (2 x 25 ml) and brine (30 ml), dried over Na_2SO_4, filtrated and evaporated in vacuo to give a slightly yellow solid which was purified by column chromatography (EtOAc:cyclohexane 7:3) to give the **308** as a colourless solid (3.49 g, 8.06 mmol, 86%).

^{1}H NMR (400 MHz, DMSO-*d*6) δ ppm 8.56;8.58 (2 d, *J* = 6.3;6.4 Hz, 1H, 2 dia), 8.36 (m, 1H), 7.27-7.17 (m, 5H), 4.98;5.02 (2 br s, 1H, 2 dia), 4.46 (m, 1H), 3.73 (m, 1H), 3.56-3.57 (2s, 3H), 3.00 (dd, *J* = 13.6 and 5.8 Hz, 1H), 2.89 (m, 1H), 2.38-2.48 (m, 2H), 1.36;1.37 (s, 9H, 2 dia)

^{13}C NMR (100 MHz, DMSO-*d*6) δ ppm 172.2, 172.1, 168.7, 156.7, 137.5, 137.4, 129.4, 129.3, 128.7, 127.0, 126.3 (q, *J* = 27.8 Hz), 79.3, 58.3, 58.0, 54.1;54.0 (2 dia), 52.1, 52.2, 37.2, 37.1, 33.4, 28.5

^{19}F (188 MHz, DMSO-*d*6) δ ppm (-73.6) –(-73.8) (m).

R_f: 0.7 (EtOAc/cyclohexane: 70/30)

mp: 94-96 °C (crude)

IR (cm^{-1}): 3351, 3288, 1739, 1709, 1683, 1164, 1124, 698

MS (ESI Positive) m/z: 456 $[M+Na]^+$

Elemental Anal. Calculated for [C19H26F3N3O5] C. 52.65, H 6.05, N. 9.69 found C 52.15, H 6.07, N 9.37

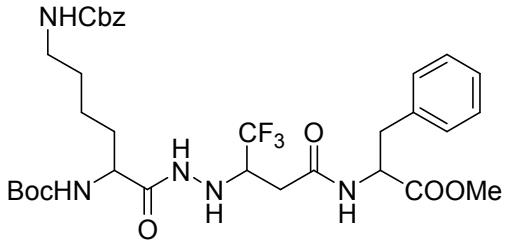

300

2-{3-[N'-(6-Benzyloxycarbonylamino-2-tert-butoxycarbonylamino-hexanoyl)-hydrazino]-4,4,4 trifluoro-butyrylamino}-3-phenyl-propionic acid methyl ester 300

A solution of **308** (197 mg, 0.44 mmol, 1.0 eq.) in DCM/TFA 3:1 (4 ml) was stirred for 2 h at RT. The solvent was evaporated in vacuo and the excess of trifluoroacetic acid was coevaporated with methanol. The resulting slightly yellow solid was dissolved in DMF (2 ml), then DIPEA (360 µl, 2.2 mmol, 5.0 eq.) and HOBt (90 mg, 0.66 mmol, 1.5 eq.) were added. Meanwhile a solution of NαBocNεZLysine (251 mg, 0.66 mmol, 1.5 eq.) and HBTU (250 mg, 0.66 mmol, 1.5 eq.) in DMF (2 mL) was stirred for half an hour. The two solutions were then combined and the resulting mixture was stirred at RT overnight. The solvent was evaporated under vacuum and the resulting yellow oil was diluted with ACOEt (10 mL) and washed with 10% aqueous solution of citric acid (2 x 10 mL), a 10% aqueous solution of K_2CO3 (2 x 10 mL) and brine (15 ml), dried over Na_2SO_4, filtrated and evaporated in vacuo to give a slightly yellow solid which was purified by column chromatography (cyclohexane:EtOAc 6:4) to give **300** as a colourless solid (207 mg, 0.30 mmol, 68%).

^{1}H NMR (400 MHz, DMSO-*d*6) δ ppm 9.42 (m, 1H), 8.61 (d, *J* = 7.6 Hz, 1H), 7.40-7.19 (m, 11 H), 6.81 (m, 1H), 5.40 (bs, 1H), 5.00 (s, 2H), 4.49 (m, 1H), 3.83 (m, 1H), 3.74 (m, 1H), 3.58 (s, 3H,), 3.05-2.89 (m, 4H), 2.46 (m, 2H), 1.46 (m, 2H), 1.40-1.28 (m, 11H), 1.26 (m, 2H)

^{13}C NMR (100 MHz, DMSO-*d*6) δ ppm 171.8, 168.1, 156.1, 155.2, 137.3, 137.0, 129.0, 128.9, 128.3, 128.2, 127.7, 126.5, 78.0, 65.1, 57.5 (q, *J* = 20.9 Hz), 53.6, 52.8, 51.8, 39.7, 36.7, 32.8, 31.3, 29.0, 28.1, 22.7

^{19}F (188 MHz, DMSO-*d*6) δ ppm -76.4 (d, *J* = 7.4 Hz), -76.5 (d, *J* = 7.2 Hz).

R_f: 0.6 (EtOAc/cyclohexane: 70/30)

mp: 92-94 °C (crude)

IR (cm^{-1}): 3321 (NH), 1741 (C=O), 1686 (C=O), 1634 (C=O), 1161 (C-O), 1127 (C-O), 698 (CF_3)

HRMS (EI) *m/e*: $[M+Na]^+$ calcd 718.3040, found 718.3019

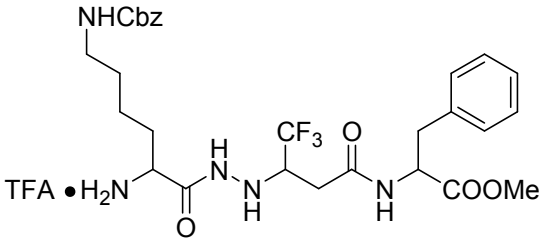

297

2-{3-[N'-(2-Amino-6-benzyloxycarbonylamino-hexyl)-hydrazino]4,4,4trifluorobutyrylamino}-3-phenyl-propionic acid methyl ester trifluoroacetic acid salt 297

A solution of **300** (318mg, 0.45 mmol, 1.0 eq.) in DCM/TFA 3:1 (4 ml) was stirred for 2 h at RT. The solvent was evaporated in vacuum and the excess of TFA was coevaporated with methanol. The crude was then precipitate with diethyl ether to afford **297** (319 mg, 0.45 mmol, quantitative) as a colourless solid.

^{1}H NMR (400 MHz, DMSO-*d*6) δ ppm 9.94 (d, *J* = 4.2 Hz, 1H), 8.62 (m, 1H), 8.17 (m, 3H), 7.38-7.12 (m, 11 H), 5.70 (m, 1H), 5.00 (s, 2H), 4.50 (m, 1H), 3.80 (m, 1H), 3.63 (m, 1H), 3.58 (s, 3H), 3.02 (m, 1H), 2.96 (m, 2H), 2.89 (m, 1H), 2.49 (m, 2H), 1.66 (m, 2H), 1.39 (m, 2H), 1.26 (m, 2H).

^{13}C NMR (100 MHz, DMSO-*d*6) δ ppm 171.8, 168.2, 168.1, 156.1, 137.2, 137.0, 129.0, 128.9, 128.3, 128.2, 127.7, 126.6, 65.1, 57.5 (q, *J* = 22.4 Hz), 53.6, 51.8, 50.9, 40.1, 36.7, 32.8, 30.6, 28.9, 21.4

^{19}F (188 MHz, DMSO-*d*6) δ ppm -76.6 (d, *J* = 7.5 Hz), -76.7 (d, *J* = 5.6 Hz).

R_f: 0.5 (EtOAc/MeOH/NH_4OH: 79/20/1)

m.p.: 92-94 °C (crude)

IR (cm^{-1}): 3297, 1666, 1172, 1130, 697

MS (ESI Negative) m/z: 708 $[M-H]^-$

Elemental Anal. Calculated for [C31H41F6N5O8] +2 H_2O 52.65, H 6.05, N 9.69 found C 52.15, H 6.07, N 9.37

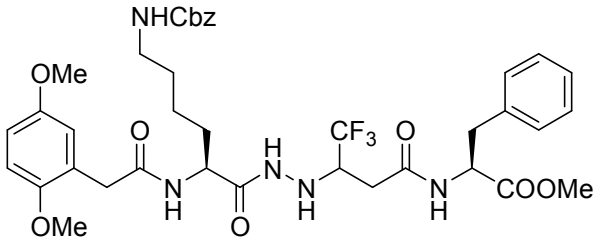

315

2-[3-(N'-{6-Benzyloxycarbonylamino-2-[2-(2,5-dimethoxy-phenyl)-acetylamino]-hexanoyl}-hydrazino)-4,4,4-trifluoro-butyrylamino]-3-phenyl-propionic acid methyl ester 315

To a solution of **297** (319 mg, 0.45 mmol, 1.0 eq.) in DMF (2 ml), DIPEA (370 µl, 2.25 mmol, 5.0 eq.) and HOBt (90 mg, 0.67 mmol, 1.5 eq.) were added. Meanwhile a solution of 2,5-dimethoxyphenylacetic acid (132 mg, 0.67 mmol, 1.5 eq.) and HBTU (254 mg, 0.67 mmol, 1.5 eq.) in DMF (2 mL) was stirred for half an hour at RT. The two solutions were then combined and the resulting mixture was stirred at RT overnight. The solvent was evaporated under vacuum and the resulting yellow oil was diluted with ACOEt (10 mL) and washed with 10% aqueous solution of citric acid (2 x 10 mL), a 10% aqueous solution of K_2CO3 (2 x 10 mL) and brine (15 ml), dried over Na_2SO_4, filtrated and evaporated in vacuo to give a slightly yellow solid which was purified by precipitation in a mixture of cyclohexane/EtOAc to give **315** as a colourless solid (298 mg, 0.38 mmol, 84%).

^{1}H NMR (300 MHz, DMSO-*d*6) δ ppm 9.53 (t, 1H, J=5.6Hz), 8.64 (dd, 1H, J=7.3Hz, J=8.7Hz), 7.95 (m, 1H), 7.36-7.20 (m, 10H), 6.87-6.76 (m, 3H), 5.01 (s, 2H), 4.50 (m, 1H), 4.20 (m, 1H) 3.79 (m, 1H), 3.69 (s, 3H), 3.68 (s, 3H), 3.59 (s, 3H), 3.42 (d, 2H, J=3.2Hz), 3.06-2.90 (m, 4H), 2.46 (m, 2H), 1.57-1.53 (m, 2H), 1.41-1.36 (m, 2H), 1.28-1.21 (m, 2H)

^{13}C NMR (75 MHz, DMSO-*d*6) δ ppm 171.7, 171.6, 171.4, 169.8, 168.1, 156.0, 152.9, 151.3, 137.2, 137.0, 136.9, 129.0, 128.9, 128.3, 128.2, 127.7, 126.5, 116.7, 111.9, 111.6, 79.4, 78.9, 78.5, 65.1, 55.8, 55.2, 53.7, 53.6, 51.8, 51.0, 50.9, 36.7, 36.6, 32.9, 31.7, 29.0, 22.4

^{19}F (188 MHz, DMSO-*d*6) δ ppm -73.74 (d, 0.4F, J=7.3Hz) I diastereomer -73.91 (d, 0.6F, J=7.5Hz) II diastereomer

R_f: 0.5 (SiO_2, EtOAc)

mp: 140-142 °C

IR (cm^{-1}): 3283, 2943, 1739, 1684, 1637, 1531, 1502, 1443, 1360, 1261, 1227, 1207 739

MS (ESI) m/z: 796.7 [M+Na$^+$]

Elemental Anal. Calculated for [$C_{38}H_{46}F_3N_5O_9$+0.75H_2O] C 57.95 H 6.09 N 8.90 found C58.04 H 6.02 N 9.01

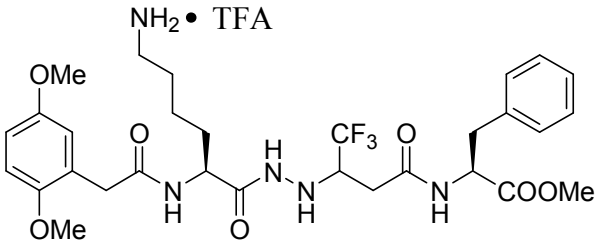

316

2-[3-(N'-{6-Amino-2-[2-(2,5-dimethoxy-phenyl)-acetylamino]-hexanoyl}-hydrazino)-4,4,4-trifluoro-butyrylamino]-3-phenyl-propionic acid methyl ester trifluoro acetic acid salt 316

To a solution of **315** (461 mg, 0.60 mmol, 1.0 eq.) in dry methanol (8 ml) was added palladium on activate charcoal 10% (46 mg, 1% massive of palladium). The mixture was stirred overnight under hydrogen atmosphere a RT. The catalyst was filtrated on a celite pad and the solvent was evaporated under vacuum obtaining a yellowish solid oil. The crude was dissolved in DCM/TFA 3:1 (8 ml) and stirred for half an hour. The solvent was evaporated in vacuum and the excess of TFA removed by coevaporation with methanol. The crude was dissolved in DCM/Et_2O with just few drops of MeOH and precipitate at -20°C. It was obtained a yellowish solid which was washed with Et_2O to afford **316** (461 mg, 0.49 mmol, 82%).

^{1}H NMR (300 MHz, MeOD) δ ppm 7.23-7.17 (m, 5H), 6.86-6.75 (m, 3H), 4.65 (m, 1H), 4.29 (m, 1H), 3.74 (s, 3H), 3.69 (s, 3H), 3.65 (s, 3H), 3.51-3.44 (m, 3H), 3.15-3.08 (m, 1H), 3.00 (m, 1H), 2.88-2.82 (m, 2H), 2.52-2.46 (m, 2H), 1.57-1.53 (m, 2H), 1.41-1.36 (m, 2H), 1.28-1.21 (m, 2H)

^{13}C NMR (75 MHz, MeOD) δ ppm 155.5, 153.5, 153.4, 152.0, 138.5, 130.6, 129.9, 129.6, 128.3, 126.3, 118.7, 114.3, 114.2, 113.1, 67.3, 60.7, 60.2, 59.9, 59.7, 56.9, 56.4, 56.0, 53.2, 53.1, 40.9, 39.0, 38.7, 34.6, 33.0, 28.4, 23.8, 15.8

^{19}F (188 MHz, MeOD) δ ppm -76.67 (d, 0.3F, J=7.3Hz), -76.62 (d, 0.7F, J=7.5Hz), for the partial overlap of the signals it is not possible calculate accurately the diastereomeric ratio, -77.34 (s, 1F)

R_f: 0.3 (SiO_2, EtOAc/MeOH/NH_4OH: 79/20/1)

mp: 120-122 °C

IR (cm^{-1}): 3324, 1639, 1503, 1126, 700

MS (ESI) m/z: 640.3 [M+H$^+$]

Elemental Anal. Calculated for [C32H41F6N5O9+0.5 H_2O] C 50.39 H 5.56 N 9.18 found C 50.04 H 5.37 N 8.73

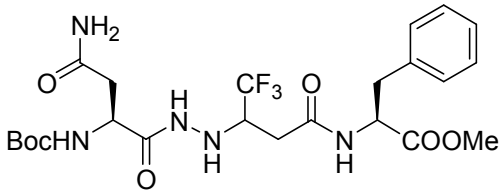

311

2-{3-[N'-(2-tert-Butoxycarbonylamino-3-carbamoyl-propionyl)-hydrazino]-4,4,4-trifluoro-butyrylamino}-3-phenyl-propionic acid methyl ester 311

A solution of **308** (218 mg, 0.49 mmol, 1.0 eq.) in DCM/TFA 3:1 (4 ml) was stirred for 2 h at RT. The solvent was evaporated in vacuo and the excess of trifluoroacetic acid was coevaporated with methanol. The resulting white solid was dissolved in DMF (2 ml), then DIPEA (400 µl, 2.45 mmol, 5.0 eq.) and HOBt (100 mg, 0.74 mmol, 1.5 eq.) were added. Meanwhile a solution of NBocAsparagine (170 mg, 0.74 mmol, 1.5 eq.) and HBTU (280 mg, 0.74 mmol, 1.5 eq.) in DMF (2 mL) was stirred for half an hour at RT. The two solutions were then combined and the resulting mixture was stirred at RT overnight. The solvent was evaporated under vacuum and the resulting yellow oil was diluted with ACOEt (10 mL) and washed with 10% aqueous solution of citric acid (2 x 10 mL), a 10% aqueous solution of K_2CO3 (2 x 10 mL) and brine (15 ml), dried over Na_2SO_4, filtrated and evaporated in vacuo to give a white solid which was purified by column chromatography (EtOAc:MeOH 9:1) to give **311** as a colourless solid (168 mg, 0.30 mmol, 63%).

^{1}H NMR (300 MHz, DMSO-*d*6) δ ppm 9.44 (m, 1H), 8.60 (d, 1H, J=7.6Hz), 7.35-7.17 (m, 5H), 6.90 (d, 2H, J=7.6Hz), 5.43 (m, 1H), 4.49 (m, 1H), 4.19 (m, 1H), 3.74 (m, 1H), 3.59 (s, 3H), 3.05-2.85 (m, 2H), 2.60-2.40 (m, 2H, under DMSO), 2.40-2.31 (m, 2H), 1.37 (s, 1H)

^{13}C NMR (75 MHz, DMSO-*d*6) δ ppm 171.6, 171.3, 171.1, 171.0, 168., 154.9, 137.0, 129.0, 128.2, 126.5, 78.1, 53.7, 51.7, 50.0, 37.1, 36.7, 32.8, 28.1,

^{19}F (188 MHz, DMSO-*d*6) δ ppm -73.71 (d, 1H, J=7.4Hz)

R_f: 0.2 (SiO_2, EtOAc:MeOH 9:1)

m.p.: 150-152 °C (crude)

IR (cm^{-1}): 3477, 2149, 1639, 1524, 1165

MS (ESI) m/z: 548.2 [M+H^+]

Elemental Anal. Calculated for [C23H32F3N5O7+ 0.15H_2O] C 50.23 H 5.93 H12.74 found C49.75 H 5.75 N 13.61

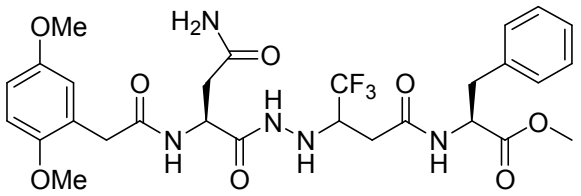

317

2-[3-(N'-{3-Carbamoyl-2-[2-(2,5-dimethoxy-phenyl)-acetylamino]-propionyl}-hydrazino)-4,4,4-trifluoro-butyrylamino]-3-phenyl-propionic acid methyl ester 317

A solution of **311** (355 mg, 0.64 mmol, 1.0 eq.) in DCM/TFA 2:1 (9 ml) was stirred for 2 h at RT. The solvent was evaporated in vacuo, the excess of trifluoroacetic acid was coevaporated with methanol and the resulting yellowish solid oil precipitated with Et_2O. The resulting white solid was dissolved in DMF (3 ml), then DIPEA (540 µl, 3.25 mmol, 5.0 eq.) and HOBt (129 mg, 0.95 mmol, 1.5 eq.) were added. Meanwhile a solution of 2,5-dimethoxyphenylacetic acid (187 mg, 0.95 mmol, 1.5 eq.) and HBTU (361 mg, 0.95 mmol, 1.5 eq.) in DMF (3 mL) was stirred for half an hour at RT. The two solutions were combined and the resulting mixture was stirred at RT overnight. The solvent was evaporated under vacuum and the resulting yellow oil was diluted with ACOEt (15 mL) and washed with 10% aqueous solution of citric acid (2 x 10 mL), water (15 ml), a 10% aqueous solution of K_2CO_3 (2 x 10 mL) and brine (15 ml), dried over Na_2SO_4, filtrated and evaporated in vacuo to give a white solid which washed several times with EtOAc, cyclohexane and Et_2O to obtain **317** (259 mg, 0.42 mmol, 65%).

^{1}H NMR (300 MHz, DMSO-*d*6) δ ppm 7.34-7.22 (m, 5H), 6.92-6.82 (m, 3H), 4.69 (dd, 1H, J=5.9Hz, J=8.8Hz), 3.78 (s, 3H), 3.75 (s, 3H), 3.68 (d, 3H, J=3.2Hz), 3.46 (s, 1H), 3.18-3.11 (m, 1H), 3.04-2.97 (m, 1H), 2.52 (m, 1H)

^{13}C NMR (75 MHz, DMSO-*d*6) δ ppm 171.8, 171.7, 171.1, 171.0, 170.6, 169.8, 168.2 ,152.9, 151.1, 137.0, 129.0, 128.2, 126.5, 116.6, 112.1, 55.9, 55.3, 53.7, 53.6, 51.7, 48.4, 37.0, 36.7, 32.8

^{19}F (188 MHz, DMSO-*d*6) δ ppm -73.72 (d, 0.7F, J=7.4Hz) I diastereomer -73.85 (d, 0.3, J=7.8Hz) II diastereomer

R_f: 0.2 (SiO_2, EtOAc)

mp: 168-170 °C

IR (cm^{-1}): 3286, 1639, 1537, 1406, 1226, 1124

MS (ESI Negative) m/z: 626.3 [M+Na$^+$]

Elemental Anal. Calculated for [C28H34F3N5O2] C 53.76 H 5.48 N 11.19 found C 53.79 H 5.30 N 10.75

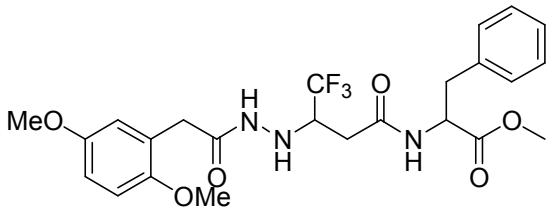

318

2-(3-{N'-[2-(2,5-Dimethoxy-phenyl)-acetyl]-hydrazino}-4,4,4-trifluoro-butyrylamino)-3-phenyl-propionic acid methyl ester 318

A solution of **308** (392 mg, 0.88 mmol, 1.0 eq.) in DCM/TFA 3:1 (4 ml) was stirred for 2 h at RT. The solvent was evaporated in vacuo and the excess of trifluoroacetic acid was coevaporated with methanol. The resulting slightly yellow solid was dissolved in DMF (3 ml), then DIPEA (730 µl, 4.4 mmol, 5.0 eq.) and HOBt (179 mg, 1.32 mmol, 1.5 eq.) were added. Meanwhile a solution of 2,5-dimethoxyphenylacetic acid (259 mg, 1.32 mmol, 1.5 eq.) and HBTU (499 mg, 1.32 mmol, 1.5 eq.) in DMF (3 mL) was stirred for half an hour at RT. The solutions were combined and the resulting mixture was stirred at RT overnight. The solvent was evaporated under vacuum and the resulting yellow oil was diluted with ACOEt (10 mL) and washed with 10% aqueous solution of citric acid (2 x 10 mL), a 10% aqueous solution of K_2CO3 (2 x 10 mL) and brine (15 ml), dried over Na_2SO_4, filtrated and evaporated in vacuo to give a slightly yellow solid which was purified by column chromatography (EtOAc) to give **318** as a colourless solid (347 mg, 0.68 mmol, 77%).

^{1}H NMR (300 MHz, DMSO-*d*6) δ ppm 9.37 (d, 1H, J=5.1Hz), 8.60 (d, 1H, J=7.4Hz), 8.03 (t, 1H, J=8.8Hz), 7.34-7.22 (m, 5H), 6.88-6.80 (m, 3H), 5.43 (d, 1H, J=3.7Hz), 4.58-4.50 (m, 2H), 3.68 (s,

3H), 3.67 (s, 3H), 3.58 (s, 3H), 3.52-3.56 (bs, 1H), 3.40 (s, 2H), 3.05-2.88 (m, 2H), 2.50-2..4 (m, 2H)

^{13}C NMR (75 MHz, DMSO-*d*6) δ ppm 172.3, 171.6, 168.4, 168.2, 153.7, 151.0, 136.4, 129.2, 129.1, 128.4, 126.9, 123.1, 117.1, 113.4, 11.5, 55.7, 53.8, 53.7, 52.4, 37.3, 37.1, 33.3

^{19}F (188 MHz, DMSO-*d*6) δ ppm -74.99 (d, 0.7F, J=7.3Hz) I diastereomer -75.37 (d, 0.3F, J=7.1Hz) II diastereomer

R_f: 0.7 (SiO_2, EtOAc)

mp: 100-102 °C

IR (cm^{-1}): 3301, 1648, 1502, 1229, 1122 698

MS (ESI) m/z: 534.4 [M+Na$^+$]

Elemental Anal. Calculated for [C24H28F3N3O] C 56.36 H 5.52 N 8.22 found C 56.08 H 5.43 N 8.01

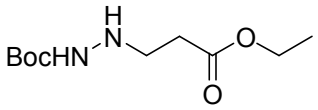

323

3-(N'-tert-Butoxycarbonyl-hydrazino)-propionic acid ethyl ester 323

A solution of 3-Bromo-propionic acid ethyl ester (2 ml, 15.7 mmol, 1.0 eq.), DIPEA (2.6 ml, 15.7 mmol, 1.0 eq.) and Boc-hydrazine (3.1 g, 3.1 g, 23.55 mmol, 1.5) in toluene was heated at 80 °C for 4 days. The solvent was evaporated and the product purified by column chromatography (cyclohexane:EtOAc 6:4) to give **323** as a slightly yellow oil (1.58 g, 6.80 mmol, 43%).

^{1}H NMR (300 MHz, $CDCl_3$) δ ppm 6.26 (bs, 1H), 4.08 (q, 2H, J=7.1Hz), 3.06 (t, 2H, J=6.6Hz), 2.41 (t, 2H, J=6.6Hz), 1.39 (s, 9H), 1.19 (dt, 3H, J=1.5Hz, J=7.1Hz)

^{13}C NMR (75 MHz, $CDCl_3$) δ ppm 172.2, 156.7, 80.3, 60.3, 47.3, 33.0, 28.2, 14.0

R_f: 0.7 (SiO_2, EtOAc)

IR (cm^{-1}): 2980, 1714, 1252, 1151, 1025

MS (ESI Negative) m/z: 233 [M+H$^+$]

Elemental Anal. Calculated for [C10H20N2O4] C 51.71 H 8.68 N 12.06 found C 51.61 H 8.25 N 11.58

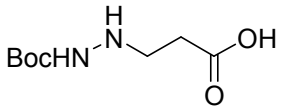

324

3-(N'-tert-Butoxycarbonyl-hydrazino)-propionic acid 324

To a solution of **323** (2.00 g, 8.6 mmol, 1.0 eq.) in THF/MeOH (10 ml/10 ml) a 2N solution of NaOH (4.8 ml, 9.6 mmol, 1.1 eq.) was added. The reaction was stirred at RT over 3 hrs. The solvent was removed under vacuum (without distilling the water) and the remaining solution was brought at pH=5 by addition of 1N solution of HCl. The aqueous phase was extracted with EtOAc (3x 20 ml). The combined organic layers were dried with $MgSO_4$, filtered and concentrated under vacuum to obtain the product **324** (1.64 g, 8.0 mmol, 93%) as a white solid which was used in the next step without further purification.

^{1}H NMR (300 MHz, DMSO-*d*6) δ ppm 8.17 (m, 1H), 2.87 (t, 2H, J=7.0Hz, 2.30 (t, 2H, J=6.9Hz), 1.39 (s, 9H)

^{13}C NMR (75 MHz, DMSO-*d*6) δ ppm 173.2, 156.3, 78.2, 46.7, 32.5, 28.0

R_f: 0.3 (SiO_2, EtOAc)

mp: 112-114 °C (crude)

IR (cm^{-1}): 3350, 2981, 1679, 1437, 1156, 860

MS (ESI Negative) m/z: 227 [$M+Na^+$], 431.1 [$2M+Na^+$]

Elemental Anal. Calculated for [C8H16N2O4] C 47.05 7.90 N 13.72 found C 47.43 H 7.90 N 13.33

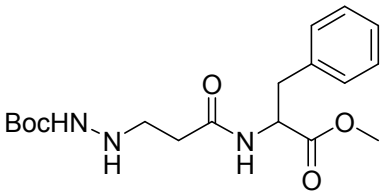

325

2-[3-(N'-tert-Butoxycarbonyl-hydrazino)-propionylamino]-3-phenyl-propionic acid methyl ester 325

To a solution of **324** (819 0g, 4.0 mmol, 1.0 eq.) and HBTU (1.52 g, 4.0 mmol, 1.0 eq.) in DMF (10 ml) pre-complexed for 30 min. were added in the order HOBt (650 mg, 4.8 mmol, 1.2 eq.), DIPEA (1.4 ml, 8.0 mmol, 2.0 eq.) and phenylalanine hydroxychloride (1.04 g, 4.8 mmol, 1.2 eq.). The reaction was performed under argon atmosphere a RT overnight. The solvent was evaporated over vacuum and the product dissolved in EtOAc (15 ml). The organic layer was washed a 10% aqueous solution of K_2CO_3 (2 x 15 ml) and brine (20 ml) and distilled water (2 x 15 ml), dried over Na_2SO_4, filtrated and evaporated in vacuo to give a slightly yellow solid which was purified by column chromatography (EtOAc) to give the **325** as a colourless solid (1.26 g, 3.3 mmol, 82%).

^{1}H NMR (300 MHz, $CDCl_3$) δ ppm 7.53 (s, 1H), 7.26-7.13 (m, 5H), 6.22 (s, 1H), 4.79 (dd, 1H, J=7.3Hz, J=13.2Hz), 3.64 (s, 3H), 3.13-2.92 (m, 4H), 2.24 (t, 2H, J=6.0Hz), 1.38 (s, 9H)

^{13}C NMR (75 MHz, $CDCl_3$) δ ppm 172.0, 171.1, 137.2, 129.2, 129.0, 128.1, 126.5, 78.3, 53.4, 51.7, 47.4, 36.7, 33.8, 28.1

R_f: 0.4 (SiO_2, EtOAc)

mp: 86-88 °C

IR (cm^{-1}): 2935, 1728, 1529, 1156, 837

MS (ESI Negative) m/z: 388.3 [M+Na^+]

Elemental Anal. Calculated for [C18H27N3O5] C 59.16 H 7.45 N 11.50 found C 59.20 H 7.20 N 11.05

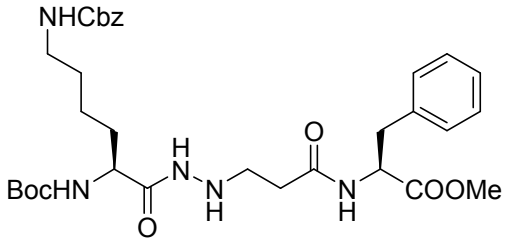

326

2-{3-[N'-(6-Benzyloxycarbonylamino-2-tert-butoxycarbonylamino-hexanoyl)-hydrazino]-propionylamino}-3-phenyl-propionic acid methyl ester 326

A solution of **325** (914 mg, 2.41 mmol, 1.0 eq.) in DCM/TFA 3:1 (12 ml) was stirred for 2 h at RT. The solvent was evaporated in vacuo and the excess of trifluoroacetic acid was coevaporated with methanol. The resulting slightly yellow solid was dissolved in DMF (5 ml), then DIPEA (2.0 ml, 12.0 mmol, 5.0 eq.) and HOBt (390 mg, 2.89 mmol, 1.2 eq.) were added. Meanwhile a solution of NαBocNεZLysine (1.10 g, 2.89 mmol, 1.2 eq.) and HBTU (1.09 mg, 2.89 mmol, 1.2 eq.) in DMF (5 mL) was stirred for half an hour at RT. The solutions were then combined and the resulting mixture was stirred at RT overnight. The solvent was evaporated under vacuum and the resulting yellow oil was diluted with ACOEt (15 mL) and washed a 10% aqueous solution of K_2CO3 (2 x 20 mL) and brine (30 ml) and water (2 x 20 ml), dried over Na_2SO_4, filtrated and evaporated in vacuo to give a slightly yellow oil which was purified by column chromatography (EtOAc) to give **20** as a colourless solid (940 mg, 1.50 mmol, 62%).

^{1}H NMR (400 MHz, $CDCl_3$) δ ppm 8.12 (s, 1H), 7.37-7.23 (m, 8H), 7.16 (m, 2H), 5.20-5.04 (m, 3H), 4.88 (dd, 1H, J=6.4Hz, J=13.9Hz), 3.99 (dd, 1H, J=7.8Hz, J=14.8Hz), 3.74 (d, 3H, J=1.9Hz), 3.20-3.15 (m, 3H), 3.10-3.05 (m, 3H), 2.27 (t, 2H, J=5.6Hz), 1.79-1.74 (m, 1H), 1.66-1.60 (m, 1H), 1.59-1.49 (m, 2H), 1.43 (s, 9H), 1.38-1.33 (m, 2H)

^{13}C NMR (100 MHz, $CDCl_3$) δ ppm 172.7, 171.5, 157.8, 156.3, 137.3, 136.6, 136.0, 128.8, 127.7, 126.7, 80.4, 67.5, 66.7, 65.8, 52.9, 52.2, 47.8, 40.2, 38.2, 37.2, 34.4, 32.4, 30.3, 28.0, 23.0

R_f: 0.2 (SiO_2, EtOAc)

mp: 106-108 °C (crude)

IR (cm^{-1}): 3309, 1686, 1653, 1524, 1248, 1167

MS (ESI Negative) m/z: 650.8 [M+Na^+]

Elemental Anal. Calculated for [C32H45N5O8] C 61.23 H 7.23 N 11.16 found C 61.03 H 7.14 N 10.94

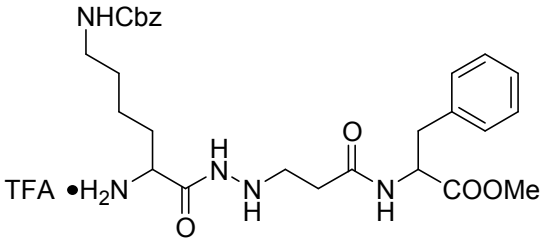

327

2-{3-[N'-(2-Amino-6-benzyloxycarbonylamino-hexanoyl)-hydrazino]-propionylamino}-3-phenyl-propionicacid methyl ester trifluoroacetic acid 327

A solution of **326** (99 mg, 0.16 mmol, 1.0 eq) in DCM/TFA 3:1 (4 ml) was stirred for 2 h at RT. The solvent was evaporated in vacuum and the excess of TFA was coevaporated with methanol. The crude was then precipitate with diethyl ether and washed with cyclohexane (3 x 15 ml) to afford **327** (101 mg, 0.16 mmol, quantitative) as a colourless solid.

^{1}H NMR (300 MHz, MeOD) δ ppm 7.33-7.20 (m, 10H), 5.06 (s, 2H), 4.69 (ddd, 1H, J=2.2Hz, J=4.7Hz, J=5.9Hz), 3.74-3.68 (m, 1H), 3.69 (s, 3H), 3.19-3.11 (m, 3H), 3.01-2.94 (m, 3H), 2.35 (dt, 2H, J=2.9Hz, J=6.5Hz), 1.86-1.80 (m, 2H), 1.57-1.51 (m, 2H), 1.42-1.37 (m, 2H)

^{13}C NMR (75 MHz, MeOD) δ ppm 174.5, 174.1, 169.5, 159.4, 138.8, 138.5, 130.8, 130.6, 130.2, 129.8, 129.4, 129.2, 128.3, 67.8, 55.7, 53.6, 53.1, 41.6, 38.7, 35.3, 32.5, 30.8, 23.5

R_f: 0.4 (SiO_2, EtOAc/MeOH/NH_4OH: 79/20/1)

m.p.: 96-98 °C (crude)

IR (cm^{-1}): 2929, 1668, 1531, 1199, 1129

MS (ESI Negative) m/z: 528 [M+H$^+$]

Elemental Anal. Calculated for [C29H38F3N5O8+1.5 H_2O] C 52.12 H 6.20 N 10.48 found C 52.48 H 6.28 N 10.13

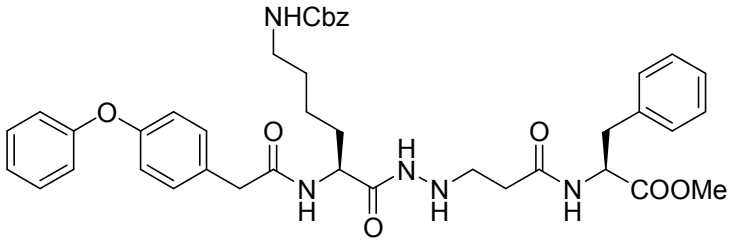

328

2-[3-(N'-{6-Benzyloxycarbonylamino-2-[2-(4-phenoxy-phenyl)-acetylamino]-hexanoyl}-hydrazino)-propionylamino]-3-phenyl-propionic acid methyl ester 328

To a solution of **327** (491 mg, 0.76 mmol, 1.0 eq.) in DMF (4 ml), DIPEA (630 µl, 3.8 mmol, 5.0 eq.) and HOBt (125 mg, 0.92 mmol, 1.2 eq.) were added. Meanwhile a solution of 2-phenoxyphenylacetic acid (210 mg, 0.92 mmol, 1.2 eq.) and HBTU (349 mg, 0.96 mmol, 1.2 eq.) in DMF (4 mL) was stirred for half an hour at RT. The solutions were combined and the resulting mixture was stirred at RT overnight. The solvent was evaporated under vacuum and the resulting yellow oil was diluted with ACOEt (20 mL) and washed with a 10% aqueous solution of K_2CO3 (2 x 15 mL), brine (20 ml) and distilled water (2 x 15 ml), dried over Na_2SO_4, filtrated and evaporated in vacuo to give a slightly yellow oil which was purified by column chromatography (EtOAc) to give **22** as a colourless solid (452 mg, 0.61 mmol, 81%).

^{1}H NMR (300 MHz, DMSO-*d*6) δ ppm 9.40 (bs, 1H), 8.38 (bs, 1H), 8.20 (bs, 1H), 7.34-7.22 (m, 15H), 7.15-6.85 (m, 6H), 5.00 (s, 2H), 4.94-4.89 (m, 1H), 4.49-4.44 (m, 1H), 4.15-4.09 (m, 1H), 3.58 (s, 3H), 3.47 (bs, 2H), 3.00-2.93 (m, 4H), 2.76-2.68 (m, 2H), 2.20-2.16 (m, 2H), 1.57-1.53 (m, 2H), 1.41-1.36 (m, 2H), 1.28-1.21 (m, 2H)

^{13}C NMR (75 MHz, DMSO-*d*6) δ ppm 165.9, 165.8, 158.3, 146.6, 139.3, 139.3, 139.0, 138.4, 137.7, 137.5, 137.5, 137.1, 135.9, 132.7, 128.6, 127.9, 113.0, 87.4, 86.6, 74.5, 63.4, 46.1, 32.2, 31.9, 25.6

R_f: 0.1 (SiO_2, EtOAc)

mp: decomposition at 70-80 °C (crude)

IR (cm^{-1}): 3264, 1645, 1529, 1210

MS (ESI Negative) m/z: 760 [M+Na$^+$], 776.5 [M+K$^+$]

Elemental Anal. Calculated for [C41H47N5O8+0.75 H_2O] C 65.58 H 6.52 N 9.53 found C 65.95 H 6.40 N 8.87

SUMMARY

In the first part of my PhD, which was done in the group of the organic chemistry of the professor Reiser in Regensburg, the δ-constrained sugar-like amino acid **256** were synthesised. To investigate its ability to induce a secondary structure if inserted in a sequence of α-δ-amino acid, the pentapeptide **261** and the heptapeptide **263** were also synthesised (Figure 133). Conformational studies and molecular modelling, which were performed in cooperation with Karine Guitot and Lucia Formicola) of both the penta- and hepta-peptide **261** and **263** showed the presence of a well ordered structure, but just on the base of the NMR spectroscopy data, it was not possible to elucidate the exact structure of the two compounds. Moreover, molecular modelling studies performed using as constraints the contacts obtained by NOESY and ROESY data, indicate for both the compounds the presence of an helix structure, which can not unfortunately completely described in the base of the data in our possession.

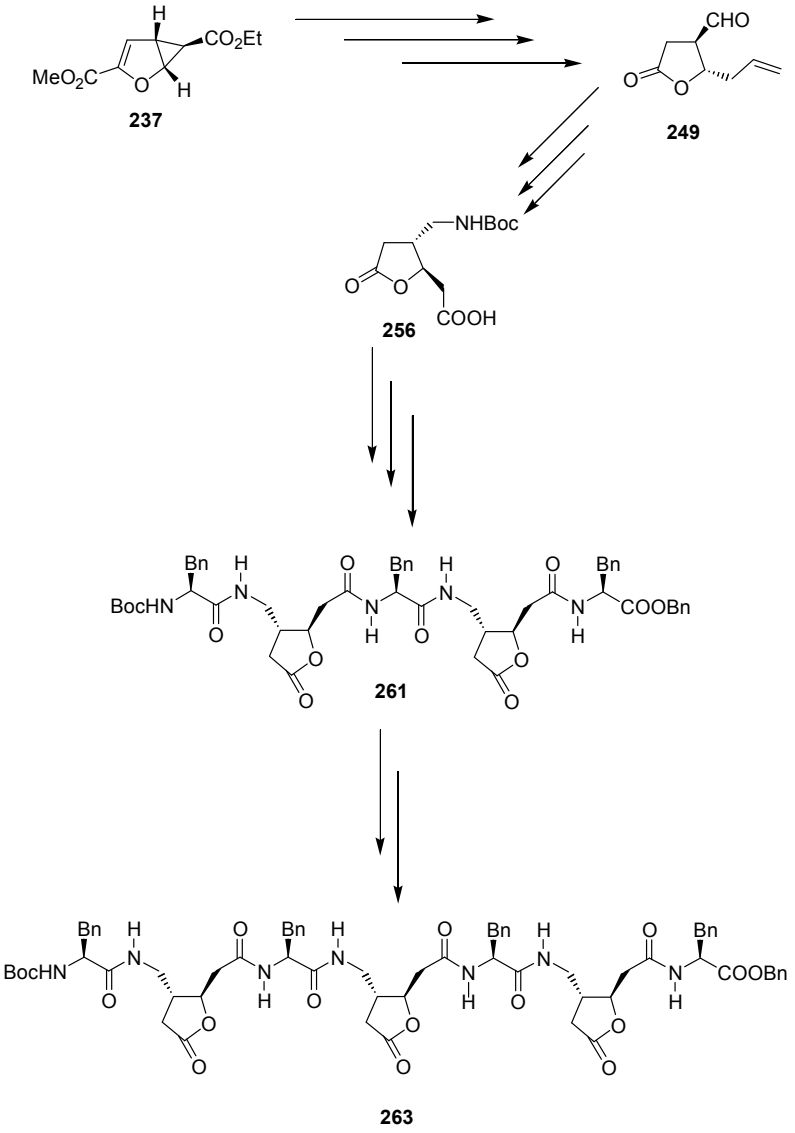

Figure 133

The lactone **249** was also used for the synthesis of some PNAs precursor (Figure 134). After the introduction and the successive protection of the nitrogen moiety to give the compound **264**, the lactone function was reduced to lactol and the acetylated to give the compound **265**. This key compound could be coupled with a freshly prepared persylilated thymine in the presence of a Lewis acid to give **266** as a mixture of diastereomers. After the PMB-removal by CAN it was also possible to separate the two diastereomers **267** and **268** and identify the absolute configuration of the anomeric carbon by means of the analysis of the ROESY spectra of both the compounds.

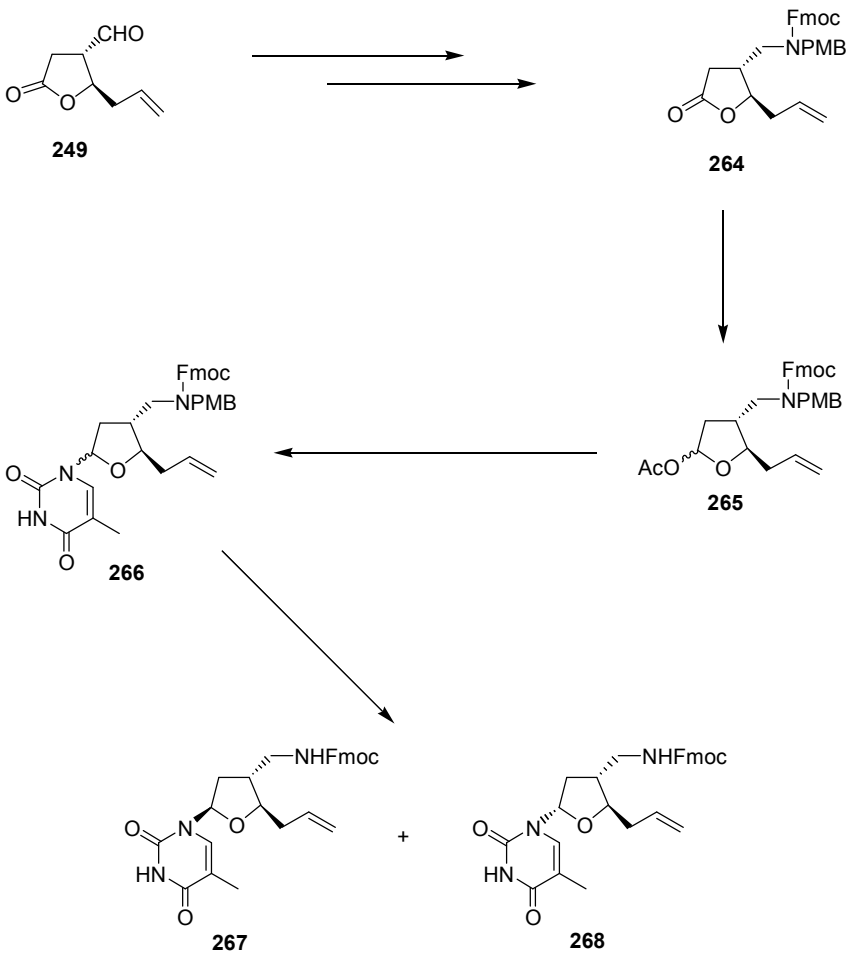

Figure 134

In the same conditions, it was also possible to perform the coupling with the persylilated adenine, but the successive Cbz-protection of the free amino group of the adenine did not give the desired compound **271** both with Cbz-Cl and Rapoport's reagent (figure 135).

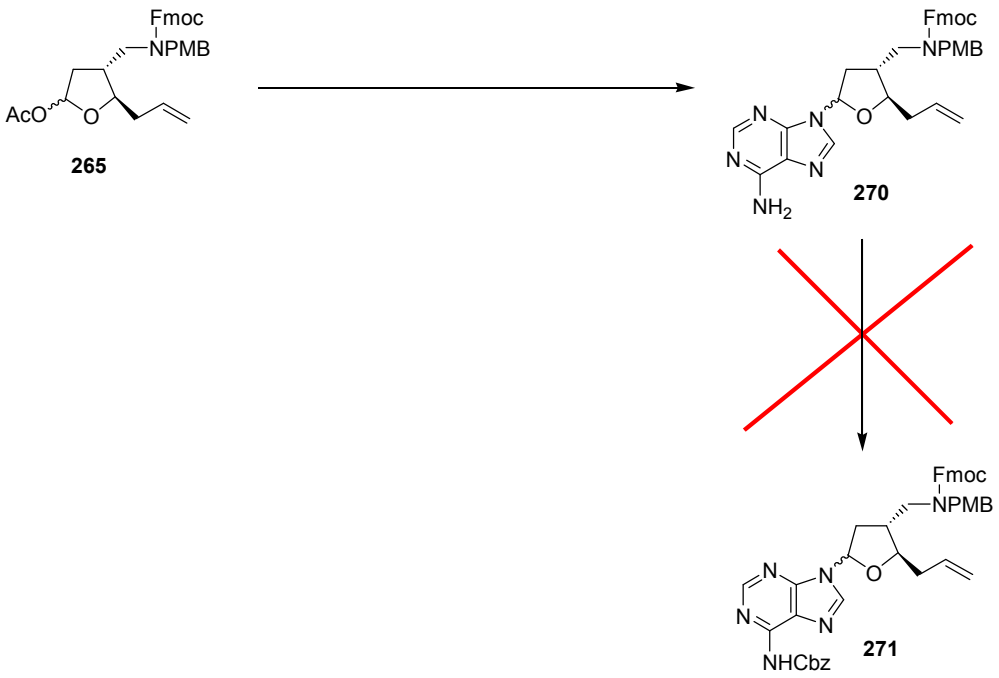

Figure 135

To solve this problem, it was so decide to perform the coupling directly with the Cbz-protected adenine. The Cbz-protected adenine resulted not enough reactive, so it was decided to activated *in situ* the compound **265** by bromination with trimethylsilyl bromide. The resulting intermediate **272** was not isolated and was directly reacted with the Cbz-protected adenine to afford the desired compound **271** in a good yield (Figure 136).

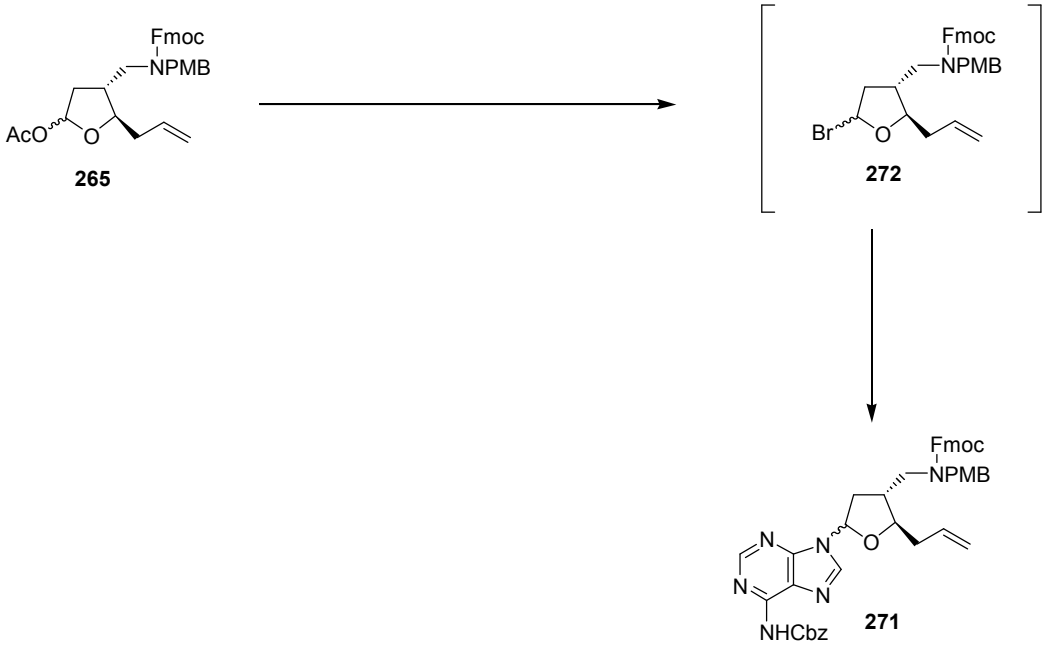

Figure 136

The second part of my PhD have been done at the University of Paris XI, in the Laboratoire de Molécules Fluorées et Chimie Médicinale, BioCIS, UMR-CNRS 8076. In the previous two years, in our lab, the challenge of the design and the synthesis of novel non covalent inhibitors of the 20S proteasome has been tackled by Lucia Formicola. Her efforts brought to the synthesis of a fluorinated pseudo amino acid (**295**) which, opportunely substituted, allows to inhibit the different active sites of the proteasome. In particular, the lead inhibitor **296**, with an IC_{50} in the order of μM for CT-L and caspase active sites, was synthesised (figure 137).

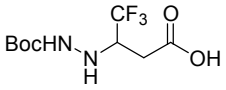

295

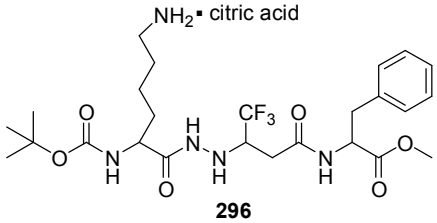

296

Figure 137

My project was try to elucidate the mechanism of the interaction between the compound **296** and the proteasome and to synthesise new more active compounds. For that purpose, the following steps were followed.

- Identification by means of literature and crystallography studies of the mechanism of interaction between the known inhibitors and the proteasome. This allowed to identify the essential features (occupation of hydrophobic pockets, hydrogen bonds etc.) necessary for the inhibition of the proteasome.

- Docking of known inhibitors to compare our results with the crystallised structures or with the reported molecular modelling studies. This allowed to define the docking parameters and to validate the model.

- Docking of the lead molecule (**296**) to formulate a first hypothesis of interaction.

- Systematic modification of the lead molecule and subsequently docking of the suggested molecules to address the synthetic work.

- Use of the biological evaluation results of the synthesised molecules to refine the docking parameters and for a well understanding of the binding interaction between molecules and proteasome.

The methodology exposed above gave as result the synthesis of a series of molecules (figure 138) which showed an inhibitory activity of the 20S proteasome.

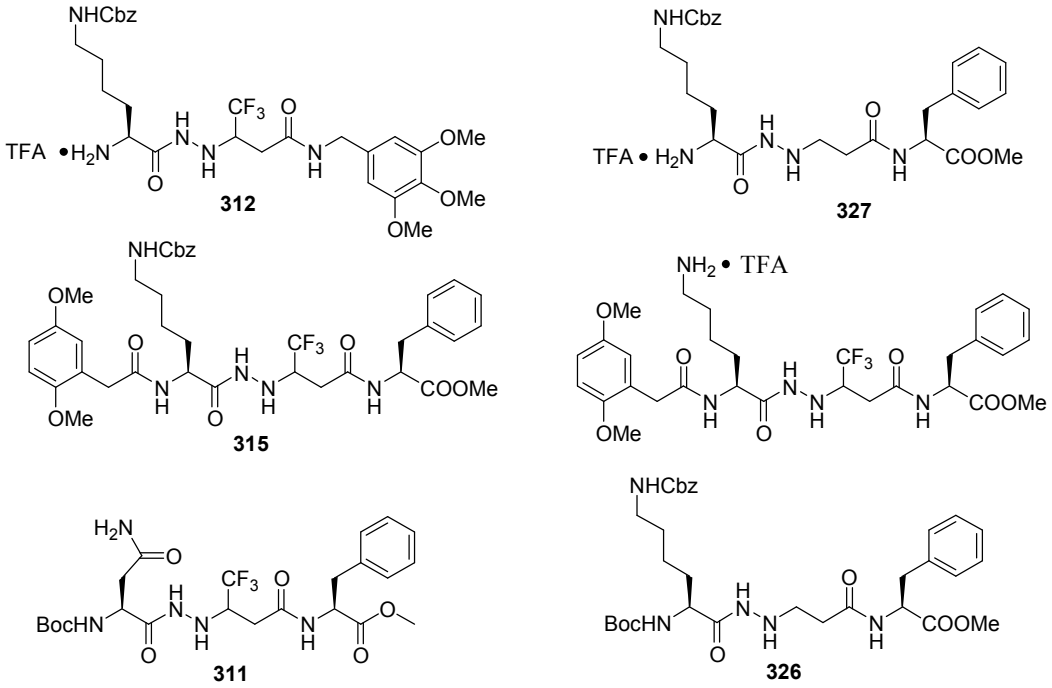

Figure 138

In conclusion, we demonstrated here that our methodology can be an useful tool to support and to drive the synthesis of new candidates for the inhibition of the 20S proteasome. Moreover, the docking can be an important help for a better understanding of the binding mechanism between small molecules and 20S proteasome. In particular, we showed that it is possible to explain the differences in the activity between sets of similar molecules which bind the receptor in a similar manner (see the docking results exposed in the paragraph 3.7). The limits in our methodology are particularly relied to the high number of torsions of the inhibitor candidates, which does not allow to obtain a good clustering, making more complicated the analysis of the results. Moreover, the structural diversity of the molecules synthesised joined with their high flexibility, makes plausible that it does not exist just one mechanism of binding interaction common to all the molecules, making more complicated the establishment of a structure-activity relationship.

References and notes

1. Wuthrich, K., Protein structure determination in solution by NMR spectroscopy. *J Biol Chem* **1990,** 265, (36), 22059-62.
2. Rich, D. H.; Singh, J., *Major Methods of Peptide Bond Formation*. New York, 1979; Vol. 1.
3. Sakakibara, S., Synthesis of Large Peptides in Solution. *Biopolymers* **1995,** 37, (1), 17-28.
4. Merrifield, R. B., Solid Phase Peptide Synthesis. I. The Synthesis of a Tetrapeptide. *J Am Chem Soc*
1963, 85, (14), 2149-2154.
5. Barany, G.; Merrifield, R. B., *The Peptides. Analysis, Synthesis, Biology. Vol. 2*. Academic Press: New York, 1979.
6. Merrifield, R. B., *Peptides. Synthesis, Structures and Applications*. Academic Press: New York, 1995.
7. DeGrado, W. F.; Summa, C. M.; Pavone, V.; Nastri, F.; Lombardi, A., De novo design and structural characterization of proteins and metalloproteins. *Annual Review of Biochemistry* **1999,** 68, 779-819.
8. Hill, R. B.; Raleigh, D. P.; Lombardi, A.; Degrado, N. F., De novo design of helical bundles as models for understanding protein folding and function. *Accounts of Chemical Research* **2000,** 33, (11), 745-754.
9. Gellman, S. H., Minimal model systems for beta sheet secondary structure in proteins. *Current Opinion in Chemical Biology* **1998,** 2, (6), 717-725.
10. Venkatraman, J.; Shankaramma, S. C.; Balaram, P., Design of folded peptides. *Chemical Reviews* **2001,** 101, (10), 3131-3152.
11. Lacroix, E.; Kortemme, T.; de la Paz, M. L.; Serrano, L., The design of linear peptides that fold as monomeric beta-sheet structures. *Current Opinion in Structural Biology* **1999,** 9, (4), 487-493.
12. Hirschmann, R., Medicinal Chemistry in the Golden-Age of Biology - Lessons from Steroid and Peptide Research. *Angewandte Chemie-International Edition in English* **1991,** 30, (10), 1278-1301.
13. Giannis, A., Peptidomimetics for Receptor Ligands Discovery, Development, and Medical Perspectives. *Angewandte Chemie-International Edition in English* **1993,** 32, (9), 1244-1267.
14. Hanessian, S.; McNaughtonSmith, G.; Lombart, H. G.; Lubell, W. D., Design and synthesis of conformationally constrained amino acids as versatile scaffolds and peptide mimetics. *Tetrahedron* **1997,** 53, (38), 12789-12854.
15. Gante, J., Peptidomimetics - Tailored Enzyme-Inhibitors. *Angewandte Chemie-International Edition* **1994,** 33, (17), 1699-1720.
16. Rizo, J.; Gierasch, L. M., Constrained Peptides - Models of Bioactive Peptides and Protein Substructures. *Annual Review of Biochemistry* **1992,** 61, 387-418.
17. Schneider, J. P.; Kelly, J. W., Templates That Induce Alpha-Helical, Beta-Sheet, and Loop Conformations. *Chemical Reviews* **1995,** 95, (6), 2169-2187.
18. Nowick, J. S.; Smith, E. M., The design, synthesis, and structural evaluation of three-stranded artificial beta-sheets. *Abstracts of Papers of the American Chemical Society* **1996,** 212, 195-ORGN.
19. Seebach, D.; Overhand, M.; Kuhnle, F. N. M.; Martinoni, B.; Oberer, L.; Hommel, U.; Widmer, H., beta-peptides: Synthesis by Arndt-Eistert homologation with concomitant peptide coupling. Structure determination by NMR and CD spectroscopy and by X-ray crystallography. Helical secondary structure of a beta-hexapeptide in solution and its stability towards pepsin. *Helvetica Chimica Acta* **1996,** 79, (4), 913-941.
20. Patch, J. A.; Barron, A. E., Mimicry of bioactive peptides via non-natural, sequence-specific peptidomimetic oligomers. *Curr Opin Chem Biol* **2002,** 6, (6), 872-7.

21. Appella, D. H.; Christianson, L. A.; Karle, I. L.; Powell, D. R.; Gellman, S. H., β-Peptide Foldamers: Robust Helix Formation in a New Family of β-Amino Acid Oligomers. *J Am Chem Soc* **1996,** 118, (51), 13071-13072.
22. Kaltenbronn, J. S.; Hudspeth, J. P.; Lunney, E. A.; Michniewicz, B. M.; Nicolaides, E. D.; Repine, J. T.; Roark, W. H.; Stier, M. A.; Tinney, F. J.; Woo, P. K. W.; Essenburg, A. D., Renin Inhibitors Containing Isosteric Replacements of the Amide Bond Connecting the P3 and P2 Sites. *Journal of Medicinal Chemistry* **1990,** 33, (2), 838-845.
23. Jenmalm, A.; Berts, W.; Li, Y. L.; Luthman, K.; Csoregh, I.; Hacksell, U., Stereoselective Epoxidation of Phe-Gly and Phe-Phe Vinyl Isosteres. *Journal of Organic Chemistry* **1994,** 59, (5), 1139-1148.
24. Jensen, A. J.; Luthman, K., Diastereoselective peracid epoxidation: Control of the face selectivity via functional group tuning and proper choice of epoxidation reagent. *Tetrahedron Letters* **1998,** 39, (20), 3213-3214.
25. Wiktelius, D.; Berts, W.; Jensen, A. J.; Gullbo, J.; Saitton, S.; Csoregh, I.; Luthman, K., Peracid dependent stereoselectivity and functional group contribution to the stereocontrol of epoxidation of (E)-alkene dipeptide isosteres. *Tetrahedron* **2006,** 62, (15), 3600-3609.
26. Mann, A.; Quaranta, L.; Reginato, G.; Taddei, M., A general synthesis of oligopeptides containing an oxirane ring in the place of a peptidic bond. *Tetrahedron Letters* **1996,** 37, (15), 2651-2654.
27. Wipf, P.; Xiao, J. B.; Geib, S. J., Imine additions of internal alkynes for the synthesis of trisubstituted (E)-alkene and cyclopropane peptide isosteres. *Advanced Synthesis & Catalysis* **2005,** 347, (11-13), 1605-1613.
28. Lopez-Ortega, B.; Jenkinson, S. F.; Claridge, T. D. W.; Fleet, G. W. J., Oxetane amino acids: synthesis of tetrameric and hexameric carbopeptoids derived from L-ribo 4-(aminomethyl)-oxetan-2-carboxylic acid. *Tetrahedron-Asymmetry* **2008,** 19, (8), 976-983.
29. Claridge, T. D. W.; Lopez-Ortega, B.; Jenkinson, S. F.; Fleet, G. W. J., Secondary structural investigations into homo-oligomers of delta-2,4-cis oxetane amino acids. *Tetrahedron-Asymmetry* **2008,** 19, (8), 984-988.
30. Johnson, S. W.; Jenkinson, S. F.; Angus, D.; Perez-Victoria, I.; Claridge, T. D. W.; Fleet, G. W. J.; Jones, J. H., The synthesis of oligomers of oxetane-based dipeptide isosteres derived from L-rhamnose or D-xylose. *Journal of Peptide Science* **2005,** 11, (6), 303-318.
31. Johnson, S. W.; Jenkinson, S. F.; Angus, D.; Jones, J. H.; Watkin, D. J.; Fleet, G. W. J., Pseudoenantiomeric oxetane delta-amino acid scaffolds derived from L-rhamnose and D-xylose: D/L-alanine-D-serine and glycine-L-serine dipeptide isosteres. *Tetrahedron-Asymmetry* **2004,** 15, (20), 3263-3273.
32. Smith, M. D.; Long, D. D.; Martin, A.; Marquess, D. G.; Claridge, T. D. W.; Fleet, G. W. J., Absence of secondary structure in a carbopeptoid tetramer of a trans-5-aminomethyl-tetrahydrofuran-2-carboxylate. *Tetrahedron Letters* **1999,** 40, (11), 2191-2194.
33. Chakraborty, T. K.; Ghosh, S.; Jayaprakash, S.; Sharma, J. A. R. P.; Ravikanth, V.; Diwan, P. V.; Nagaraj, R.; Kunwar, A. C., Synthesis and conformational studies by peptidomimetics containing furanoid sugar amino acids an a sugar diacid. *Journal of Organic Chemistry* **2000,** 65, (20), 6441-6457.
34. van Well, R. M.; Meijer, M. E. A.; Overkleeft, H. S.; van Boom, J. H.; van der Marel, G. A.; Overhand, M., Synthesis of bridged sugar amino acids: a new entry into conformationally locked delta- and epsilon-amino acids. *Tetrahedron* **2003,** 59, (14), 2423-2434.
35. Hanessian, S.; Brassard, M., Stereoselective synthesis of constrained oxacyclic hydroxyethylene isosteres of aspartyl protease inhibitors. Nitroaldol methodology toward 2,3-substituted tetrahydrofurans. *Tetrahedron* **2004,** 60, (35), 7621-7628.
36. Chakraborty, T. K.; Reddy, V. R.; Sudhakar, G.; Kumar, S. U.; Reddy, T. J.; Kumar, S. K.; Kunwar, A. C.; Mathur, A.; Sharma, R.; Gupta, N.; Prasad, S., Conformational studies of 3,4-

dideoxy furanoid sugar amino acid containing analogs of the receptor binding inhibitor of vasoactive intestinal peptide. *Tetrahedron* **2004,** 60, (38), 8329-8339.
37. Chakraborty, T. K.; Sudhakar, G., Synthesis of C6-substituted 3,4-dideoxy furanoid sugar amino acids. *Tetrahedron-Asymmetry* **2005,** 16, (1), 7-9.
38. vonRoedern, E. G.; Lohof, E.; Hessler, G.; Hoffmann, M.; Kessler, H., Synthesis and conformational analysis of linear and cyclic peptides containing sugar amino acids. *Journal of the American Chemical Society* **1996,** 118, (42), 10156-10167.
39. Overkleeft, H. S.; Verhelst, S. H. L.; Pieterman, E.; Meeuwenoord, W. J.; Overhand, M.; Cohen, L. H.; van der Marel, G. A.; van Boom, J. H., Design and synthesis of a protein : farnesyltransferase inhibitor based on sugar amino acids. *Tetrahedron Letters* **1999,** 40, (21), 4103-4106.
40. Stockle, M.; Voll, G.; Gunther, R.; Lohof, E.; Locardi, E.; Gruner, S.; Kessler, H., Synthesis and NMR Studies of Cyclopeptides Containing a Sugar Amino Acid. In 2002; Vol. 4, pp 2501-2504.
41. Risseeuw, M. D. P.; Mazurek, J.; van Langenvelde, A.; van der Marel, G. A.; Overkleeft, H. S.; Overhand, M., Synthesis of alkylated sugar amino acids: conformationally restricted L-Xaa-L-Ser/Thr mimics. *Organic & Biomolecular Chemistry* **2007,** 5, (14), 2311-2314.
42. Belvisi, L.; Colombo, L.; Manzoni, L.; Potenza, D.; Scolastico, C., Design, synthesis, conformational analysis and application of azabicycloalkane amino acids as constrained dipeptide mimics. *Synlett* **2004**, (9), 1449-1471.
43. Wang, W.; Yang, J. Q.; Ying, J. F.; Xiong, C. Y.; Zhang, J. Y.; Cai, C. Z.; Hruby, V. J., Stereoselective synthesis of dipeptide beta-turn mimetics: 7-benzyl and 8-phenyl substituted azabicyclo[4.3.0]nonane amino acid esters. *Journal of Organic Chemistry* **2002,** 67, (18), 6353-6360.
44. Millet, R.; Domarkas, J.; Rombaux, P.; Rigo, B.; Houssin, R.; Henichart, J. P., Synthesis of an azabicycloalkane amino acid scaffold as potential rigid dipeptide mimetic. *Tetrahedron Letters* **2002,** 43, (29), 5087-5088.
45. Dragovich, P. S.; Zhou, R.; Prins, T. J., Synthesis of an optically active, bicyclic 2-pyridone dipeptide mimetic. *Journal of Organic Chemistry* **2002,** 67, (3), 741-746.
46. Tong, Y. S.; Fobian, Y. M.; Wu, M. Y.; Boyd, N. D.; Moeller, K. D., Conformationally constrained substance P analogues: The total synthesis of a constrained peptidomimetic for the Phe(7)-Phe(8) region. *Journal of Organic Chemistry* **2000,** 65, (8), 2484-2493.
47. Maison, W.; Grohs, D. C.; Prenzel, A. H. G. P., Efficient synthesis of structurally diverse diazabicycloalkanes: Scaffolds for modular dipeptide mimetics with tunable backbone conformations. *European Journal of Organic Chemistry* **2004**, (7), 1527-1543.
48. Chiou, W. H.; Mizutani, N.; Ojima, I., Highly efficient synthesis of azabicyclo[x.y.0]alkane amino acids and congeners by means of Rh-catalyzed cyclohydrocarbonylation. *Journal of Organic Chemistry* **2007,** 72, (6), 1871-1882.
49. Bencsik, J. R.; Kercher, T.; O'Sullivan, M.; Josey, J. A., Efficient, stereoselective synthesis of oxazolo[3,2-a]pyrazin-5-ones: Novel bicyclic lactam scaffolds from the bicyclocondensation of 3-aza-1,5-ketoacids and amino alcohols. *Organic Letters* **2003,** 5, (15), 2727-2730.
50. Sellstedt, M.; Almqvist, F., Synthesis of a Novel Tricyclic Peptidomimetic Scaffold. In *Organic Letters*, 2008; Vol. 10, pp 4005-4007.
51. Lastdrager, B.; Timmer, M. S. M.; van der Marel, G. A.; Overkleeft, H. S.; Overhand, M., Transformation of glucose into a novel carbasugar amino acid dipeptide isostere. *Journal of Carbohydrate Chemistry* **2007,** 26, (1), 41-59.
52. Hann, M. M.; Sammes, P. G.; Kennewell, P. D.; Taylor, J. B., On the Double Bond lsostere of the Peptide Bond: Preparation of an Enkephalin Analogue. *Journal of the Chemical Society, Perkin Transactions 1* **1982**, 307-314.
53. Hann, M. M.; Sammes, P. G.; Kennewell, P. D.; Taylor, J. B., On Double Bond Isosteres of the Peptide Bond; an Enkephalin Analogue. *J. Chem. Soc. Chem. Commun.* **1980**, 234-235.

54. Cox, M. T.; Gormley, J. J.; Hayward, C. F.; Petter, N. N., Incorporation of trans -0lefinic Dipeptide Isosteres into Enkephalin and Substance P Analogues. *J. Chem. Soc. Chem. Commun.* **1980**, 800-802.
55. Manzenrieder, F.; Frank, A. O.; Huber, T.; Dorner-Ciossek, C.; Kessler, H., Synthesis and biological evaluation of phosphino dipeptide isostere inhibitor of human β-secretase (BACE1). *Bioorg. Med. Chem.* **2007,** 15, (12), 4136.
56. Manzenrieder, F.; Frank, A. O.; Huber, T.; Dorner-Ciossek, C.; Kessler, H., Synthesis and biological evaluation of phosphino dipeptide isostere inhibitor of human beta-secretase (BACE1). *Bioorganic & Medicinal Chemistry* **2007,** 15, (12), 4136-4143.
57. Yang, X. M.; Zou, X. M.; Fu, Y. Q.; Mou, K.; Fu, G.; Ma, C.; Xu, P., Synthesis of beta-secretase inhibitors containing a hydroxyethylene dipeptide isostere. *Synthetic Communications* **2007,** 37, (1-3), 9-24.
58. Hom, R. K.; Gailunas, A. F.; Mamo, S.; Fang, L. Y.; Tung, J. S.; Walker, D. E.; Davis, D.; Thorsett, E. D.; Jewett, N. E.; Moon, J. B.; John, V., Design and Synthesis of Hydroxyethylene-Based Peptidomimetic Inhibitors of Human β-Secretase. *J. Med. Chem.* **2004,** 47, (1), 158-164.
59. Ghosh, A. K.; Bilcer, G.; Harwood, C.; Kawahama, R.; Shin, D.; Hussain, K. A.; Hong, L.; Loy, J. A.; Nguyen, C.; Koelsch, G.; Ermolieff, J.; Tang, J., Structure-Based Design: Potent Inhibitors of Human Brain Memapsin 2 (β-Secretase). *J. Med. Chem.* **2001,** 44, (18), 2865-2868.
60. Maibaum, J.; Stutz, S.; Göschke, R.; Rigollier, P.; Yamaguchi, Y.; Cumin, F.; Rahuel, J.; Baum, H.-P.; Cohen, N.-C.; Schnell, C. R.; Fuhrer, W.; Gruetter, M. G.; Schilling, W.; Wood, J. M., Structural modification of the P2' position of 2, 7-dialkyl-substituted 5(S)-amino-4(S)-hydroxy-8-phenyl-octanecarboxamides: the discovery of Aliskiren, a potent nonpeptide human renin inhibitor active after once daily dosing in marmosets. *Journal of Medicinal Chemistry* **2007,** 50, 4832-4844.
61. Baldauf, C.; Günther, R.; Hofmann, H.-J., delta-Peptides and delta-Amino Acids as Tools for Peptide Structure DesignsA Theoretical Study. *J. Org. Chem.* **2004,** 69, (19), 6214.
62. Gardner, R. R.; Liang, G.-B.; Gellman, S. H., An achiral dipeptide mimetic that promotes β-hairpin formation. *J. Am. Chem. Soc.* **1995**, (117), 3280-3281.
63. Gardner, R. R.; Liang, G.-B.; Gellman, S. H., β-Turn and β-Hairpin Mimicry with Tetrasubstituted Alkenes. *J. Am. Chem. Soc.* **1999,** 121, (9), 1806-1816.
64. Zhao, X.; Jia, M.-X.; Jiang, X.-K.; Wu, L.-Z.; Li, Z.-T.; Chen, G.-J., Zipper-Featured δ-Peptide Foldamers Driven by Donor-Acceptor Interaction. Design, Synthesis, and Characterization. *J. Org. Chem.* **2004,** 69, (2), 270-279.
65. Hungerford, N. L.; Claridge, T. D. W.; Watterson, M. P.; Aplin, R. T.; Moreno, A.; Fleet, G. W. J., Tetrahydrofuran amino acids: Secondary structure in tetrameric and octameric carbopeptoids derived from a D-allo 5-(aminomethyl)-tetrahydrofuran-2-carboxylic acid. *J. Chem. Soc., Perkin Trans. 1* **2000**, 3666.
66. Claridge, T. D. W.; Long, D. D.; Baker, C. M.; Odell, B.; Grant, G. H.; Edwards, A. A.; Tranter, G. E.; Fleet, G. W. J.; Smith, M. D., Helix-forming carbohydrate amino acids. *Journal of Organic Chemistry* **2005,** 70, (6), 2082-2090.
67. Smith, M. D.; Claridge, T. D. W.; Sansom, M. S. P.; Fleet, G. W. J., Bend ribbon-forming tetrahydrofuran amino acids. *Organic & Biomolecular Chemistry* **2003,** 1, (21), 3647-3655.
68. Chakraborty, T. K.; Jayaprakash, S.; Srinivasu, P.; Madhavendra, S. S.; Sankar, A. R.; Kunwar, A. C., Furanoid sugar amino acid based peptidomimetics: well-defined solution conformations to gel-like structures. *Tetrahedron* **2002,** 58, (14), 2853-2859.
69. Davies, D. E.; Doyle, P. M.; Farrant, R. D.; Hill, R. D.; Hitchcock, P. B.; Sanderson, P. N.; Young, D. W., Synthesis of an external beta-turn based on the GLDV motif of cell adhesion proteins. *Tetrahedron Letters* **2003,** 44, (49), 8887-8891.

70. Nielsen, P. E.; Egholm, M.; Berg, R. H.; Buchardt, O., Sequence-selective recognition of DNA by strand displacement with a thymine-substituted polyamide. *Science* **1991,** 254, (5037), 1497-500.
71. Egholm, M.; Buchardt, O.; Nielsen, P. E.; Berg, R. H., Peptide Nucleic-Acids (Pna) - Oligonucleotide Analogs with an Achiral Peptide Backbone. *Journal of the American Chemical Society* **1992,** 114, (5), 1895-1897.
72. Hyrup, B.; Nielsen, P. E., Peptide nucleic acids (PNA): Synthesis, properties and potential applications. *Bioorganic & Medicinal Chemistry* **1996,** 4, (1), 5-23.
73. Nielsen, P. E.; Haaima, G., Peptide nucleic acid (PNA). A DNA mimic with a pseudopeptide backbone. *Chemical Society Reviews* **1997,** 26, (2), 73-78.
74. Uhlmann, E.; Peyman, A.; Breipohl, G.; Will, D. W., PNA: Synthetic polyamide nucleic acids with unusual binding properties. *Angewandte Chemie-International Edition* **1998,** 37, (20), 2797-2823.
75. Heimer, E. P.; Gallotorres, H. E.; Felix, A. M.; Ahmad, M.; Lambros, T. J.; Scheidl, F.; Meienhofer, J., Synthesis of Analogs and Oligomers of N-(2-Aminoethyl)Glycine and Their Gastrointestinal Absorption in the Rat. *International Journal of Peptide and Protein Research* **1984,** 23, (2), 203-211.
76. Thomson, S. A.; Josey, J. A.; Cadilla, R.; Gaul, M. D.; Hassman, C. F.; Luzzio, M. J.; Pipe, A. J.; Reed, K. L.; Ricca, D. J.; Wiethe, R. W.; Noble, S. A., Fmoc Mediated Synthesis of Peptide Nucleic-Acids. *Tetrahedron* **1995,** 51, (22), 6179-6194.
77. Stetsenko, D. A.; Lubyako, E. N.; Potapov, V. K.; Azhikina, T. L.; Sverdlov, E. D., New approach to solid phase synthesis of polyamide nucleic acids analogues (PNA) and PNA-DNA conjugates. *Tetrahedron Letters* **1996,** 37, (20), 3571-3574.
78. Breipohl, G.; Will, D. W.; Peyman, A.; Uhlmann, E., Novel synthetic routes to PNA monomers and PNA-DNA linker molecules. *Tetrahedron* **1997,** 53, (43), 14671-14686.
79. Kofoed, T.; Hansen, H. F.; Orum, H.; Koch, T., PNA synthesis using a novel Boc/acyl protecting group strategy. *Journal of Peptide Science* **2001,** 7, (8), 402-412.
80. Bialy, L.; Diaz-Mochon, J. J.; Specker, E.; Keinicke, L.; Bradley, M., Dde-protected PNA monomers, orthogonal to Fmoc, for the synthesis of PNA-peptide conjugates. *Tetrahedron* **2005,** 61, (34), 8295-8305.
81. Hudson, R. H. E.; Goncharenko, M.; Wallman, A. P.; Wojciechowski, F., PNA-directed triple-helix formation by N-7-xanthine. *Synlett* **2005**, (9), 1442-1446.
82. Liu, Z. C.; Shin, D. S.; Lee, K. T.; Jun, B. H.; Kim, Y. K.; Lee, Y. S., Synthesis of photolabile o-nitroveratryloxycarbonyl (NVOC) protected peptide nucleic acid monomers. *Tetrahedron* **2005,** 61, (33), 7967-7973.
83. Lee, H.; Jeon, J. H.; Lim, J. C.; Choi, H.; Yoon, Y.; Kim, S. K., Peptide nucleic acid synthesis by novel amide formation. *Org Lett* **2007,** 9, (17), 3291-3.
84. Vysabhattar, R.; Ganesh, K. N., Cyanuryl peptide nucleic acid: synthesis and DNA complexation properties. *Tetrahedron Letters* **2008,** 49, (8), 1314-1318.
85. Wojciechowski, F.; Hudson, R. H., A convenient route to N-[2-(Fmoc)aminoethyl]glycine esters and PNA oligomerization using a Bis-N-Boc nucleobase protecting group strategy. *J Org Chem* **2008,** 73, (10), 3807-16.
86. Dueholm, K. L.; Egholm, M.; Buchardt, O., An Efficient Synthesis of Boc-Aminoacetaldehyde and Its Application to the Synthesis of N-(2-Boc-Aminoethyl)Glycine Esters. *Organic Preparations and Procedures International* **1993,** 25, (4), 457-461.
87. Finn, P. J.; Gibson, N. J.; Fallon, R.; Hamilton, A.; Brown, T., Synthesis and properties of DNA-PNA chimeric oligomers. *Nucleic Acids Research* **1996,** 24, (17), 3357-3363.
88. Will, D. W.; Langner, D.; Knolle, J.; Uhlmann, E., The Synthesis of Polyamide Nucleic-Acids Using a Novel Monomethoxytrityl Protecting-Group Strategy. *Tetrahedron* **1995,** 51, (44), 12069-12082.

89. Breipohl, G.; Knolle, J.; Langner, D.; OMalley, G.; Uhlmann, E., Synthesis of polyamide nucleic acids (PNAs) using a novel Fmoc/Mmt protecting-group combination. *Bioorganic & Medicinal Chemistry Letters* **1996,** 6, (6), 665-670.
90. Hyrup, B.; Egholm, M.; Nielsen, P. E.; Wittung, P.; Norden, B.; Buchardt, O., Structure-Activity Studies of the Binding of Modified Peptide Nucleic-Acids (Pnas) to DNA. *Journal of the American Chemical Society* **1994,** 116, (18), 7964-7970.
91. Hyrup, B.; Nielsen, P. E., Peptide nucleic acids (PNA): synthesis, properties and potential applications. *Bioorg Med Chem* **1996,** 4, (1), 5-23.
92. Krotz, A. H.; Buchardt, O.; Nielsen, P. E., Synthesis of Retro-Inverso Peptide Nucleic-Acids .1. Characterization of the Monomers. *Tetrahedron Letters* **1995,** 36, (38), 6937-6940.
93. Krotz, A. H.; Buchardt, O.; Nielsen, P. E., Synthesis of Retro-Inverso Peptide Nucleic-Acids .2. Oligomerization and Stability. *Tetrahedron Letters* **1995,** 36, (38), 6941-6944.
94. Krotz, A. H.; Larsen, S.; Buchardt, O.; Eriksson, M.; Nielsen, P. E., A 'retro-inverso' PNA: structural implications for DNA and RNA binding. *Bioorg Med Chem* **1998,** 6, (11), 1983-92.
95. Haaima, G.; Lohse, A.; Buchardt, O.; Nielsen, P. E., Peptide nucleic acids (PNAs) containing thymine monomers derived from chiral amino acids: Hybridization and solubility properties of D-lysine PNA. *Angewandte Chemie-International Edition in English* **1996,** 35, (17), 1939-1942.
96. Balaji, B. S.; Gallazzi, F.; Jia, F.; Lewis, M. R., An efficient, convenient solid-phase synthesis of amino acid-modified peptide nucleic acid monomers and oligomers. *Bioconjug Chem* **2006,** 17, (2), 551-8.
97. Ganesh, K. N.; Gourishankar, A.; Vysabhattar, R.; Bokil, P., Property editing of peptide nucleic acids (PNA): gem-dimethyl, cyanuryl and 8-aminoadenine PNAs. *Nucleic Acids Symp Ser (Oxf)* **2007**, (51), 17-8.
98. Kosynkina, L.; Wang, W.; Liang, T. C., A Convenient Synthesis of Chiral Peptide Nucleic-Acid (Pna) Monomers. *Tetrahedron Letters* **1994,** 35, (29), 5173-5176.
99. Englund, E. A.; Appella, D. H., Synthesis of gamma-substituted peptide nucleic acids: A new place to attach fluorophores without affecting DNA binding. *Organic Letters* **2005,** 7, (16), 3465-3467.
100. Kleiner, R. E.; Brudno, Y.; Birnbaum, M. E.; Liu, D. R., DNA-templated polymerization of side-chain-functionalized peptide nucleic acid aldehydes. *J Am Chem Soc* **2008,** 130, (14), 4646-59.
101. Altmann, K. H.; Chiesi, C. S.; GarciaEcheverria, C., Polyamide based nucleic acid analogs - Synthesis of delta-amino acids with nucleic acid bases bearing side chains. *Bioorganic & Medicinal Chemistry Letters* **1997,** 7, (9), 1119-1122.
102. Cantin, M.; Schutz, R.; Leumann, C. J., Synthesis of the monomeric building blocks of Z-olefinic PNA (Z-OPA) containing the bases adenine and thymine. *Tetrahedron Letters* **1997,** 38, (24), 4211-4214.
103. Schutz, R.; Cantin, M.; Roberts, C.; Greiner, B.; Uhlmann, E.; Leumann, C., Olefinic Peptide Nucleic Acids (OPAs): New Aspects of the Molecular Recognition of DNA by PNA The team at the University of Bern thanks the Swiss National Science Foundation and Novartis Pharma AG, Basel, for generous financial support. *Angew Chem Int Ed Engl* **2000,** 39, (7), 1250-1253.
104. Bergmeier, S. C.; Fundy, S. L., Synthesis of oligo(5-aminopentanoic acid)-nucleobases (APN): Potential antisense agents. *Bioorganic & Medicinal Chemistry Letters* **1997,** 7, (24), 3135-3138.
105. D'Costa, M.; Kumar, V.; Ganesh, K. N., Aminoethylprolyl (aep) PNA: mixed purine/pyrimidine oligomers and binding orientation preferences for PNA:DNA duplex formation. *Org Lett* **2001,** 3, (9), 1281-4.
106. D'Costa, M.; Kumar, V. A.; Ganesh, K. N., Aminoethylprolyl peptide nucleic acids (aepPNA): chiral PNA analogues that form highly stable DNA:aepPNA2 triplexes. *Org Lett* **1999,** 1, (10), 1513-6.

107. Kumar, V.; Pallan, P. S.; Meena, M.; Ganesh, K. N., Pyrrolidine nucleic acids: DNA/PNA oligomers with 2-hydroxy/aminomethyl- 4-(thymin-1-yl)pyrrolidine-N-acetic acid. *Org Lett* **2001,** 3, (9), 1269-72.
108. Sharma, N. K.; Ganesh, K. N., Expanding the repertoire of pyrrolidyl PNA analogues for DNA/RNA hybridization selectivity: aminoethylpyrrolidinone PNA (aepone-PNA). *Chemical Communications* **2003**, (19), 2484-2485.
109. Myers, M. C.; Witschi, M. A.; Larionova, N. V.; Franck, J. M.; Haynes, R. D.; Hara, T.; Grajkowski, A.; Appella, D. H., A cyclopentane conformational restraint for a peptide nucleic acid: design, asymmetric synthesis, and improved binding affinity to DNA and RNA. *Org Lett* **2003,** 5, (15), 2695-8.
110. Puschl, A.; Boesen, T.; Zuccarello, G.; Dahl, O.; Pitsch, S.; Nielsen, P. E., Synthesis of pyrrolidinone PNA: a novel conformationally restricted PNA analogue. *J Org Chem* **2001,** 66, (3), 707-12.
111. Shirude, P. S.; Kumar, V. A.; Ganesh, K. N., (2S,5R/2R,5S)-aminoethylpipecolyl aepip-aegPNA chimera: synthesis and duplex/triplex stability. *Tetrahedron* **2004,** 60, (42), 9485-9491.
112. Goodnow, R. A.; Richou, A. R.; Tam, S., Synthesis of thymine, cytosine, adenine, and guanine containing N-Fmoc protected amino acids: Building blocks for construction of novel oligonucleotide backbone analogs. *Tetrahedron Letters* **1997,** 38, (18), 3195-3198.
113. Goodnow, R. A.; Tam, S.; Pruess, D. L.; McComas, W. W., Oligomer synthesis and DNA/RNA recognition properties of a novel oligonucleotide backbone analog: Glucopyranosyl nucleic amide (GNA). *Tetrahedron Letters* **1997,** 38, (18), 3199-3202.
114. Böhm, C.; Schinnerl, M.; Bubert, C.; Zabel, M.; Labahn, T.; Parisini, E.; Reiser, O., A New Strategy for the Stereoselective Synthesis of 1,2,3-Trisubstituted Cyclopropanes. *European Journal of Organic Chemistry* **2000,** 2000, (16), 2955-2965.
115. Reiser, O.; Schinnerl, M.; Bohm, C.; Glos, M., New bisoxazolin ligands with secondary binding sites for asymmetric catalysis. *Abstracts of Papers of the American Chemical Society* **2000,** 219, U140-U140.
116. Cram, D. J.; Elhafez, F. A. A., Studies in Stereochemistry. X. The Rule of “Steric Control of Asymmetric Induction” in the Syntheses of Acyclic Systems. In 1952; Vol. 74, pp 5828-5835.
117. Chérest, M.; Felkin, H.; Prudent, N., Torsional strain involving partial bonds. The stereochemistry of the lithium aluminium hydride reduction of some simple open-chain ketones. *Tetrahedron Letters* **1968,** 9, (18), 2199-2204.
118. Cram, D. J.; Elhafez, F. A. A., Studies in Stereochemistry. X. The Rule of “Steric Control of Asymmetric Induction” in the Syntheses of Acyclic Systems. *Journal of the American Chemical Society* **1952,** 74, (23), 5828-5835.
119. Hutchinson, C. R., Reductive amination of .alpha.-formyl lactones. II. Synthesis of tulipalin A and B and the acylglucoside, Tuliposide A, fungitoxic agents from Tulipa gesneriana. Carbon-13 nuclear magnetic resonance analysis of anomeric configuration in acylglucosides. *J Org Chem* **1974,** 39, (13), 1854-1858.
120. Meindl, W. R.; Von Angerer, E.; Schoenenberger, H.; Ruckdeschel, G., Benzylamines: synthesis and evaluation of antimycobacterial properties. *J Med Chem* **1984,** 27, (9), 1111-1118.
121. Barchuk, A.; Ngai, M. Y.; Krische, M. J., Allylic Amines via Iridium-Catalyzed C-C Bond Forming Hydrogenation: Imine Vinylation in the Absence of Stoichiometric Byproducts or Metallic Reagents. *J Am Chem Soc* **2007,** 129, (27), 8432-8433.
122. Yoshimura, J.; Yamaura, M.; Suzuki, T.; Hashimoto, H., Oxidative Removal of N-(Para-Methoxybenzyl) Group on Diketopiperazine Skeleton with Ceric Ammonium-Nitrate. *Chemistry Letters* **1983**, (7), 1001-1002.
123. Robinson, R. P.; Laird, E. R.; Blake, J. F.; Bordner, J.; Donahue, K. M.; Lopresti-Morrow, L. L.; Mitchell, P. G.; Reese, M. R.; Reeves, L. M.; Stam, E. J.; Yocum, S. A., Structure-Based Design

and Synthesis of a Potent Matrix Metalloproteinase-13 Inhibitor Based on a Pyrrolidinone Scaffold. *J Med Chem* **2000,** 43, (12), 2293-2296.
124. Yee, N. K.; Dong, Y.; Kapadia, S. R.; Song, J. J., A Practical and Improved Synthesis of (3S,5S)-3-[(tert-Butyloxycarbonyl)methyl]- 5-[(methanesulfonyloxy)methyl]-2- pyrrolidinone. *J Org Chem* **2002,** 67, (24), 8688-8691.
125. Kagoshima, H.; Okamura, T.; Akiyama, T., The Asymmetric [3+2] Cycloaddition Reaction of Chiral Alkenyl Fischer Carbene Complexes with Imines: Synthesis of Optically Pure 2,5-Disubstituted-3-pyrrolidinones. *J Am Chem Soc* **2001,** 123, (29), 7182-7183.
126. Elworthy, T. R.; Brill, E. R.; Chiou, S. S.; Chu, F.; Harris, J. R.; Hendricks, R. T.; Huang, J.; Kim, W.; Lach, L. K.; Mirzadegan, T.; Yee, C.; Walker, K. A. M., Lactams as EP4 Prostanoid Receptor Agonists. 3. Discovery of N-Ethylbenzoic Acid 2-Pyrrolidinones as Subtype Selective Agents. *J Med Chem* **2004,** 47, (25), 6124-6127.
127. Chakraborty, T.; Ghosh, A., A Convenient Synthesis of Chiral beta^3-Amino Acids. *Synlett* **2002**, (12).
128. Baer, H. H.; Zamkanei, M., Stereospecific synthesis of (-)-anisomycin from D-galactose. *J Org Chem* **1988,** 53, (20), 4786-4789.
129. Ralph Steffans, C. L., Nucleic Acid Analogs with Constraint Conformational Flexibility in the Sugar-Phosphate Backbone ldquoTricyclo-DNArdquo. Part 1. Preparation of [(5prime<I>R</I>,6prime<I>R</I>)-2prime-deoxy-3prime,5prime-ethano-5prime,6prime-methano-beta-<FONT SIZE='-2'>D</FONT>-ribofuranosyl]thymine and -adenine, and the corresponding phosphoramidites for oligonucleotide synthesis. *Helvetica Chimica Acta* **1997,** 80, (8), 2426-2439.
130. Paquette, L. A.; Seekamp, C. K.; Kahane, A. L.; Hilmey, D. G.; Gallucci, J., Stereochemical features of Lewis acid-promoted glycosidations involving 4'-spiroannulated DNA building blocks. *J Org Chem* **2004,** 69, (22), 7442-7.
131. Paquette, L. A.; Seekamp, C. K.; Kahane, A. L.; Hilmey, D. G.; Gallucci, J., Stereochemical Features of Lewis Acid-Promoted Glycosidations Involving 4‘-Spiroannulated DNA Building Blocks. *Journal of Organic Chemistry* **2004,** 69, (22), 7442-7447.
132. Leif Christensen, R. F. B. G. K. H. P. H. F. H. T. K. M. E. O. B. P. E. N. J. C. R. H. B., Solid-Phase synthesis of peptide nucleic acids. *journal of Peptide Science* **1995,** 1, (3), 175-183.
133. Thomson, S. A.; Josey, J. A.; Cadilla, R.; Gaul, M. D.; Hassman, C. F.; Luzzio, M. J.; Pipe, A. J.; Reed, K. L.; Ricca, D. J.; Wiethe, R. W., Fmoc Mediated Synthesis of Peptide Nucleic Acids. *Tetrahedron* **1995,** 51, (22), 6179-6194.
134. Hershko, A.; Ciechanover, A., The ubiquitin system. *Annu Rev Biochem* **1998,** 67, 425-79.
135. Pagano, M.; Tam, S. W.; Theodoras, A. M.; Beer-Romero, P.; Del Sal, G.; Chau, V.; Yew, P. R.; Draetta, G. F.; Rolfe, M., Role of the ubiquitin-proteasome pathway in regulating abundance of the cyclin-dependent kinase inhibitor p27. *Science* **1995,** 269, (5224), 682-5.
136. Meng, L.; Mohan, R.; Kwok, B. H.; Elofsson, M.; Sin, N.; Crews, C. M., Epoxomicin, a potent and selective proteasome inhibitor, exhibits in vivo antiinflammatory activity. *Proc Natl Acad Sci U S A* **1999,** 96, (18), 10403-8.
137. Palombella, V. J.; Conner, E. M.; Fuseler, J. W.; Destree, A.; Davis, J. M.; Laroux, F. S.; Wolf, R. E.; Huang, J.; Brand, S.; Elliott, P. J.; Lazarus, D.; McCormack, T.; Parent, L.; Stein, R.; Adams, J.; Grisham, M. B., Role of the proteasome and NF-kappaB in streptococcal cell wall-induced polyarthritis. *Proc Natl Acad Sci U S A* **1998,** 95, (26), 15671-6.
138. Rock, K. L.; Goldberg, A. L., Degradation of cell proteins and the generation of MHC class I-presented peptides. *Annu Rev Immunol* **1999,** 17, 739-79.
139. Schubert, U.; Anton, L. C.; Gibbs, J.; Norbury, C. C.; Yewdell, J. W.; Bennink, J. R., Rapid degradation of a large fraction of newly synthesized proteins by proteasomes. *Nature* **2000,** 404, (6779), 770-4.

140. Jensen, T. J.; Loo, M. A.; Pind, S.; Williams, D. B.; Goldberg, A. L.; Riordan, J. R., Multiple proteolytic systems, including the proteasome, contribute to CFTR processing. *Cell* **1995,** 83, (1), 129-35.
141. Ward, C. L.; Omura, S.; Kopito, R. R., Degradation of CFTR by the ubiquitin-proteasome pathway. *Cell* **1995,** 83, (1), 121-7.
142. Qu, D.; Teckman, J. H.; Omura, S.; Perlmutter, D. H., Degradation of a mutant secretory protein, alpha1-antitrypsin Z, in the endoplasmic reticulum requires proteasome activity. *J Biol Chem* **1996,** 271, (37), 22791-5.
143. Holzl, H.; Kapelari, B.; Kellermann, J.; Seemuller, E.; Sumegi, M.; Udvardy, A.; Medalia, O.; Sperling, J.; Muller, S. A.; Engel, A.; Baumeister, W., The regulatory complex of Drosophila melanogaster 26S proteasomes. Subunit composition and localization of a deubiquitylating enzyme. *J Cell Biol* **2000,** 150, (1), 119-30.
144. Lowe, J.; Stock, D.; Jap, B.; Zwickl, P.; Baumeister, W.; Huber, R., Crystal structure of the 20S proteasome from the archaeon T. acidophilum at 3.4 A resolution. *Science* **1995,** 268, (5210), 533-9.
145. Groll, M.; Kim, K. B.; Kairies, N.; Huber, R.; Crews, C. M., Crystal structure of epoxomicin : 20S proteasome reveals a molecular basis for selectivity of alpha ',beta '-epoxyketone proteasome inhibitors. *Journal of the American Chemical Society* **2000,** 122, (6), 1237-1238.
146. Groll, M.; Ditzel, L.; Lowe, J.; Stock, D.; Bochtler, M.; Bartunik, H. D.; Huber, R., Structure of 20S proteasome from yeast at 2.4 A resolution. *Nature* **1997,** 386, (6624), 463-71.
147. Orlowski, M.; Wilk, S., Catalytic activities of the 20 S proteasome, a multicatalytic proteinase complex. *Arch Biochem Biophys* **2000,** 383, (1), 1-16.
148. Arendt, C. S.; Hochstrasser, M., Identification of the yeast 20S proteasome catalytic centers and subunit interactions required for active-site formation. *Proc Natl Acad Sci U S A* **1997,** 94, (14), 7156-61.
149. Groll, M.; Heinemeyer, W.; Jager, S.; Ullrich, T.; Bochtler, M.; Wolf, D. H.; Huber, R., The catalytic sites of 20S proteasomes and their role in subunit maturation: a mutational and crystallographic study. *Proc Natl Acad Sci U S A* **1999,** 96, (20), 10976-83.
150. Heinemeyer, W.; Fischer, M.; Krimmer, T.; Stachon, U.; Wolf, D. H., The active sites of the eukaryotic 20 S proteasome and their involvement in subunit precursor processing. *J Biol Chem* **1997,** 272, (40), 25200-9.
151. Orlowski, M., The multicatalytic proteinase complex, a major extralysosomal proteolytic system. *Biochemistry* **1990,** 29, (45), 10289-97.
152. Dick, T. P.; Nussbaum, A. K.; Deeg, M.; Heinemeyer, W.; Groll, M.; Schirle, M.; Keilholz, W.; Stevanovic, S.; Wolf, D. H.; Huber, R.; Rammensee, H. G.; Schild, H., Contribution of proteasomal beta-subunits to the cleavage of peptide substrates analyzed with yeast mutants. *J Biol Chem* **1998,** 273, (40), 25637-46.
153. Nussbaum, A. K.; Dick, T. P.; Keilholz, W.; Schirle, M.; Stevanovic, S.; Dietz, K.; Heinemeyer, W.; Groll, M.; Wolf, D. H.; Huber, R.; Rammensee, H. G.; Schild, H., Cleavage motifs of the yeast 20S proteasome beta subunits deduced from digests of enolase 1. *Proc Natl Acad Sci U S A* **1998,** 95, (21), 12504-9.
154. Kisselev, A. F.; Akopian, T. N.; Castillo, V.; Goldberg, A. L., Proteasome active sites allosterically regulate each other, suggesting a cyclical bite-chew mechanism for protein breakdown. *Mol Cell* **1999,** 4, (3), 395-402.
155. Thornberry, N. A.; Lazebnik, Y., Caspases: enemies within. *Science* **1998,** 281, (5381), 1312-6.
156. Cardozo, C.; Michaud, C.; Orlowski, M., Components of the bovine pituitary multicatalytic proteinase complex (proteasome) cleaving bonds after hydrophobic residues. *Biochemistry* **1999,** 38, (30), 9768-77.
157. Seemuller, E.; Lupas, A.; Stock, D.; Lowe, J.; Huber, R.; Baumeister, W., Proteasome from Thermoplasma acidophilum: a threonine protease. *Science* **1995,** 268, (5210), 579-82.

158. Rock, K. L.; Gramm, C.; Rothstein, L.; Clark, K.; Stein, R.; Dick, L.; Hwang, D.; Goldberg, A. L., Inhibitors of the proteasome block the degradation of most cell proteins and the generation of peptides presented on MHC class I molecules. *Cell* **1994,** 78, (5), 761-71.
159. Vinitsky, A.; Cardozo, C.; Sepp-Lorenzino, L.; Michaud, C.; Orlowski, M., Inhibition of the proteolytic activity of the multicatalytic proteinase complex (proteasome) by substrate-related peptidyl aldehydes. *J Biol Chem* **1994,** 269, (47), 29860-6.
160. Palombella, V. J.; Rando, O. J.; Goldberg, A. L.; Maniatis, T., The ubiquitin-proteasome pathway is required for processing the NF-kappa B1 precursor protein and the activation of NF-kappa B. *Cell* **1994,** 78, (5), 773-85.
161. Tsubuki, S.; Saito, Y.; Tomioka, M.; Ito, H.; Kawashima, S., Differential inhibition of calpain and proteasome activities by peptidyl aldehydes of di-leucine and tri-leucine. *J Biochem* **1996,** 119, (3), 572-6.
162. Figueiredo-Pereira, M. E.; Berg, K. A.; Wilk, S., A new inhibitor of the chymotrypsin-like activity of the multicatalytic proteinase complex (20S proteasome) induces accumulation of ubiquitin-protein conjugates in a neuronal cell. *J Neurochem* **1994,** 63, (4), 1578-81.
163. Harding, C. V.; France, J.; Song, R.; Farah, J. M.; Chatterjee, S.; Iqbal, M.; Siman, R., Novel dipeptide aldehydes are proteasome inhibitors and block the MHC-I antigen-processing pathway. *J Immunol* **1995,** 155, (4), 1767-75.
164. Adams, J.; Behnke, M.; Chen, S.; Cruickshank, A. A.; Dick, L. R.; Grenier, L.; Klunder, J. M.; Ma, Y. T.; Plamondon, L.; Stein, R. L., Potent and selective inhibitors of the proteasome: dipeptidyl boronic acids. *Bioorg Med Chem Lett* **1998,** 8, (4), 333-8.
165. Omura, S.; Fujimoto, T.; Otoguro, K.; Matsuzaki, K.; Moriguchi, R.; Tanaka, H.; Sasaki, Y., Lactacystin, a novel microbial metabolite, induces neuritogenesis of neuroblastoma cells. *J Antibiot (Tokyo)* **1991,** 44, (1), 113-6.
166. Omura, S.; Matsuzaki, K.; Fujimoto, T.; Kosuge, K.; Furuya, T.; Fujita, S.; Nakagawa, A., Structure of lactacystin, a new microbial metabolite which induces differentiation of neuroblastoma cells. *J Antibiot (Tokyo)* **1991,** 44, (1), 117-8.
167. Corey, E. J.; Li, W. D., Total synthesis and biological activity of lactacystin, omuralide and analogs. *Chem Pharm Bull (Tokyo)* **1999,** 47, (1), 1-10.
168. Fenteany, G.; Standaert, R. F.; Lane, W. S.; Choi, S.; Corey, E. J.; Schreiber, S. L., Inhibition of proteasome activities and subunit-specific amino-terminal threonine modification by lactacystin. *Science* **1995,** 268, (5211), 726-31.
169. Dick, L. R.; Cruikshank, A. A.; Grenier, L.; Melandri, F. D.; Nunes, S. L.; Stein, R. L., Mechanistic studies on the inactivation of the proteasome by lactacystin: a central role for clasto-lactacystin beta-lactone. *J Biol Chem* **1996,** 271, (13), 7273-6.
170. Feling, R. H.; Buchanan, G. O.; Mincer, T. J.; Kauffman, C. A.; Jensen, P. R.; Fenical, W., Salinosporamide A: a highly cytotoxic proteasome inhibitor from a novel microbial source, a marine bacterium of the new genus salinospora. *Angew Chem Int Ed Engl* **2003,** 42, (3), 355-7.
171. Maldonado, L. A.; Fenical, W.; Jensen, P. R.; Kauffman, C. A.; Mincer, T. J.; Ward, A. C.; Bull, A. T.; Goodfellow, M., Salinispora arenicola gen. nov., sp. nov. and Salinispora tropica sp. nov., obligate marine actinomycetes belonging to the family Micromonosporaceae. *Int J Syst Evol Microbiol* **2005,** 55, (Pt 5), 1759-66.
172. Eustaquio, A. S.; Moore, B. S., Mutasynthesis of fluorosalinosporamide, a potent and reversible inhibitor of the proteasome. *Angew Chem Int Ed Engl* **2008,** 47, (21), 3936-8.
173. Bogyo, M.; McMaster, J. S.; Gaczynska, M.; Tortorella, D.; Goldberg, A. L.; Ploegh, H., Covalent modification of the active site threonine of proteasomal beta subunits and the Escherichia coli homolog HslV by a new class of inhibitors. *Proc Natl Acad Sci U S A* **1997,** 94, (13), 6629-34.
174. Meng, L.; Kwok, B. H.; Sin, N.; Crews, C. M., Eponemycin exerts its antitumor effect through the inhibition of proteasome function. *Cancer Res* **1999,** 59, (12), 2798-801.
175. Kloetzel, P. M., The proteasome system: a neglected tool for improvement of novel therapeutic strategies? *Gene Ther* **1998,** 5, (10), 1297-8.

176. Koguchi, Y.; Kohno, J.; Nishio, M.; Takahashi, K.; Okuda, T.; Ohnuki, T.; Komatsubara, S., TMC-95A, B, C, and D, novel proteasome inhibitors produced by Apiospora montagnei Sacc. TC 1093. Taxonomy, production, isolation, and biological activities. *J Antibiot (Tokyo)* **2000,** 53, (2), 105-9.
177. Kohno, J.; Koguchi, Y.; Nishio, M.; Nakao, K.; Kuroda, M.; Shimizu, R.; Ohnuki, T.; Komatsubara, S., Structures of TMC-95A-D: novel proteasome inhibitors from Apiospora montagnei sacc. TC 1093. *J Org Chem* **2000,** 65, (4), 990-5.
178. Groll, M.; Koguchi, Y.; Huber, R.; Kohno, J., Crystal structure of the 20 S proteasome:TMC-95A complex: a non-covalent proteasome inhibitor. *J Mol Biol* **2001,** 311, (3), 543-8.
179. Groll, M.; Gotz, M.; Kaiser, M.; Weyher, E.; Moroder, L., TMC-95-based inhibitor design provides evidence for the catalytic versatility of the proteasome. *Chemistry & Biology* **2006,** 13, (6), 607-614.
180. Nam, S.; Smith, D. M.; Dou, Q. P., Ester bond-containing tea polyphenols potently inhibit proteasome activity in vitro and in vivo. *Journal of Biological Chemistry* **2001,** 276, (16), 13322-13330.
181. Basse, N.; Piguel, S.; Papapostolou, D.; Ferrier-Berthelot, A.; Richy, N.; Pagano, M.; Sarthou, P.; Sobczak-Thepot, J.; Reboud-Ravaux, M.; Vidal, J., Linear TMC-95-based proteasome inhibitors. *Journal of Medicinal Chemistry* **2007,** 50, (12), 2842-2850.
182. Garcia-Echeverria, C.; Imbach, P.; France, D.; Furst, P.; Lang, M.; Noorani, M.; Scholz, D.; Zimmermann, J.; Furet, P., A new structural class of selective and non-covalent inhibitors of the chymotrypsin-like activity of the 20S proteasome. *Bioorganic & Medicinal Chemistry Letters* **2001,** 11, (10), 1317-1319.
183. Lin, Z. P.; Boller, Y. C.; Amer, S. M.; Russell, R. L.; Pacelli, K. A.; Patierno, S. R.; Kennedy, K. A., Prevention of brefeldin A-induced resistance to teniposide by the proteasome inhibitor MG-132: involvement of NF-kappaB activation in drug resistance. *Cancer Res* **1998,** 58, (14), 3059-65.
184. Wojcik, C.; Schroeter, D.; Stoehr, M.; Wilk, S.; Paweletz, N., An inhibitor of the chymotrypsin-like activity of the multicatalytic proteinase complex (20S proteasome) induces arrest in G2-phase and metaphase in HeLa cells. *Eur J Cell Biol* **1996,** 70, (2), 172-8.
185. Drexler, H. C.; Risau, W.; Konerding, M. A., Inhibition of proteasome function induces programmed cell death in proliferating endothelial cells. *Faseb J* **2000,** 14, (1), 65-77.
186. Drexler, H. C., Activation of the cell death program by inhibition of proteasome function. *Proc Natl Acad Sci U S A* **1997,** 94, (3), 855-60.
187. Orlowski, R. Z.; Eswara, J. R.; Lafond-Walker, A.; Grever, M. R.; Orlowski, M.; Dang, C. V., Tumor growth inhibition induced in a murine model of human Burkitt's lymphoma by a proteasome inhibitor. *Cancer Res* **1998,** 58, (19), 4342-8.
188. Lopes, U. G.; Erhardt, P.; Yao, R.; Cooper, G. M., p53-dependent induction of apoptosis by proteasome inhibitors. *J Biol Chem* **1997,** 272, (20), 12893-6.
189. Pahl, H. L., Activators and target genes of Rel/NF-kappaB transcription factors. *Oncogene* **1999,** 18, (49), 6853-66.
190. Borman, S., Drugs by design. *Chemical & Engineering News* **2005,** 83, (48), 28-30.
191. Moitessier, N.; Englebienne, P.; Lee, D.; Lawandi, J.; Corbeil, C. R., Towards the development of universal, fast and highly accurate docking/scoring methods: a long way to go. *British Journal of Pharmacology* **2008,** 153, S7-S26.
192. Goodsell, D. S.; Morris, G. M.; Olson, A. J., Automated docking of flexible ligands: Applications of AutoDock. *Journal of Molecular Recognition* **1996,** 9, (1), 1-5.
193. Goodsell, D. S.; Olson, A. J., Automated Docking of Substrates to Proteins by Simulated Annealing. *Proteins-Structure Function and Genetics* **1990,** 8, (3), 195-202.

194. Morris, G. M.; Goodsell, D. S.; Halliday, R. S.; Huey, R.; Hart, W. E.; Belew, R. K.; Olson, A. J., Automated docking using a Lamarckian genetic algorithm and an empirical binding free energy function. *Journal of Computational Chemistry* **1998,** 19, (14), 1639-1662.
195. Goldberg, D. E., *Genetic Algorithms in Search, Optimization & Machine Learning.* 1989.
196. Sousa, S. F.; Fernandes, P. A.; Ramos, M. J., Protein-ligand docking: Current status and future challenges. *Proteins-Structure Function and Bioinformatics* **2006,** 65, (1), 15-26.
197. Michalewicz, Z., *Genetic Algorithms + Data Structures = Evolution Programs*. 1996.
198. Hagmann, W. K., The many roles for fluorine in medicinal chemistry. *J Med Chem* **2008,** 51, (15), 4359-69.
199. Bégué, J.-P.; Bonnet-Delpon, D., *Bioorganic and medicinal chemistry of fluorine*. Wiley: 2008.
200. Bohm, H. J.; Banner, D.; Bendels, S.; Kansy, M.; Kuhn, B.; Muller, K.; Obst-Sander, U.; Stahl, M., Fluorine in medicinal chemistry. *Chembiochem* **2004,** 5, (5), 637-43.
201. Halgren, T. A., Maximally diagonal force constants in dependent angle-bending coordinates. II. Implications for the design of empirical force fields. *J Am Chem Soc* **1990,** 112, (12), 4710-4723.
202. Unno, M.; Mizushima, T.; Morimoto, Y.; Tomisugi, Y.; Tanaka, K.; Yasuoka, N.; Tsukihara, T., The structure of the mammalian 20S proteasome at 2.75 A resolution. *Structure* **2002,** 10, (5), 609-18.
203. Hu, G.; Lin, G.; Wang, M.; Dick, L.; Xu, R. M.; Nathan, C.; Li, H., Structure of the Mycobacterium tuberculosis proteasome and mechanism of inhibition by a peptidyl boronate. *Mol Microbiol* **2006,** 59, (5), 1417-28.
204. Groll, M.; Berkers, C. R.; Ploegh, H. L.; Ovaa, H., Crystal structure of the boronic acid-based proteasome inhibitor bortezomib in complex with the yeast 20S proteasome. *Structure* **2006,** 14, (3), 451-6.
205. Borissenko, L.; Groll, M., 20S proteasome and its inhibitors: crystallographic knowledge for drug development. *Chem Rev* **2007,** 107, (3), 687-717.
206. Smith, D. M.; Daniel, K. G.; Wang, Z.; Guida, W. C.; Chan, T. H.; Dou, Q. P., Docking studies and model development of tea polyphenol proteasome inhibitors: applications to rational drug design. *Proteins* **2004,** 54, (1), 58-70.
207. Cozzini, P.; Dottorini, T., Is it possible docking and scoring new ligands with few experimental data? Preliminary results on estrogen receptor as a case study. *Eur J Med Chem* **2004,** 39, (7), 601-9.
208. Furet, P.; Imbach, P.; Noorani, M.; Koeppler, J.; Laumen, K.; Lang, M.; Guagnano, V.; Fuerst, P.; Roesel, J.; Zimmermann, J.; Garcia- Echeverria, C., Entry into a new class of potent proteasome inhibitors having high antiproliferative activity by structure-based design. *Journal of Medicinal Chemistry* **2004,** 47, (20), 4810-4813.
209. Cheguillaume, A.; Doubli-Bounoua, I.; Baudy-Floc'h, M.; Le Grel, P., New potential monomers for solid phase synthesis of hydrazinopeptoids: the N-alpha-substituted-N-beta-protected hydrazinoglycines and hydrazinoglycinals. *Synlett* **2000**, (3), 331-334.
210. Busnel, O.; Baudy-Floc'h, M., Preparation of new monomers aza-beta(3)-aminoacids for solid-phase syntheses of aza-beta(3)-peptides. *Tetrahedron Letters* **2007,** 48, (33), 5767-5770.

ANNEX I Docking results

CASPASE In this active site it is not present the D114

Name	clust rank	N° conf	deltaG	dist Thr1	T21	G23	G47	A49	D114	Others HB	S1	S3
315	2	1	-6.76	4.0	n	n	y	n	X	Y	1	4
315R	1	1	-6.29	HB	n	n	y	n	X	T22, S129	4	2
	3	1	-5.62	3.9	n	n	n	y	X	S129	4	1
311	1	1	-6.18	HB	y	n	y	n	X	T22	1	4
	2	3	-5.31	HB	y	y	n	n	X		4	1
311R	2	1	-6.24	HB	y	n	y	n	X		1	4
	3	1	-5.68	HB	y	n	y	n	X	R19, T22	1	4
297	1	1	-8.37	6.0	n	n	n	n	X	H114	X	2
297R	Not found conformations corresponding to the selected criteria											
296	1	4	-4.94	4.8	y	n	n	n	X	D51	4	1
296R	1	1	-5.43	HB	n	n	n	y	X	D51	4	1
298	2	1	-6.07	5.0	y	y	n	n	X	D51 Q91 N94	1	4
298R	3	1	-6.21	3.5	n	n	n	y	X	T22 D51	1	4
299	2	1	-6.53	3.6	n	n	n	n	X	A50	1	4
299R	2	2	-6.05	3.3	y	n	n	n	X	T22, A50	1	4
300	Not found conformations corresponding to the selected criteria											
300R	Not found conformations corresponding to the selected criteria											
301	Not found conformations corresponding to the selected criteria											
301R	Not found conformations corresponding to the selected criteria											
302	Not found conformations corresponding to the selected criteria											
302R	Not found conformations corresponding to the selected criteria											
318	1	1	-5.96	2.2	y	n	n	y	X	S118 H114	2	4
318R	1	1	-6.33	3.1	y	n	n	n	X	R45 H114 D120	1	2
317	2	4	-5.97	3.5	n	y	n	y	X	H114 S118 A50	4	1
317R	1	5	-5.92	3.6	y	n	n	n	X	S48 A50 T98	4	1
312	Not found conformations corresponding to the selected criteria											
312R	3	1	-5.52	HB	y	n	n	n	X	S118 V30	2	1

316	4	1	-5.23	3.0	y	y	n	y	X	D120	1	2
316R	1	1	-5.89	4.1	y	n	n	n	X	A50 D120	1	2

CHYMOTRYPSIN-LIKE

Name	**clust rank**	**N° conf**	**deltaG**	**dist Thr1**	**T21**	**G23**	**G47**	**A49**	**D114**	**Others HB**	**S1**	**S3**
315	1	1	-7.85	3.4	y	n	n	y	n		CF3	1
315R	2	2	-6.08	4.0	n	n	n	y	y		1	2
311	1	1	-6.30	2.9	y	n	y	y	y		1	4
311R	2	1	-6.08	HB	y	n	y	n	y	S168	1	4
297	1	1	-8.21	3.8	y	y	n	y	y		CF3	1 m
297R	1	1	-8.70	6.0	y	n	y	n	y		4	2
296	1	1	-9.20	3.1	y	n	y	y	y	S118	1	4
296R	2	1	-6.30	4.8	y	n	n	n	y	S118	1	4
298	2	1	-6.73	3.4	y	n	y	n	y		1	4
298R	1	1	-7.79	2.9	y	n	n	y	y		1	2
299	1	1	-7.78	3.0	n	n	n	y	y		1	2
299R	1	1	-7.60	HB	y	n	y	y	y		4	1
301	Not found conformations corresponding to the selected criteria											
301R	1	1	-8.51	2.6	y	n	y	n	n		4	1
300	Not found conformations corresponding to the selected criteria											
300R	Not found conformations corresponding to the selected criteria											
302	Not found conformations corresponding to the selected criteria											
302R	2	1	-8.13	3.5	n	n	n	n	y		1	2
318	1	1	-6.00	HB	y	n	y	y	y	S96	4	2
318R	3	1	-6.33	HB	y	n	y	y	n	S112	2	4
317	1	1	-7.54	HB	y	n	n	y	y	Q53	4	1
317R	1	2	-7.77	HB	y	n	n	y	y	D50	4	1
312	1	2	-7.16	2.8	y	n	y	y	y		4	2
312R	1	3	-8.22	3.7	y	y	n	y	y		4	2
316	1	1	-6.37	3.3	n	n	n	n	y	A50	1	4
316R	3	2	5.39	3.5	n	y	n	n	y		4	1

TRIPSIN-LIKE

Name	clust rank	N° conf	deltaG	dist Thr1	T21	G23	G47	A49	D114	Others HB	S1	S3
315	1	1	-6.25	<2.5	n	y	n	n	n		Cbz	X
315R	1	1	-6.08	5.3	y	n	n	y	n		1	X
311	1	1	-6.21	<2.5	y	n	n	y	n		4	1-2
311R	1	1	-5.89	3.0	y	y	y	n	n	Q22	1	4
297	1	1	-5.89	4.9	y	y	n	n	n		Cbz	CF3
297R	1	1	-7.44	<2.5	y	n	y	n	y		CF3	Cbz
296	1	1	-6.01	3.0	y	n	n	n	n	G22 D120	1	2
296R	1	2	-7.24	2.9	y	n	n	n	y	D120	1	2
	2	3	-6.64	3.1	y	n	n	y	y	D120	1	2
298	1	3	-8.96	3.3	y	n	n	y	y	D120	1	2
298R	1	1	-9.60	5.0	y	n	n	n	y	D120	1	2
	2	2	-9.02	5.3	y	n	n	n	n	R91 D120	1	2
	3	4	-9.01	3.0	y	n	n	n	y	D120	1	2
299	1	2	-6.85	2.8	n	n	n	y	n	T48	1	X
299R	1	1		3.1	n	n	n	y	n	T48 R91	1	X
300	Not found conformations corresponding to the selected criteria											
300R	Not found conformations corresponding to the selected criteria											
301	Not found conformations corresponding to the selected criteria											
301R	Not found conformations corresponding to the selected criteria											
302	Not found conformations corresponding to the selected criteria											
302R	Not found conformations corresponding to the selected criteria											
318	1	1	-6.46	3.2	y	n	n	y	y	I119	1	2
318R	1	2	-6.50	2.9	y	n	y	y	y	D120	1	2
317	1	2	-6.90	3.8	y	n	n	y	y		4	1
317R	Not found conformations corresponding to the selected criteria											
312	1	1	-6.72	3.0	y	n	n	y	y	C118	4	1
312R	1	1	-9.09	<2.5	n	n	n	n	y	S20	4	1
316	1	1	-7.24	<2.5	y	n	n	n	y	T48 D120	1	2
316R	1	1	-6.73	2.8	y	n	n	n	y	R91 T48	1	2

Clust. rank = cluster ranking of the conformation obtained by the Autodock score function

N° conf = number of conformation in the cluster (with an RMSD < 2Å)

Delta G = energy of binding calculated by Autodock

Dist Thr1 = distance between the ligand and the threonine 1, HB if it is detected an hydrogen bond

T21, G23, G47, A49, D114 = y: it is present an hydrogen bond between the ligand and this residue

N = no hydrogen bonds detected

Others HB = presence of additionally hydrogen bonds

S1 = group of the molecule which fills the S1 pocket (*Vide supra*, Paragraph 3.6.3, Fig 116)

S3 = group of the molecule which fills the S3 pocket (*Vide supra*, Paragraph 3.6.3, Fig 116)

ANNEX II NMR SPECTRA

(1R,5R,6R)-(+)-2-Oxabicyclo[3.1.0]hex-3-ene-3,6-dicarboxylic-6-ethylester-3-methyl ester (237) in $CDCl_3$

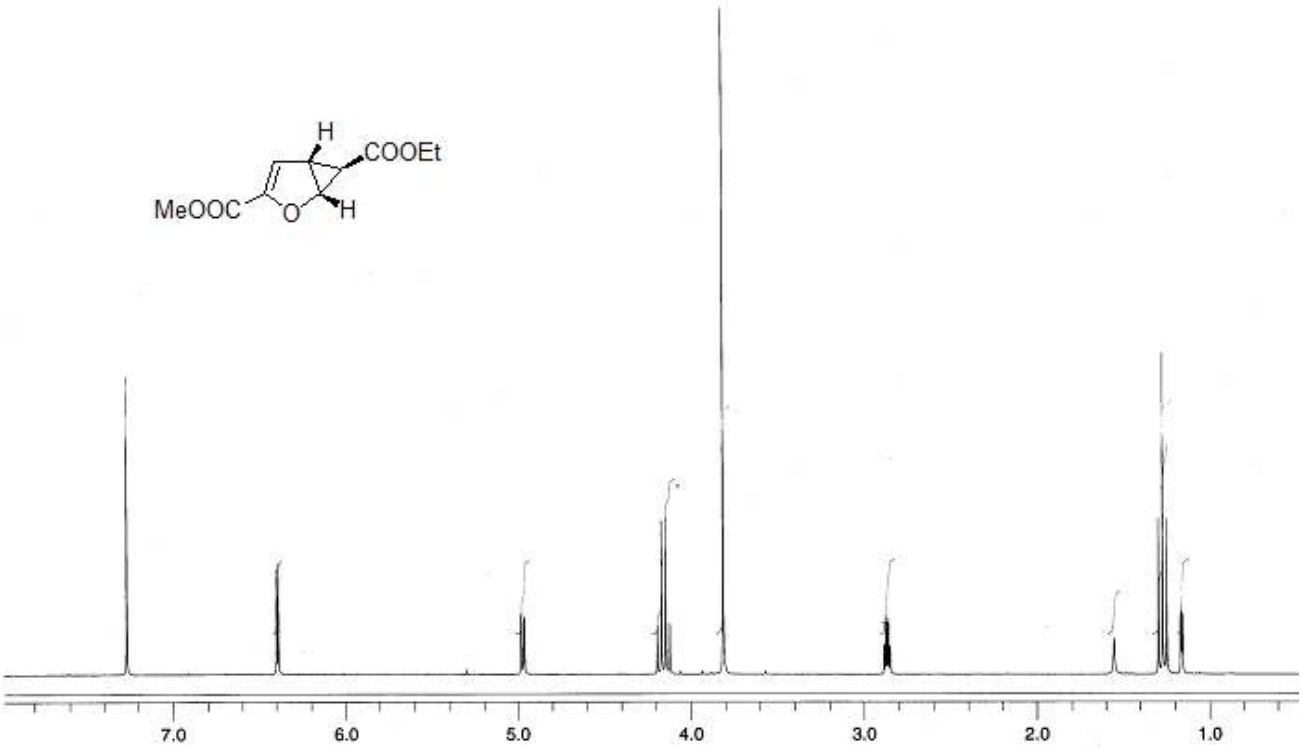

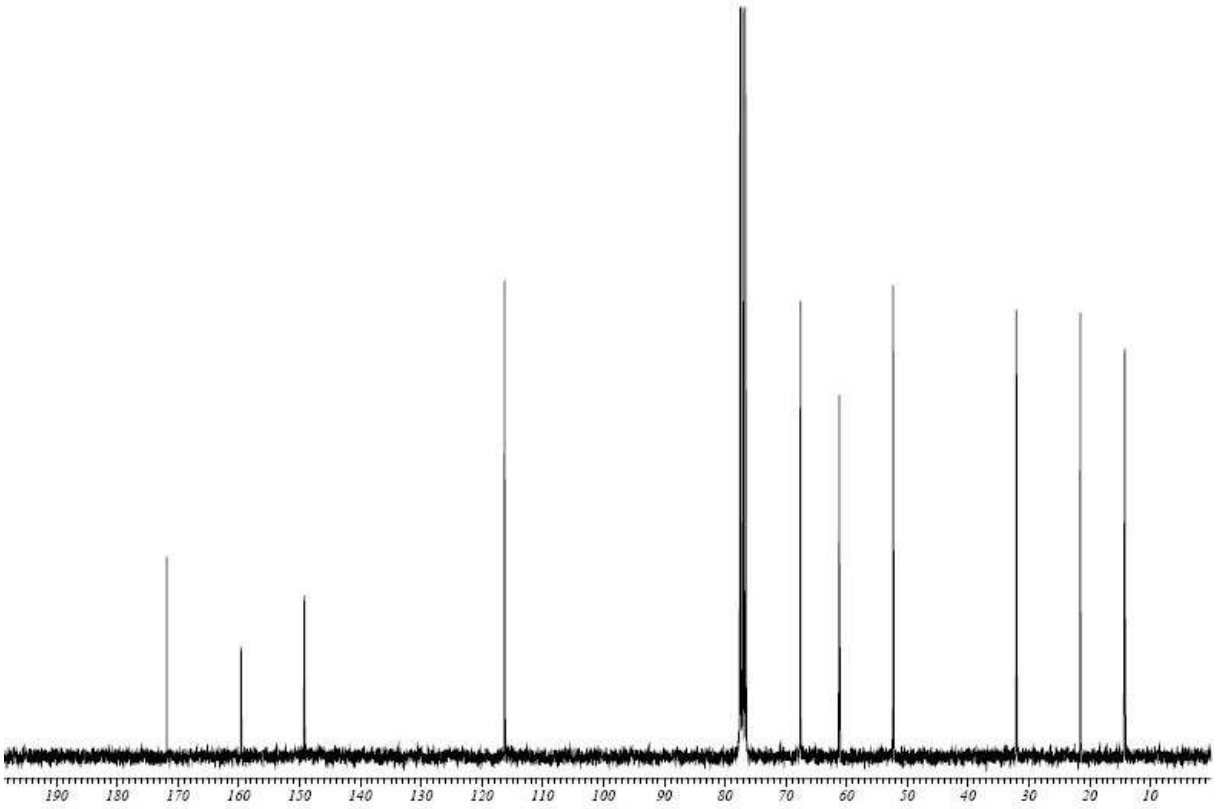

(1R,2R,3R)-(+)-Oxalic acid 2-ethoxycarbonyl 3-formyl-cyclopropyl ester methyl ester 242

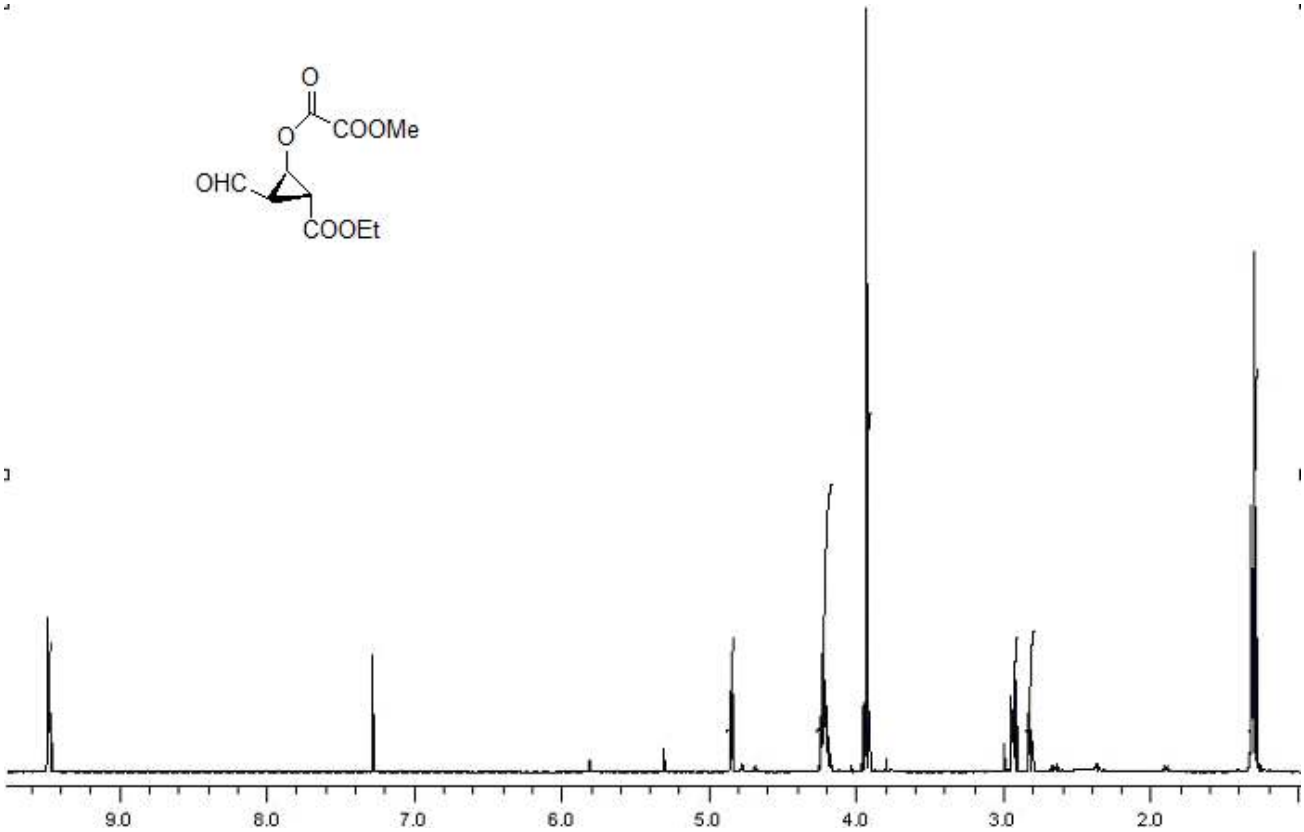

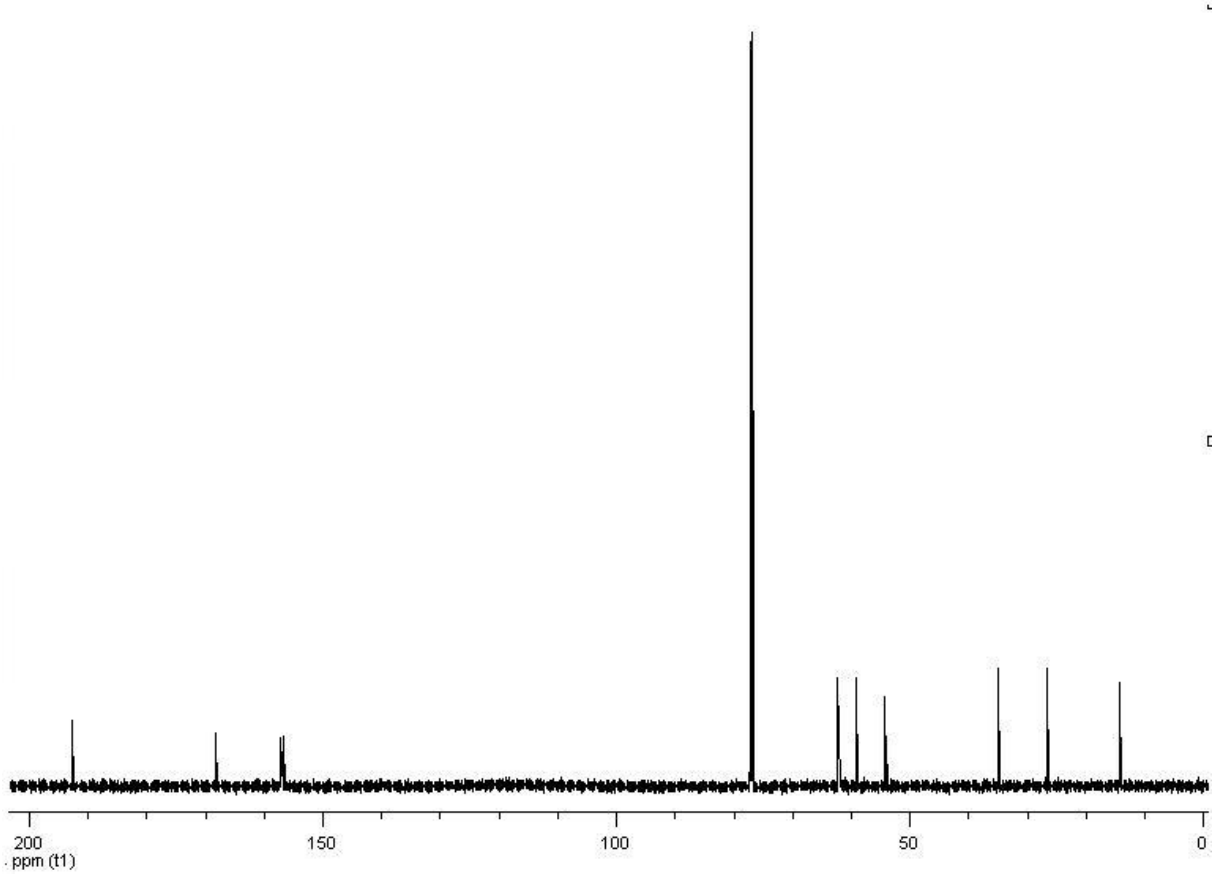

(1R, 1'R/R,2R, 3R)-Oxalicacid-hydroxy-but-3'-enyl-3-ethoxycarbonyl-cyclopropylester methylester 244

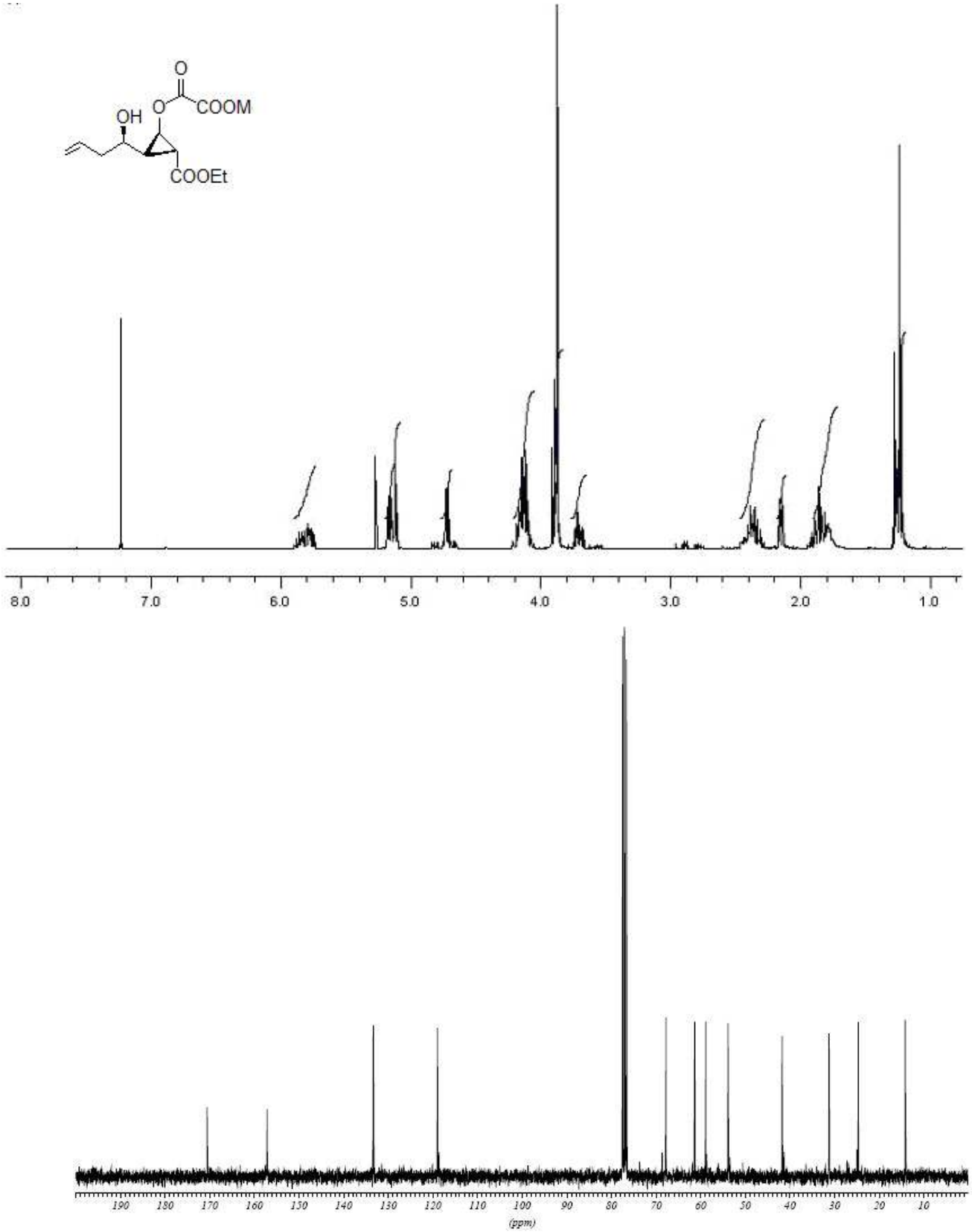

2R/S,3R)-2-Allyl-5-oxotetrahydrofuran-3-carbaldehyde 249

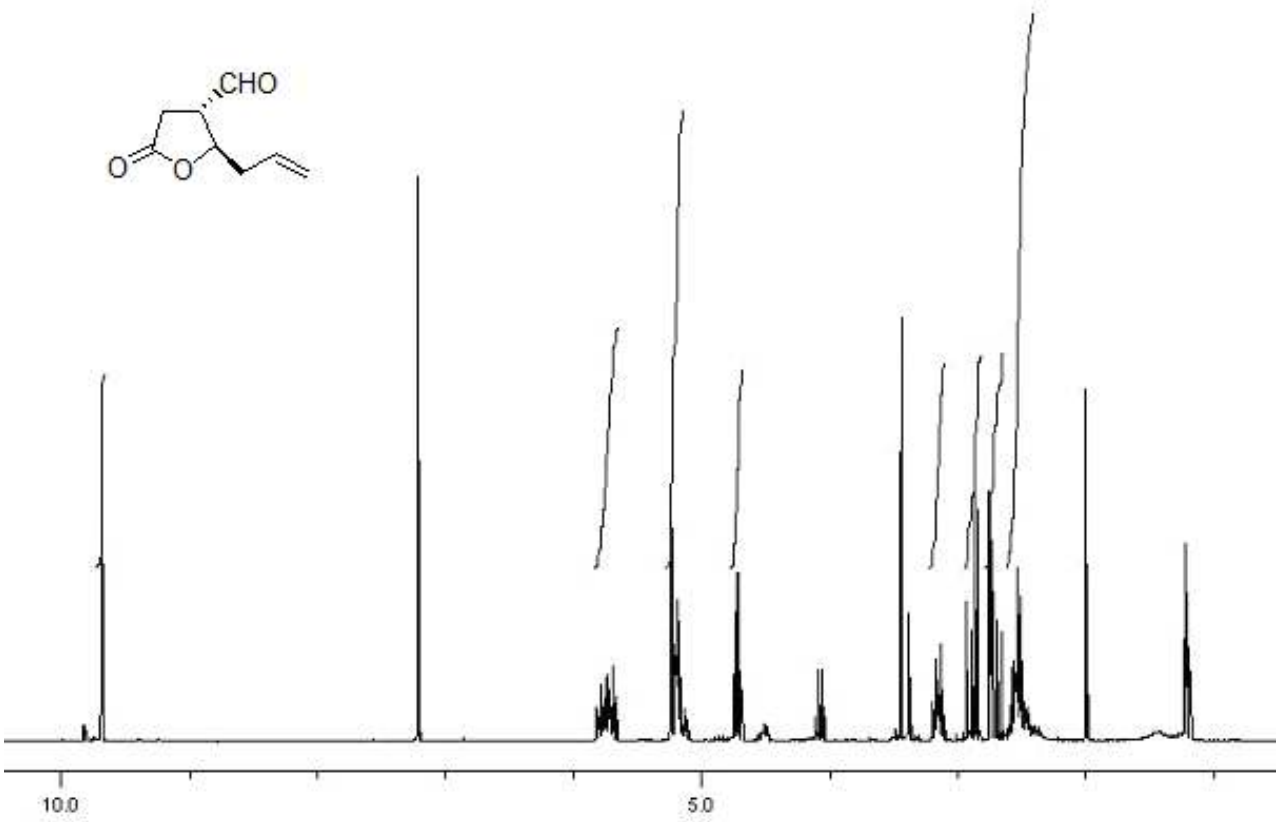
CHO
O
O
10.0
5.0

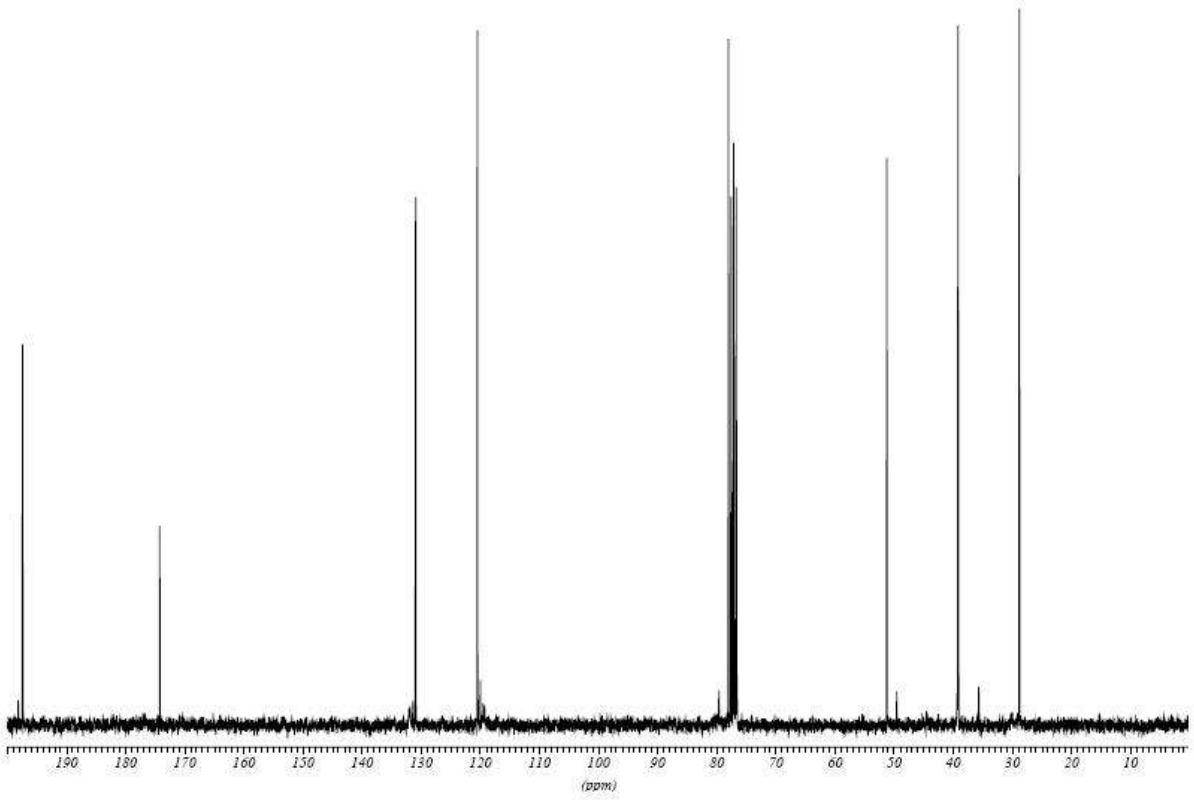
190
180
170
160
150
140
130
120
110
100
90
80
70
60
50
40
30
20
10
(ppm)

(2R/S, 3R, 4R, 5R)-5-Allyl-4-formyl-2-hydroxy-tetrahydro-furan-2,3-dicarboxylic acid 3-ethyl ester 2-methyl ester 251

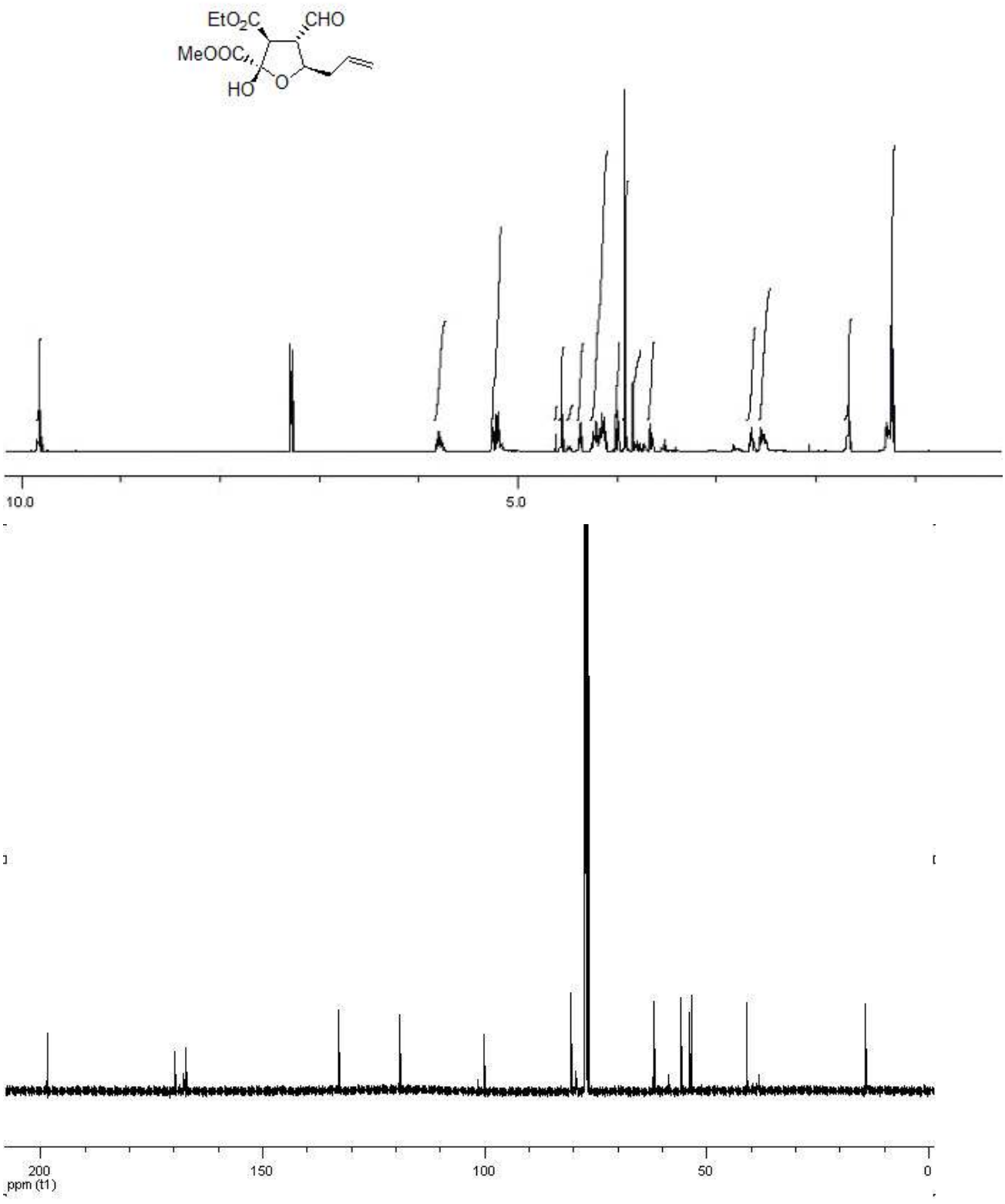

(4R,5R)-5-Allyl-4-[(4-methoxy-benzylamino)-methyl]-dihydro-furan-2-one 252

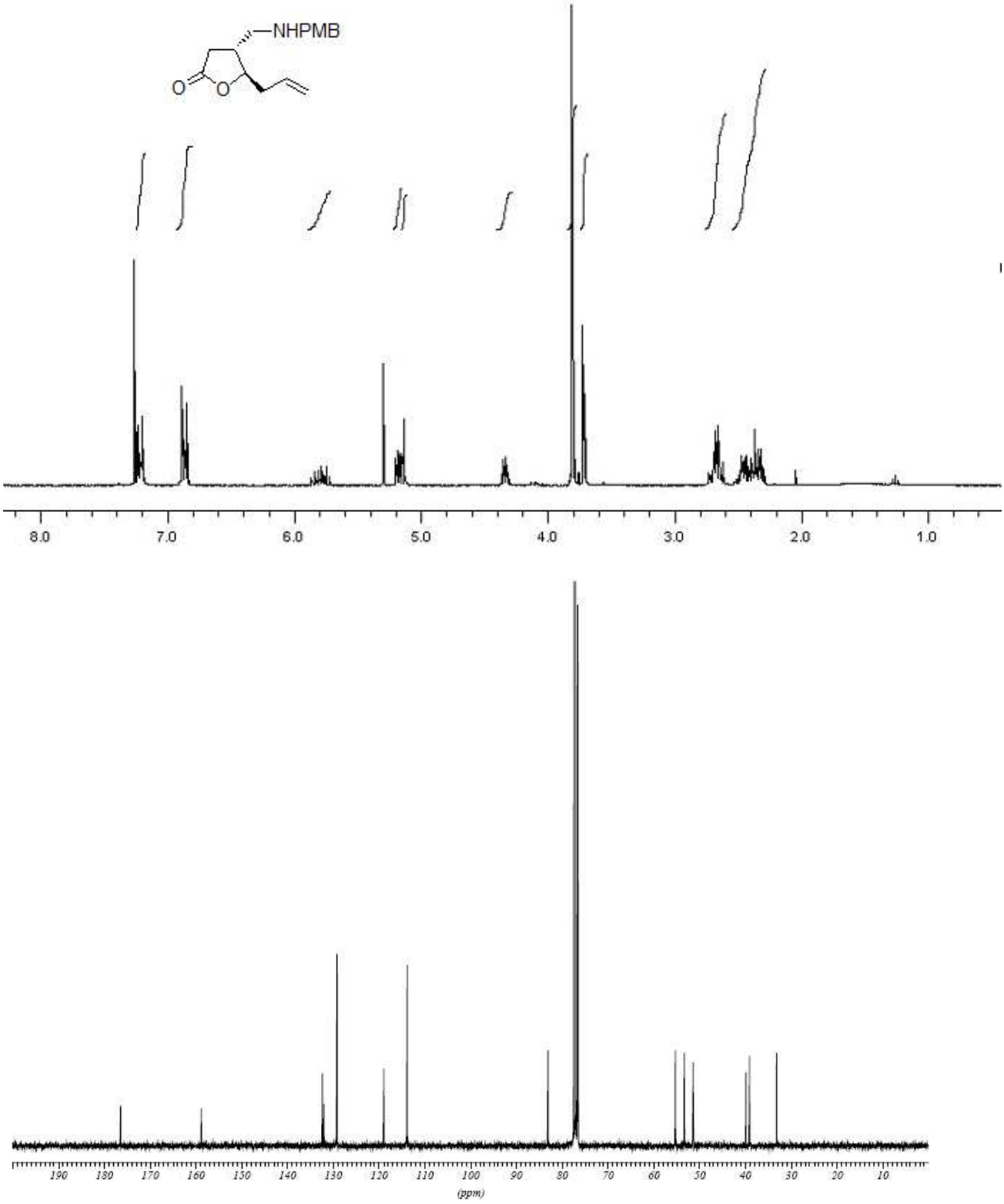

4R, 1'R)-4-(1-Hydroxy-but-3-enyl)-1-(4-methoxy-benzyl)-pyrrolidin-2-one 253

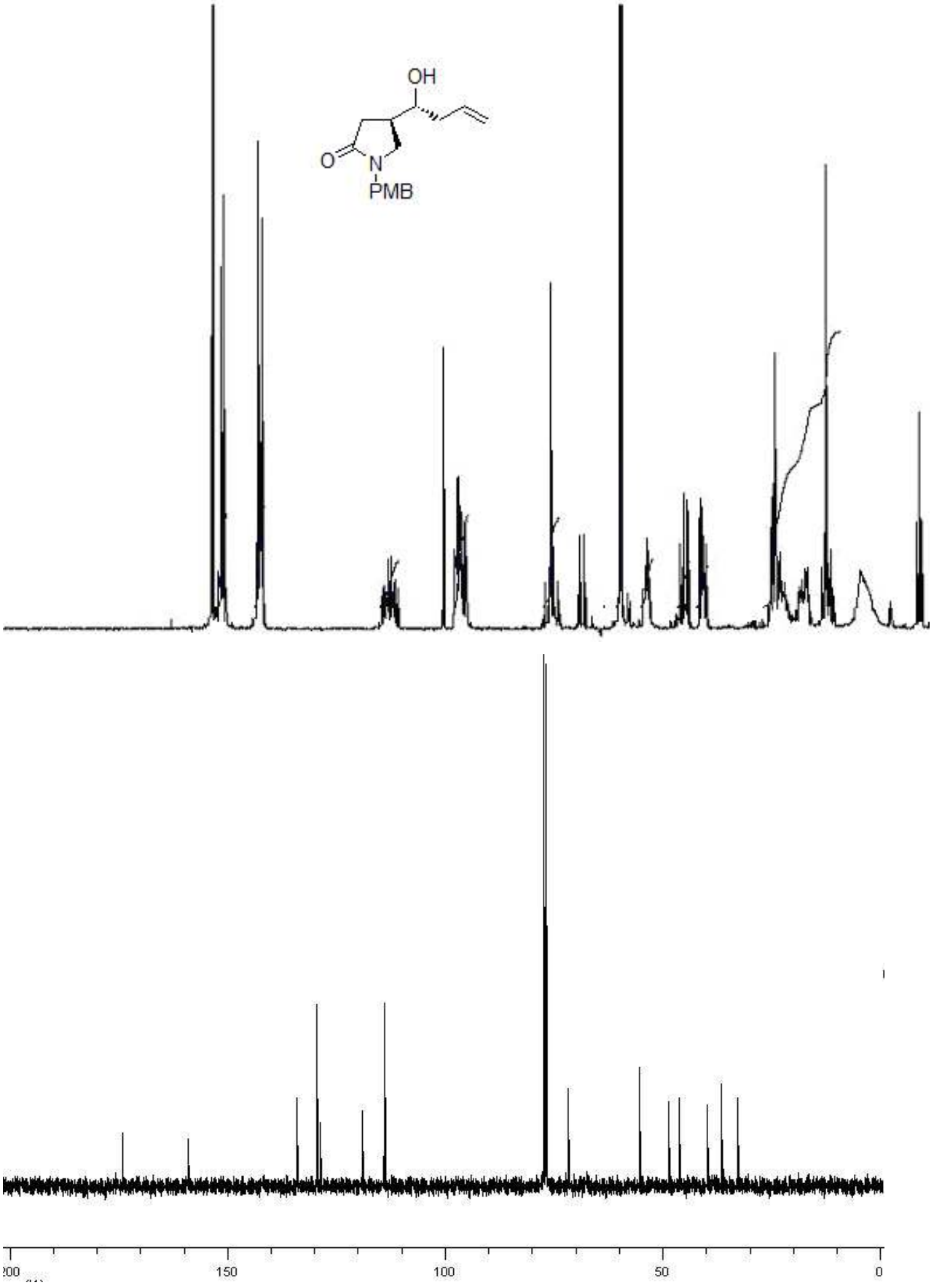

(2R,3R)-(2-Allyl-5-oxo-tetrahydro-furan-3-ylmethyl)-(4-methoxy-benzyl)-carbamic acid tert-butyl ester 254

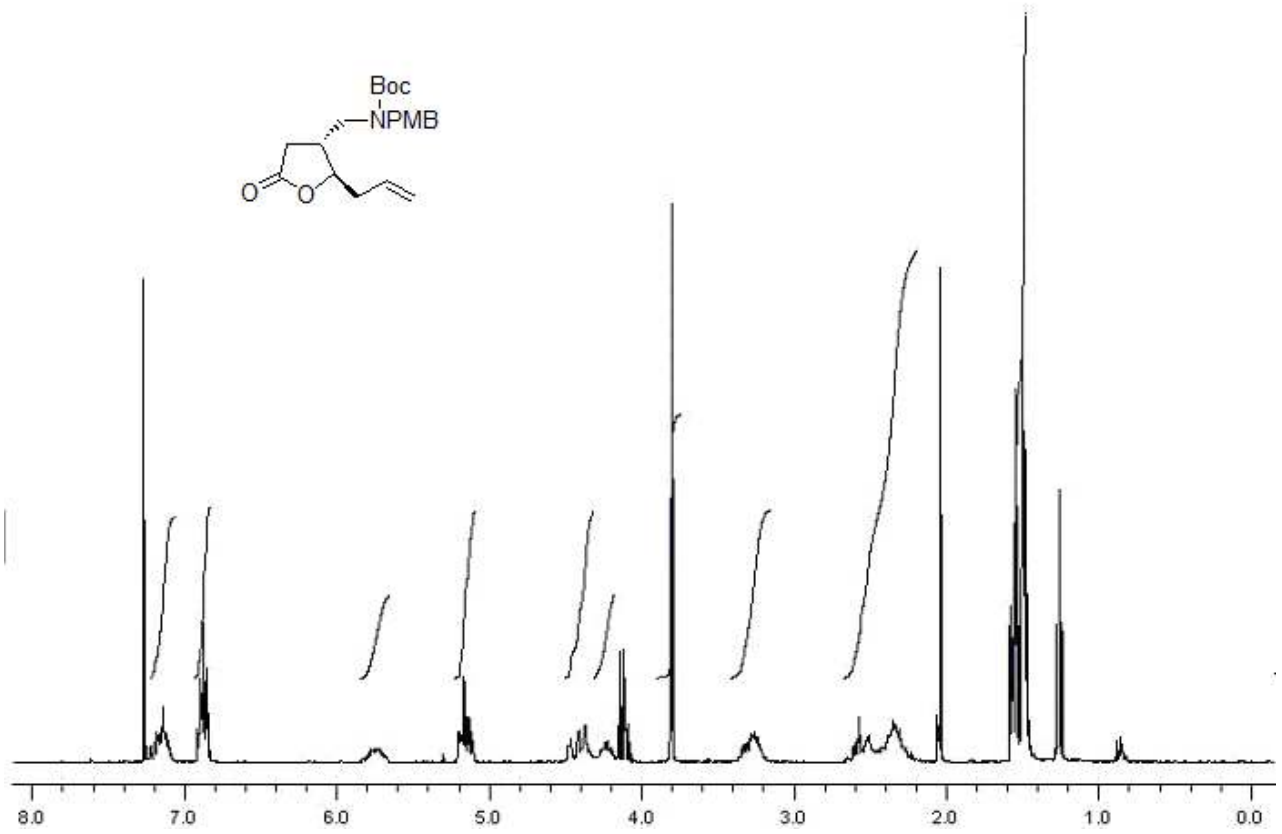

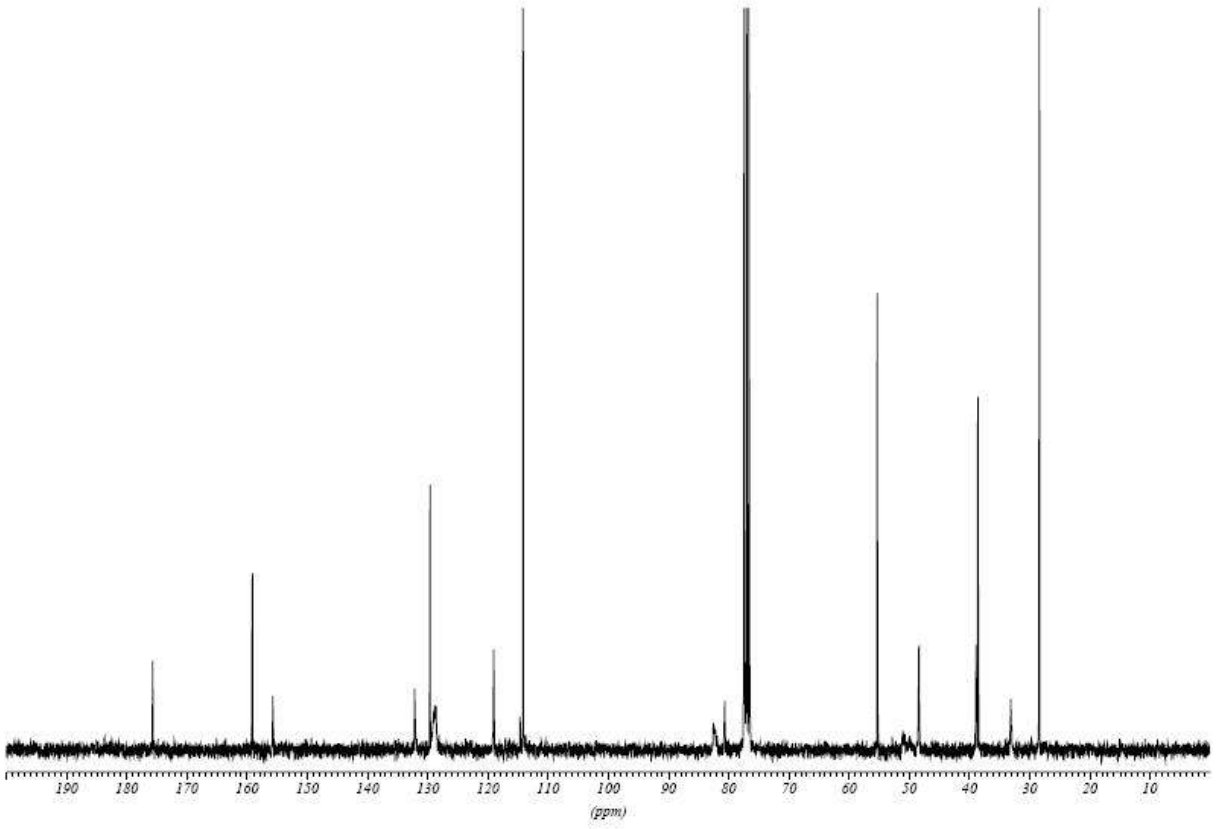

(2R,3R)-(2-Allyl-5-oxo-tetrahydro-furan-3-ylmethyl)-carbamic acid tert-butyl ester 255

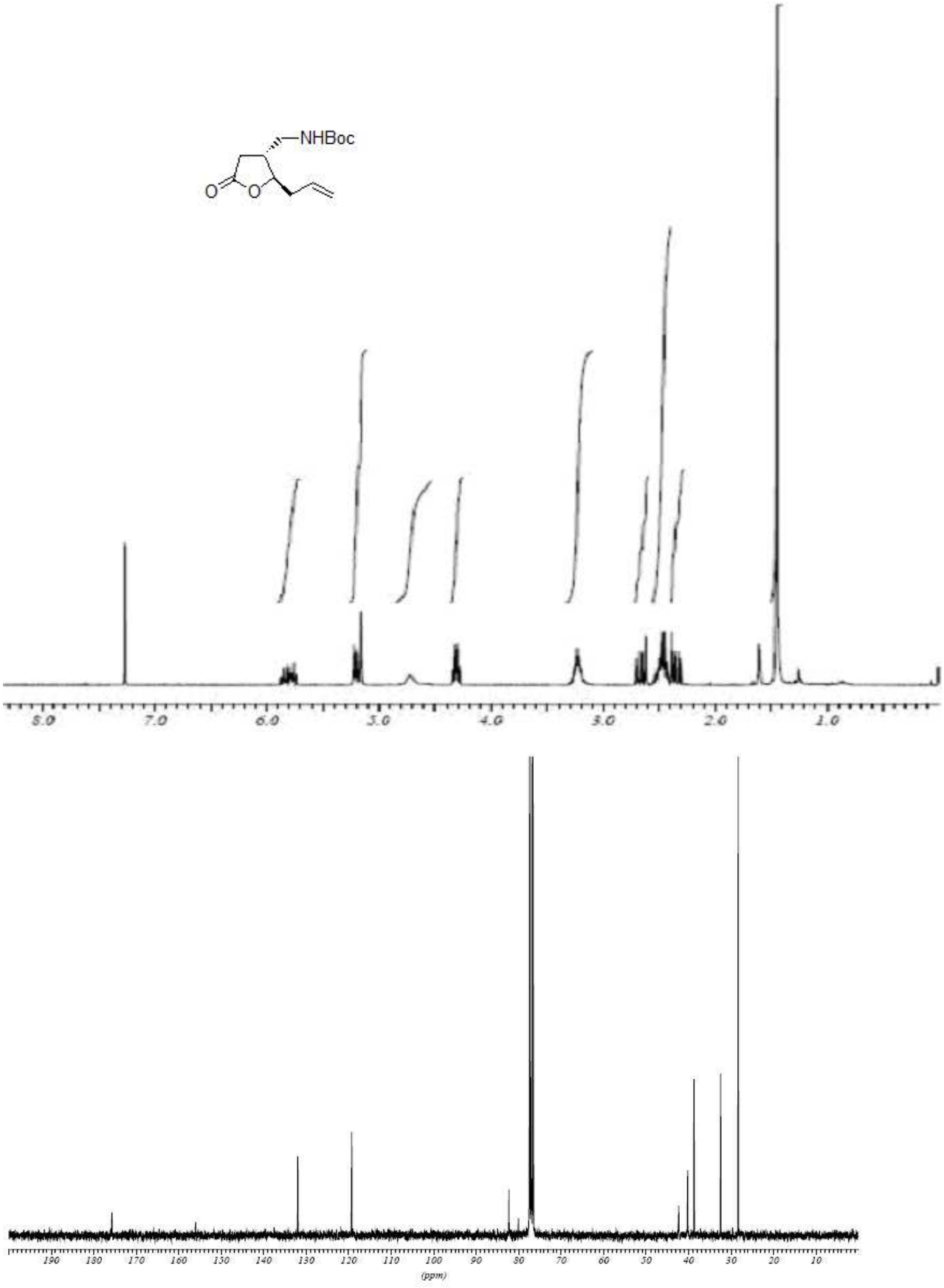

(2R,3R)-[3-(tert-Butoxycarbonylamino-methyl)-5-oxo-tetrahydro-furan-2-yl]-acetic acid 256 or (+)-GBA

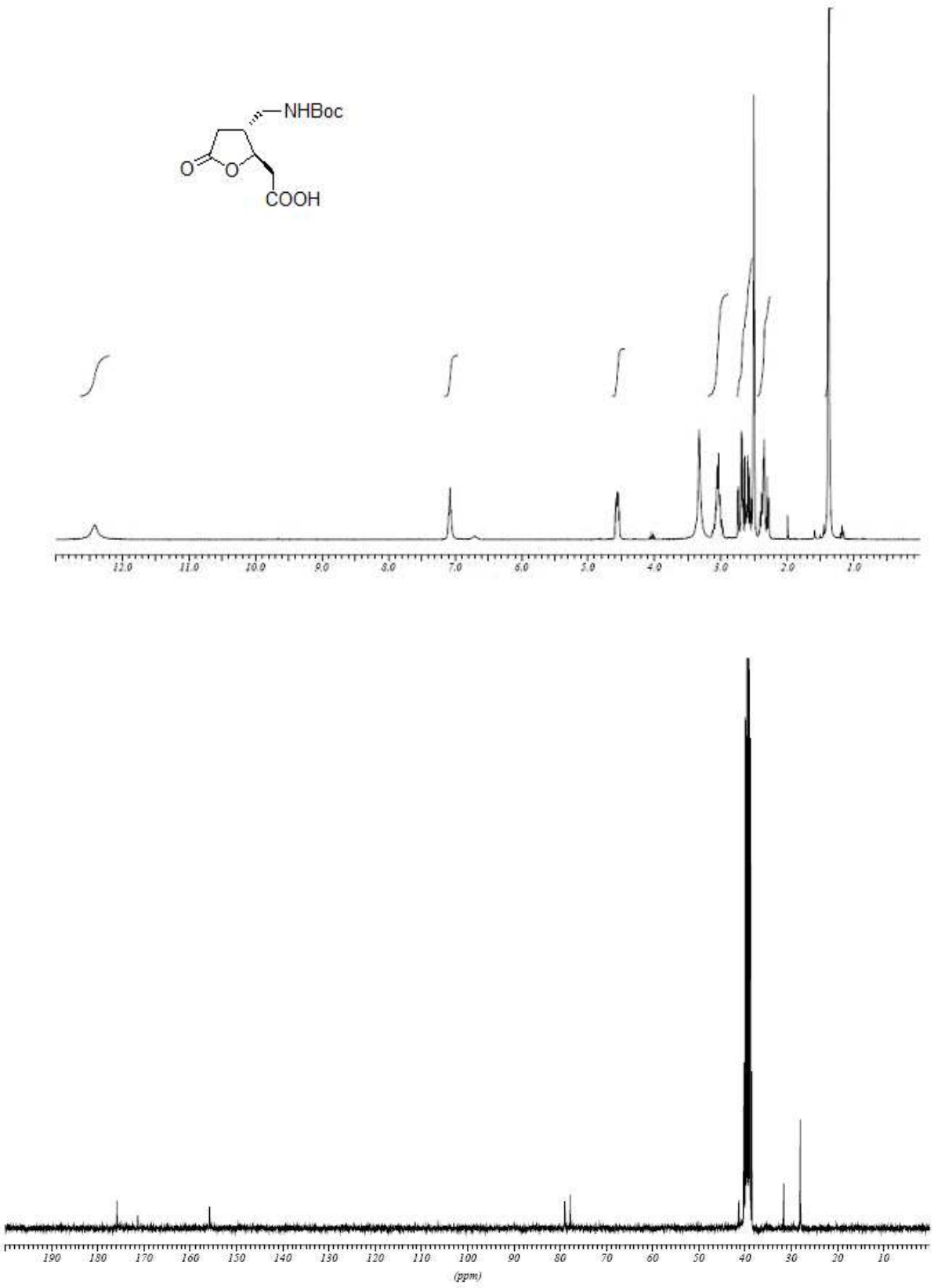

Boc-(+)-GBA-L-Phe-COOBn 258

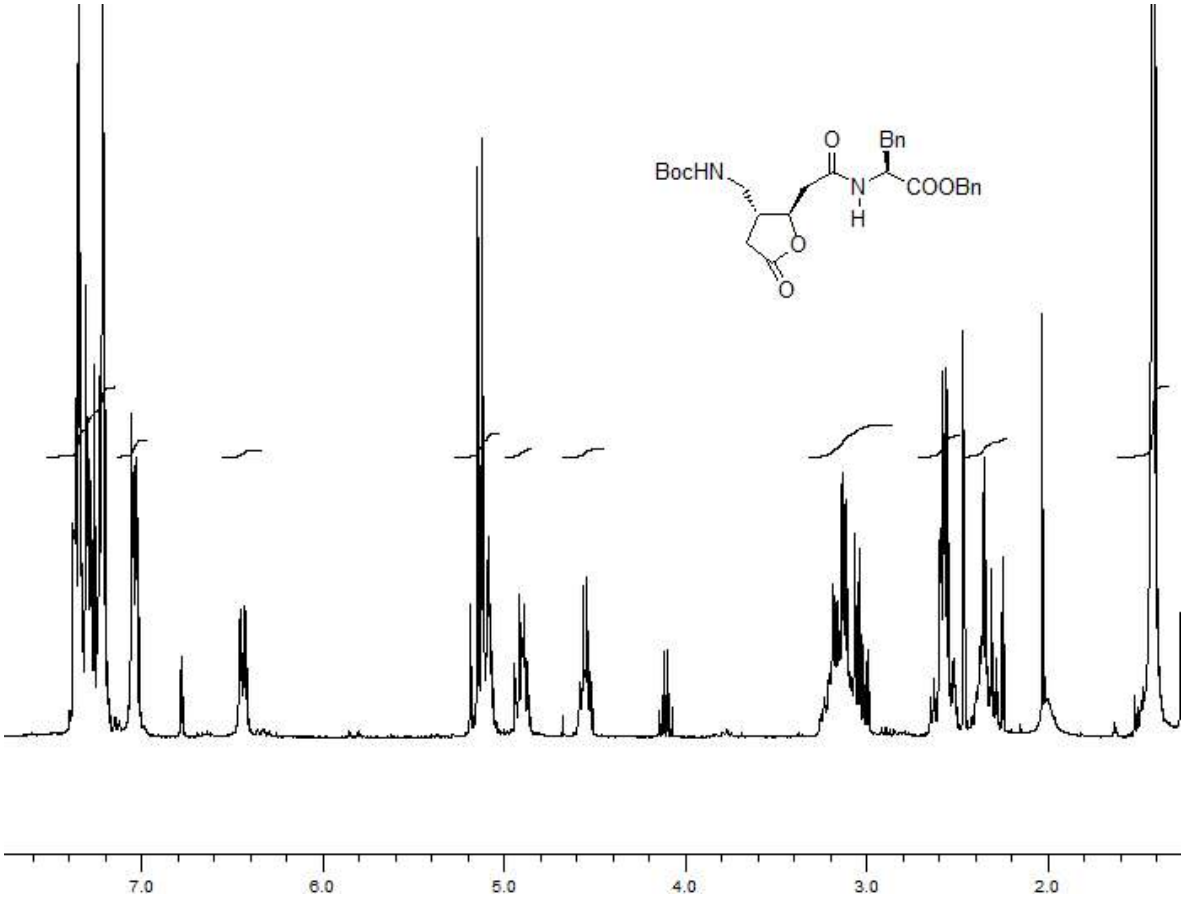

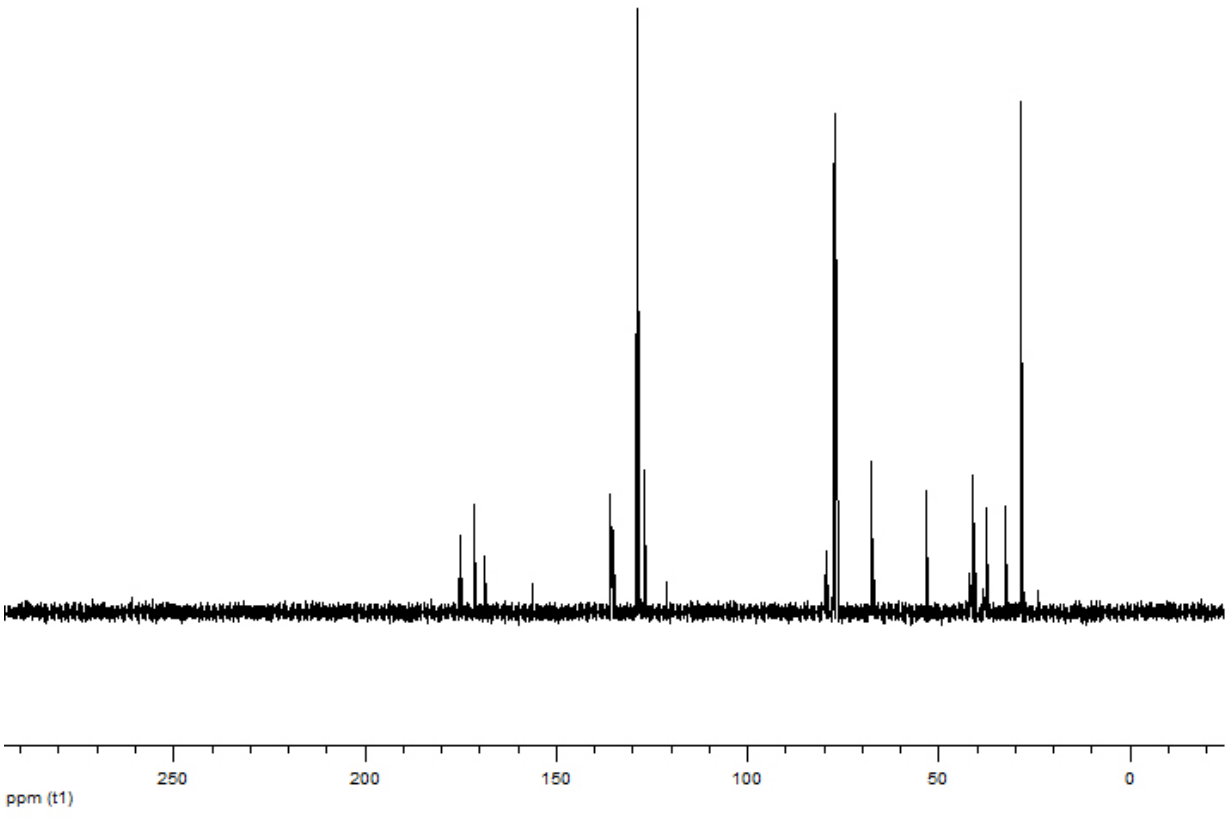

Boc-(L)-Phe-(+)-GBA-(L)-Phe-COOBn 259

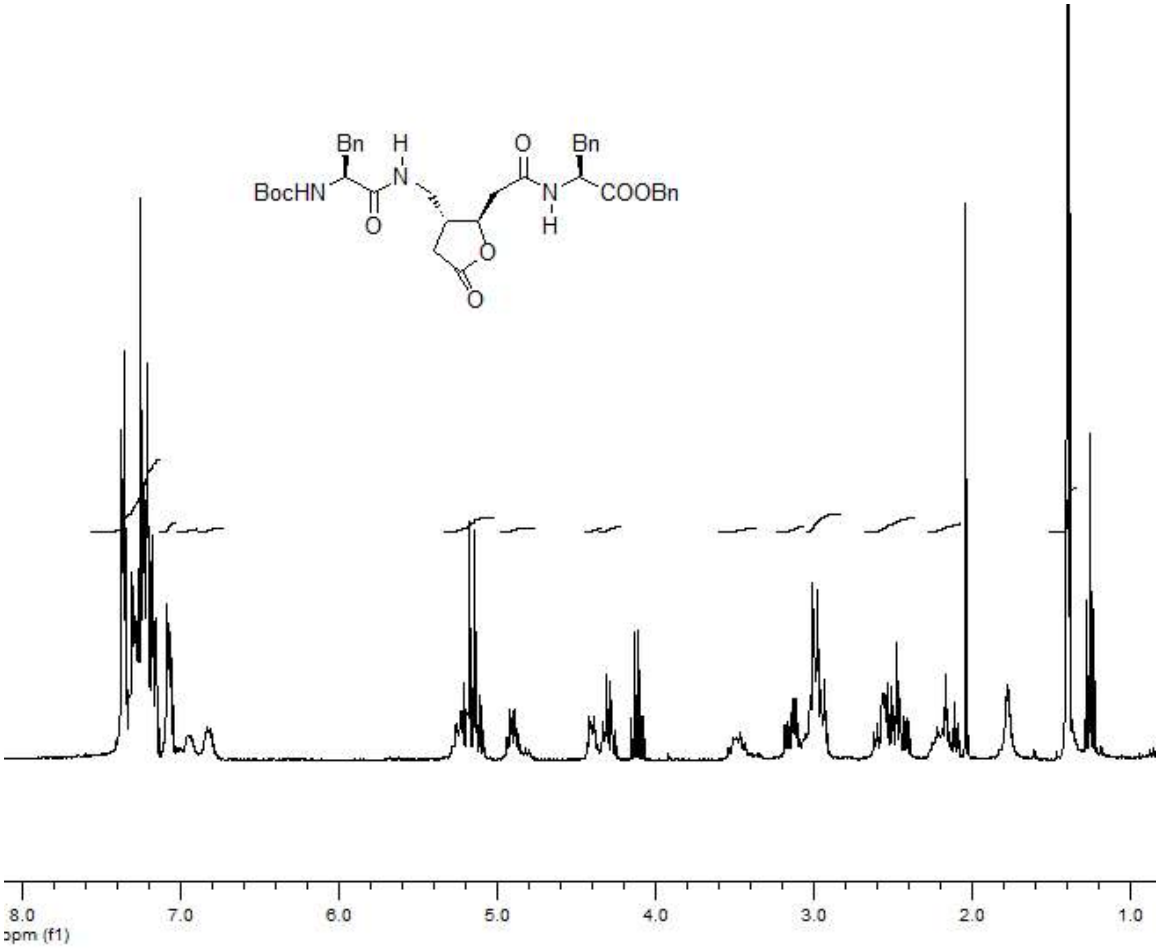

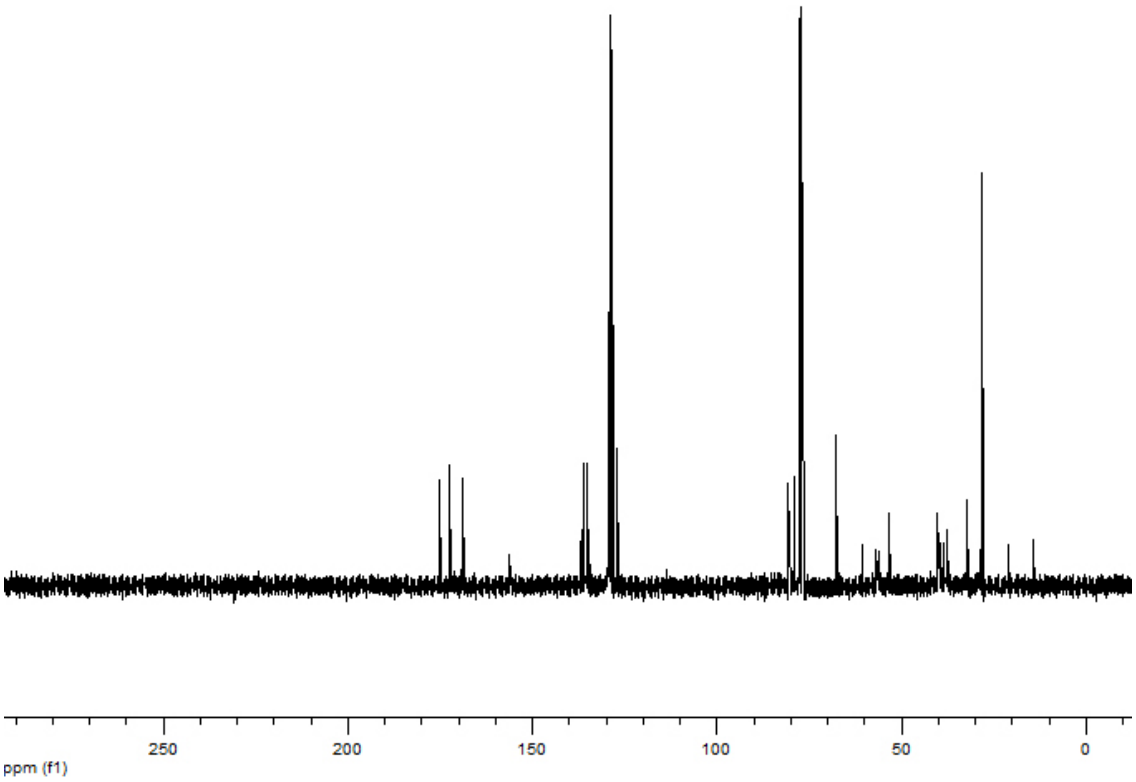

Boc-(+)-GBA-(L)-Phe-(+)-GBA-(L)-Phe-COOBn 260

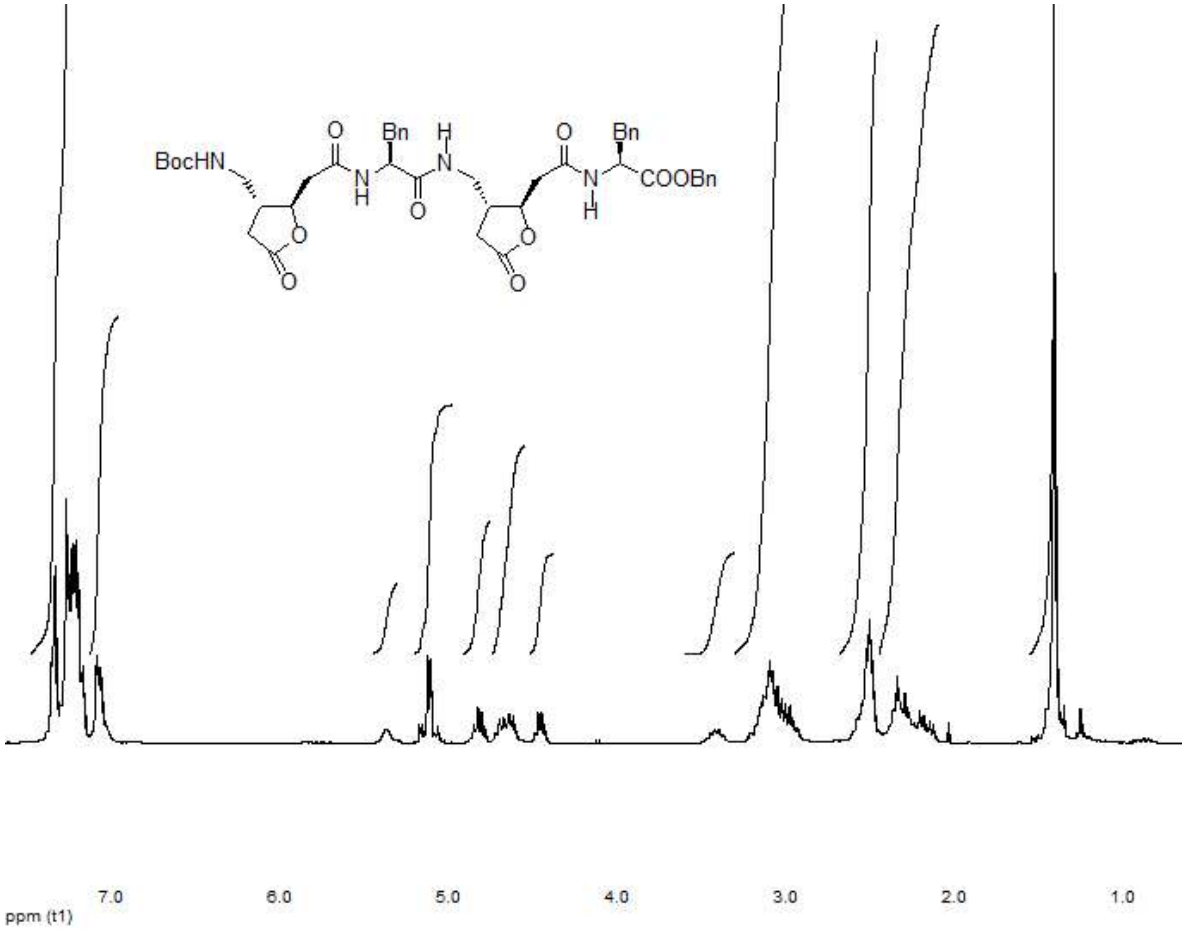

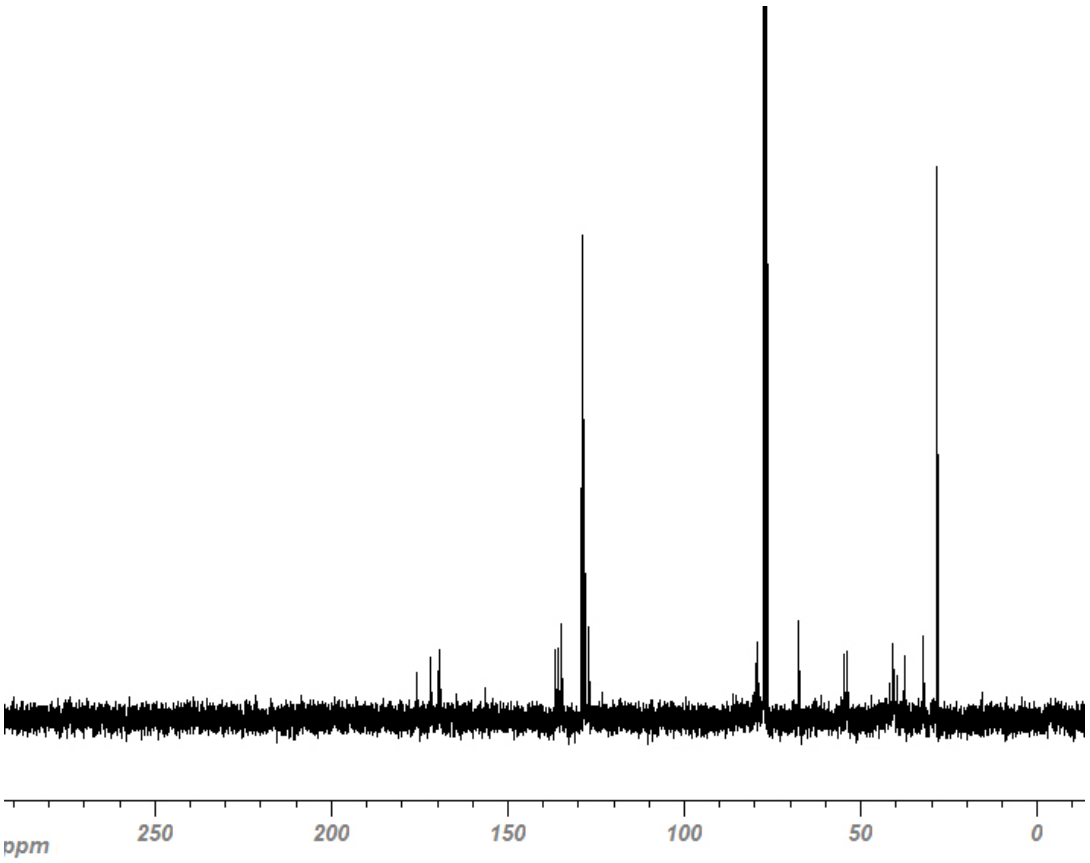

Boc-(L)-Phe-(+)-GBA-(L)-Phe-(+)-GBA-(L)-Phe-COOBn 261

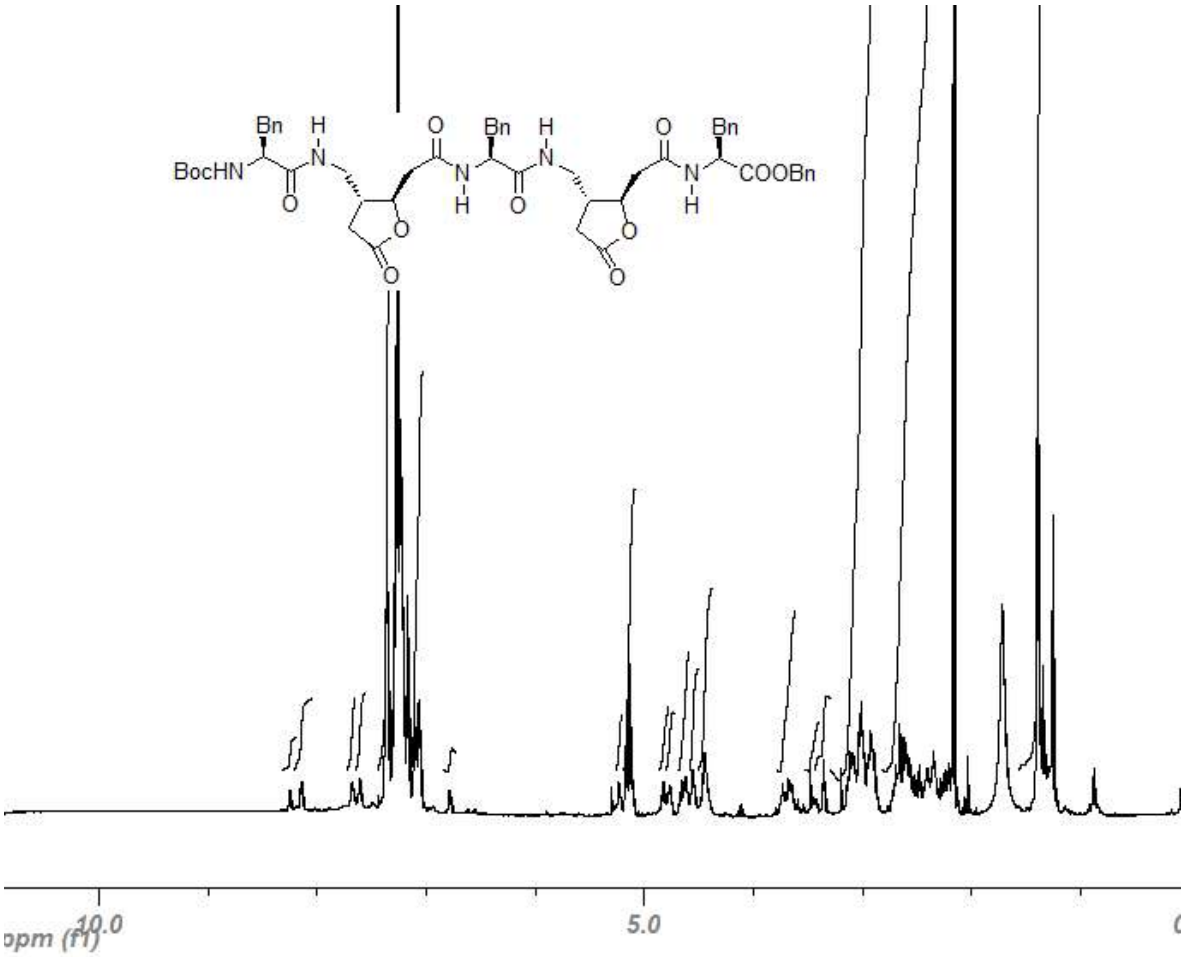

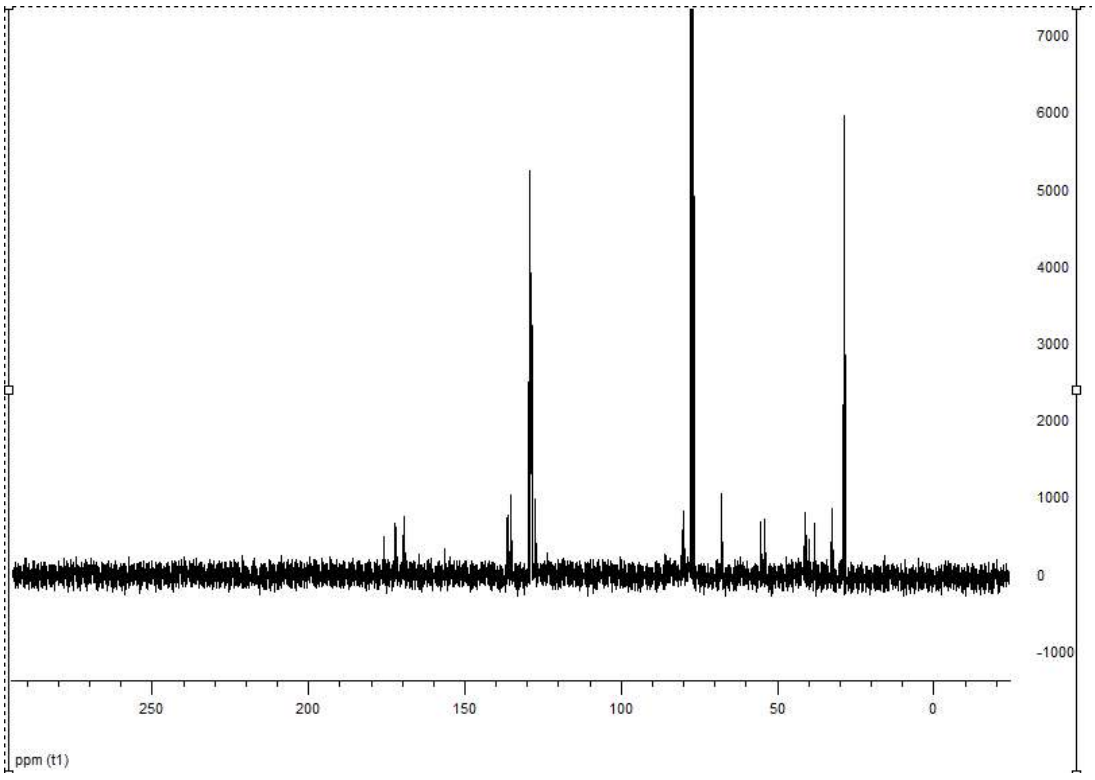

Boc-(+)-GBA-(L)-Phe-(+)-GBA-(L)-Phe-(L)-Phe-(+)-GBA -COOBn 262

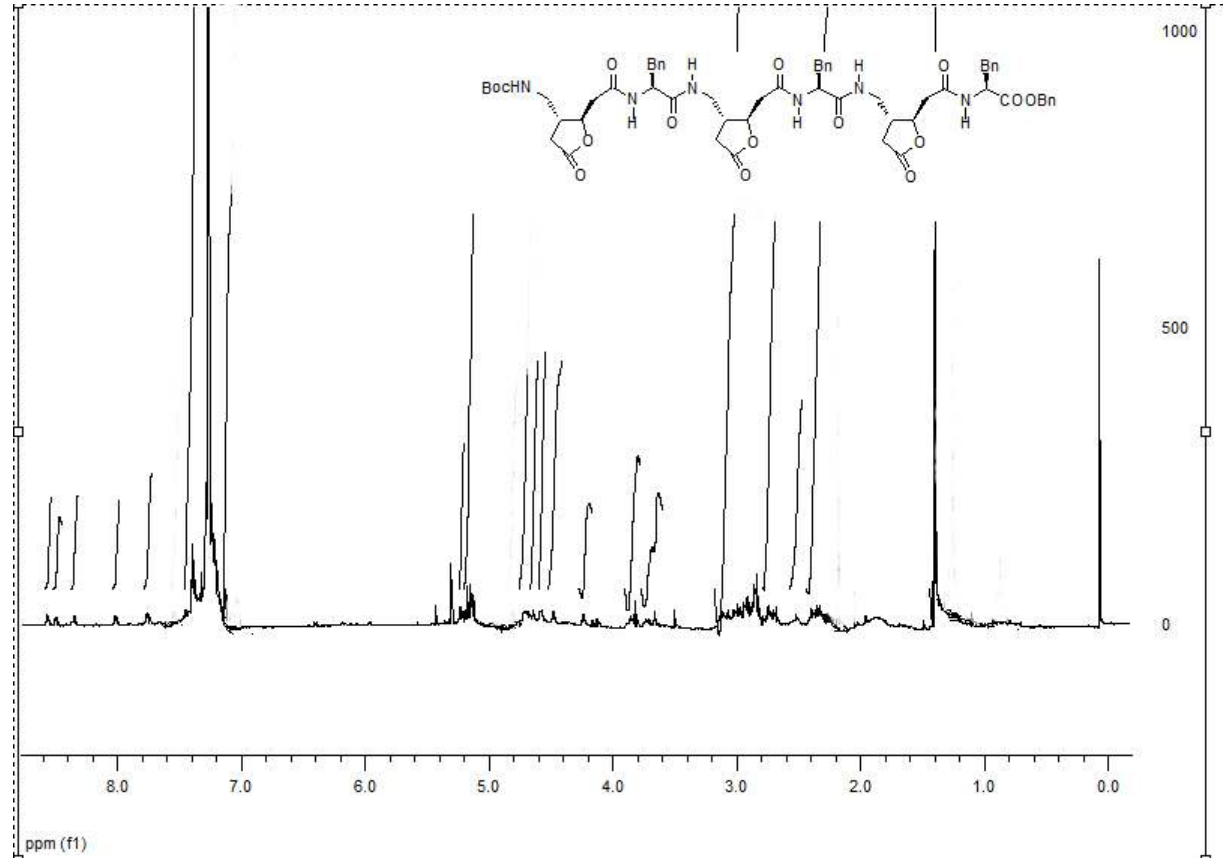

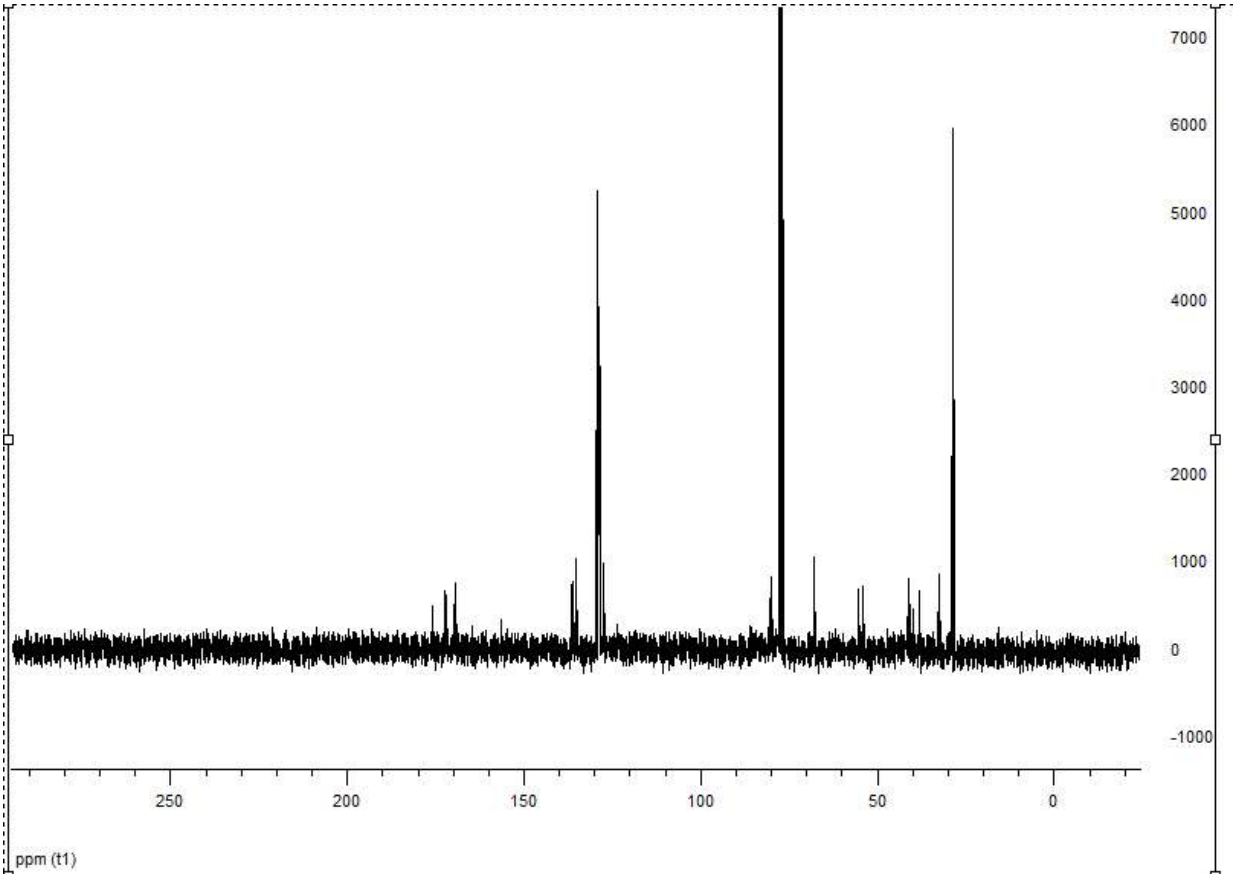

Boc-(L)-Phe-(+)-GBA-(L)-Phe-(+)-GBA-(L)-Phe-(+)-GBA-(L)-Phe-(+)-COOBn 263

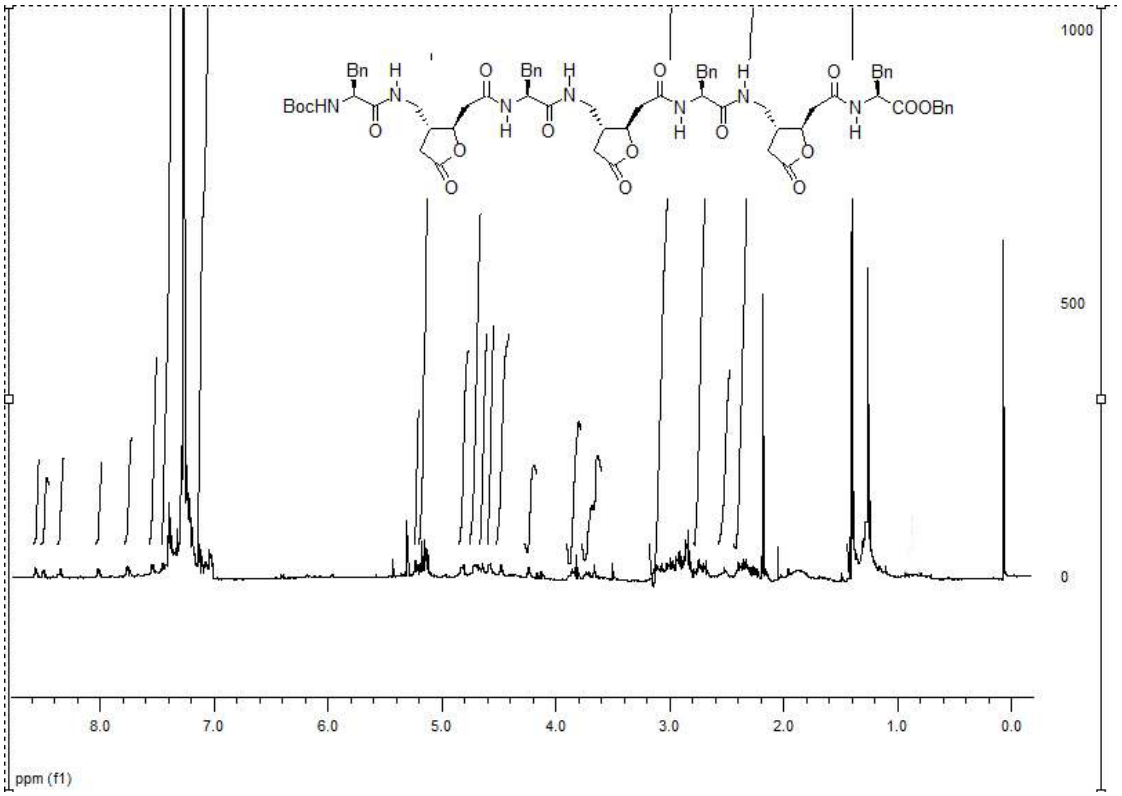

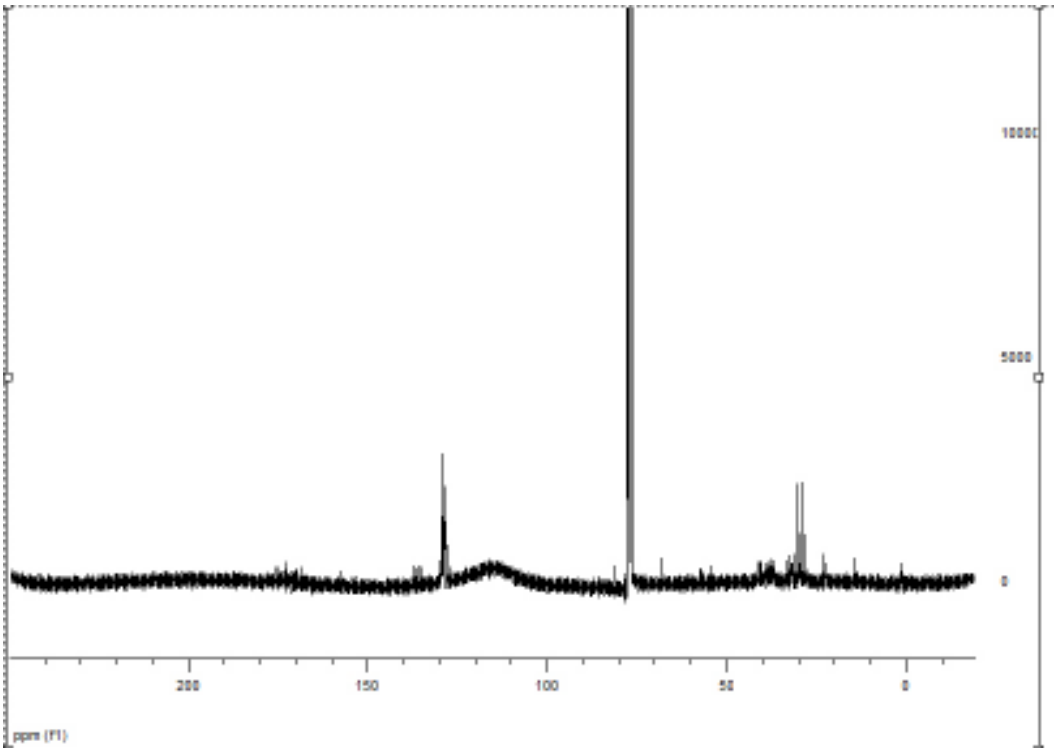

(2R,3R)-(2-Allyl-5-oxo-tetrahydro-furan-3-ylmethyl)-(4-methoxy-benzyl)-carbamic acid 9H-fluoren-9-ylmethyl ester 264

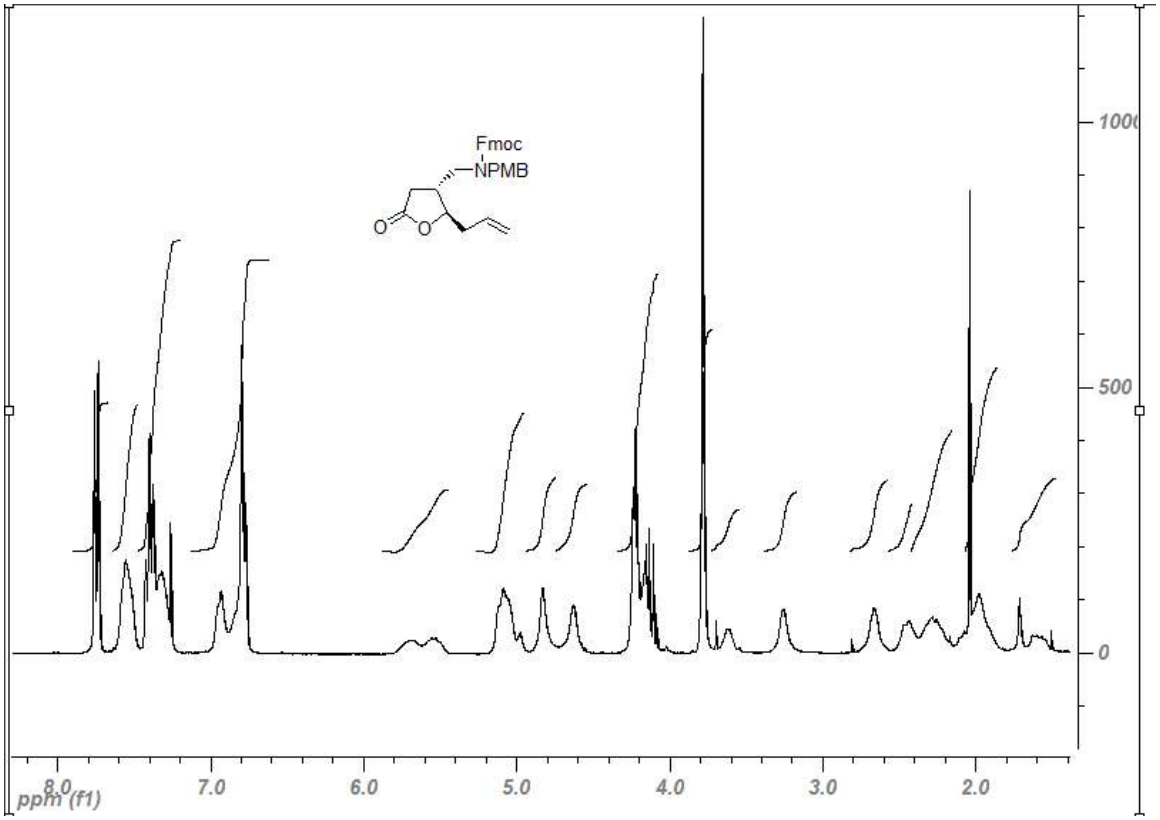

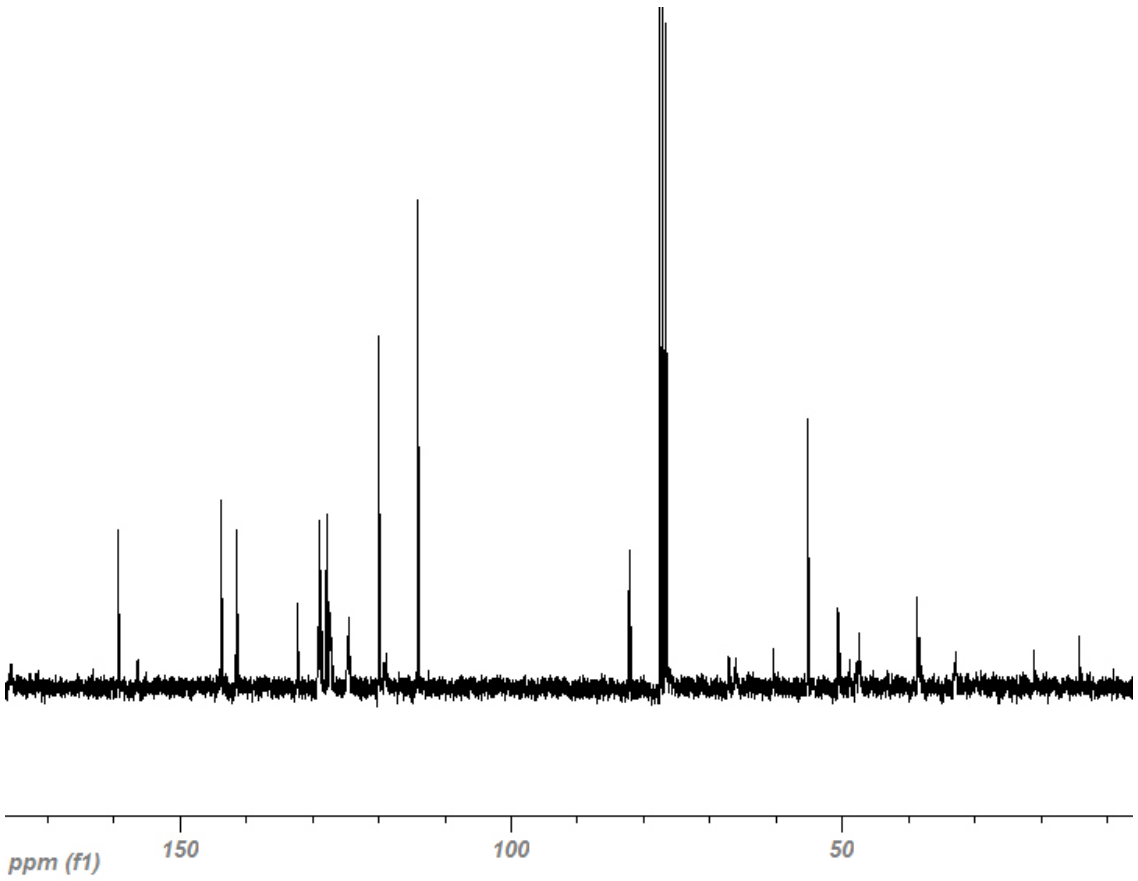

(4R,5R)- Acetic acid 5-allyl-4-v-tetrahydro-furan-2-yl ester 265

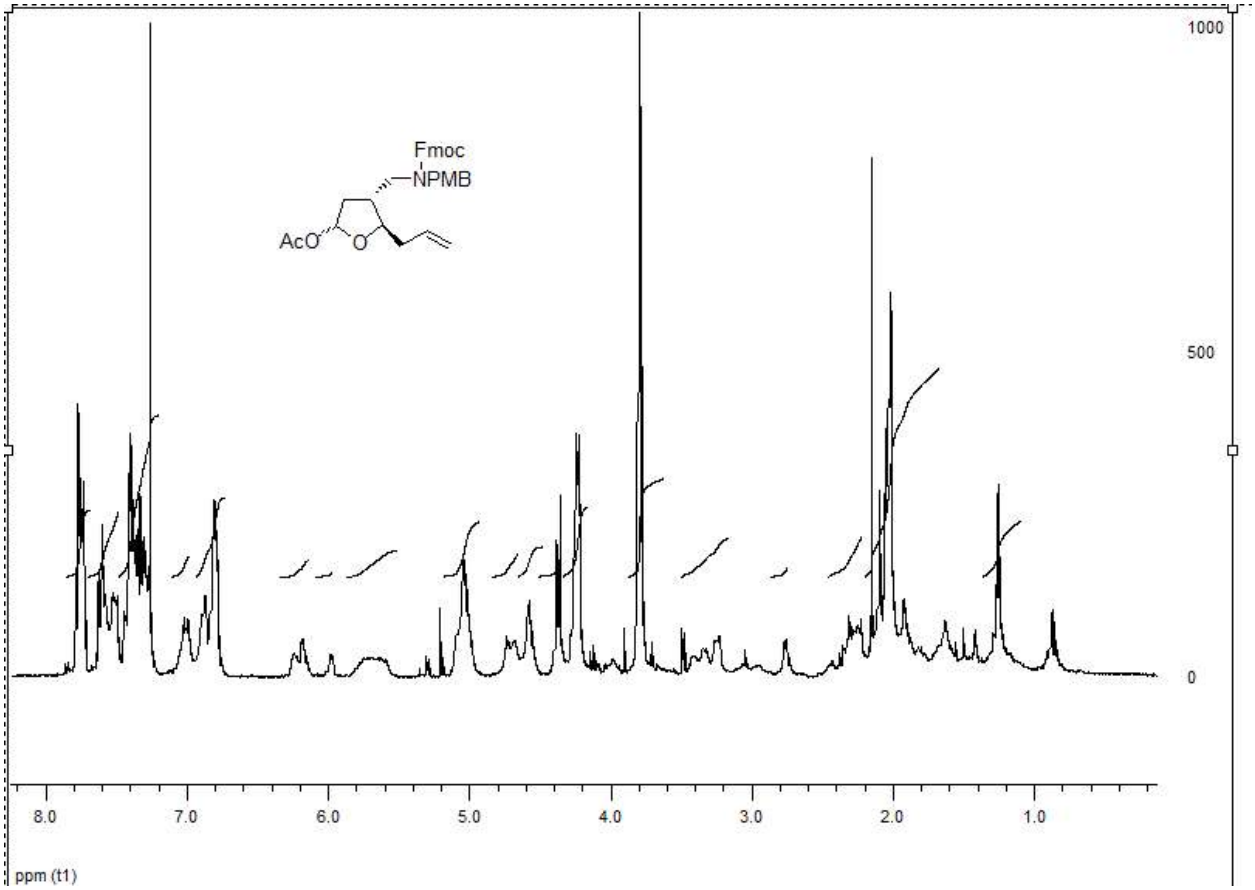

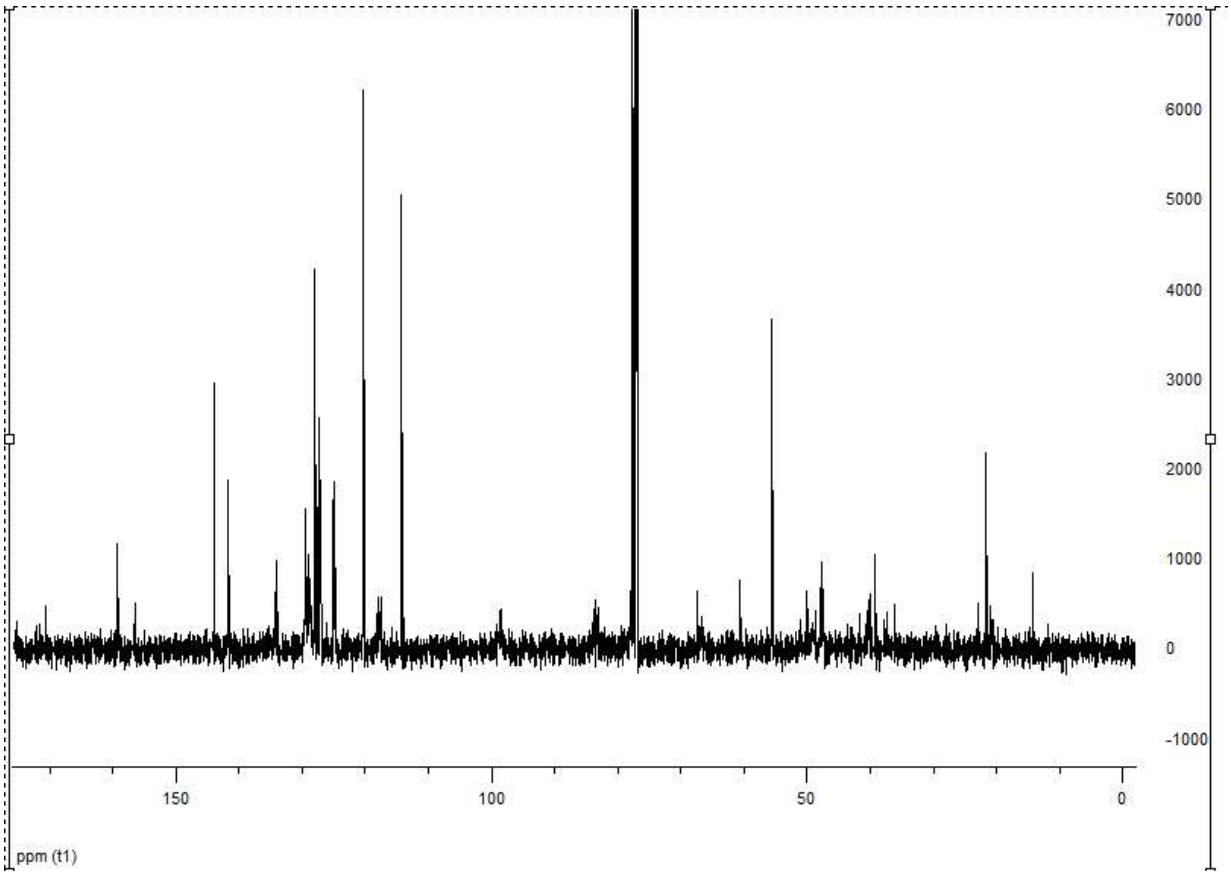

(4R,5R)-[2-Allyl-5-(5-methyl-2,4-dioxo-3,4-dihydro-2H-pyrimidin-1-yl)-tetrahydro-furan-3-ylmethyl]- (4-methoxy-benzyl)-carbamic acid 9H-fluoren-9-ylmethyl ester 266

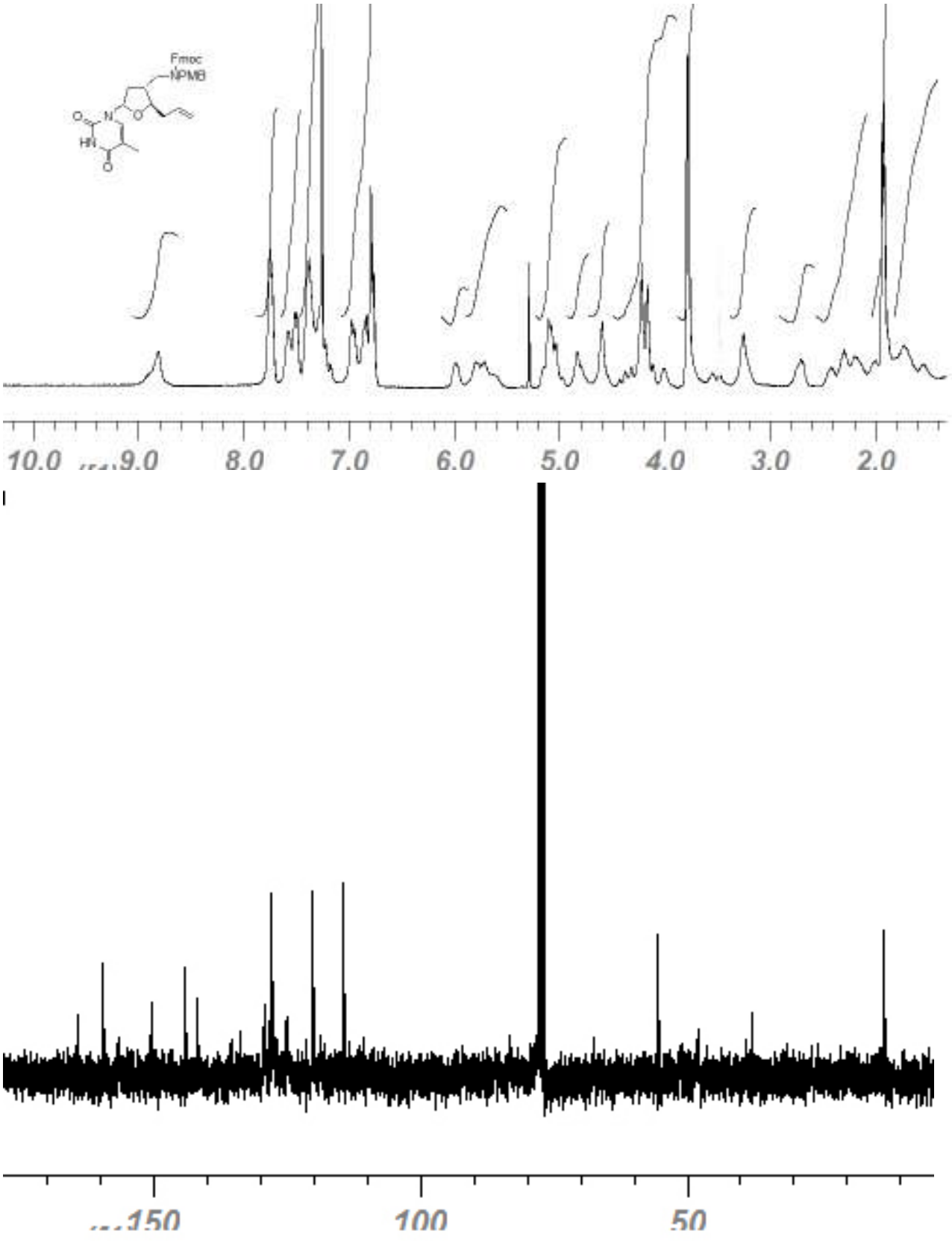

(2R, 4R, 5R)-[2-Allyl-5-(5-methyl-2,4-dioxo-3,4-dihydro-2H-pyrimidin-1-yl)-tetrahydro-furan-3-ylmethyl]-carbamic acid 9H-fluoren-9-ylmethyl ester 267

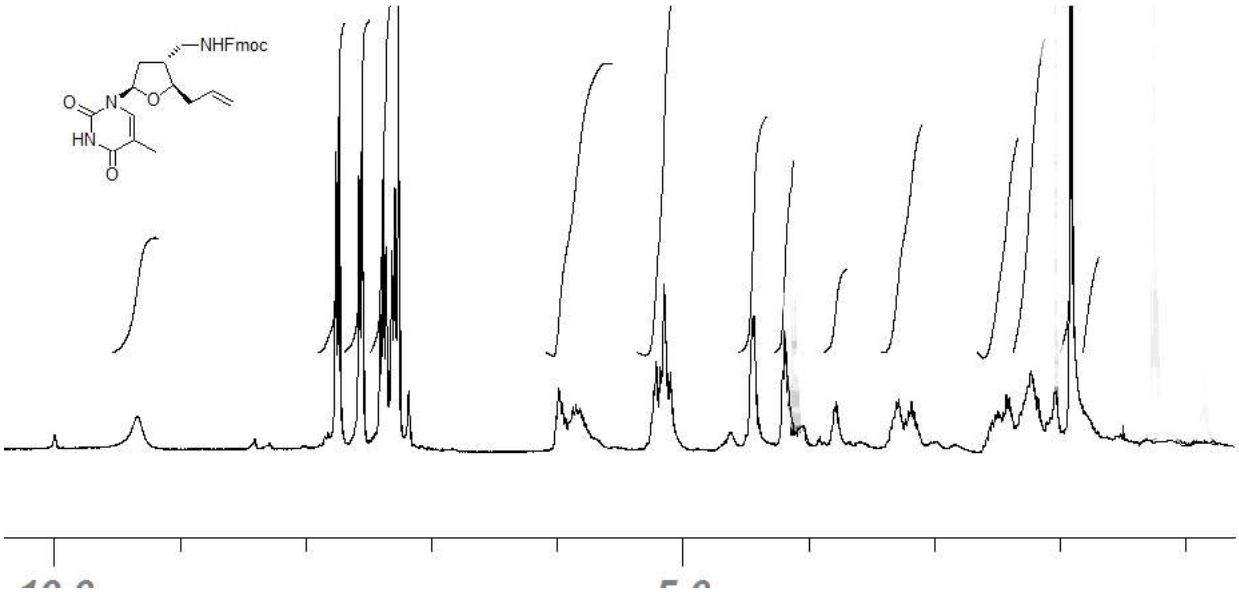

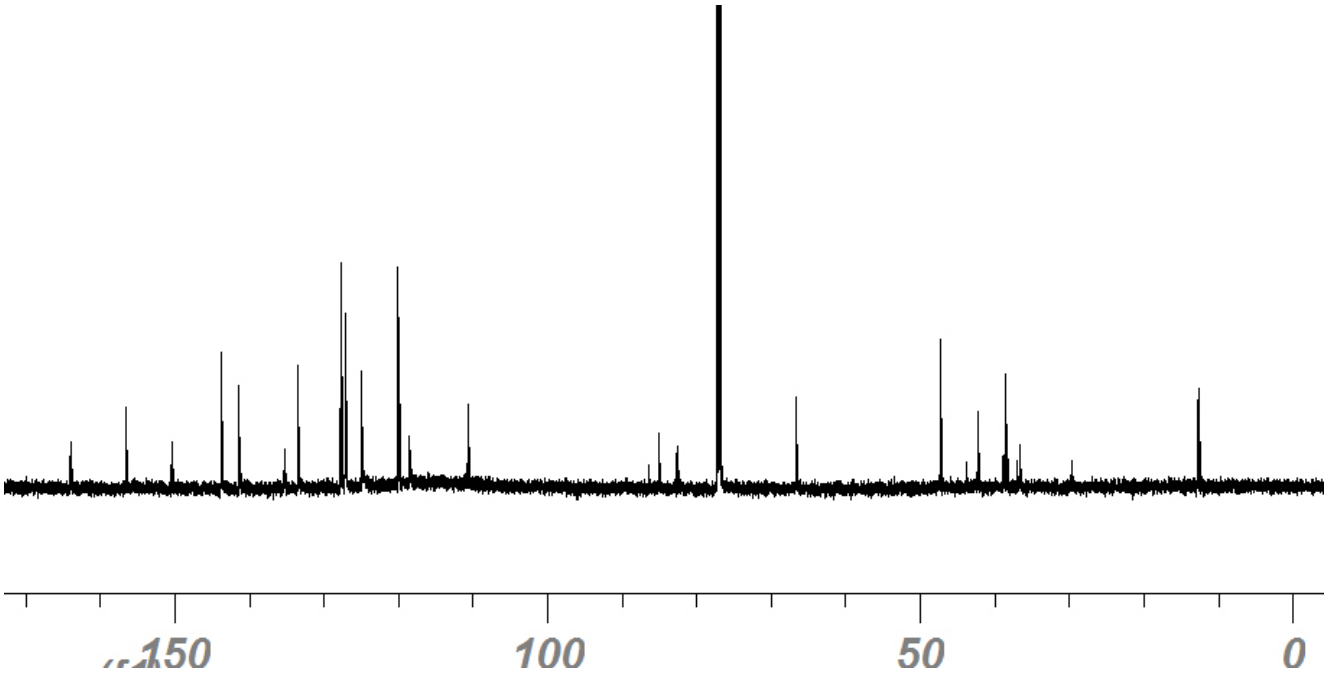

(2S, 4R, 5R)-[2-Allyl-5-(5-methyl-2,4-dioxo-3,4-dihydro-2H-pyrimidin-1-yl)-tetrahydro-furan-3-ylmethyl]-carbamic acid 9H-fluoren-9-ylmethyl ester 268

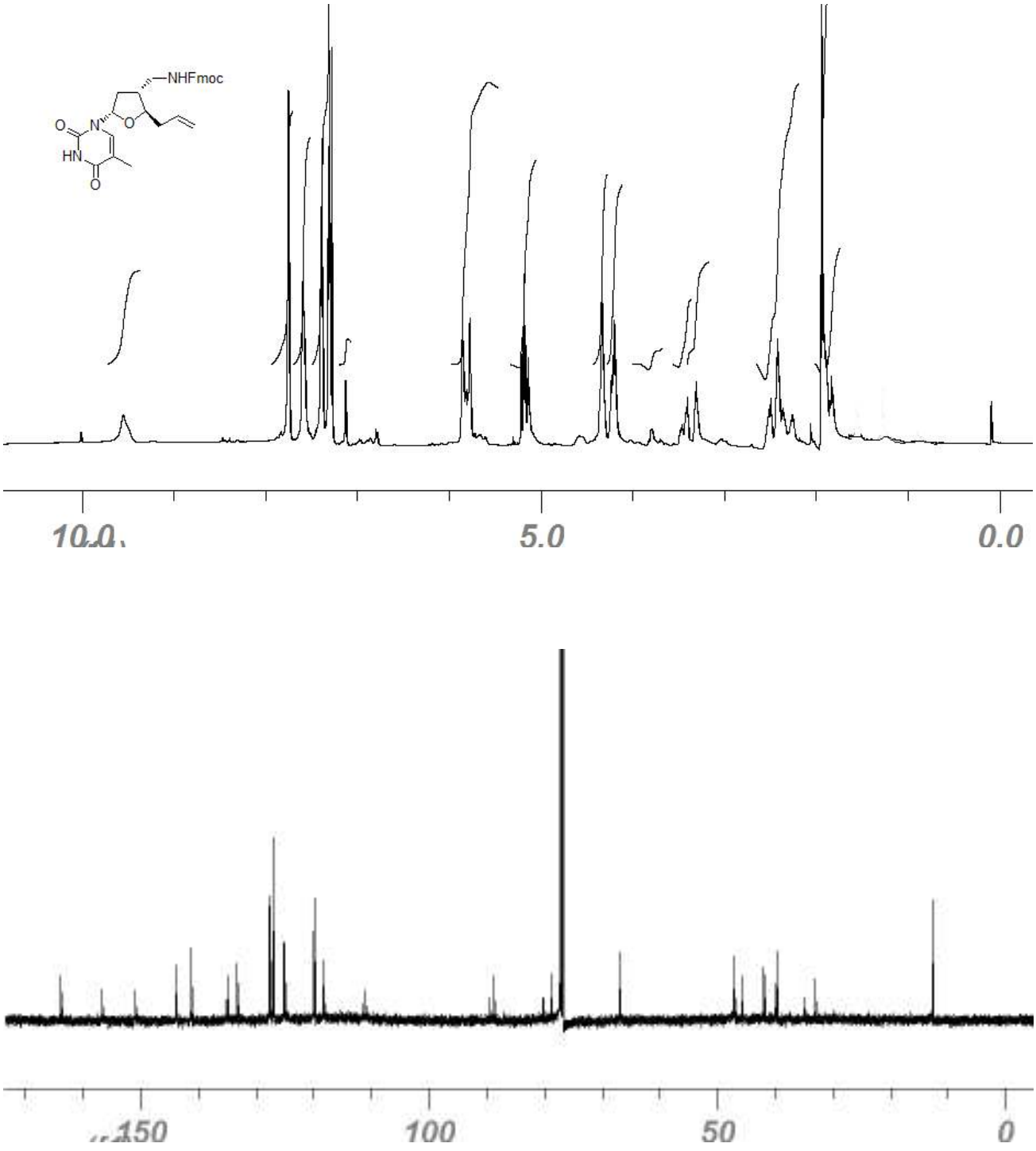

(2R/S,3R,5R)-[2-Allyl-5-(6-amino-purin-9-yl)-tetrahydro-furan-3-ylmethyl]-(4-methoxy-benzyl)-carbamic acid 9H-fluoren-9-ylmethyl ester 270

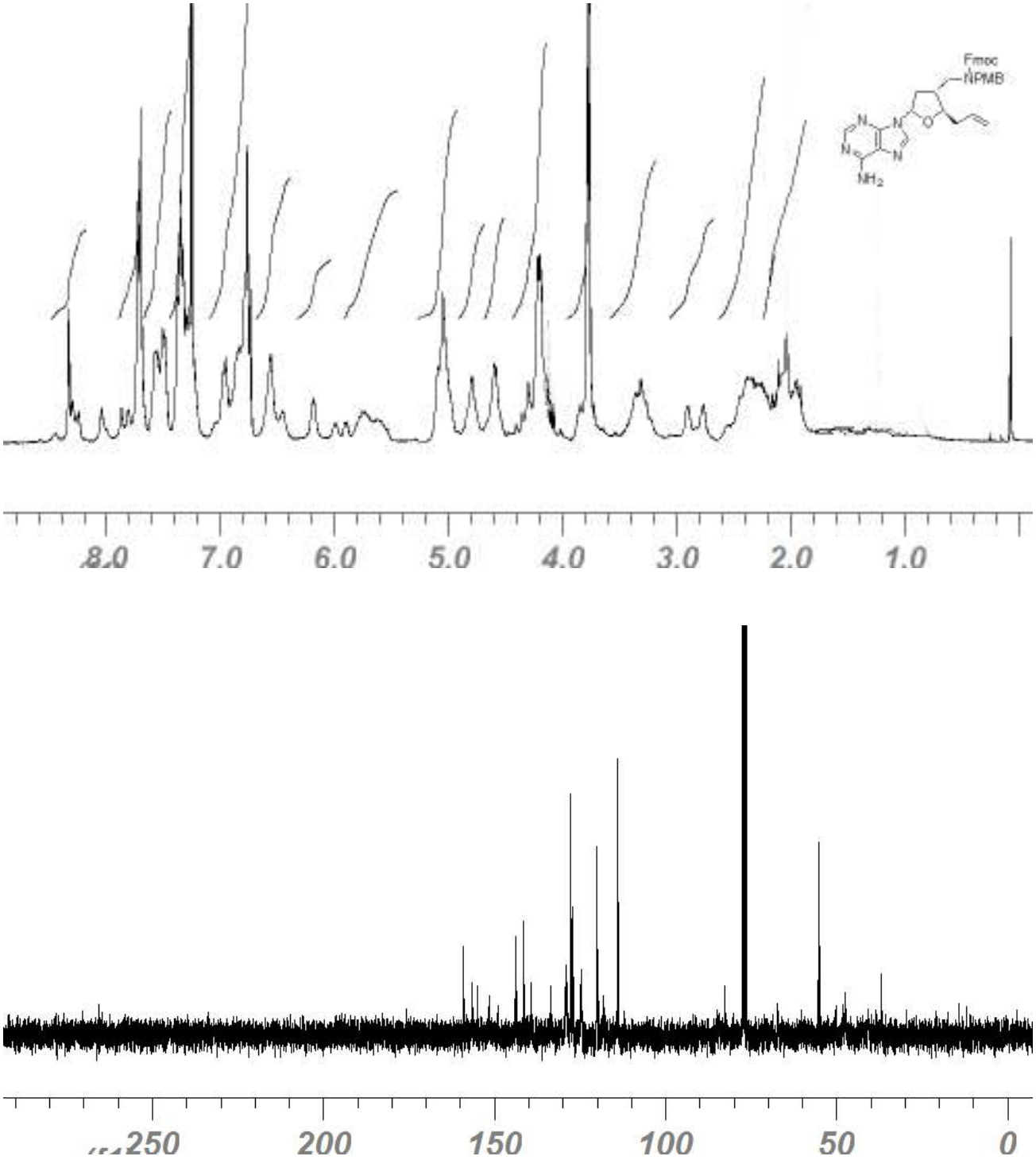

[9-(5-Allyl-4-{[(9H-fluoren-9-ylmethoxycarbonyl)-(4-methoxy-benzyl)-amino]-methyl}-tetrahydro-furan-2-yl)-9H-purin-6-yl]-carbamic acid benzyl ester 271

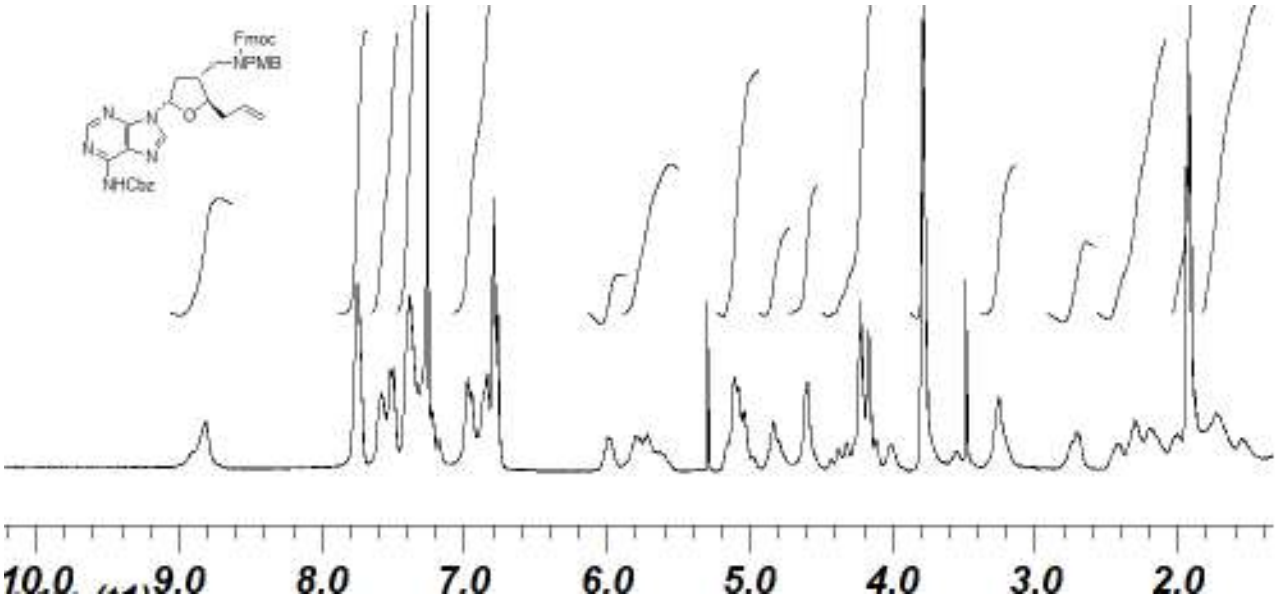

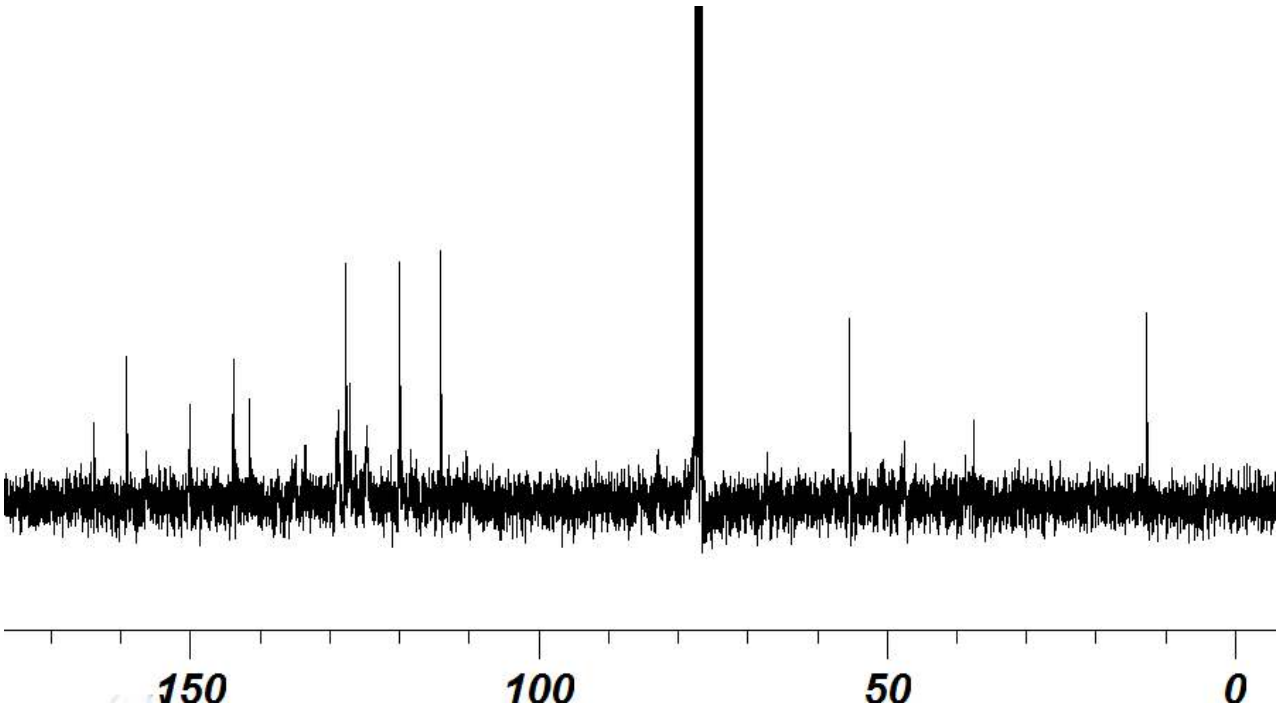

N'-{2,2,2-Trifluoro-1-[(3,4,5-trimethoxy-benzylcarbamoyl)-methyl]-ethyl}-hydrazinecarboxylic acid tert-butyl ester 307

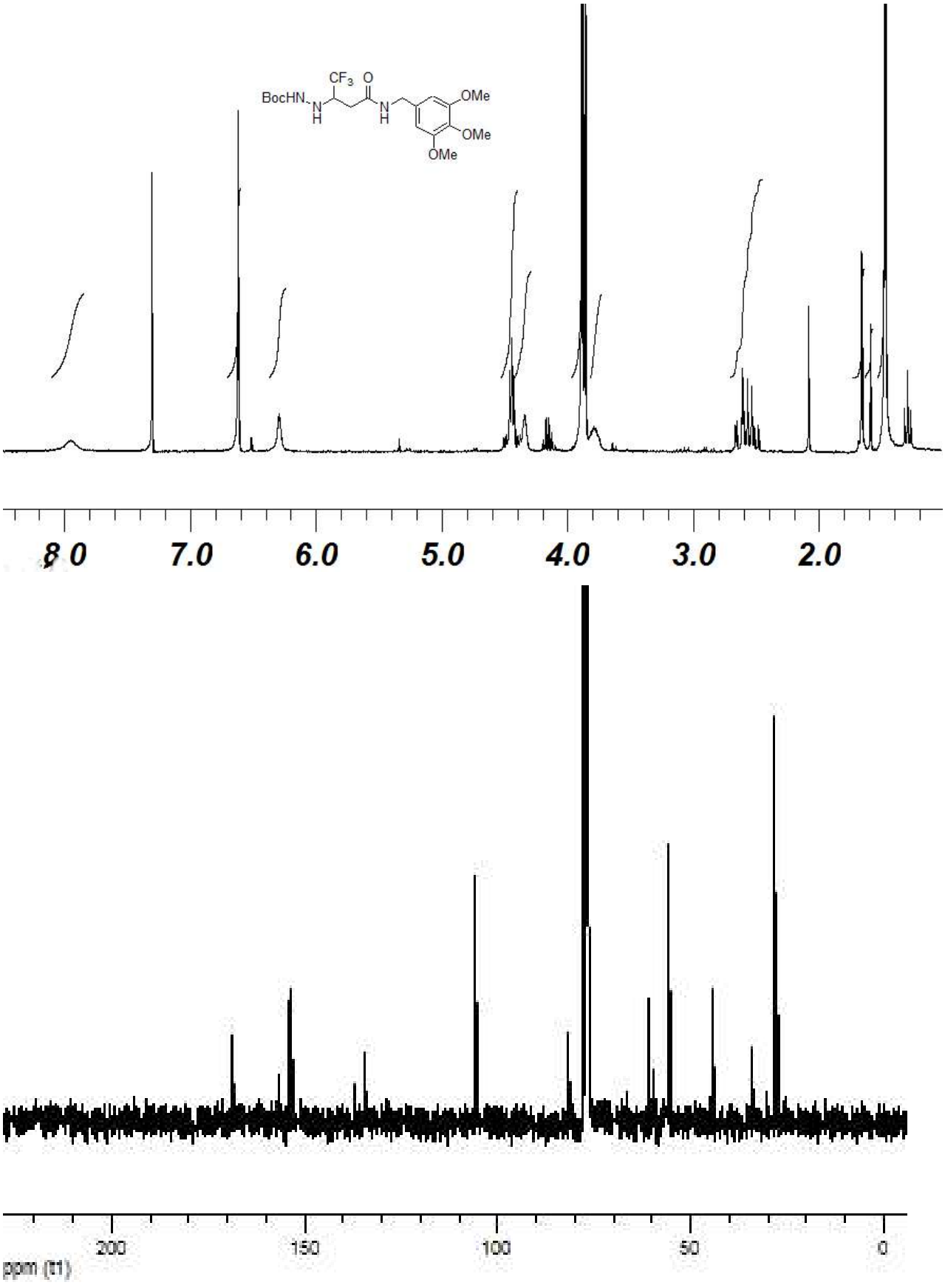

[5-tert-Butoxycarbonylamino-5-(N'-{2,2,2-trifluoro-1-[(3,4,5-trimethoxy-benzylcarbamoyl)-methyl]-ethyl}-hydrazinocarbonyl)-pentyl]-carbamic acid benzyl ester 309

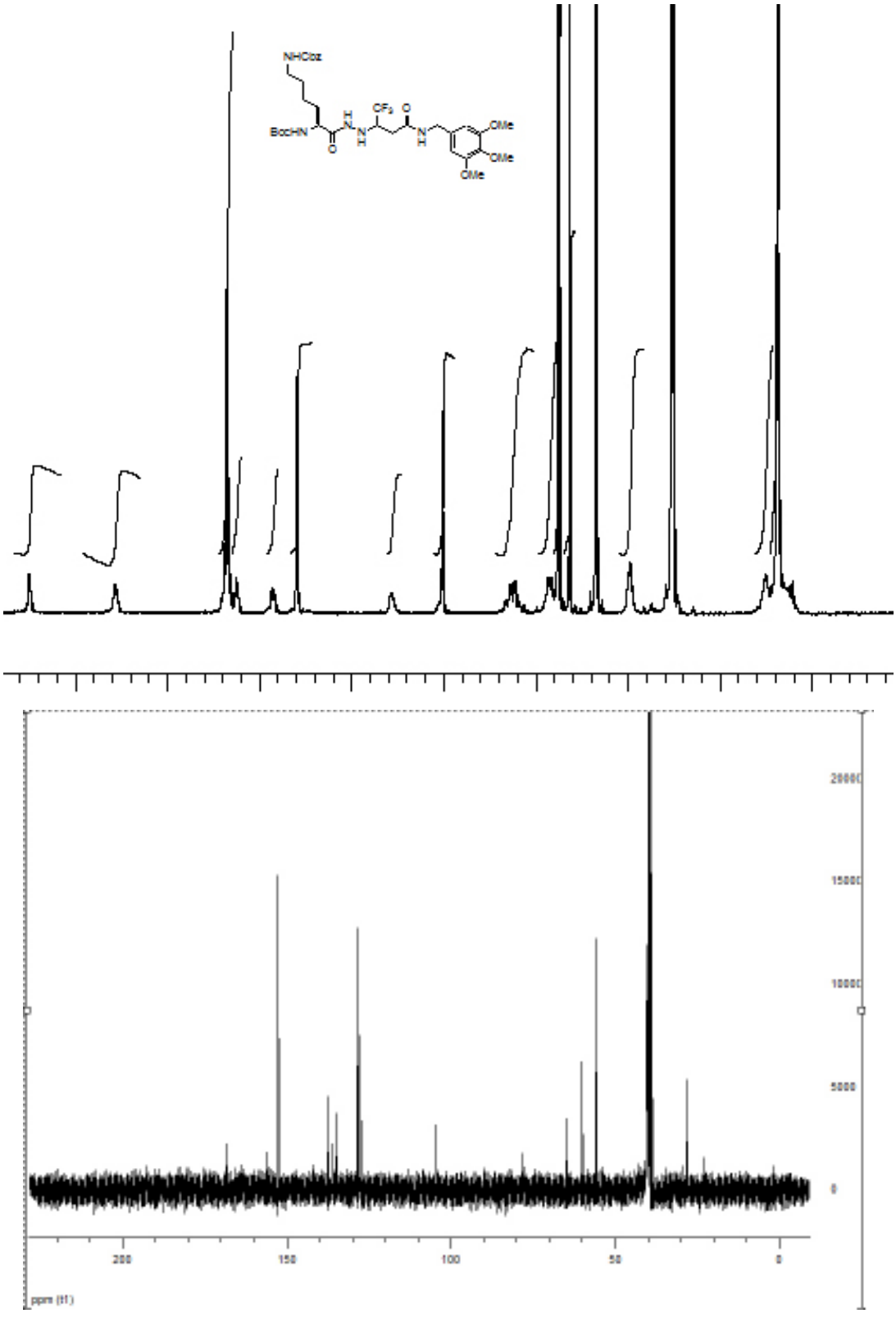

[5-Amino-5-(N'-{2,2,2-trifluoro-1-[(3,4,5-trimethoxy-benzylcarbamoyl)-methyl]-ethyl}-hydrazinocarbonyl)-pentyl]-carbamic acid benzyl ester trifluoroacetic acid salt 312

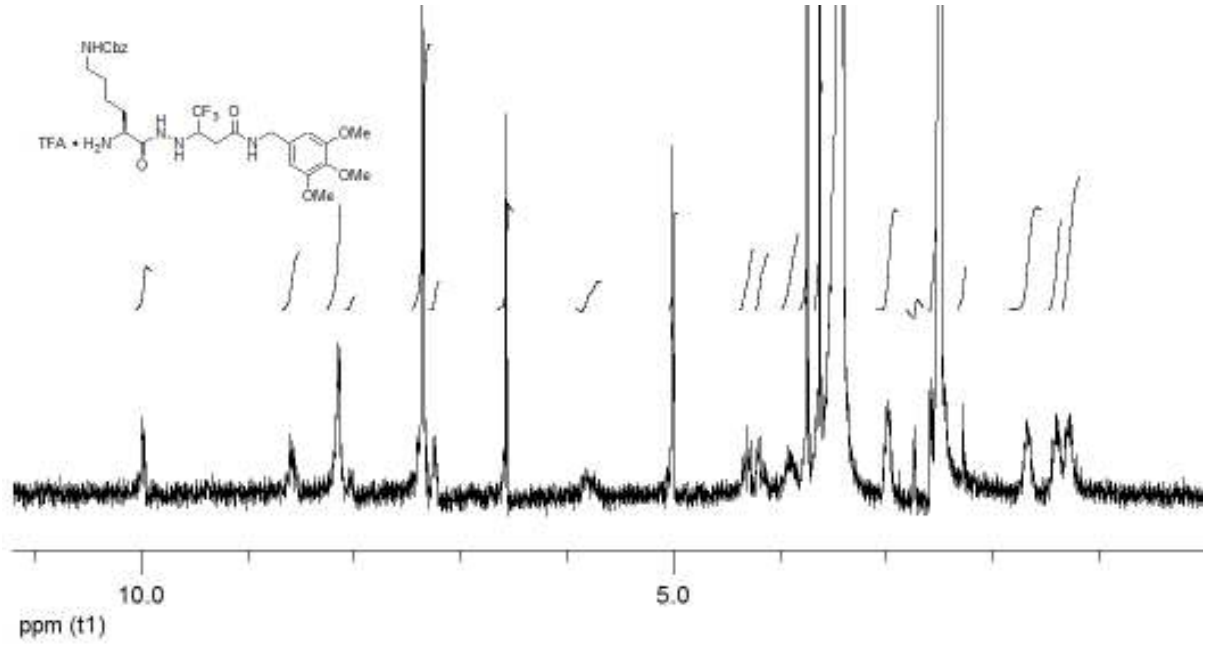

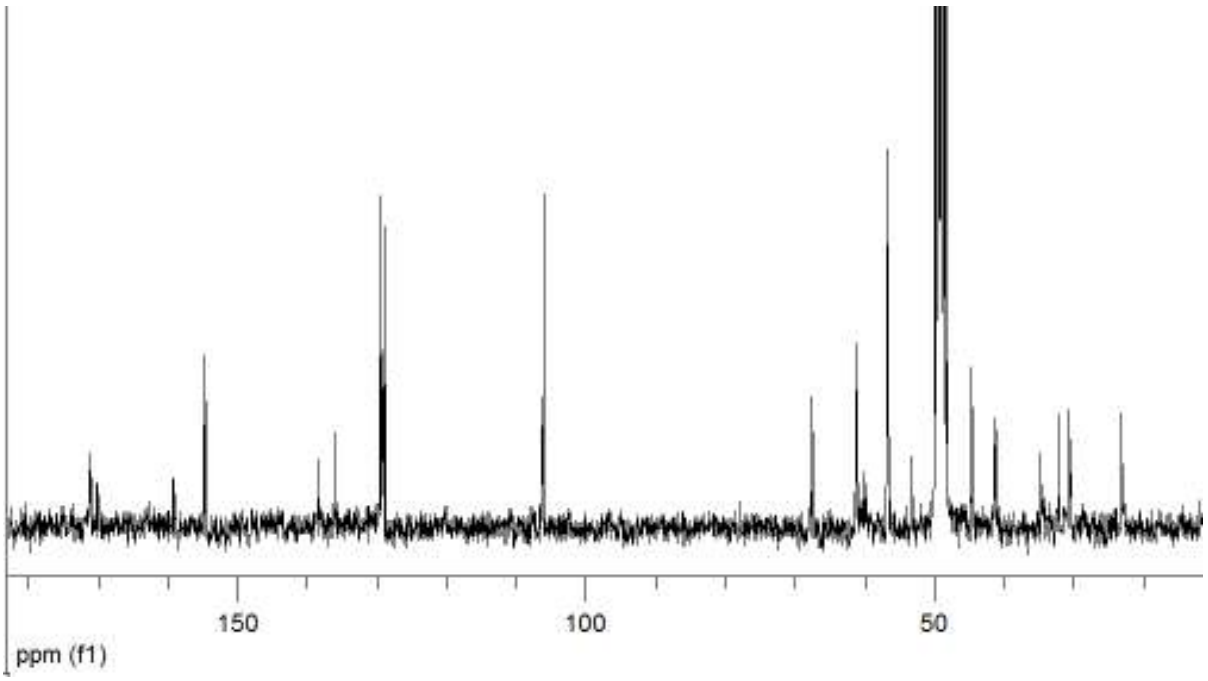

[5-[2-(2,5-Dimethoxy-phenyl)-acetylamino]-5-(N'-{2,2,2-trifluoro-1-[(3,4,5-trimethoxy-benzylcarbamoyl)-methyl]-ethyl}-hydrazinocarbonyl)-pentyl]-carbamic acid benzyl ester 313

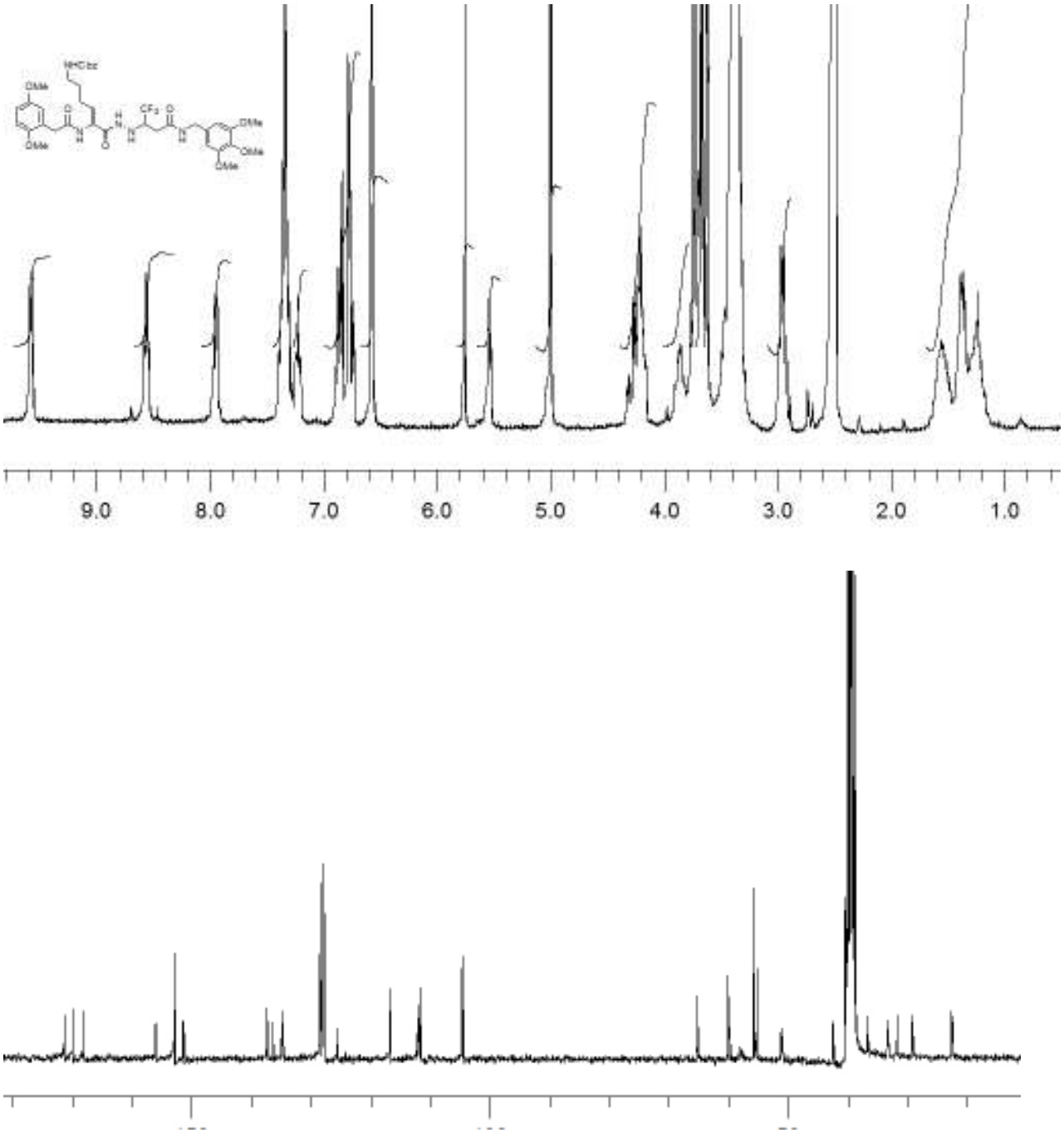

[2-Carbamoyl-1-(N'-{2,2,2-trifluoro-1-[(3,4,5-trimethoxy-benzylcarbamoyl)-methyl]-ethyl}-hydrazinocarbonyl)-ethyl]-carbamic acid tert-butyl ester 310

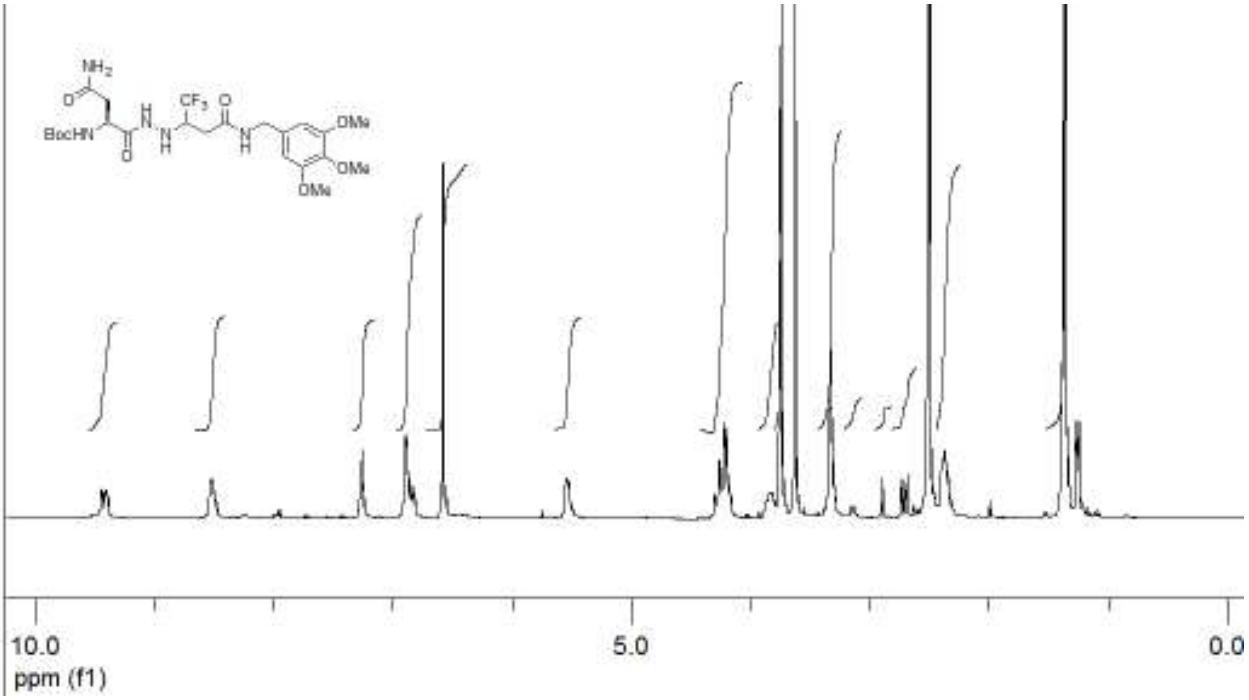

2-[3-(N'-{6-Benzyloxycarbonylamino-2-[2-(2,5-dimethoxy-phenyl)-acetylamino]-hexanoyl}-hydrazino)-4,4,4-trifluoro-butyrylamino]-3-phenyl-propionic acid methyl ester 315

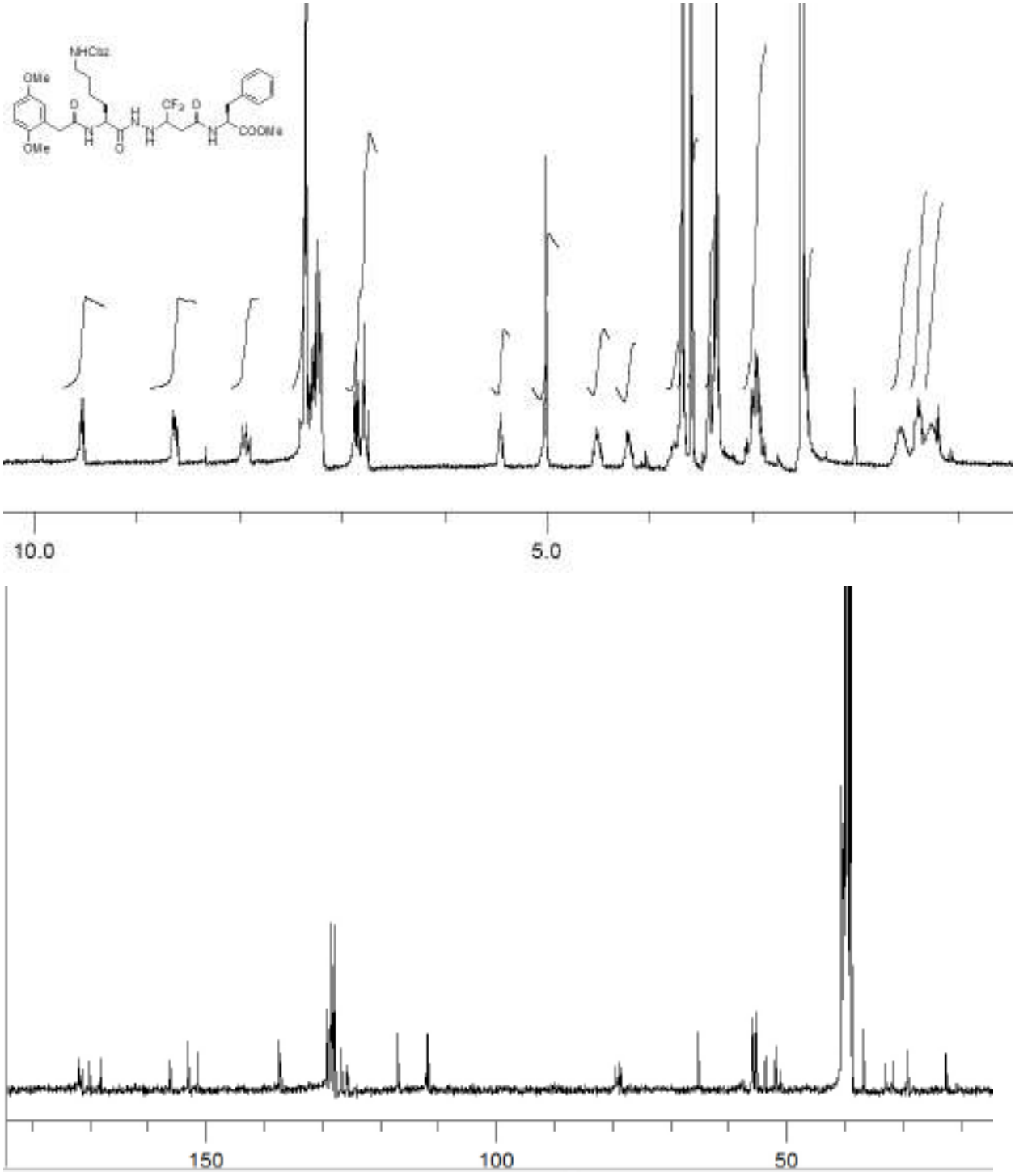

2-[3-(N'-{6-Amino-2-[2-(2,5-dimethoxy-phenyl)-acetylamino]-hexanoyl}-hydrazino)-4,4,4-trifluoro-butyrylamino]-3-phenyl-propionic acid methyl ester trifluoro acetic acid salt 316

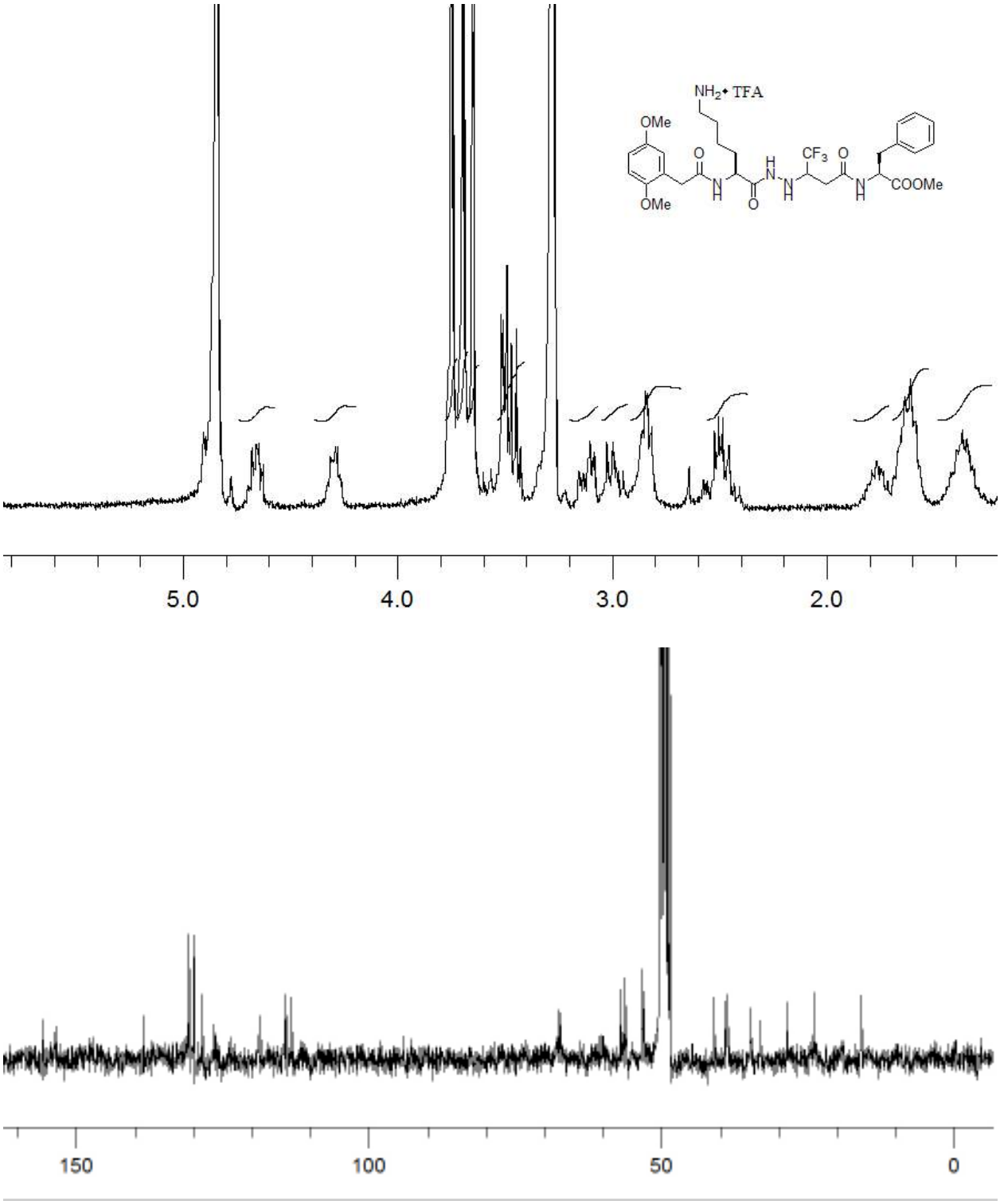

2-{3-[N'-(2-tert-Butoxycarbonylamino-3-carbamoyl-propionyl)-hydrazino]-4,4,4-trifluoro-butyrylamino}-3-phenyl-propionic acid methyl ester 311

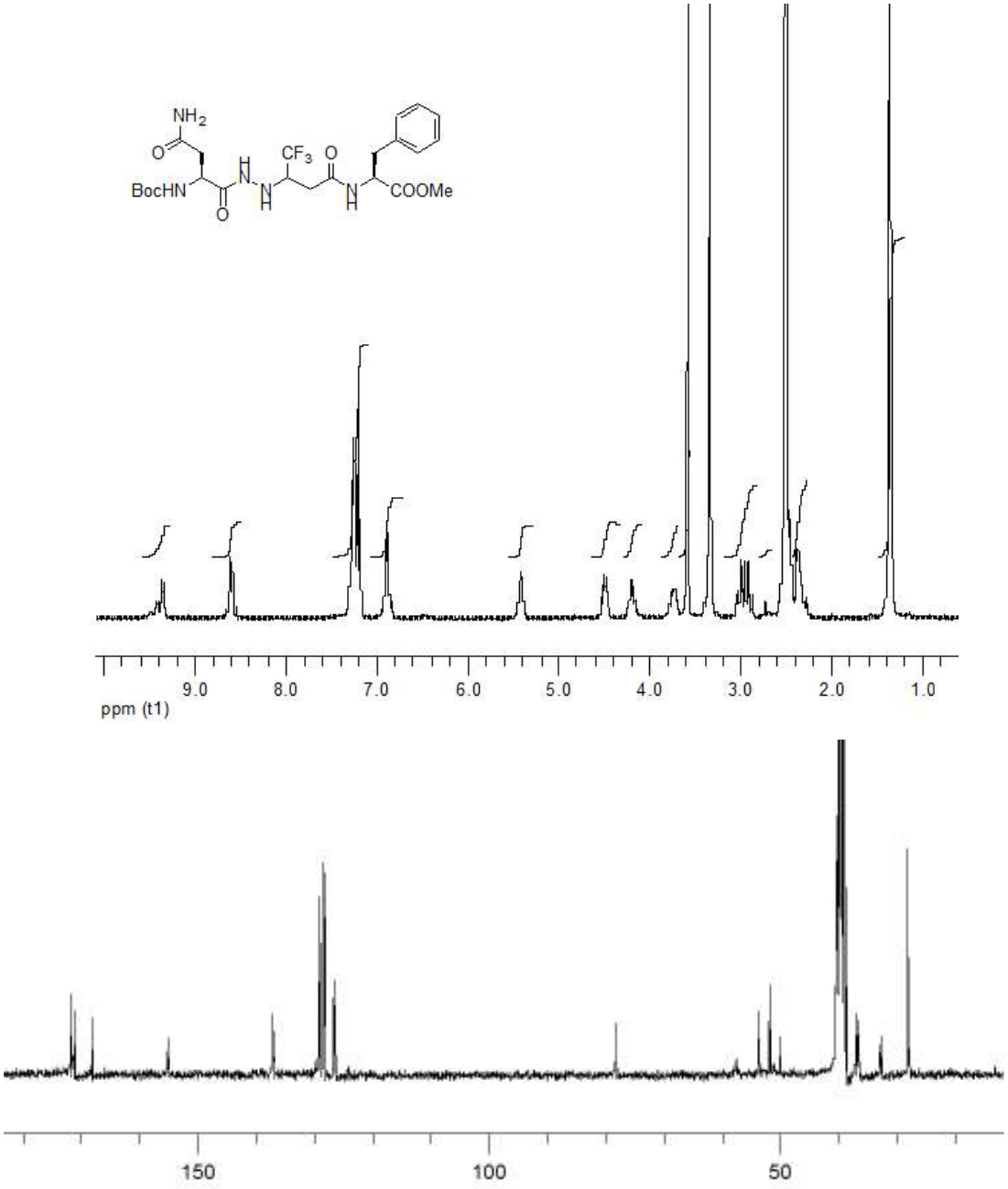

2-[3-(N'-{3-Carbamoyl-2-[2-(2,5-dimethoxy-phenyl)-acetylamino]-propionyl}-hydrazino)-4,4,4-trifluoro-butyrylamino]-3-phenyl-propionic acid methyl ester 317

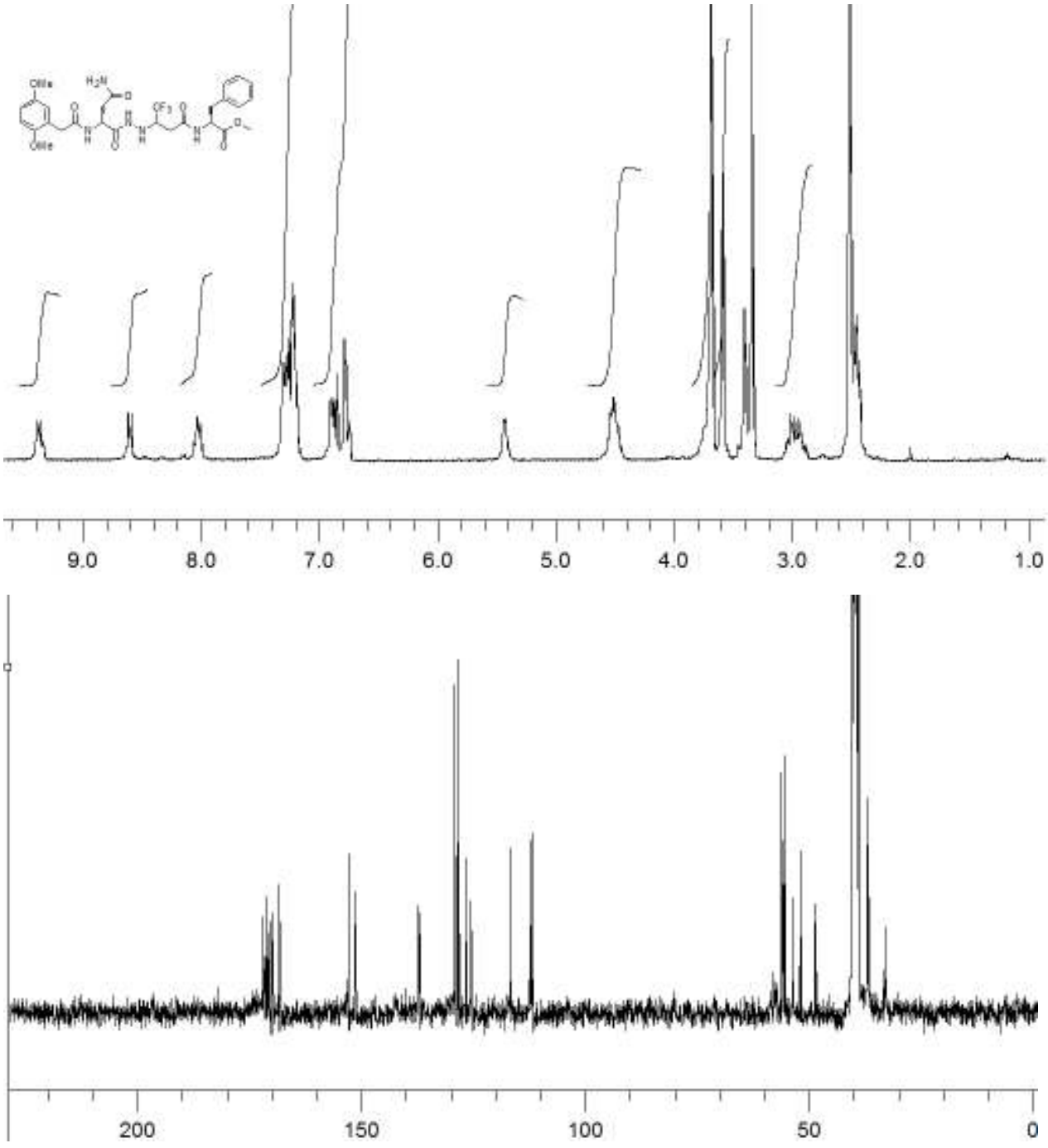

2-(3-{N'-[2-(2,5-Dimethoxy-phenyl)-acetyl]-hydrazino}-4,4,4-trifluoro-butyrylamino)-3-phenyl-propionic acid methyl ester 318

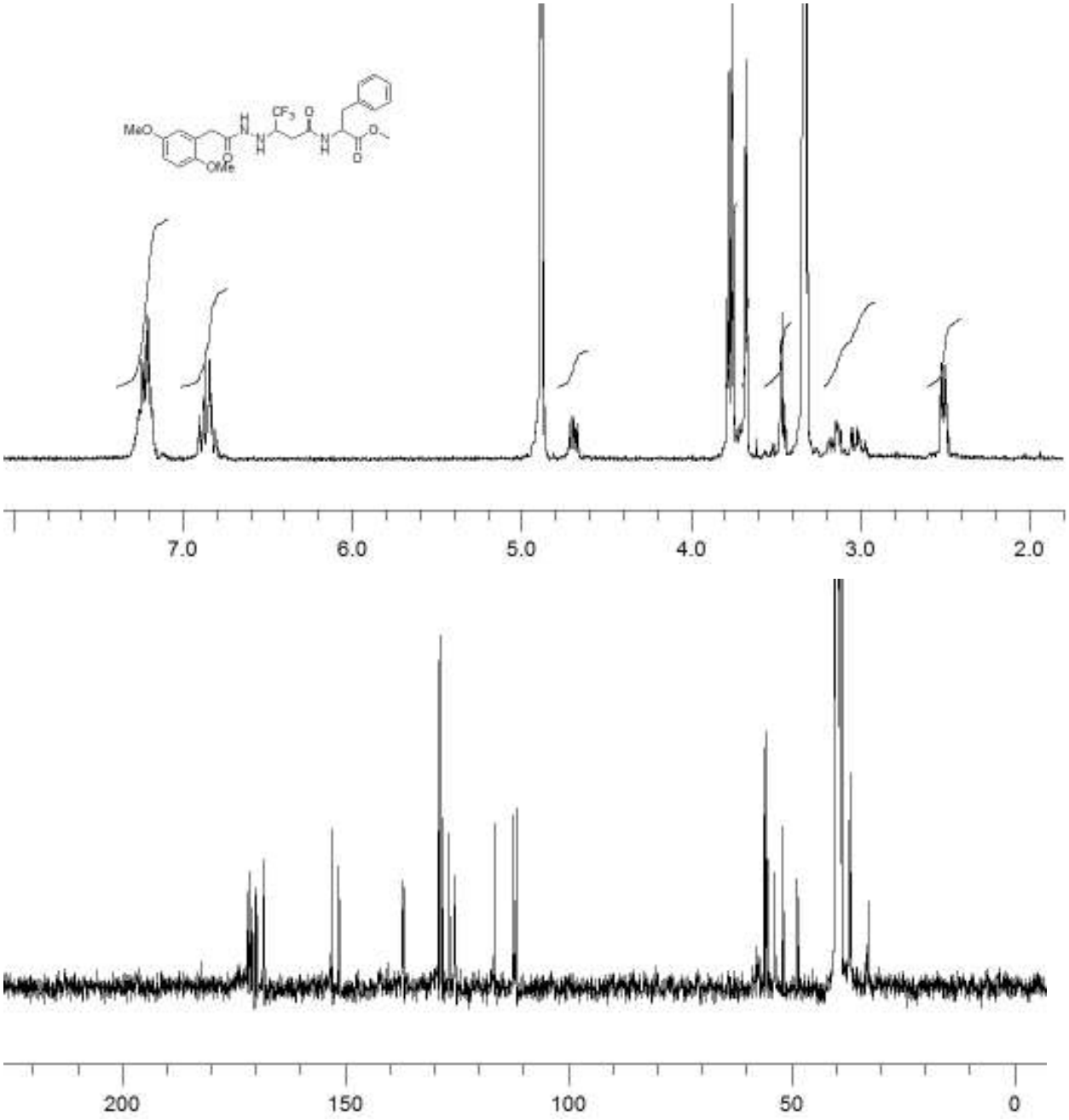

3-(N'-tert-Butoxycarbonyl-hydrazino)-propionic acid ethyl ester 323

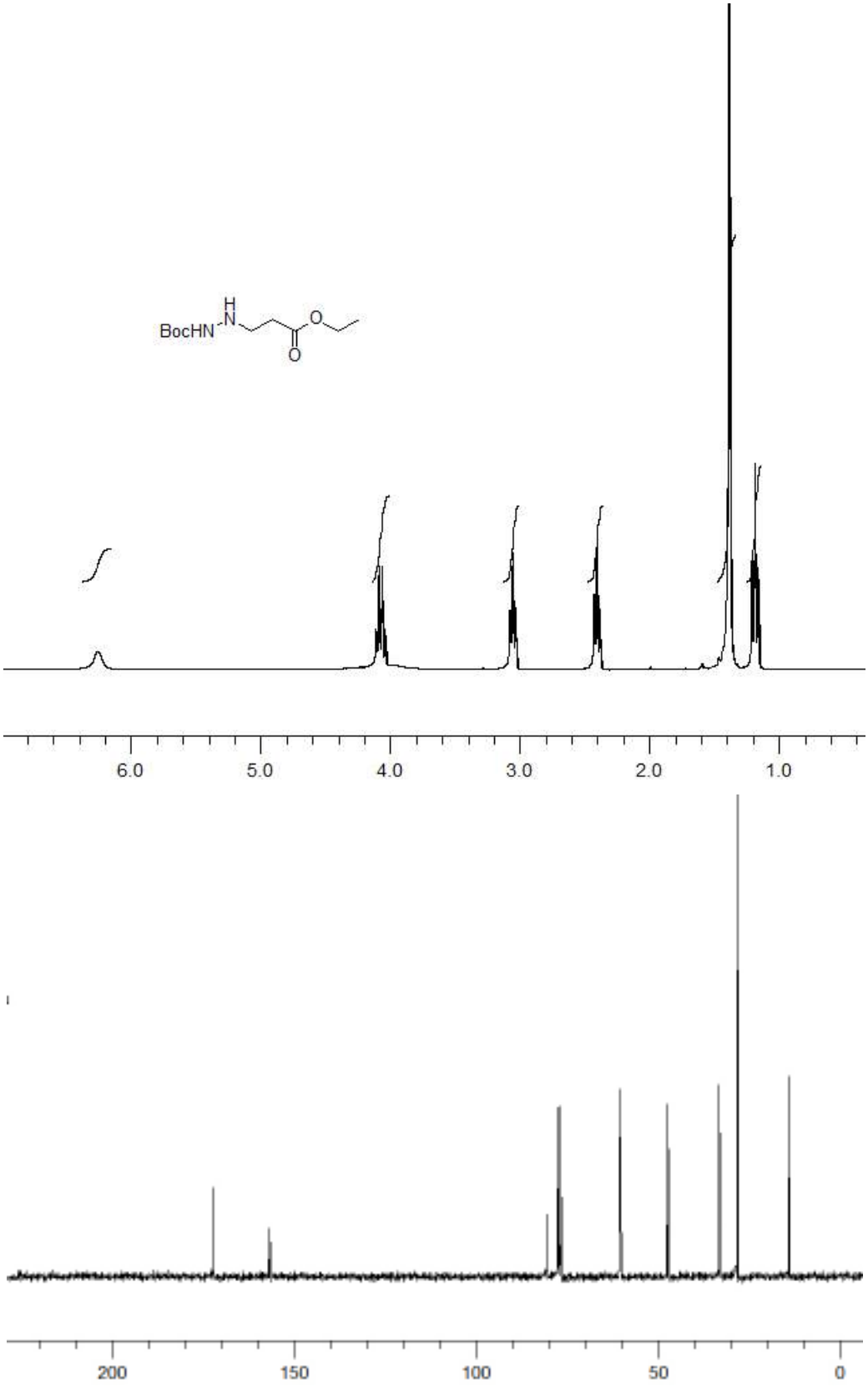

3-(N'-tert-Butoxycarbonyl-hydrazino)-propionic acid 324

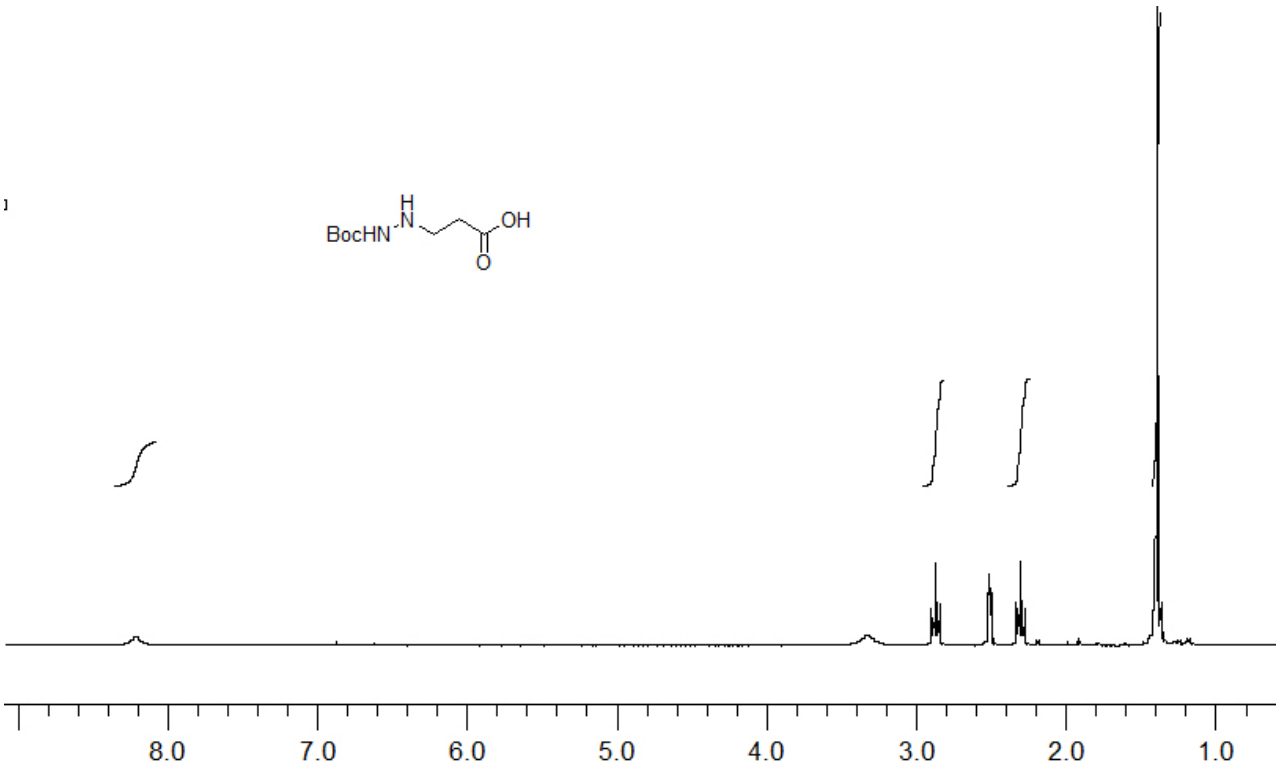

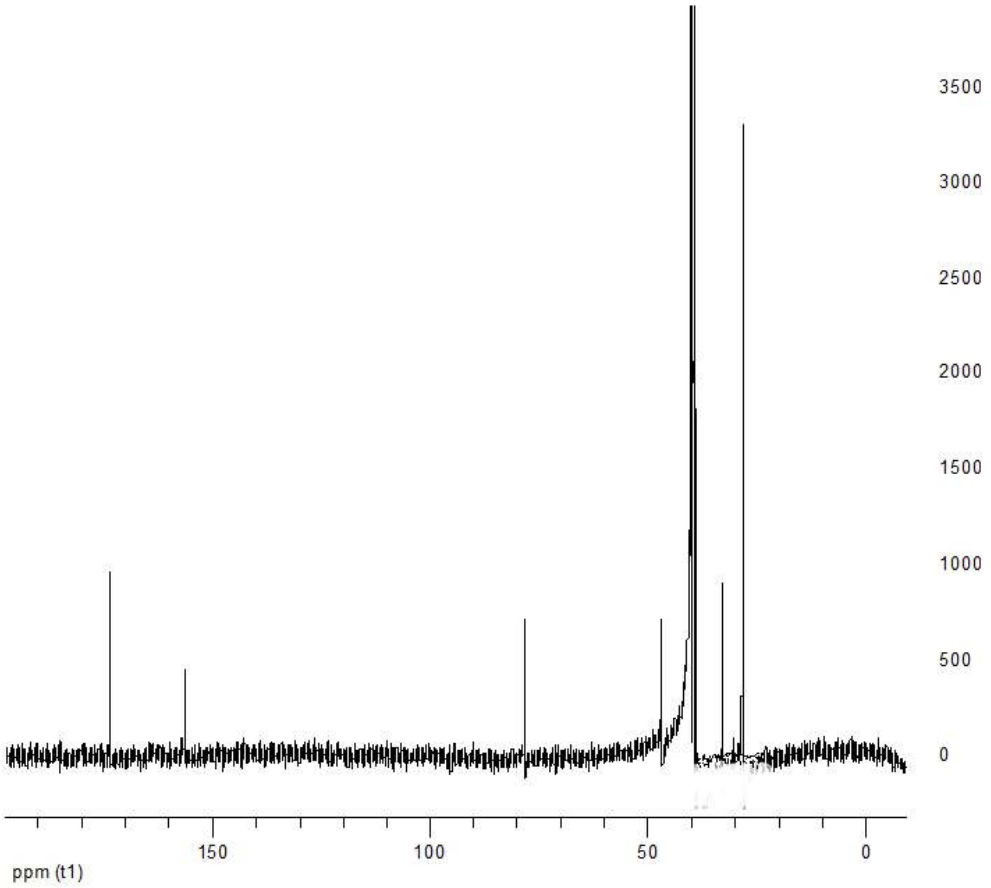

2-[3-(N'-tert-Butoxycarbonyl-hydrazino)-propionylamino]-3-phenyl-propionic acid methyl ester 325

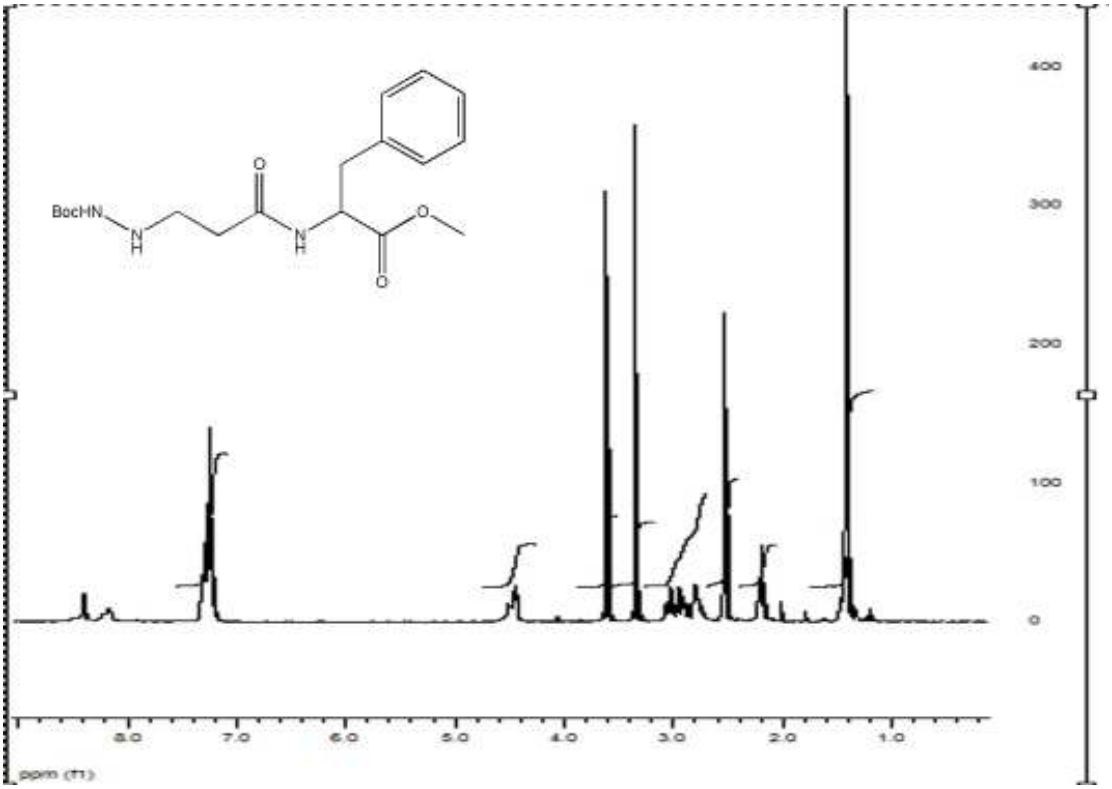

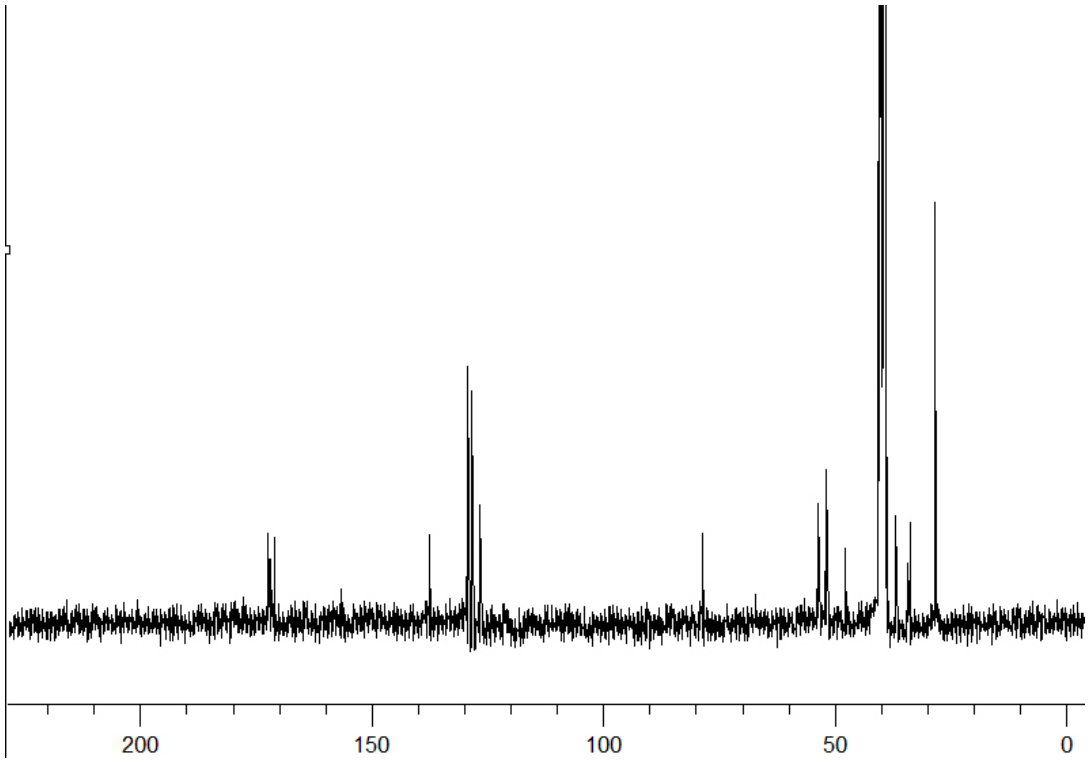

2-{3-[N'-(6-Benzyloxycarbonylamino-2-tert-butoxycarbonylamino-hexanoyl)-hydrazino]-propionylamino}-3-phenyl-propionic acid methyl ester 326

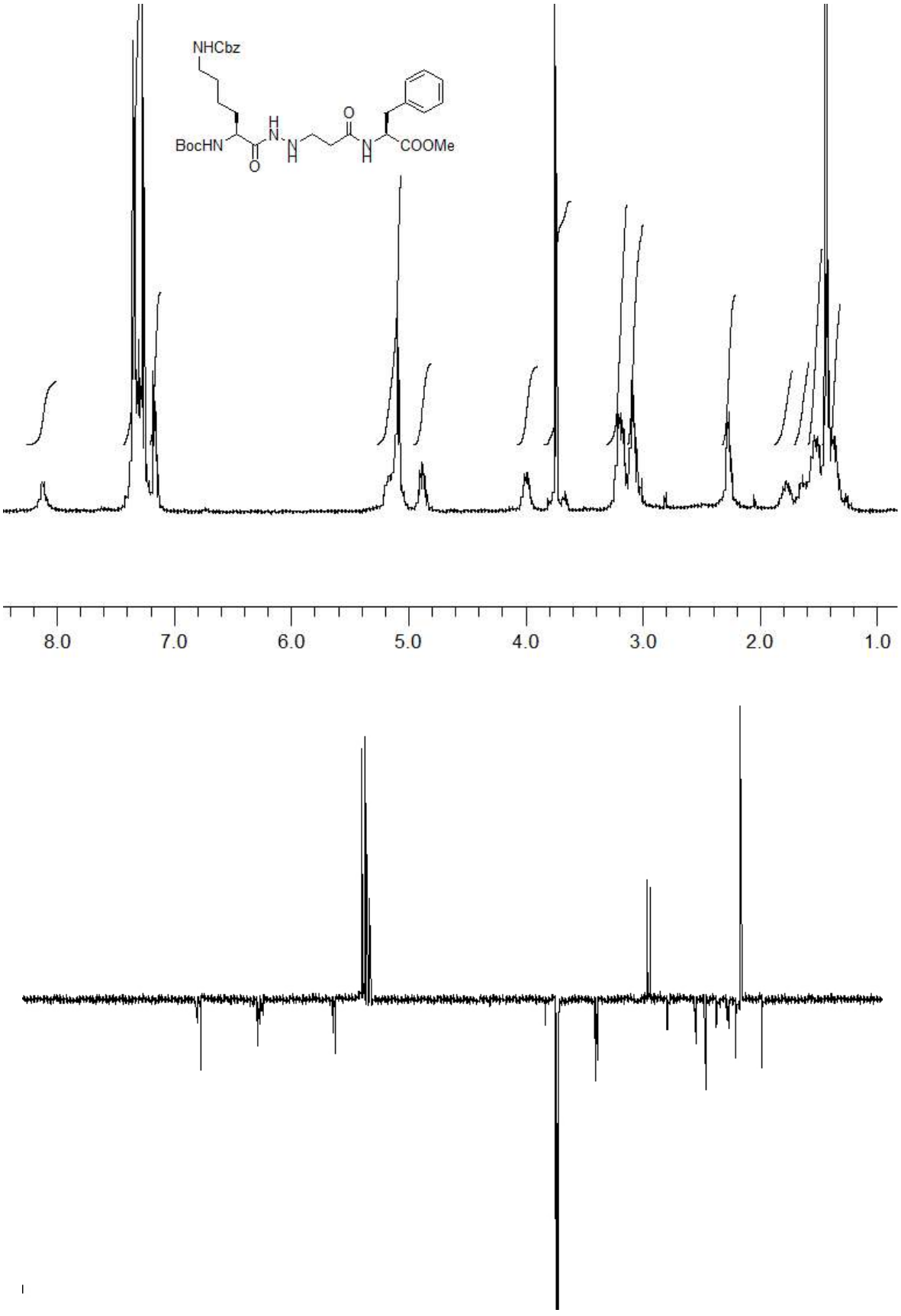

2-{3-[N'-(2-Amino-6-benzyloxycarbonylamino-hexanoyl)-hydrazino]-propionylamino}-3-phenyl-propionicacid methyl ester trifluoroacetic acid 327

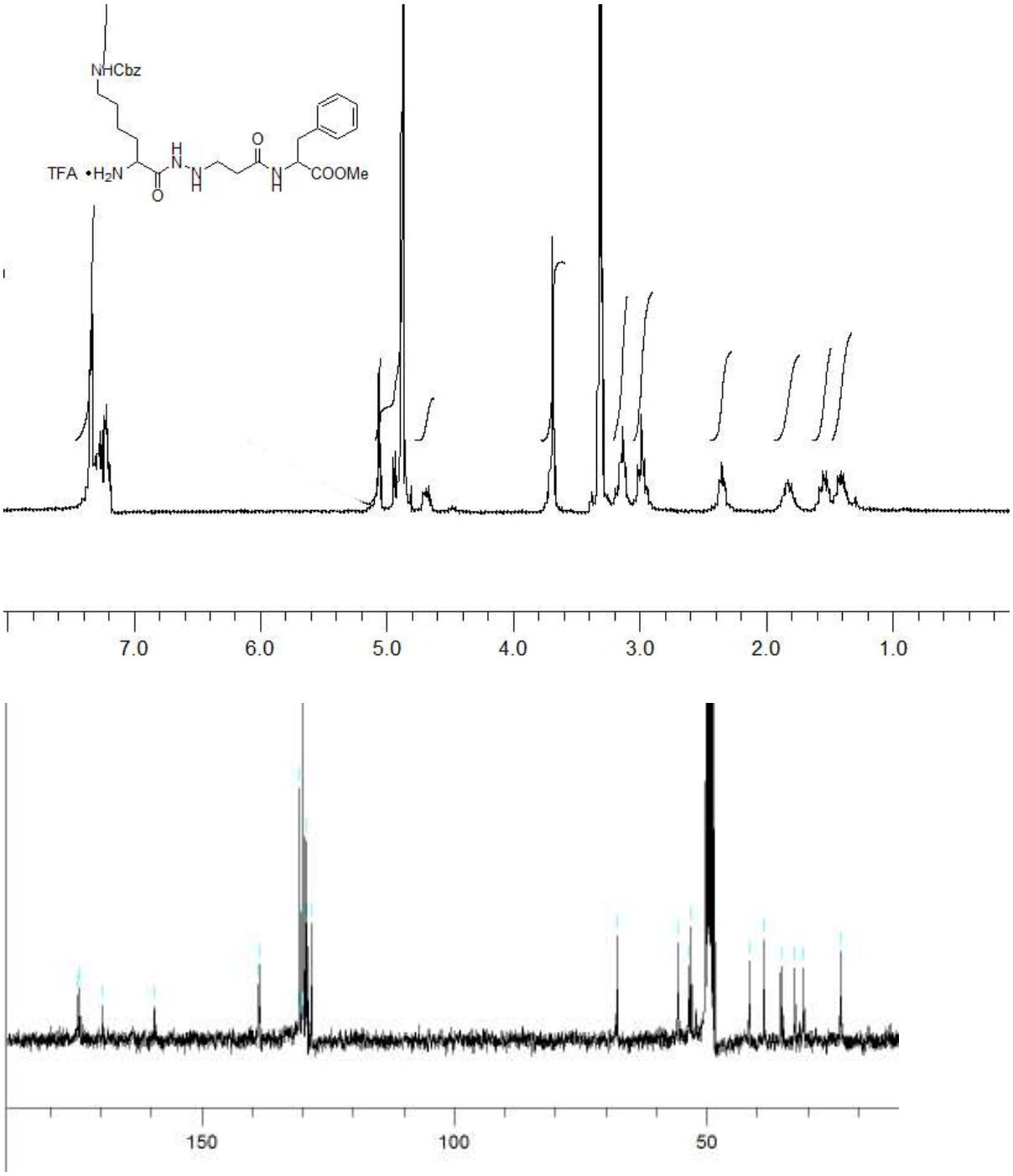

2-[3-(N'-{6-Benzyloxycarbonylamino-2-[2-(4-phenoxy-phenyl)-acetylamino]-hexanoyl}-hydrazino)-propionylamino]-3-phenyl-propionic acid methyl ester 328

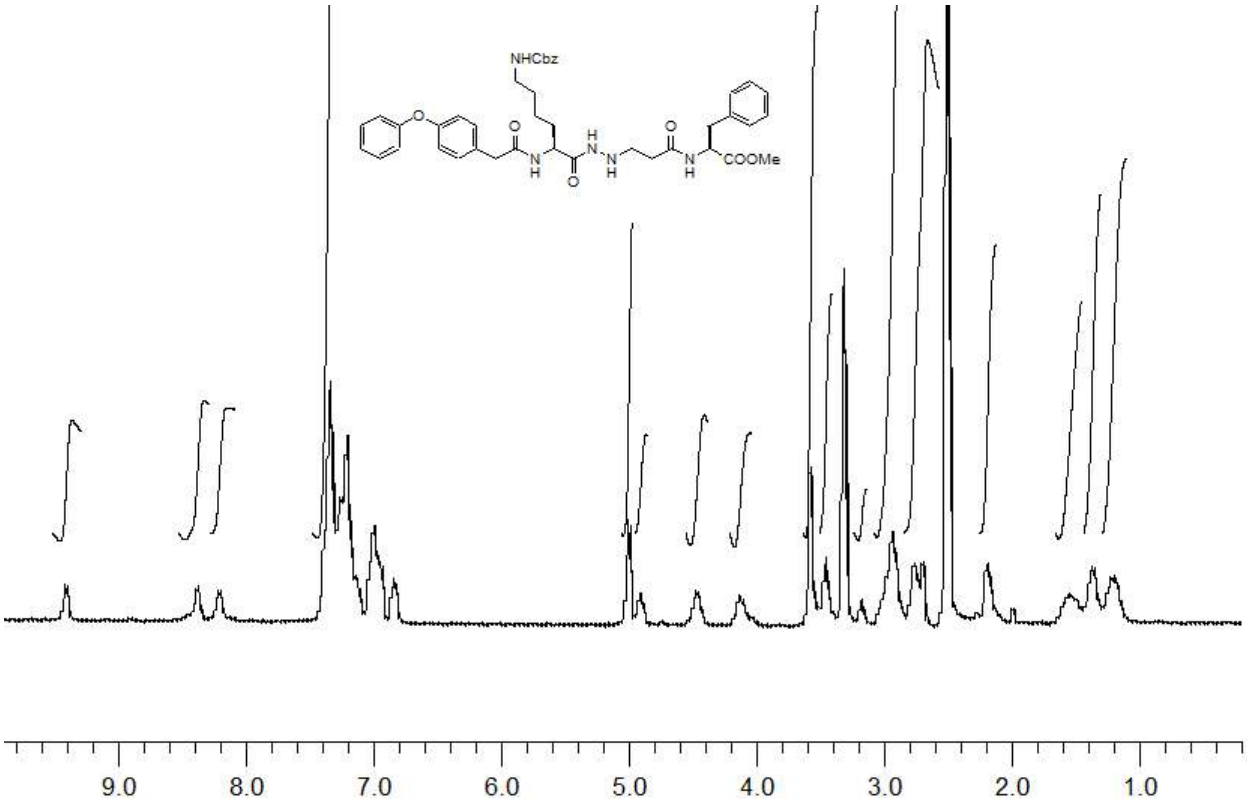

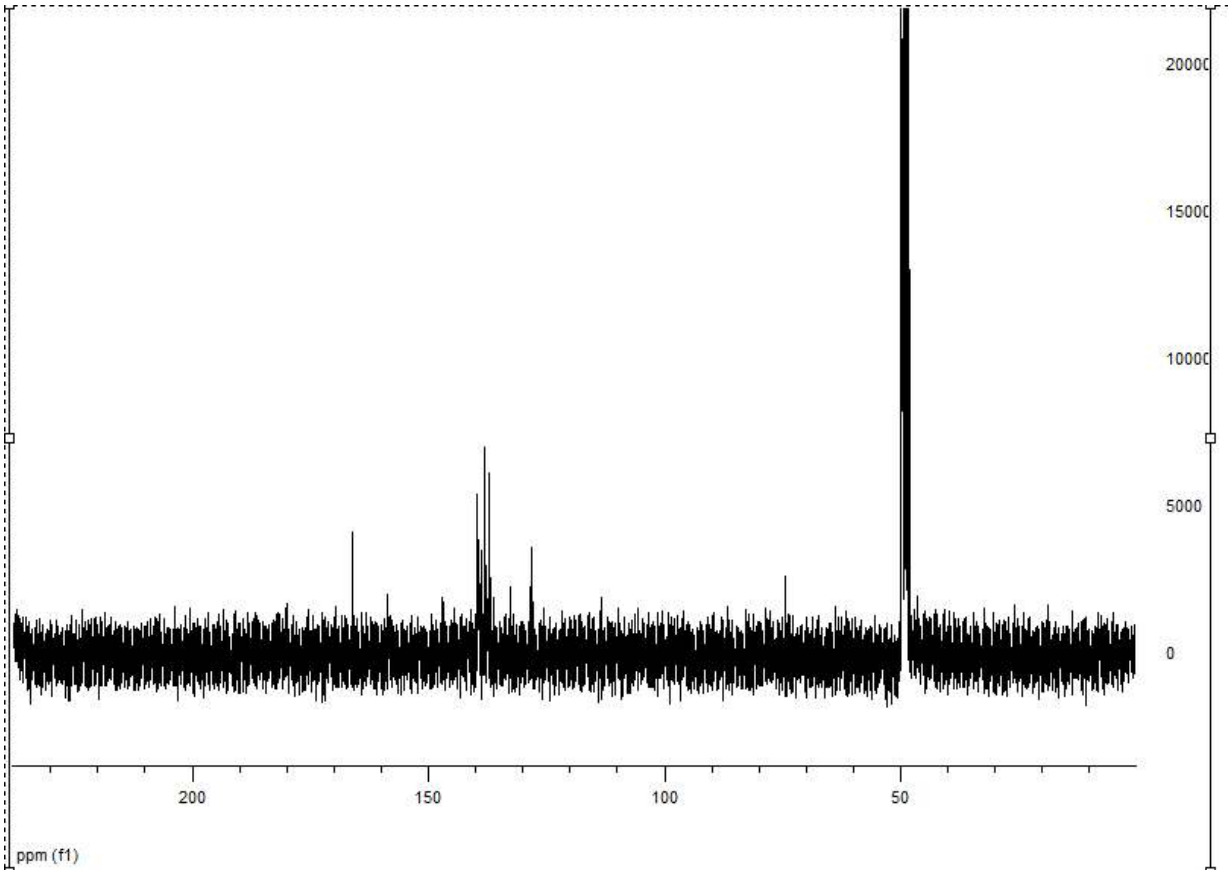
20000
15000
10000
5000
0
200
150
100
50
ppm (f1)